AN INVESTIGATION INTO THE EFFECT OF POTENTIAL MODIFIERS ON THE FLOTATION OF A COPPER SULPHIDE ORE

Lucia Dzinza

A thesis submitted to the faculty of Engineering and the Built Environment, University of Cape Town in the fulfilment of the requirements for the degree of Master of Science in Chemical Engineering

April 2018

Declaration

I declare that this thesis is my own work. It has not been submitted prior to this for any degree at this university or any other institution. I know the meaning of plagiarism and declare that all work in this document, save for that which is properly acknowledged is my own. This thesis has been submitted to the Turnitin module and I confirm that my supervisor has seen my report and any concerns revealed by such have been resolved with my supervisor.

Lucia Dzinza Signed by candidate

12 April 2018

Acknowledgements

To the best supervisors I have met in my life, Dr. Kirsten Corin and Mrs Jenny Wiese, I cannot thank you enough for believing in me and giving me the room to prove myself. Thank you for the undying support and motivation throughout this research journey. You never gave up on me.

To the CMR staff, Shireen Govender, Refilwe, Monde and Kenneth, thank you for the laboratory support and ensuring that my experiments would progress despite some draw backs I experienced in the laboratory.

To Dr. Margreth Tadie and Wonder Chimonyo, thank you for the support and advice on rest potential measurements. You were always available and patient enough to respond to all those million questions I had on electrochemistry.

To Theophilus Dzingai, thank you for the support on froth stability measurements.

To Malibongwe Manono, Lisa October, Jestos Taguta, Jemitias Chivavava, Motlokoa Khasu and Ben Abikoye, thank you for the help and advice on some aspects of this research.

To our helper, Florence Matseka, thank you for helping with taking care of our kids when I needed to get going with this research. You also contributed in making this research a success.

To my beautiful roses, Talicia and Tamuda, thank you for making me a happy mother. It gave me the strength and motivation to carry out this research. You are the pillars of my strength.

To my husband, Charles Nyausaru, I am out of words for the extra-ordinary support and sacrifices you went through in order for 'us' to obtain this Master's degree. Thank you so much for your love, support and motivation to keep me going through these studies. I really appreciate.

My utmost gratitude goes to my late father, Brighton Dzinza, my mum Margaret Dzinza, my sister Irene Dzinza and my other siblings, you have made me to be who I am today. Thank you for your love.

A special mention goes to the National Research Foundation (NRF) and the South African Department of Science and Technology (DST) for the financial support on this project.

Above all, to God whose name is Jehovah, you were faithful enough to take me through this journey with your armour of love. I thank you infinitely for making this research a success.

Synopsis

Oxidation, adsorption and reduction reactions are electrochemical in nature in the flotation of sulphide minerals which have semiconducting properties. Electrochemical mechanisms have two valuable implications in flotation, the potential across the mineral/solution interface determines flotation recovery and the anodic oxidation reaction involving the collector is an important parameter in imparting floatability. The reactions are dependent on the redox conditions in the pulp phase. Chemical control of redox potential (Eh) using potential modifiers may be exploited in flotation processes of sulphide minerals to improve their floatability, recoveries and grades; owing to the formation of a hydrophobic dithiolate or metal thiolate in the case of thiol collectors. In addition, chemical control of Eh is advantageous as it renders a more uniform electrochemical environment around the sulphide particles as compared to the external control of pulp potential. The adjustment of pulp potential using potential modifiers is being exploited as one of the main control parameters in sulphide flotation studies as it provides a diagnostic tool to develop flotation strategies and alleviate flotation challenges. Though potential modifiers have been previously investigated, no literature has addressed the correlation between their flotation performances on copper sulphides to their respective rest potentials at different concentrations. The present study explored the use of potential modifiers such as sodium hypochlorite (NaClO), potassium permanganate ($KMnO_4$) and potassium dichromate ($K_2Cr_2O_7$) on the flotation of a copper sulphide ore from Kansanshi Copper mine in Zambia.

The potential modifiers were investigated at $1x10^{-4}$, $1x10^{-3}$ and $1x10^{-2}$ mols which gave rise to various Eh values for each modifier. Batch flotation and froth stability tests were carried out at the ore's natural pH whilst varying Eh. The dynamic stability factor (∑) was used to quantify froth stability. Electrochemical techniques have been considered as an appropriate approach in the study of collector-mineral interactions. To complement results obtained from batch flotation and froth stability tests, rest potential measurements were carried out to determine the characteristic species formed on the chalcopyrite mineral surface at specific conditions. The potential modifier-collector-mineral interactions were investigated through rest

potential measurements using the aforementioned potential modifiers, a thiol collector sodium iso-butyl xanthate (SIBX) and a pure chalcopyrite mineral.

It was hypothesized that assuming an X^-/X_2 equilibrium potential below 100 mV for SIBX, a redox potential range of 100-400 mV promotes good copper floatability due to the formation of dixanthogen and thus hydrophobic mineral particles which would result in a moderately stable froth. Rest potentials above 500 mV were hypothesized to reduce copper floatability due to the presence of very hydrophobic mineral particles, which would increase bubble coalescence and bubble breakage or result in highly stable froth. In this study, the equilibrium potential of SIBX at $6.24x10^{-4}$ M was measured to be 80 mV. Furthermore, equilibrium potential of SIBX was determined to be concentration dependent. Rest potential measurements for all conditions investigated were in excess of the measured equilibrium potential, therefore implying that the dixanthogen species was formed as postulated. It was found that an increase in concentration of potential modifiers increased froth stability or bubble coalescence depending on the potential modifier used. Furthermore, concentrations of potential modifiers resulting in Eh values of 137-476 mV resulted in high copper recoveries >88%, with $1x10^{-2}$ mols of $KMnO_4$ at 540 mV giving a very low copper recovery of 4.8%. However, though high copper recoveries were obtained between concentrations that gave rise to an Eh range of 137-476 mV, a slight decrease in copper recoveries of approximately <4%, was observed with even larger increases in concentrations of potential modifiers.

The findings of this study showed that the use of potential modifiers improved copper grades as a result of the reduction in gangue material recovery. In addition, the present study has shown that though concentration or Eh induced by potential modifiers may affect the flotation performance of sulphide ores, the most dominant factor that has shown to have a greater impact is the nature of the potential modifier. Comparing the findings of this work to literature findings for NaClO, it was determined that different sulphide minerals indeed exhibit different rates of redox reactions at given conditions. Ultimately, an inverse relationship was determined to exist between copper recoveries and rest potential measurements.

This study has provided insight into the use of potential modifiers in the flotation of copper sulphides from an electrochemical perspective.

Table of Contents

List of Figures

List of Tables

Abbreviations

A	Cross sectional area of the column
Ag/AgCl	Silver/Silver chloride
C	Xanthate concentration at electrode
C1	First concentrate
C2	Second concentrate
C3	Third concentrate
C4	Fourth concentrate
CPS	Controlled Potential Sulphidisation
^0C	Degrees Celsius
E	Cell potential
E^0	Standard cell potential
Eh	Redox potential
F	Faraday constant
g/t	grams per tonne
H_{max}	Maximum froth height
$KMnO_4$	Potassium permanganate
k_1	Rate constant
$K_2Cr_2O_7$	Potassium dichromate
L/min	Litres per minute
M	Molarity

ml	Millilitres
NaClO	Sodium hypochlorite
$Na_2B_4O_7.10H_20$	Di-sodium tetraborate decahydrate
Na_2SO_4	Sodium sulphate
PXRD	Powder X-Ray Diffraction
Q	Gas volumetric flow rate
R	Universal gas constant
SIBX	Sodium iso-butyl xanthate
SHE	Standard Hydrogen Electrode
SPW	Synthetic Plant Water
TDS	Total dissolved solids
µl	Microlitre
V_f	Volume of foam or froth at equilibrium
X^-	Xanthate ion
X_2	Dixanthogen
XRF	X-Ray Fluorescence
ZRA	Zero Resistance Ammeter

Greek symbols

τ	Average bubble lifetime
θ	Contact angle
$\sum$	Dynamic froth stability factor
Υ_{sl}	Surface energy between solid and water
Υ_{sv}	Surface energy between solid and air
Υ_{lv}	Surface energy between water and air
α	Symmetry factor
β	Transfer coefficient

1 Introduction

1.1 Background

The Kansanshi Copper mine in Zambia is the largest copper mine in Africa and the eighth largest in the world. The ore deposit comprises of the primary and secondary copper minerals which are further classified into three groups namely, sulphides, oxides and mixed ore. The sulphide ore constitutes mainly of coarse grained pyrite with chalcopyrite set in a matrix of feldspar, quartz and muscovite mica. The high grade copper sulphide ore constitutes 3.9% chalcopyrite whereas the low grade ore constitutes 1% chalcopyrite (Kalichini, 2015), to which the former was the focus of this study.

On-site, copper recoveries are currently being optimized by the use of Controlled Potential Sulphidisation (CPS). It is well established that the activation of oxidised copper ores such as chrysocolla involves their treatment with hydrosulphide ions. Sulphidisation is considered best under controlled potential to improve recoveries (Woods, 2010). It has been reported in literature that the use of potential modifiers in the flotation of copper sulphides presents yet another economic benefit to the mining industry considering that minute quantities of potential modifiers are required to improve valuable mineral recoveries (Plackowski et al., 2014, Chimonyo et al., 2017). However, some draw backs with the CPS method involve under-sulphidising mineral particles which may result in poor mineral recoveries and over-sulphidising which may depress the valuable mineral (Kalichini, 2015). In addition, tarnishing of mineral surfaces, which involves loss of lustre on mineral surfaces may occur and reproducibility is difficult at plant scale. Alternatively, this study seeks to exploit the control of potential during flotation of a copper ore by the use of potential modifiers with the intention of improving the flotation performance of the copper mineral.

Owing to the fact that sulphide minerals have semi-conducting properties, their reactions are usually electrochemical in nature (Kocabag and Guler, 2007). The reactions are dependent on the redox environment of the pulp phase which is determined by all redox reactions occurring. The redox environment may be induced by potential modifiers, which are considered as one of the most important parameters affecting electrochemically controlled

flotation of sulphide minerals (Hu et al., 2009). It is of great importance to understand how potential modifiers can be manipulated in order to obtain maximum recoveries. The redox potential at the mineral-solution interface has been used as a diagnostic tool in flotation processes (Ralston, 1991).

Although literature has reported on the effects of potential modifiers on valuable minerals (Guo and Yen, 2002, Senior et al., 2009, Peng et al., 2012), it has not highlighted the fundamental understanding of potential modifiers from an electrochemical point of view. Therefore, this study seeks to compare different types of potential modifiers and give a fundamental understanding to their impact on the flotation performance of copper sulphides.

1.2 Scope of thesis

The scope of this study includes the evaluation of the effect of selected potential modifiers on the flotation performance of a copper sulphide ore. The flotation performance was evaluated by chemical analysis for the element copper, determination of gangue material recovered under the conditions investigated and the evaluation of potential modifier type and concentration. In addition, froth stability tests were used to determine the effect of the various types and concentrations of potential modifiers on the froth phase. Rest potential measurements were conducted to complement batch flotation and froth stability tests.

In the initial stages of the study, preliminary tests were carried out to determine whether pH varies with Eh for the particular potential modifiers investigated. It was determined that pH remained constant for all conditions with changes in Eh.

A summary of this work is illustrated in Figure 1.1. The inputs of this work are highlighted in green and orange and the outputs are highlighted in purple.

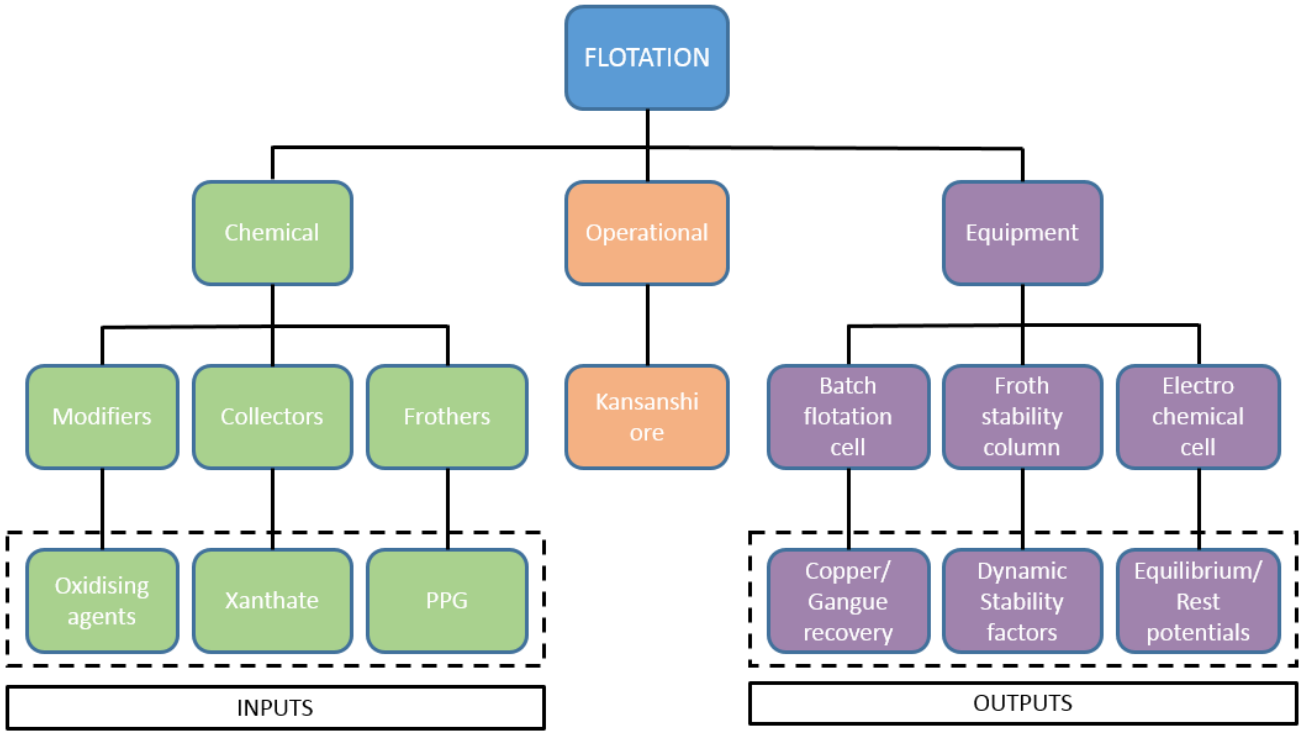

Figure 1.1: Schematic diagram representing the scope of this study.

Operating conditions such as air flow rate that can readily affect froth stability were kept constant in all froth stability investigations. Efforts were made to keep the particle size distribution similar by maintaining the same milling time and using the same milling media. This thesis does not include analysis of the effects of dissolved oxygen and ionic strength on the flotation of the copper sulphide ore. All other experimental parameters except for changes in potential modifier type and concentrations were maintained.

2 Literature Review

2.1 Introduction

The control of potential by redox reagents has been reported in literature as an important tool to control sulphide mineral recoveries in the flotation process. The effects of various potential modifiers at various amounts in the flotation of copper sulphides and their interactions with mineral surfaces has not been explored.

This chapter critically reviews literature that is within the scope of the study. The chapter begins with outlining the principles of froth flotation and subsequently reviews factors that affect froth stability and how froth stability may be measured. A critical synthesis of the mechanisms involved in thiol collector interactions with mineral surfaces and flotation recoveries as a function of chemically controlled potential, shall follow. After-which the techniques used to identify characteristic species formed on mineral surfaces will be discussed. A mineralogical review of the ore and a brief summary of ore processing are also given. The chapter will be concluded by a summary of the literature that brings to surface the gap that has been created in literature by pertinent studies.

2.2 Principles of froth flotation

Flotation is a physical-chemical separation process that employs differences in wettabilities between valuable minerals and non-valuable gangue material (Wills and Napier-Munn, 2006). It is a process that consists of two well-defined phases, the pulp phase, where all process conditions are applied and mineral recovery is initiated; and the froth phase, where the valuable concentrate is recovered. Wills & Napier-Munn (2006) went further to describe the recovery of material in the flotation process (Figure 2.1) from the pulp phase as a process that involves three mechanisms. The first and most dominant mechanism is true flotation. This involves selective attachment of minerals to bubbles, true flotation contributes to most of the concentrate that reports to the froth phase. The second mechanism is entrainment in the water which passes through the froth phase, this process is unselective. The third mechanism

is entrapment, where the valuable and gangue material in the froth phase is trapped between the air bubbles and the other particles in the froth.

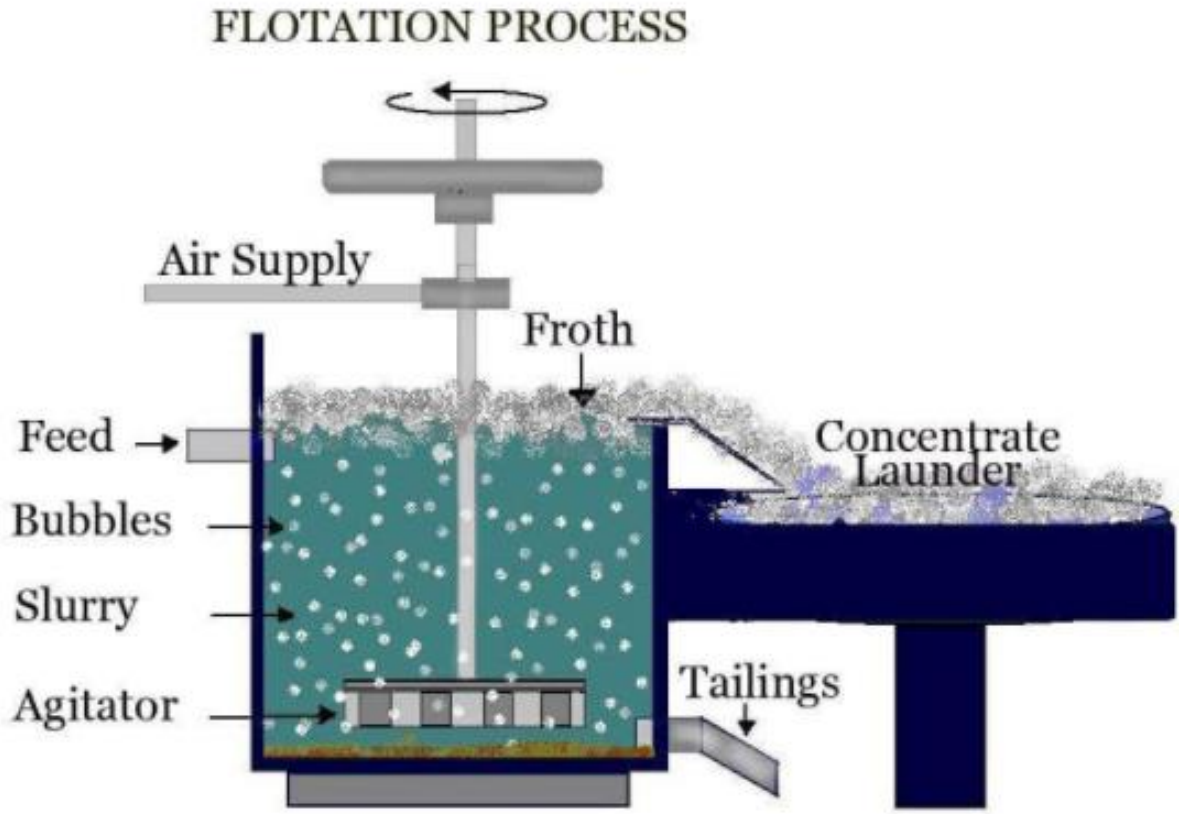

Figure 2.1: Schematic diagram of a conventional flotation cell (adapted from 911 Metallurgist, 2015).

The flotation process has therefore been postulated to be a complex process that is affected by various parameters, that can be categorized into three main groups as in Figure 2.2 (Klimpel, 1995).

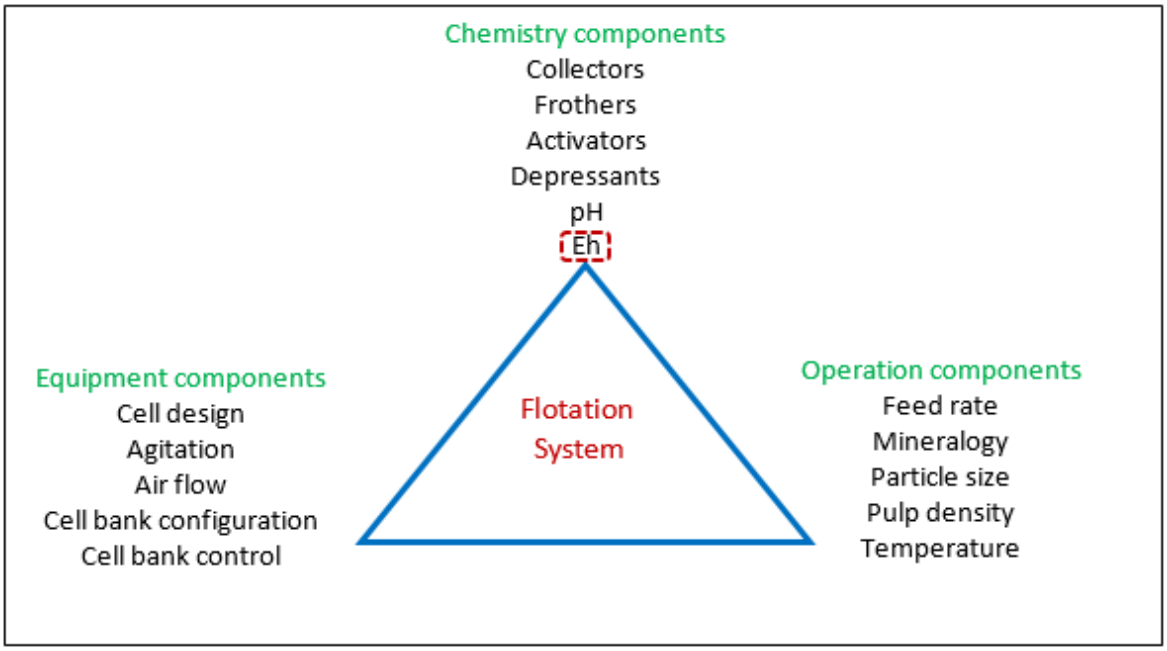

Figure 2.2: Flotation system includes many interrelated components (adapted from Klimpel, 1995).

The complexity of the flotation process is ascribed to the interlinked relationship between flotation parameters (Klimpel, 1995). Considering Figure 2.2, the highlighted chemistry component is where the focus of this work lies.

2.1.1 Hydrophobicity/Hydrophilicity

Considering that the basis of the flotation process is in the wettability differences of mineral particles, it is therefore important to distinguish between the hydrophobic (water repellent) particles from the hydrophilic (easily wettable) particles (Wills and Napier-Munn, 2006). For a successful flotation process to occur, mineral surfaces should be rendered hydrophobic for them to be selectively attached to air bubbles (Kawatra and Eisele, 2014). The mineral laden air bubbles are carried to the froth layer where the mineral is isolated as a separate product. Since the hydrophilic particles have a less tendency to attach to the air bubbles, they remain in suspension and are lost in the tailings. Some minerals are naturally hydrophobic whereas others must be modified by chemical reagents. The hydrophobicity of a mineral increases with a contact angle between a bubble and a particle (Figure 2.3). Contact angle has been extensively studied as a measure of hydrophobicity of mineral surfaces (Ramachandra Rao, 2004). However, the limitation is that it cannot be used to surmise the kinetic process as it is a thermodynamic property.

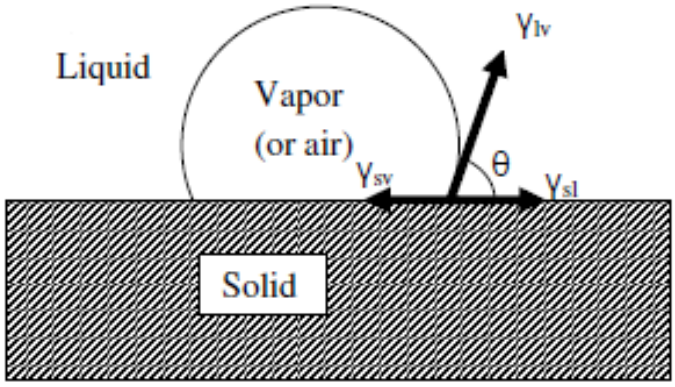

Figure 2.3: Contact angle between bubble and particle in an aqueous medium (Kawatra and Eisele, 2014).

At equilibrium, the Young/Dupre Equation 2.1 applies;

$$\gamma_{Iv}cos\theta = \gamma_{sv} - \gamma_{sI} \quad \text{Eqn 2.1}$$

Where γ_{sv}, γ_{sI} and γ_{Iv} are surface energies between solid and air, solid and water, water and air respectively and θ is the contact angle between the mineral surface and the air bubble. A contact angle of around 90^0 is presumed as adequate enough to enhance effective froth flotation (Kawatra and Eisele, 2014).

2.3 The froth phase

The froth phase is formed when frother surfactants are principally added to the pulp phase so that a transient, mineralised froth may be formed at the top of the flotation cell. The transport of mineral laden bubbles from the collection zone of the flotation cell to the concentrate launder is considered to be a vital step in the flotation process, and this transportation occurs in the froth phase (Tsatouhas et al., 2006). A transient froth is desirable in the flotation process as bubble coalescence or bubble collapse should occur once the froth reports to the concentrate launder. Froth stability and froth structure are important parameters that determine mineral grade and recovery (Farrokhpay, 2011). Froth stability is referred to as thin film rupture, bubble coalescence and the reduction in froth volume (Tsatouhas et al., 2006). A moderately stable froth is a pre-requisite in the flotation process as a highly unstable froth results in a significant loss of the valuable mineral from the froth phase to the pulp phase and eventually to the tailings stream and conversely a highly stable

froth causes undesirable problems in pumping (Tsatouhas et al., 2006) and furthermore can result in a significant contamination of the valuable product with gangue material due to high water recovery (Zheng et al., 2006, Kawatra and Eisele, 2014).

The term 'foam' shall be used in the current work to refer to a two-phase system comprising of air and liquid whereas the term 'froth' shall be used to refer to the three-phase system comprising of air, solid particles and liquid.

2.3.1 Factors affecting froth stability

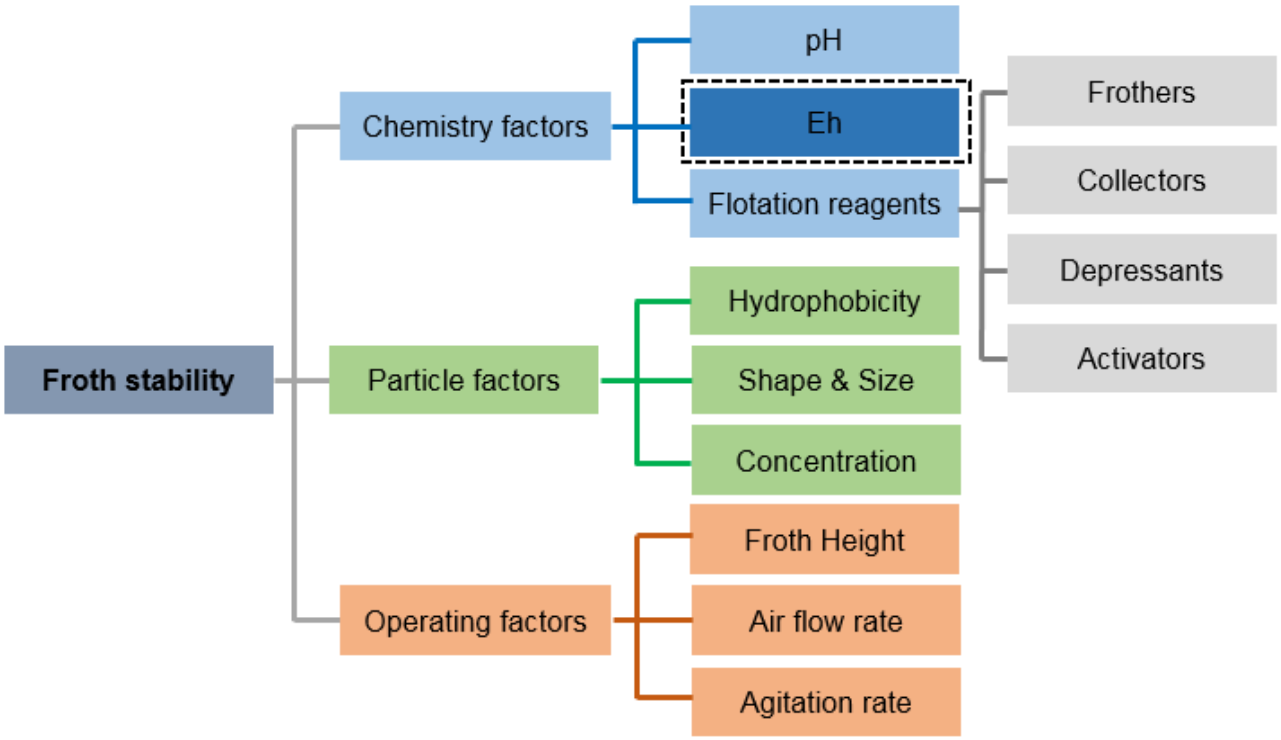

Figure 2.4: Summary of factors that affect froth stability.

Froth stability is mainly dependent on frother type and concentration but other parameters such as flotation reagents play a role too. Furthermore, quality of process water (Farrokhpay and Zanin, 2011), pH and Eh are some chemistry parameters that have been perceived to also have an effect on froth stability. The latter shall be the focus of our study. The amount, hydrophobicity and size of particles have also been reported in literature to also affect the stability of the froth (Gonzenbach et al., 2007, Horozov, 2008, Hunter et al., 2008). Furthermore, operating factors such as froth height (Barbian et al., 2003), gas dispersion

(Barbian et al., 2005) and impeller speed (Koh and Smith, 2011) also contribute in froth stability. All the factors mentioned will be briefly discussed in this section.

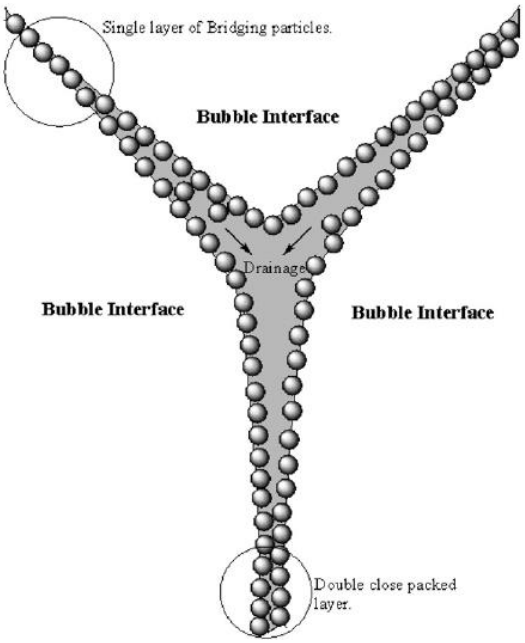

Figure 2.5: Particle stabilised polyhedral type of froth.

The presence of particles on bubble films contributes to froth stabilisation because foams are thermodynamically unstable as their decay results in the decrease in free energy (Horozov, 2008, Hunter et al., 2008). The lateral mobility of particles at the bubble film surface helps them to create a steric barrier to bubble coalescence. Foam systems are known to have increased drainage effects so the presence of particles on the interfilm (Figure 2.5) therefore reduces the drainage and increases the maximum capillary pressure, P_c^{max}, which can be resisted by the liquid menisci around the particles, thus increasing froth stability (Horozov, 2008). Bridging of particles in between froth is important as it forms a high forced contact area in the froth phase. Mechanisms of particle stabilised froth (Figure 2.6) have been reported as being due to a bridging monolayer created on the surface of the bubble film, or a bilayer of closely packed particles or a network of particles aggregates formed around bubble film surfaces (Horozov, 2008).

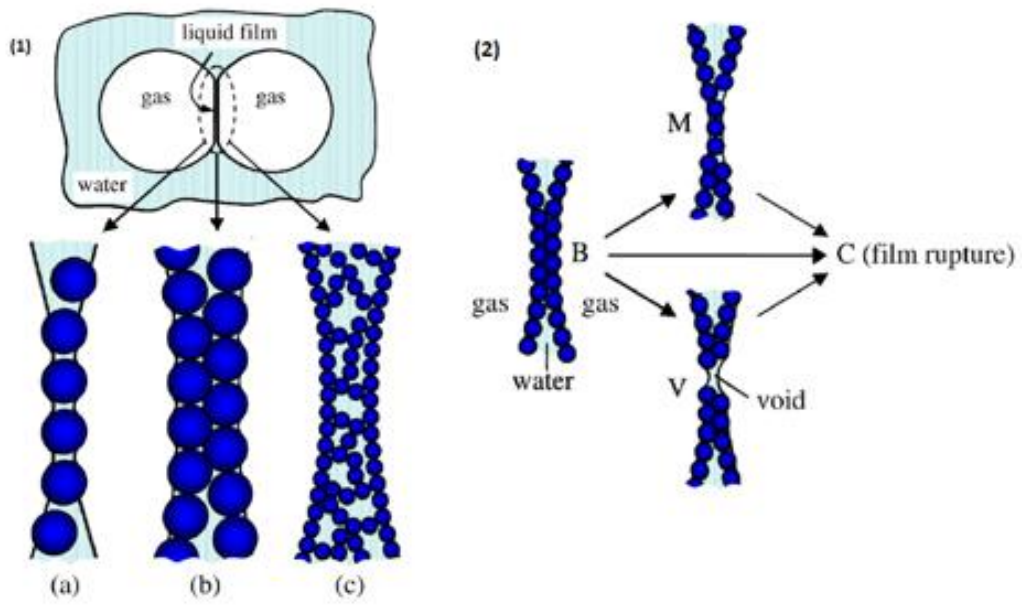

Figure 2.6: (1)- Possible mechanisms of liquid film stabilisation by (a) a monolayer of bridging particles (b) a bilayer of close-packed particles and (c) a network of particle aggregates inside the film (2)- Possible mechanisms of rupture of a water film stabilised by a bilayer of particles: (B-C) direct rupture without rearrangement of a particles, (B-M-C) via bilayer to monolayer transition and (B-V-C) via void formation (Horozov, 2008).

Particles in monolayer systems are very vulnerable to hydrodynamic forces so they can easily get swept away from the film centre, leaving the film unprotected and subsequently causes film rupture. Alternatively, closely packed monolayers resist drag and thus prevent film thinning and film rupture (Figure 2.6 **(1)**). Film rupture occurs at lower critical capillary pressure by two step mechanisms which involve particle rearrangement from a bilayer to a monolayer or the formation of a void where strong cohesion forces are experienced (Figure 2.6 **(2)**).

Hydrophobic particles with a contact angle of above 90^0 act as froth destabilisers (Ata et al., 2003, Hunter et al., 2008), hence particles that have a contact angle between 70 - 86^0 have been found to enhance the bridging monolayer and bilayer mechanisms of film stabilisation (Horozov, 2008). Particles with a size within a range of several tens of nanometers and several micrometers have been reported to be effective froth stabilisers too (Gonzenbach et al., 2007).

Maximum equilibrium froth height was found to increase with an increase in frother concentration and an increase in air flow rate, conversely a higher frother concentration and

a higher air flow rate will destabilise froth and thus results in a decrease in the maximum equilibrium froth height (Barbian et al., 2005). If a relationship between the fraction of air overflowing a flotation cell and flotation performance is known then the froth height can be manipulated to produce optimal froth stability and flotation performance (Barbian et al., 2003).

With regards to agitation rates, it was simulated that lower agitation rates allow for a longer contact time for the particle to attach onto the bubble film surface consequently resulting in high froth stability (Koh and Smith, 2011).

Chemistry factors such as pH and Eh are considered to also have an impact on froth stability. An increase in pH to 11 and an increase in Eh to 700 mV have been found to increase froth stability (Sheni, 2016). In their study, pH was controlled using sodium hydroxide (NaOH) and consequently Eh was controlled using NaClO. With an increase in pH, the author ascribed an increase in froth stability to be due to the presence of OH^- ions in the system, contrarily Farrokhpay & Zanin (2011) reported a decrease in pH (4) using hydrochloric acid (HCl) to cause high froth stability due to an increase in viscosity and particle aggregation. Considering the findings from the two authors, probably the ions from the reagents used to control pH might be contributing in froth stability. On the other hand, Sheni (2016) reported that in addition to froth stability, increases in Eh resulted in an increase in gangue material recovery and increase in entrainment, thus resulting in an increase in bubble coalescence. This was in contradiction to what had been previously reported in literature were an increase in entrained solids resulted in a substantial reduction of bubble coalescence due to reduced liquid drainage in bubble films (Ata et al., 2003).

2.3.2 Quantitative analysis of froth stability

Froth stability is known to play a significant role in determining mineral grades and recoveries achieved during a flotation process. Froth stability has been quantified in literature as a measure of froth recovery (Tsatouhas et al., 2006, Zanin et al., 2009), air recovery (Morar, 2006), bubble size and solids loading on bubbles (Ventura-Medina et al., 2003), bubble growth rate (Ata et al., 2003), froth rise velocity (Bikerman, 1973, Barbian et al., 2005). The latter method of analysis will be used in this work. The technique was originally developed by Bikerman (1973). It is based on a dynamic test and uses a non-overflowing froth column to quantify the froth stability. Static tests have also been used to quantify froth stability in industrial flotation circuits (Tsatouhas et al., 2006). The current work shall focus on the dynamic test in quantifying froth stability.

In the dynamic test, a vertical transparent column is used. When air is introduced into the column, the froth rises up inside the column and a froth height, H, is measured as a function of time, t, with reference to the pulp-froth interface. Depending on operating conditions and stability of the froth, the froth reaches equilibrium and a constant froth height, H_{max}, is achieved and measured (Barbian et al., 2005). The dynamic stability factor, ∑, is further calculated. It was defined by Bikerman (1973) as the ratio of the maximum volume of foam or froth generated to air flowrate:

$$\sum = \frac{V_f}{Q} = \frac{H_{max} x A}{Q} \quad \text{.....Eqn 2.2}$$

Where V_f is the volume of foam or froth at equilibrium, Q is the gas volumetric flow rate, H_{max} is the foam or froth height at equilibrium and A is the cross sectional area of the column.

The rate at which the foam or froth rises is also an important parameter. The froth height in the column is recorded visually or electronically with time and can be fitted by an exponential model of the foam or froth:

$$H(t) = H_{max}\left(1 - e^{-t/\tau}\right) \quad \text{.....Eqn 2.3}$$

Where τ is the characteristic average bubble lifetime. H_{max} can be measured accurately from the column with time or inferred from the data taken from the rise period in which the H_{max} and τ are fitted (Figure 2.7).

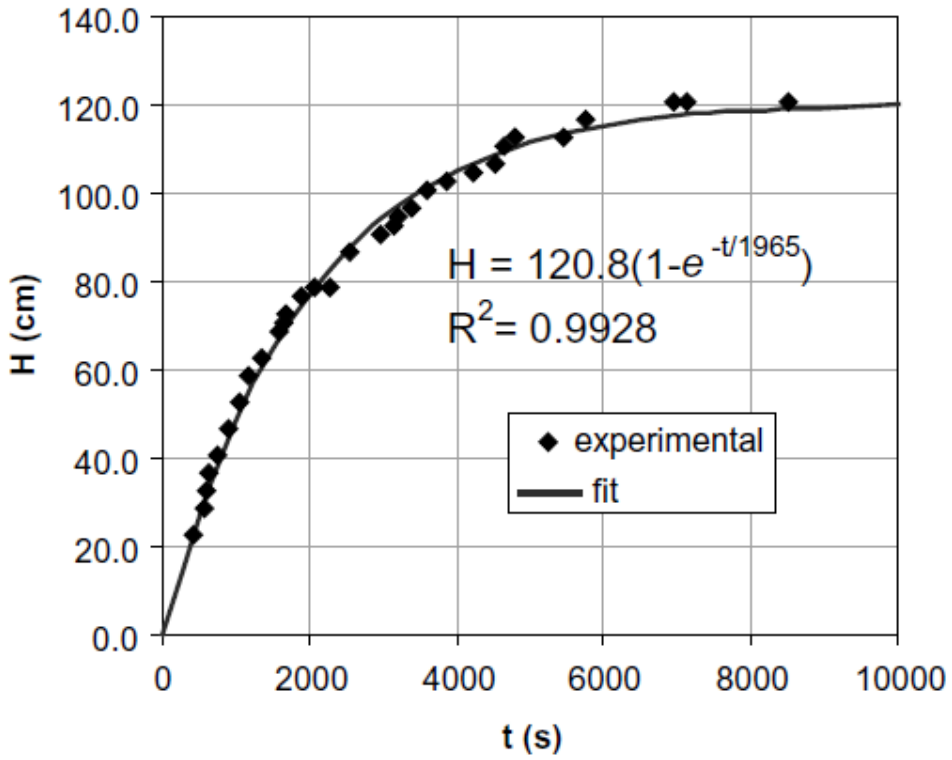

Figure 2.7: Typical variation of froth height with time in an industrial flotation cell (Barbian et al., 2005).

2.4 The pulp phase

The pulp phase significance stems from the fact that it is a phase where the whole flotation process is initialised. It is a necessity to apply conditions, both physical and chemical, that will create an environment that allows for successful flotation recoveries of valuable minerals. Conditions such as the correct impeller speed should be applied to provide enough turbulence that will allow for the successful collision of particles and bubbles which eventually will assist in the attachment of the valuable particles to bubbles and their subsequent transport to the froth phase (Wills and Napier-Munn, 2006). Air is also necessary as it allows for the formation of bubbles that will carry mineral laden bubbles to the froth phase. On the chemical aspect, reagents such as depressants, activators, collectors, frothers and modifiers have to be added adequately, to aid in the selective flotation of the valuable minerals.

2.5 Flotation reagents

As indicated earlier in this chapter in Figure 2.2, chemistry components include flotation reagents that are added to the pulp phase in order to modify the mineral/bubble surface, thereby imparting differences in mineral hydrophobicity to facilitate the separation of valuable mineral from gangue material. The reagents are classified as collectors, frothers, activators, depressants and modifying reagents and are discussed below.

2.5.1 Frothers

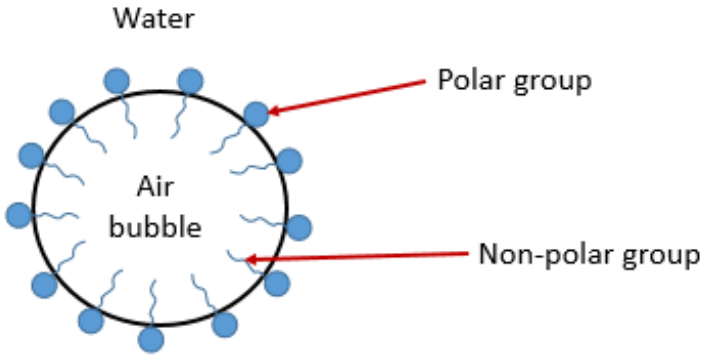

Figure 2.8: Action of a frother.

Frothers are heteropolar organic surfactants that create a reasonably stable froth to allow for selective drainage of entrained gangue from the froth thus increasing the kinetics of flotation (Ramachandra Rao, 2004, Wills and Napier-Munn, 2006). Their heteropolar structure allows them to be adsorbed on the air-water interface (Figure 2.8) (Finch et al., 2008). When the pulp is sufficiently aerated, the hydrophobic mineral particles attach onto the air bubbles after-which they are buoyed to the froth phase, where the valuable mineral is recovered. A good frother is considered to have negligible collecting power and should produce reasonable froth that is stable enough to allow for the transfer of a floated mineral from a cell surface to a collecting launder (Wills and Napier-Munn, 2006). Furthermore good frothers have been reported to have branched hydrocarbon radicals and form loosely packed gaseous films at the air-water interface (Laskowski, 1993). Solubility in water is another important aspect when considering good frothers, as this allows them to be evenly distributed in an aqueous solution and further allows for their surface active properties to be fully effective (Wills and

Napier-Munn, 2006). Alcohols (Figure 2.9), are an example of good frothers that are widely used, particularly Methyl Isobutyl Carbinol (MIBC) or 4-methyl-2-pentanol, a branched chain aliphatic alcohol or water-soluble based polymers based on propylene oxide (PO) such as polypropylene glycols (Kawatra and Eisele, 2014).

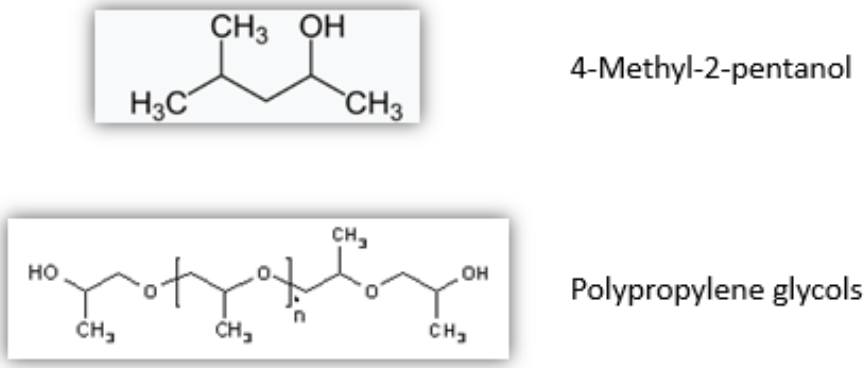

Figure 2.9: Examples of effective frothers.

2.5.2 Activators

Activators are referred to as chemical compounds that alter the chemical nature of a mineral surface to promote its interaction with a collector (Ramachandra Rao, 2004, Bulatovic, 2007). Activators are usually soluble salts which ionise in water to react with the mineral surface (Wills and Napier-Munn, 2006). Prior to the addition of the activator in the flotation process, adequate conditioning time is required to allow the activator to interact with the mineral surface. Copper sulphate has been reported in literature as a good activator in the flotation of sulphide minerals (Finkelstein, 1997). It reacts on the surface of sphalerite to improve collector adsorption and consequently increase its floatability, due to the formation of copper sulphide (Equation 2.4). The copper sulphide formed on the sphalerite surface readily reacts with a xanthate collector to form an insoluble copper xanthate, rendering the sphalerite surface hydrophobic (Wills and Napier-Munn, 2006).

$$ZnS + Cu^{2+} \leftrightarrow CuS + Zn^{2+} \quad \text{Eqn 2.4}$$

2.5.3 Depressants

Depressants are chemical compounds that alter the mineral surface to supress the action of a collector (Ramachandra Rao, 2004). They are used to depress the flotation of the unwanted mineral to allow for selective flotation of the wanted mineral. A reagent may act as a depressant by removing collector coatings from the mineral surface making it hydrophilic and non-flotable (Bulatovic, 2007). Beyond a certain threshold level, sodium sulphide replaces collector molecules from galena and sulphide mineral surfaces, resulting in the depression of these minerals. This shows that controlling the concentration levels of these chemical compounds is an important aspect in flotation of minerals. Regardless of the ability of depressants to react with collectors, they may adsorb on a mineral surface, thus preventing the collector from interacting with the mineral surface thereby rendering the mineral surface hydrophilic (Bulatovic, 2007).

2.5.4 Collectors

Collectors are surfactants that selectively adsorb on the valuable mineral surface to impart hydrophobicity (Ramachandra Rao, 2004, Wills and Napier-Munn, 2006, Kawatra and Eisele, 2014). Adsorption of collectors on the mineral surface sites may be due to chemical, electrical or physical attraction forces between polar regions of the collector and the selective sites on the mineral surface (Ramachandra Rao, 2004, Wills and Napier-Munn, 2006). The non-polar regions protrude into the bulk solution rendering the mineral surface hydrophobic (Figure 2.10). Collectors are introduced into the pulp phase and time is allowed for adsorption onto the mineral surface during agitation in what is referred to as the conditioning period (Wills and Napier-Munn, 2006). They form a thin film of non-polar hydrophobic hydrocarbons on the mineral surface thereby destabilising the hydrated layer which separates the mineral surface from the air bubble to a point where attachment of the mineral particle to the bubble is made possible. Collectors are usually used in small quantities that can form a monolayer on the mineral surface. Large quantities and high concentrations have an adverse effect on the recovery of valuable minerals, due to formation of multilayers which may reduce the proportion of hydrocarbon radicals (Wills and Napier-Munn, 2006). They may be classified as non-ionic or ionic. The latter can be further classified according to the ion (whether cation or

anion) that produces a water repellent effect in water (Bulatovic, 2007). A summary of collector classification is shown in Figure 2.11.

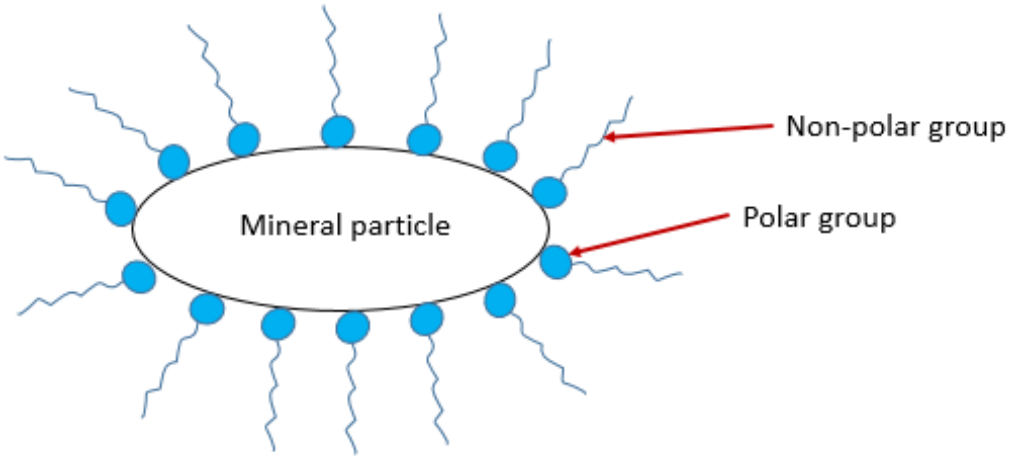

Figure 2.10: Adsorption of collector on mineral surface.

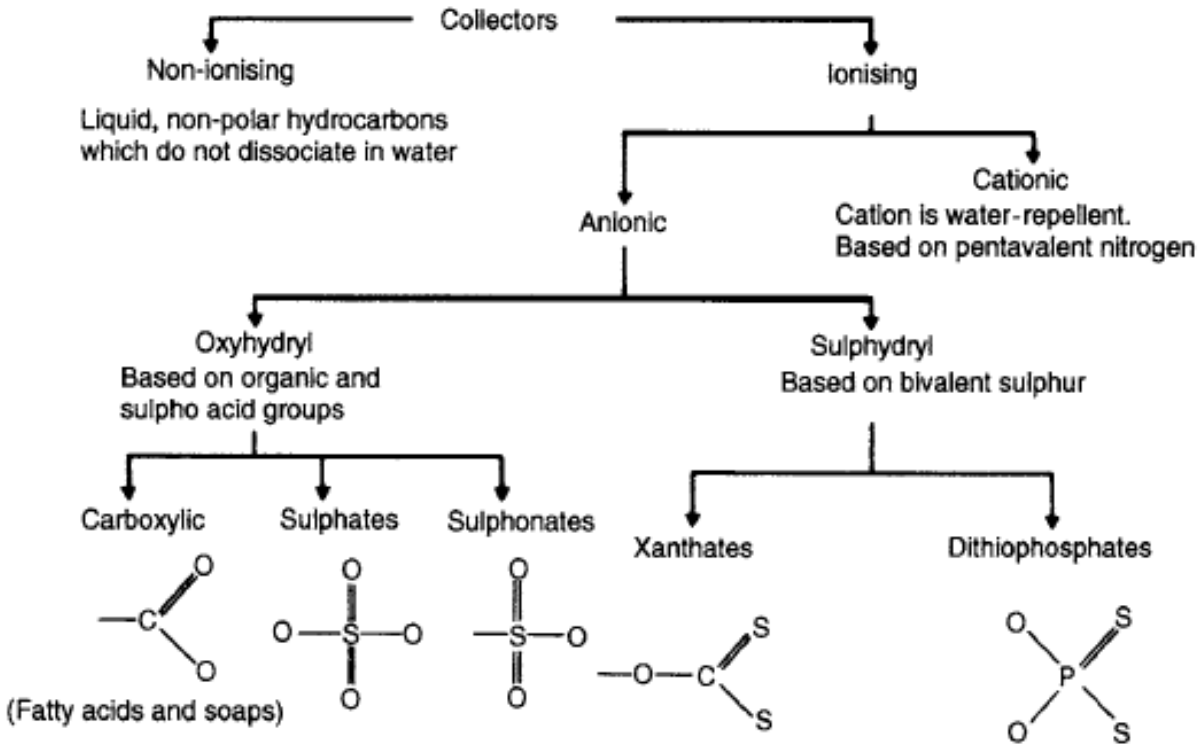

Figure 2.11: Classification of collectors after Glembotskii et al., 1972, adapted from Wills & Munn (2006).

Non-ionic collectors such as hydrocarbon fuel oils and kerosene are used to float surfaces that are partially hydrophobic such as coal, molybdenite, elemental sulphur and talc (Kawatra and Eisele, 2014). These improve hydrophobicity of valuable minerals by selectively attaching onto the particle surfaces. Their advantages extend from low-cost to good surface coverage on the valuable mineral surfaces (Kawatra and Eisele, 2014).

Cationic collectors use the amine group and positively charged pentavalent nitrogen to adsorb onto the negatively charged mineral surface sites. The adsorption is considered to be due to electrostatic forces. This type of attraction is regarded to be weak or irreversible, hence cationic collectors are weak in their collecting power. The anionic part (usually halides) does not take part in the reaction with minerals. Cationic collectors are most commonly used in the flotation of silicates and certain rare-metal oxides (Wills and Napier-Munn, 2006).

Unlike cationic collectors, anionic collectors use negatively charged polar groups to adsorb onto the positively charged mineral surface sites. These are usually weak acids or acid salts that ionise in water to produce a negatively charged end that will selectively attach onto the mineral surface (Kawatra and Eisele, 2014). They are the most commonly used collectors in mineral flotation and are sub-divided into oxyhydryl and sulphydryl collectors according to their polar group structure. Oxyhydryl collectors are organic acids or soaps that have organic and sulpho-acid anionic polar groups. Sulphydryl collectors have the polar group comprising of bivalent sulphur (thio compounds) and are widely used compared to the oxyhydryl collectors. Examples of sulphydryl collectors are xanthates and dithiophosphates, which have been used in the effective flotation of sulphide minerals (Langa et al., 2014).

Xanthates adsorb onto the mineral surface by chemical forces resulting in the formation of insoluble metal xanthates which are considered hydrophobic (Wills and Napier-Munn, 2006). Hydrophobic entities such as the adsorbed xanthate on mineral surfaces and formation of dixanthogen have also been reported in literature (Allison et al., 1972, Kocabag and Guler, 2008). Xanthates attach to the mineral surfaces by chemical forces using the $OCSS^-$ thiol group. Typical examples of the most widely used xanthates are sodium ethyl xanthate (SEX), sodium normal propyl xanthate (SNPX), sodium isobutyl xanthate (SIBX) and potassium amyl xanthate (PAX) - Figure 2.12.

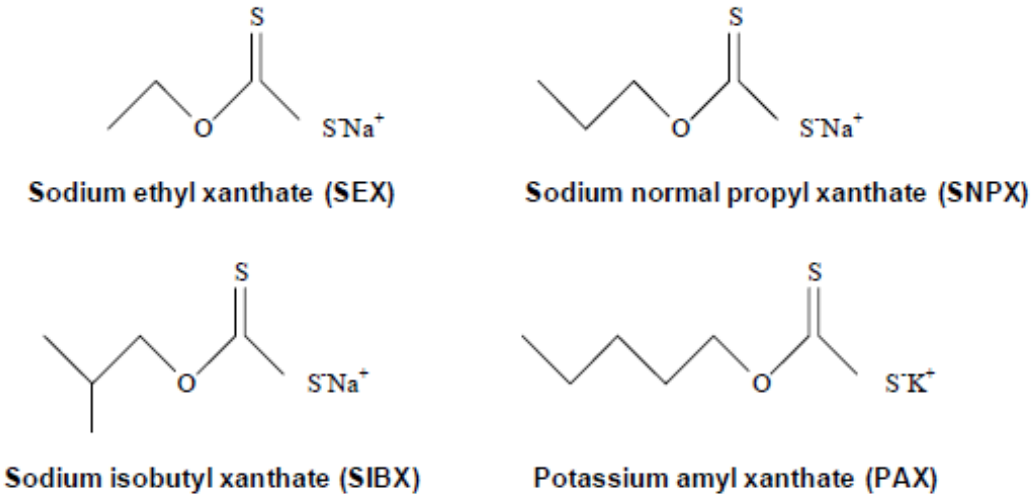

Figure 2.12: Widely used xanthate collectors.

Dithiophosphates (Figure 2.13) have a pentavalent phosphorus polar group which is the anion that attaches to the mineral surface (Wills and Napier-Munn, 2006). The cationic group, like other anionic collectors, does not take part in the reaction with the mineral surface. They can be used on their own or in combination with xanthates in the recovery of sulphide minerals, precious minerals and platinum group of metals (Bulatovic, 2007).

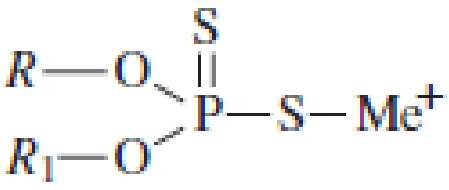

Figure 2.13: Typical structure of Dithiophosphates, adapted from Bulatovic (2007).

2.5.5 Mechanisms of mineral/collector interaction

The mechanisms of attachment of thiol collectors with sulphide minerals have been debated since the middle of the 20th century. Taggart et al, (1930) proposed the formation of metal thiols which did not fit thermodynamics, Wark & Cox (1934) and Gaudin (1939) proposed adsorption of thiols which did not fit the stability criteria and Cook & Nixon (1950) proposed the adsorption of ions which did not fit charge requirements (Woods, 2010). After carrying out some electrochemical research on corrosion science, Nixon (1957) reconciled the three eminent theories by an electrochemical approach. He proposed that the interaction of thiol

collectors with sulphide minerals is electrochemical in nature. He concluded that this approach can be best explained by a mixed potential mechanism in which an anodic oxidation reaction of the thiol collector transfers electrons to the mineral surface and a cathodic reduction reaction of oxygen returns the charge back to the solution (Woods, 2010). Moreover, oxygen has been determined to play a crucial role in the removal of the charged species formed on mineral surfaces (Cook and Nixon, 1949). Therefore, the interaction of thiol collectors on mineral surfaces has been proposed in literature to undergo three mechanisms, which shall be reviewed below.

2.5.5.1 Collector adsorption

The first mechanism is the adsorption of a collector on a mineral surface through a chemisorption reaction (Buckley and Woods, 1994), which involves the formation of chemical bonds between the collector molecules and the metal atoms on the mineral surface. Woods (2010) illustrated how sulphur molecules from the xanthate collector can be equally bonded to the lead atoms (Figure 2.14). Chemisorption has been highlighted to be the initial step that is thermodynamically favoured in the interaction of thiol collectors with sulphide mineral surfaces (Buckley and Woods, 1997). The mechanism has been identified in literature through the use of Spectroelectro-chemical studies in combination with some complementary techniques such as Ultraviolet-visible spectroscopy amongst other techniques (Buckley et al., 2003).

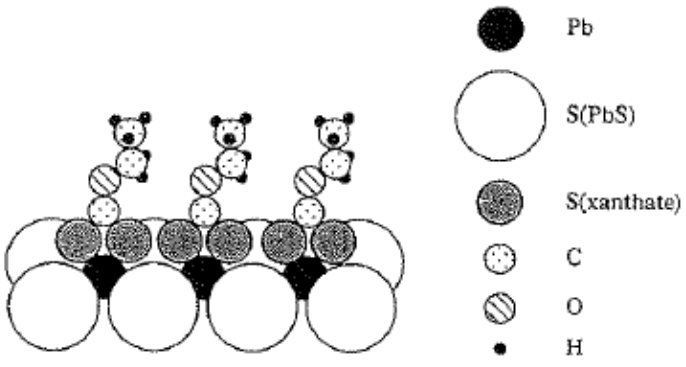

Figure 2.14: Schematic diagram representing the chemisorption of xanthate molecules onto a galena surface (Woods, 2010).

The electrochemical approach involves collector adsorption as the anodic reaction and a simultaneous cathodic oxygen reduction (Figure 2.16 (a)), with the mineral surface acting as a surface for electron transfer (Woods, 1971).

It has been indicated in literature that for chemisorption to be viable, a pre-oxidised mineral surface is an essential prerequisite, in which dissolved oxygen in an aqueous solution alone is insufficient to provide the extent of surface oxidation required for the chemisorption reaction (Page and Hazell, 1989). This inference was in contradiction to an investigation where similar techniques of X-ray photoelectron spectroscopic (XPS) and electrochemical studies were used and it was reported that the chemisorption reaction of xanthate on galena is possible in the presence of air (Buckley and Woods, 1990) . Xanthate was further determined to be adsorbed and desorbed repeatedly on a galena surface within a potential range of -0.47 and 0.2 V in voltammetry studies. It was substantiated that xanthate is adsorbed in three forms, firstly a specifically adsorbed ion that does not render the galena surface hydrophobic, secondly a chemisorbed radical that renders the mineral surface slightly hydrophobic and lastly physical adsorption of dixanthogen which renders the mineral strongly hydrophobic (Woods, 1971). In a chalcocite system, chemisorption was said to occur at a potential that is 30 mV below the potential at which the copper xanthate species is formed. Chemisorption has been widely studied and experimentally identified on various mineral sulphide systems and still remains one of the mechanisms that is believed to occur in thiol collector interaction with sulphide mineral surfaces (Woods et al., 1990, Buckley and Woods, 1994, Buckley and Woods, 1997). Assuming adsorption occurs under Temkin adsorption conditions, the rate of the forward reaction is as denoted in equation (Equation 2.5).

$$i_1 = Fk_1C(1-\theta)\exp\left(\frac{\beta FE}{RT}\right)\exp(-\alpha f\theta) \quad \text{Eqn 2.5}$$

Where k_1 is the rate constant, C is the xanthate concentration at the electrode, β is a transfer coefficient, E is the electrode potential, α is a symmetry factor, f is a constant, θ is the coverage of adsorbed intermediate and the other terms have their usual significance.

2.5.5.2 Formation of metal thiolate

The second mechanism of thiol collector interaction with sulphide minerals involves the formation of a metal thiolate species. This mechanism can occur as a single step (Figure 2.16(b)) or as a two-step process which involves surface oxidation (Figure 2.16(c)) and through ion exchange (Figure 2.16(d)). At higher pH conditions and lower xanthate concentrations, copper-xanthate species that formed on a mineral surface were reported to be unstable due to hydrolysis which resulted in the formation of Cu_2O and X^- as indicated in Figure 2.15 (Woods et al., 1990).

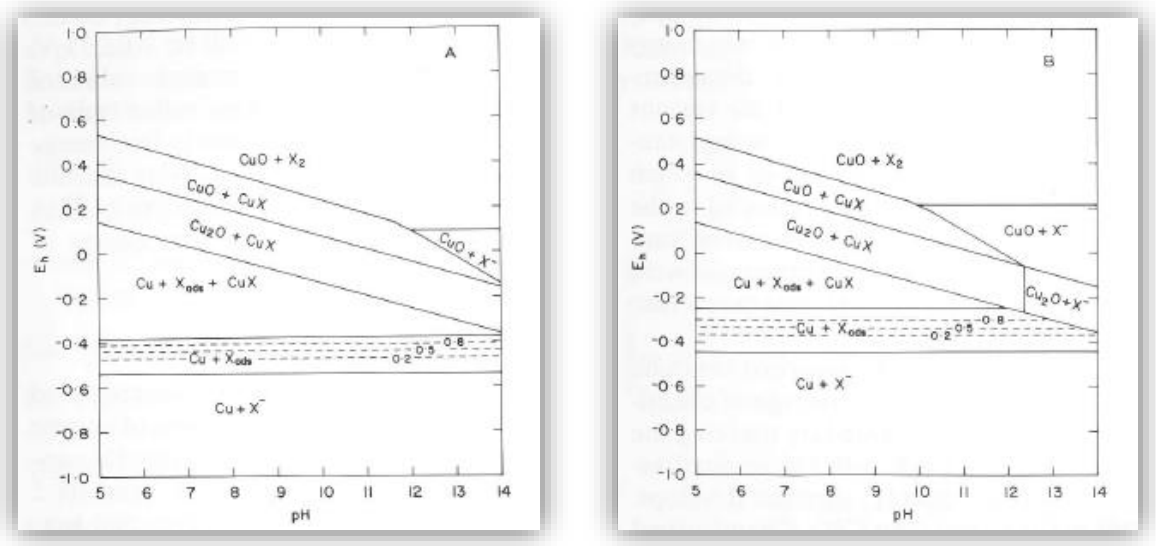

Figure 2.15: Eh-pH diagrams for the copper/water/ethyl xanthate system for an initial xanthate concentration of (A)-10^{-3} M, (B)-10^{-5} M. The dashed lines indicate the fractional surface coverages (Woods, et al., 1990).

It was reported that the interaction of xanthates with a galena surface at high potentials gives rise to the formation of a lead xanthate species, from which the chemisorbed xanthate is considered to be the precursor. At lower potentials, lead xanthate is converted back to lead metal (Buckley and Woods, 1994). XPS (X-ray photoelectron spectroscopy) studies on the interaction of potassium ethyl xanthate on galena revealed that multilayers of lead xanthate can form on a mineral surface, as this was indicated by S (2p) spectra that were determined to be relatively intense (Woods et al., 1990).

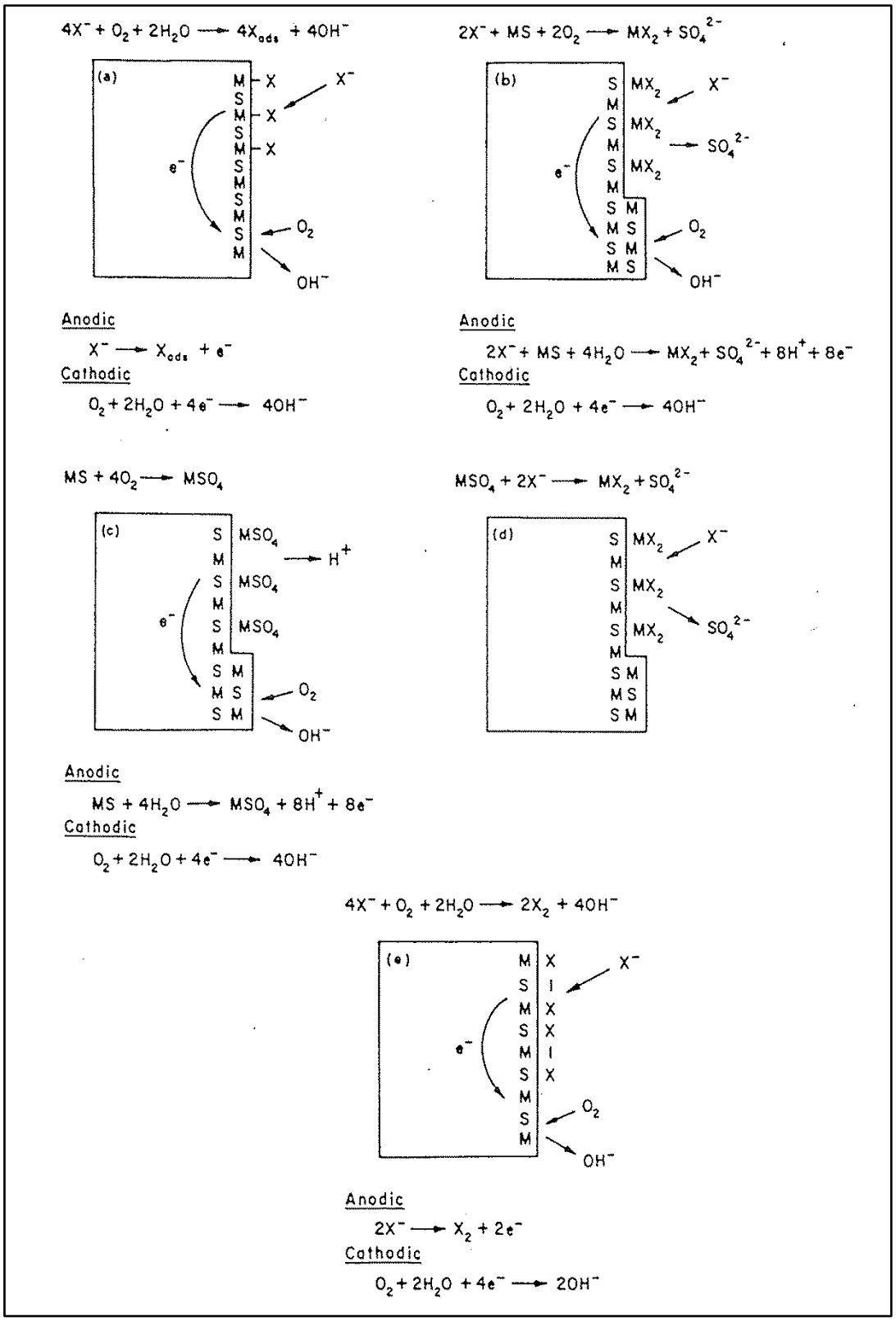

Figure 2.16: Schematic diagram of the mixed potential mechanisms of thiol collectors (X^-) with sulphide minerals in which the anodic process is (a) chemisorption; (b) reaction to form a metal collector compound; (c & d) the reaction in (b) occurring in two stages-(c) oxidation of the mineral and (d) ion exchange with the collector; and (e) formation of the dithiolate (Woods, 2010).

2.5.5.3 Formation of dithiolate

The anodic oxidation of thiol collectors has been reported to form a dithiolate, which has been successfully determined to be the most hydrophobic species that forms on sulphide mineral surfaces (Figure 2.16-(e)). Woods (1971) found that diethyl dixanthogen forms a physically adsorbed layer on the mineral surface which is insoluble and thus is equivalent to a separate dixanthogen phase which could adhere to an electrode surface. Though dixanthogen is said to physically adsorb on sulphide mineral surfaces, of all other mechanisms reported, this mechanism renders the mineral strongly hydrophobic (Woods, 1971). Electrochemical studies have shown that dixanthogen can only form above the equilibrium potential of the xanthate-dixanthogen couple (Vermaak et al., 2004). The formation of the dixanthogen species was proposed to first proceed via a chemisorption step, after-which the multilayers of dixanthogen formed, bind to the chemisorbed monolayer by the interaction of the hydrocarbon parts of the molecule (Woods and Gardner, 1974).

2.5.5.4 The mixed potential theory

For the overall reactions in Figure 2.16 to occur, there should exist a mixed potential/rest potential, at which the anodic oxidation reactions which involve the formation of dixanthogen and the metal thiolate and the cathodic reduction of oxygen/oxidising reagents, proceed at finite rates (Hu et al., 2009). The mixed potential mechanism was accepted in the 1980's after it had been demonstrated that flotation recoveries were indeed a function of potential. Potential is said to be mixed potential when there are two or more electrochemical reactions taking place on a homogenous surface. The mixed potential theory assumes that at open circuit potential, the potential measured is as a result of the sum of rates of oxidation reactions matching the sum of rates of reduction reactions (Tadie, 2015).

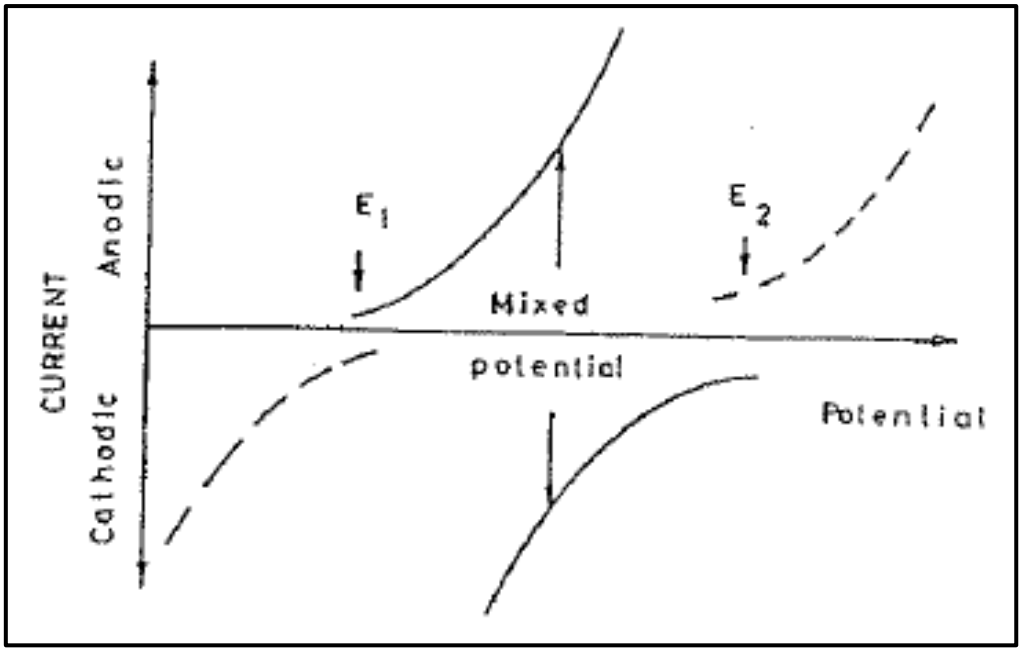

Figure 2.17: Schematic diagram showing current-potential curves with reversible potentials of two redox couples and their mixed potential (Woods, 2010).

As illustrated in Figure 2.17, the mixed potential occurs when the oxidation and the reduction reactions proceed at finite rates and give equal and opposite currents such that the net charge transfer is zero.

The information obtained from the mixed potential of a system helps to determine the type of reactions taking place on a mineral surface. Allison et al. (1972) demonstrated the type of reactions and species formed on various mineral surfaces at specific rest potentials (Table 2.1). The authors concluded that the minerals on which the dixanthogen species is formed as a major reaction product, must have rest potentials that are anodic to the equilibrium potential of the dixanthogen/xanthate couple, and those minerals on which the metal xanthate was formed, must have rest potentials below the equilibrium potential of the dixanthogen/xanthate couple. Though covellite had a rest potential that was below the equilibrium potential of the dixanthogen/xanthate couple, it indicated the presence of dixanthogen on its surface, this behaviour was simply related to the decomposition of cupric xanthate (Allison et al., 1972).

Table 2.1: Rest Potential values for different minerals and the respective species formed on mineral surfaces in a potassium ethyl xanthate concentration of $6.24x10^{-4}$ M at a pH of 7. Equilibrium potential of the dixanthogen/xanthate couple= 0.13 V (Allison et al., 1972).

Mineral	Species formed on mineral surface	Rest Potential after 10 minutes vs NHE
Arsenopyrite	X_2	+0.22
Pyrite	X_2	+0.22
Pyrrhotite	X_2	+0.21
Molybdenite	X_2	+0.16
Alabandite	X_2	+0.15
Chalcopyrite	X_2	+0.14
Bornite	MX	+0.06
Galena	MX	+0.06
Covellite	X_2	+0.05

Their study was of paramount significance as it shows that either dixanthogen or a metal xanthate is formed on mineral surfaces, and not a mixture of the two species. Rest potential measurements obtained were complemented by Spectrophotometric methods.

2.5.6 Potential (Eh) modifiers

Modifying agents also known as modulating or regulating agents are regarded as the most important chemicals used in mineral processing. They are known to control the interaction of collectors with mineral surfaces by intensifying or reducing its water repellent effect on the mineral surface (Wills and Napier-Munn, 2006, Bulatovic, 2007). Redox potential (Eh) modifiers are an important group of chemical compounds that are gaining popularity in electrochemically controlled flotation of sulphide minerals (Hu et al., 2009). The addition of Eh modifiers establishes a redox/pulp potential that might or might not promote the flotation of valuable minerals. Examples of Eh modifiers that have been reported in literature include sodium hypochlorite (Senior et al., 2009, Chimonyo et al., 2017), hydrogen peroxide (Goktepe, 2010, Sasaki et al., 2010), sodium hydrosulphide (Goktepe, 2010), sodium

dithionite (Kocabag and Guler, 2007), potassium permanganate (Razmjouee et al., 2012), potassium dichromate (Kocabag and Guler, 2008), just to mention but a few.

2.5.6.1 The pulp potential

The pulp potential, also known as the redox potential (Eh) occurs at the mineral/liquid interface. It is an essential variable in determining flotation recoveries and can be measured by noble metal electrodes that can be inserted into the pulp phase. Pulp potential can be controlled by externally applying potential into the system or by chemically controlling the potential using redox reagents. Most studies have shown that flotation recoveries can successfully be improved by controlling pulp potential using redox reagents (Kocabag and Guler, 2008, Chimonyo et al., 2017). Therefore, potential can be used as a diagnostic tool for developing flotation strategies and for resolving flotation problems. However, pH has also been reported to also play an important role in the electrochemical control of sulphide flotation (Hu et al., 2009). It is believed that a relationship exists between Eh and pH.

The correlation between Eh and pH can be best represented on Pourbaix diagrams, also known as Eh-pH diagrams. These diagrams plot out possible equilibrium phases of an electrochemical system for different redox states of an element as a function of pH.

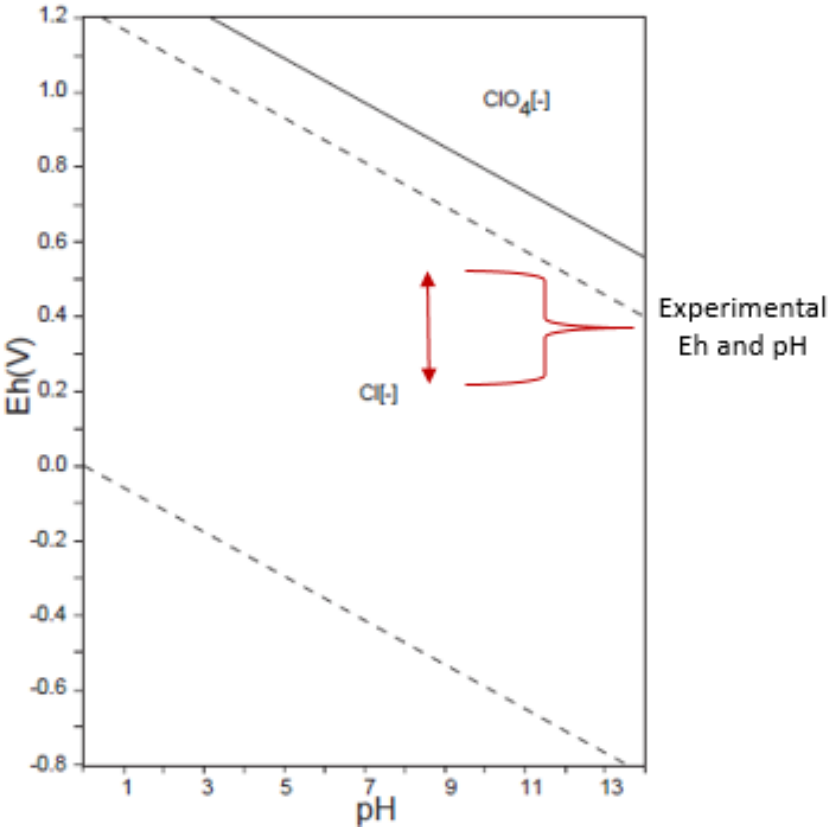

Figure 2.18: Pourbaix diagram for a NaClO system.

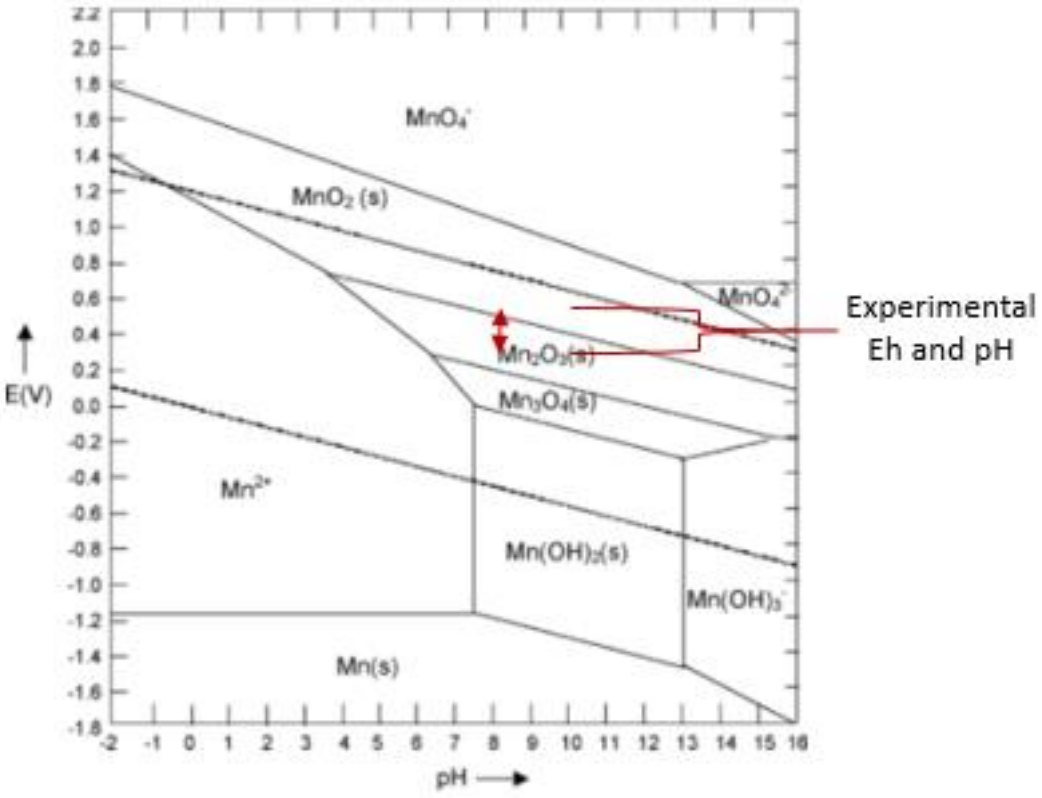

Figure 2.19: Pourbaix diagram for a $KMnO_4$ system.

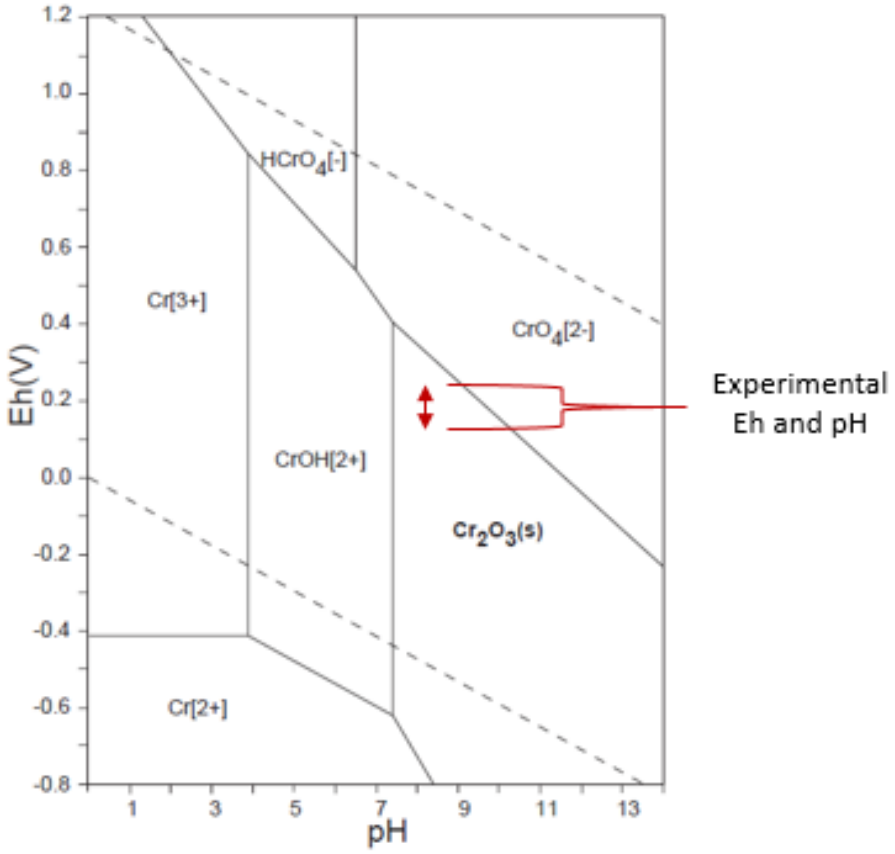

Figure 2.20: Pourbaix diagram for a $K_2Cr_2O_7$ system.

Figures 2.18-2.20 indicate the species formed for the NaClO, $KMnO_4$ and $K_2Cr_2O_7$ systems respectively, as a function of the Eh and pH of the solution. The primary ion boundaries are represented by lines as shown in Figures 2.18-2.20 above. Each diagram represents the stable phases formed for each respective system. The marked regions on each diagram shows the operational Eh and pH regions for the current work and shall be referred to in the discussion chapter.

2.5.6.2 Flotation recovery as a function of potential control

Hydrogen peroxide (H_2O_2) and dithionite have been used to adjust Eh during grinding of pyrite in a collectorless system (Peng et al., 2012). Peng et al., (2012), varied electrochemical potential from -185 mV, -10 mV to +260 mV and it was postulated that the more reducing the grinding condition was, the higher the pyrite recovery obtained. It was then inferred that the flotation of sulphide minerals is possible in mildly to moderately oxidizing conditions using hydrogen peroxide. Separation of chalcopyrite with pyrite was reported to be possible around a potential of 250 mV at a pH of 9.5, with 0.7 mg/l Potassium amyl xanthate (KAX), at which

the best potential range for floatability of both chalcopyrite and pyrite was reported to be within -100 to 200 mV (Figure 2.21). Higher dosages of hydrogen peroxide and sodium hydrogen sulphide were observed to have a drastic effect on mineral recoveries (Goktepe, 2010). Despite the fact that the importance of redox potential has been highlighted to be that of improving recoveries of valuable minerals, the work by Gőktepe (2010) has indicated how redox potentials may also be used in the separation of valuable minerals. The authors went further to note that minute quantities of the potential modifiers are required to enhance flotation of valuable minerals.

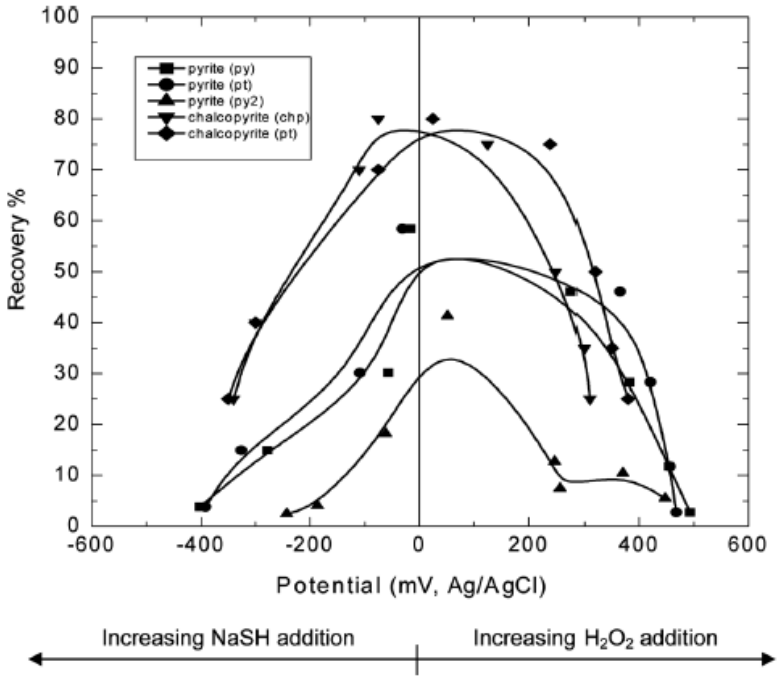

Figure 2.21: Potential vs recovery of chalcopyrite and pyrite in flotation, (chp) chalcopyrite electrode, (pt) platinum electrode, and (py) pyrite electrode, (py): flotations were performed at pH 6 and 2 mg/l Sodium iso-butyl xanthate (SIBX)., (py2): flotations were performed at same conditions with chalcopyrite flotation, pH 9.5 and 0.7 mg/l potassium amyl xanthate (KAX) (Goktepe, 2010).

With regards to the use of sodium hypochlorite (NaClO) as a potential modifier, Chimonyo et al. (2017) showed that very low concentrations of NaClO and H_2O_2 (0.001 M), which gave Eh values of 200-300 mV, significantly increased copper recoveries in the presence of a xanthate collector. NaClO and sodium dithionite ($Na_2S_2O_4$) were used to control pulp potential in an enargite system and it was found that potentials of +500 mV increased recoveries to 82% with potentials of +100 mV and – 400 mV reducing the mineral recoveries significantly to 52% and 11% respectively (Plackowski et al., 2014). The same system of redox reagents to that used

by Plackowski et al. (2014), was used to determine the flotation of gersdorffite and it was deduced that the mineral floated very well at potentials above -230 mV (Senior et al., 2009). Guo & Yen (2002) investigated the effect of applied potential using NaClO on chalcopyrite and reported good floatabilities within a potential range of -0.2 to 0.2 V at a pH of 10 and a potential range of -0.25 to 0.3 V at a pH of 7.

Studies on the effect of potassium permanganate on flotation recoveries are very limited and not much literature has been reported. Nevertheless, the effect of potassium permanganate on the floatability of chalcocite was investigated. Good floatabilities of 73% chalcocite were reported in moderately reducing conditions at which the Eh was -222 mV and in contrast lower recoveries of 18% were obtained by increasing the potential to 602 mV (Razmjouee et al., 2012). Potassium permanganate was surmised to have a depressing effect on sulphide minerals such as sphalerite, pyrrhotite and chalcopyrite (Bulatovic, 2007). The questions that would arise are to what extent does the potassium permanganate affect the sulphide minerals and what is the threshold level? Tajadod (1997) investigated the effect of $KMnO_4$ on chalcopyrite with 20 mg/l potassium amyl xanthate and found that copper recoveries were maintained between 78-81% for a concentration of 0.1-10 mg/l $KMnO_4$. The author reported the threshold level to be 10mg/l and further reported recoveries of 39% at 100mg/l $KMnO_4$. However, the author did not report on how the copper grades were affected and their work does not fall under published literature. The low recoveries in their study were therefore assigned to the strong depressing effect of the manganese oxides that could have formed on the chalcopyrite surface (Tajadod, 1997).

Similar to potassium permanganate, very limited literature has been reported on the effect of potassium dichromate ($K_2Cr_2O_7$) on sulphide mineral flotation. $K_2Cr_2O_7$ has been used in selective sulphide flotation, in the separation of galena and chalcopyrite. The $Cr_2O_7^{2-}$ ion was reported to have a depressing effect on galena due to the formation of lead chromate and chromic hydroxide and alternatively induced flotation of chalcopyrite in the anodic potentials as this was surmised to the formation of oxidation products of the mineral that formed on the mineral surface (Kocabag and Guler, 2008). Earlier in their study Kocabag & Guler (2007) reported good flotation recoveries of chalcopyrite to be between 65%-70% at an Eh of 400

mV with potassium dichromate. The authors highlighted that at high pH values of 6-12, the potential induced by $K_2Cr_2O_7$ did not have an effect on the flotation of chalcopyrite.

2.6 Electrochemical measurements

Various electrochemical techniques have been used to study the species formed on mineral surfaces after their interaction with thiol collectors. The techniques provide useful information on the oxidising/ reducing characteristics of sulphide minerals in particular (Khan and Kelebek, 2004). These techniques amongst others include rest potential measurements and cyclic voltammetry measurements (Khan and Kelebek, 2004, Ekmekci et al., 2010). Both techniques will be reviewed with the former technique being the focus of our study. Ultra-violet visible spectroscopy, surface-enhanced Raman scattering, Fourier transform infrared and electron spectroscopic studies provide complementary information on the nature of adsorbed species on the mineral surface (Buckley and Woods, 1997, Vermaak et al., 2005). The complementary techniques are not used in our investigation, therefore they are not included within the scope of this review.

2.6.1 Cyclic voltammetry

Cyclic voltammetry also known as the sweep reversal method is one of the most powerful electrochemical techniques used to study the interaction of collectors with mineral surfaces. The potential of an electrode is controlled via a potentiostat, scanned linearly in time traversing regions (or at the switching potential) in which no reaction occurs to the regions where the adsorption of collectors occurs (Woods, 2010). In this technique, the potential is reversed at a certain value and the scan in the opposite direction allowing electrochemical reactions of products formed on initial scan to be examined (Woods, 2010). The current flowing through the electrode is then recorded. The area under voltametric peaks is the charge passed in the electrochemical process, consequently when the electrochemical process is adsorption, the area under the peaks is an indication of a measure of surface coverage of the xanthate collector on the galena mineral surface (Woods, 2010).

A typical example of the application of cyclic voltammetry is used in the investigation of the interaction of ethyl xanthate with a galena surface as shown in Figure 2.22 (Woods, 1971). The initial scan began at -0.5 V against standard hydrogen electrode (SHE). An anodic peak was observed at 0 V, which was assigned to the chemisorption of a monolayer of ethyl xanthate on the galena surface. An increase in the anodic peak, was as a result of the oxidation reaction of ethyl xanthate to lead ethyl xanthate and diethyl dixanthogen. On the return scan, a cathodic peak at -0.3 V, was due to the reduction of the anodic oxidation products back to galena and ethyl xanthate. The author further complemented their findings with the XPS technique. Cyclic voltammetry investigations on the platinum, gold and copper surfaces were also carried out in the investigation. It was concluded that ethyl xanthate collector oxidised to diethyl dixanthogen on the mineral surfaces, and the oxidation proceeds through an adsorbed xanthate radical, in which the adsorption step obeys the Elovich adsorption kinetics. Chemisorption is indeed a thermodynamically favoured reaction in the interaction of thiols with sulphide minerals.

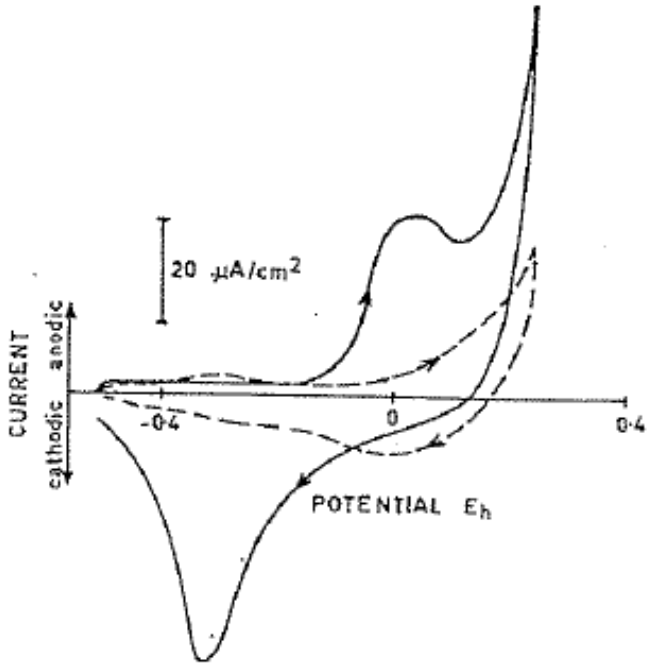

Figure 2.22: Voltammograms for a galena electrode in a 0.1 M borate solution at a temperature of 25^{0}C and a pH 9.2; triangular potential sweep at 10 mV s^{-1}; ethyl xanthate 9.5x10^{-3} M (solid line), 0 (dashed line) (Woods, 1971).

Cyclic voltammetry was also used to identify the species formed on a pyrrhotite surface in the presence of a xanthate collector. Ferric hydroxide and/or sulphur species such as elemental sulphur, polysulphide and sulphate were reported to form on a pyrrhotite surface in anodic potentials (Buswell and Nicol, 2002, Khan and Kelebek, 2004, Ekmekci et al., 2010) . Buswell & Nicol (2002) have highlighted one of the limitations in investigating the interaction of xanthate collectors on pyrrhotite surfaces as pyrrhotite oxidises at potentials at which the anodic adsorption of xanthate is expected.

In a Pd-Bi-Te system, the peaks formed in cyclic voltammetry were assigned to the oxidation of ethyl xanthate to diethyl dixanthogen and mineral oxidation and the cathodic peaks were assigned to reduction of dixanthogen and mineral oxidation. To which these findings were substantiated by the Raman Spectroscopy (Vermaak et al., 2005).

Cyclic voltammetry has proved to be a reliable method of investigating the interactions of thiol collectors with mineral surfaces.

2.6.2 Rest potential measurements

Rest potential also known as the open circuit potential or zero current potential is an important technique used to investigate the interactions of thiols with mineral surfaces. The potential measured is the mixed potential which shows the equilibrium between cathodic and anodic reactions (Ekmekci et al., 2010). Mixed potential mechanisms have been explored in a number of fields including corrosion of metals, cementation, hydrometallurgical processes, supergene alteration of sulphide ore bodies, spontaneous oxidation of sulphide minerals during transportation and storage (Woods, 2010).

Alison et al. (1972) carried out one of the first important investigations on an electrochemical approach in the identification of oxidised species that form on mineral surfaces in xanthate solutions using rest potential measurements. Their study showed the importance of applying rest potential measurements in electrochemical studies. Their study gave an insight on the characteristic species that form on mineral surfaces and their possible mechanisms. Most work that has been carried out afterwards has since confirmed their findings.

A standard rest potential measurement profile for a collectorless and a thiol-collector system has been summarised by Tadie (2015), as presented in Figure 2.23. In a collectorless system, the mixed potential results due to a balance of the oxygen- reduction reaction and mineral-oxidation reactions. A shift in the original rest potential is noted upon addition of a collector because of the interaction of the collector with the mineral surface. The mixed potential in a collector system is a balance of the oxygen-reduction reactions and the mineral and collector-oxidation reactions.

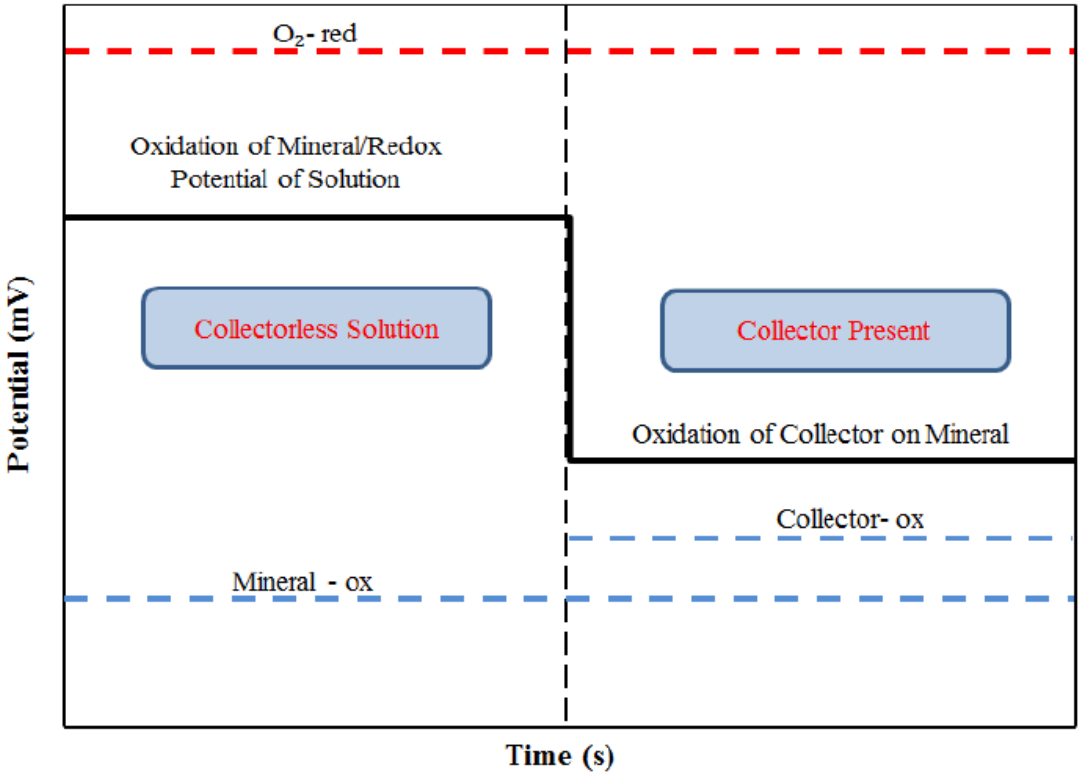

Figure 2.23: Standard rest potential measurement profile (Tadie, 2015).

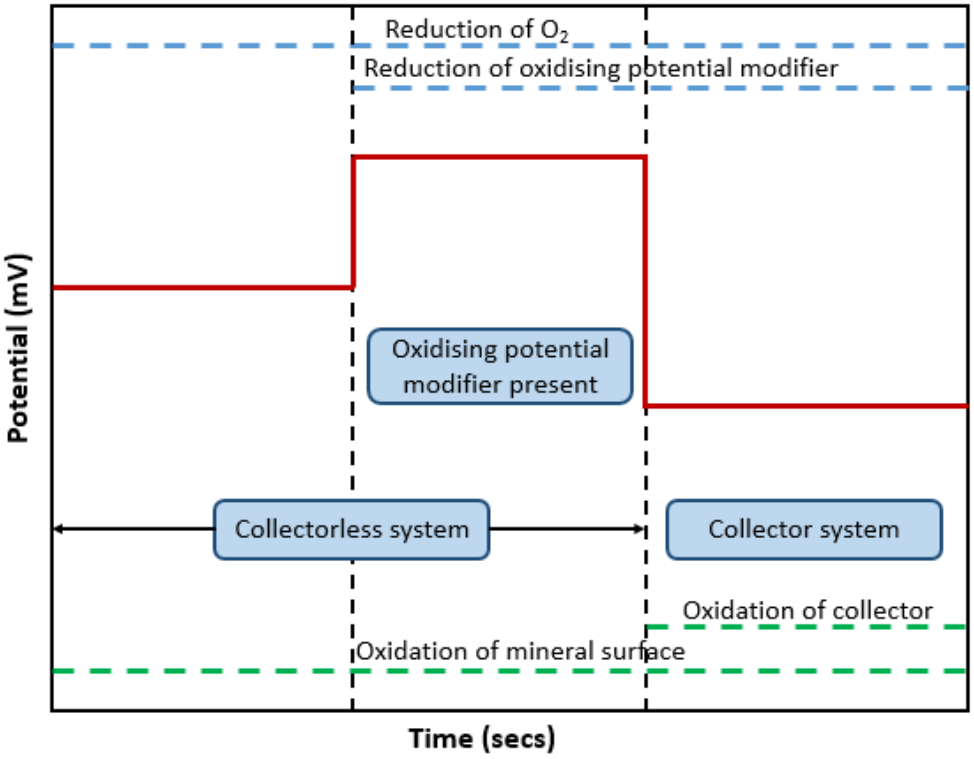

Figure 2.24: Standard rest potential measurement profile in the presence of an oxidising potential modifier (modified from Tadie, 2015).

Figure 2.24 shows a modified standard rest potential measurement profile with regards to the use of oxidising potential modifiers prior to the addition of a collector. The rest potential measurements with respect to Figure 2.24 are as a result of the oxidation and reduction reactions as shown in the diagram.

Rest potential measurements in a pyrrhotite, pentlandite system, were determined to be essential in the selective separation of pentlandite (Khan and Kelebek, 2004). It was observed that dixanthogen was formed on both mineral surfaces in oxygen-saturated conditions whereas in oxygen deficient conditions, pyrrhotite did not form dixanthogen on its surface because it had rest potentials that were below the equilibrium potential for dixanthogen formation. Furthermore in a pyrrhotite, pentlandite system in the presence of $2x10^{-3}$ M xanthate, the rest potential obtained for pentlandite was much lower than that obtained for pyrrhotite which indicated that xanthate adsorption was preferential on a pentlandite mineral surface than on a pyrrhotite surface (Bozkurt et al., 1998). The formation of the oxidised species as identified by rest potential measurements were complemented by Infra-red spectra. With regards to galvanic interactions, if two minerals are in contact, the mineral

with a more anodic rest potential becomes the cathode and the mineral with a cathodic rest potential becomes the anode. These interactions are common in a pentlandite and pyrrhotite system (Bozkurt et al., 1998).

Rest potential measurements have been extensively used to determine the range of potentials in which the flotation process should be carried out in order to improve floatability of the valuable mineral (Buswell and Nicol, 2002). The rest potentials measured by Buswell and Nicol (2002) were potentials in which ferric hydroxide, a hydrophilic species formed on a pyrrhotite surface, thus a potential below that of the formation of ferric hydroxide was recommended to allow for the anodic adsorption of xanthate on the mineral surface thus enhancing good floatability.

2.7 Mineralogy

The Kansanshi Copper Mine in Zambia is the largest copper mine in Africa and the eighth largest in the world. It is located approximately 10 kilometres north of Solwezi town and 180 kilometres to the northwest of the Copperbelt town of Chingola. Copper deposits within the Central African Copperbelt lie within the Neoproterozoic meta-sedimentary rocks of Katanga Super group (Figure 2.25). The Copperbelt stretches for approximately 800 kilometres along the Lufilian Arc that runs along the border of Zambia and the Democratic Republic of Congo (DRC) (Kampunzu et al., 2009). The Kansanshi mine is hosted within the Kundelungu group of the Katanga Supergroup (Broughton et al., 2002).

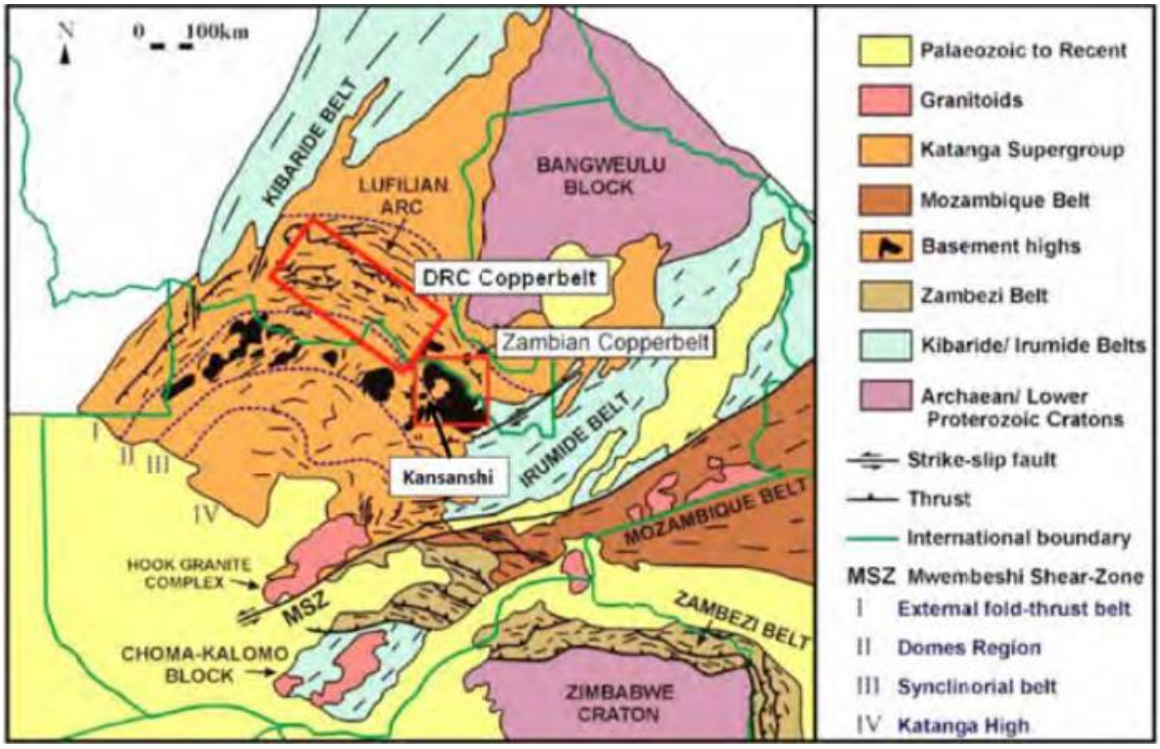

Figure 2.25: Regional geological map of the Central African Copperbelt, including structural geological features (modified from Porada & Berhorst, 2000). The DRC & Zambian Copperbelts are outlined by the red rectangles.

The ore from the Kansanshi deposit comprises of primary and secondary copper minerals (Table 2.2). These are further classified into three groups namely, sulphides, oxides and mixed ore. The sulphide ore is comprised mainly of coarse grained pyrite with chalcopyrite set in a matrix of quartz, feldspar and muscovite mica. The oxide ore is made up of chrysocolla with less malachite set in a matrix of quartz, iron oxides and iron hydroxides. The mixed ore is dominated by oxide, supergene oxide and hypogene sulphide copper. Each group type is either of high grade quality or low grade quality. The high grade copper sulphide was used for our study. The major sulphide mineral in the high grade copper ore was identified to be chalcopyrite at 3.9 % chalcopyrite with the low grade ore containing 1 % chalcopyrite (Kalichini, 2015). The major gangue materials in this deposit were identified as dolomite, calcite, quartz, pyrite and pyrrhotite (Broughton et al., 2002).

Table 2.2: Major copper bearing minerals in the Kansanshi deposit.

Mineral	Type	Formula	% Cu in mineral
Chalcopyrite	Primary sulphide	$CuFeS_2$	34.6
Bornite	Secondary sulphide	Cu_5FeS_4	63.3
Digenite	Secondary sulphide	Cu_9S_5	78.1
Chalcocite	Secondary sulphide	Cu_2S	79.9
Covellite	Secondary sulphide	CuS	66.5
Cuprite	Oxide	Cu_2O	88.8
Chrysocolla	Silicate	$\tilde{}Cu_4H_4Si_4O_{10}(OH)_8.nH_2O$	33.9
Malachite	Carbonate	$Cu_2(CO_3)(OH)_2$	57.5

At the Kansanshi mine, mineral processing of the ore types is carried out through either an oxide circuit or a sulphide and transitional ore mixed float circuit. Processing of the ore involves crushing, milling and flotation for recovery of the copper in the concentrate. The mine is currently optimizing copper recoveries by using the CPS (Controlled Potential Sulphidisation) method. Sulphidisation involves modification of mineral surfaces in order for them to resemble sulphide minerals to enhance flotation recoveries, thus it is of paramount importance to ensure correct dosages of sulphidising reagents, as under sulphidising would lead to poor mineral recoveries and over sulphidising would depress minerals.

2.8 Summary of literature

Our study seeks to evaluate the flotation performance of a copper sulphide ore by controlling potential with the aid of redox reagents. It is of importance to investigate how redox reagents would affect flotation recoveries as the CPS method used at the Kansanshi mine requires extreme care in using sulphidising agents, since under-sulphidising would lead to poor mineral recoveries and over-sulphidising would depress minerals. Other draw backs of CPS also include mineral surface tarnishing (Kalichini, 2015) and poor reproducibility at plant scale (Chadwick, 2011). Furthermore the use of redox reagents is advantageous in that it renders a more uniform electrochemical environment around mineral surfaces and redox reagents have been reported in literature as flotation reagents that have the potential to improve valuable mineral recoveries (Razmjouee et al., 2012, Plackowski et al., 2014). Gőktepe (2010) reported that redox reagents are required in minute amounts to improve recoveries of valuable minerals, thereby highlighting the economic benefit of using them in flotation studies.

Rest potential measurements are used in this study to predict reactions and the oxidising and reducing characteristics formed on a chalcopyrite surface as these measurements can be used as a reliable electrochemical technique that has been vastly used in literature.

Overall, though studies have been carried out to show how potential can be controlled by redox reagents, no literature has compared the effects of different types of potential modifiers at various amounts on the flotation performance of sulphide minerals. Moreover, no literature has reported on the interactions of potential modifiers with mineral surfaces in electrochemical studies. Thus, this study seeks to close this gap that has been created in literature.

3 Research Objectives

3.1 Objectives

The objectives of this study were:

1. To determine the effect of potential modifiers on copper recoveries and grades; and froth stability.
2. To determine the equilibrium potential of SIBX at $6.24x10^{-4}$ M.
3. To determine the electrochemical interactions of chalcopyrite with potential modifiers and SIBX.

3.2 Key Questions

The research questions developed from the study objectives were:

1. To what extent do potential modifiers affect:
    a. Froth stability?
    b. Copper recoveries and grades?
2. What is the equilibrium potential of SIBX at $6.24x10^{-4}$ M?
3. Does varying concentration of SIBX affect its equilibrium potential?
4. What is the effect of using potential modifiers on the rest potentials of chalcopyrite and the subsequent species forming on the mineral surface?
5. Is there a relationship between rest potentials and flotation recoveries?

3.3 Hypotheses

The following hypotheses were developed:

1. Assuming an equilibrium potential below 100 mV for SIBX, a redox potential range of 100 to 400 mV promotes good floatability of valuable minerals because:
    a. It triggers the oxidation of thiol collectors on the mineral surface, which results in the formation of the most hydrophobic species, dixanthogen.

b. A moderately stable froth is produced as a result of the formation of hydrophobic mineral particles which will enhance good mineral particle recoveries.

2. Redox potentials ≥500 mV may reduce floatability of valuable minerals due to the:
    a. Generation of an oxidation product film which increases the hydrophilicity of a mineral surface by reducing the binding force between dixanthogen and the mineral surface thereby reducing the adsorption amount of dixanthogen.
    b. Highly hydrophobic mineral particles formed which will increase the rate of bubble coalescence and bubble breakage or a very highly stable froth might form. Both conditions will result in the loss of the valuable minerals from the froth phase to the pulp phase.

4 Experimental methods

4.1 Introduction

This chapter describes the materials and methods used to test the hypotheses proposed in Chapter 3. Since potential modifiers are used to manipulate the potential at the mineral/liquid interface to enhance flotation of valuable minerals, tests were carried out to investigate the effect of NaClO, $KMnO_4$ & $K_2Cr_2O_7$ on the flotation of chalcopyrite. Test work considered both an ore and pure chalcopyrite in the absence and presence of potential modifiers with SIBX collector.

4.2 Ore Sampling and preparation

The ore used in this study was a high-grade copper sulphide obtained from Kansanshi Mine in Solwezi, Zambia. The ore was prepared at the Kansanshi Mine Metallurgical laboratory, after collection from a pit (Kalichini, 2015). One tonne of the ore was sun and air dried on stainless steel trays that are found on site. The ore was then crushed to -1 cm using a laboratory scale TM Engineering Terminator jaw crusher. Blending and splitting were carried out using a rotary riffle splitter. To ensure sufficient blending and splitting, each batch of crushed ore was brought to the splitter thrice. The representative samples were packaged in plastic bags with a mass of 1 kg per sample. These samples were then shipped to the Centre of Minerals Research (CMR) at the University of Cape Town (UCT).

4.3 Milling procedure

Milling within the CMR was conducted using an Eriez Magnetics MASCLAB belt driven stainless steel laboratory scale rod mill. The mill has an internal diameter of 200 mm and length of 297 mm (Figure 4.1). Twenty rods of three varying diameters were used as grinding media. Mill charge parameters are as shown in (Table 4.1).

Table 4.1: Mill charge parameters.

Diameter (mm)	Number of rods	Total charge weight (kg)
25	6	4.90
20	8	3.67
16	6	1.53
Total	**20**	**10.10**

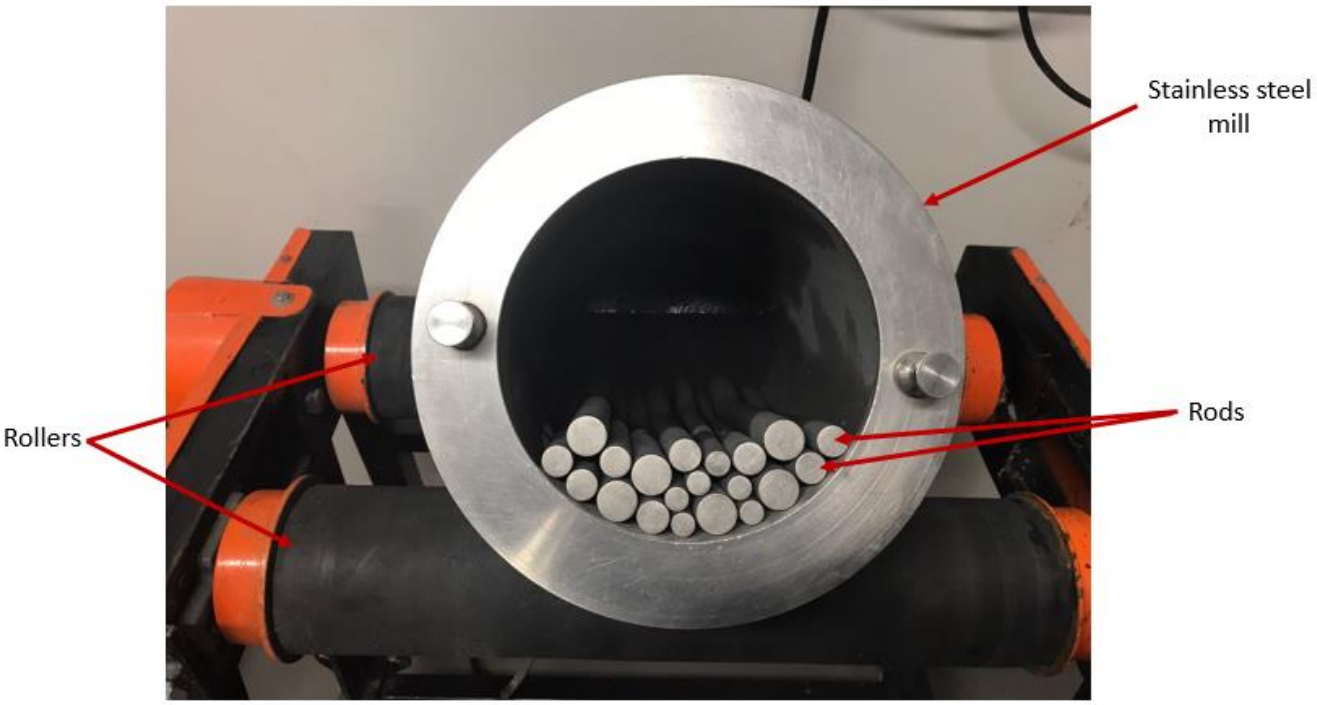

Figure 4.1: Eriez Magnetics MASCLAB stainless steel rod mill.

A 1 kg sample of the high-grade copper sulphide ore and 1 L of synthetic plant water (SPW) were charged into the mill and the mill was operated at 256 rpm, as determined by previous studies within the CMR. A grind of 80% passing 75 µm was used for all the batch flotation and froth stability tests, as this is the size used on site as well as widely used in literature (Ross and Van Deventer, 1985, Sasaki et al., 2010, Chimonyo et al., 2017). The grind size for this specific ore was attained by milling for 7 minutes and 12 seconds, as determined and experimentally confirmed by Kalichini (2015).

4.4 Water

All batch flotation and froth stability tests were conducted using synthetic plant water, where distilled water was modified with various chemical salts, to achieve a total dissolved solids (TDS) content of 1023 ppm (Wiese et al., 2005). The SPW was prepared according to the CMR standard procedure in 40 L batches and contained ionic concentrations as indicated in Table 4.2 below. The chemical salts were supplied by Merck in powder form.

Table 4.2: Ion concentrations of synthetic plant water.

Ion	**Ca^{2+}**	**Mg^{2+}**	**Na^{+}**	**Cl^{-}**	**SO_4^{2-}**	**NO_3^{-}**	**CO_3^{2-}**	**TDS**
Concentration (ppm)	80	70	153	287	240	176	17	**1023**

4.5 Reagents

All chemicals used in this study were of analytical grade and solutions were made up with distilled water.

The choice of potential modifying reagents used was based on the oxidising agents used in literature for copper sulphide minerals flotation (Goktepe, 2010, Razmjouee et al., 2012, Plackowski et al., 2014, Chimonyo, 2016). NaClO, $K_2Cr_2O_7$ and $KMnO_4$ were used as potential modifiers in all the tests. The potential modifiers were supplied by Kimix. $K_2Cr_2O_7$ and $KMnO_4$ were supplied as powders and NaClO was supplied as a stock solution of 12%. The potential modifiers were made up to solutions with $1x10^{-2}$, $1x10^{-3}$ and $1x10^{-4}$ mols using distilled water.

Flotation reagents were kept constant throughout the test work. SIBX, supplied by Senmin (Pty) Ltd, was used as the collector at a dosage of 100 g/t. A fresh 1% collector solution made up using distilled water was prepared prior to all the experimental runs. DOW 200, supplied by BetaChem, is a low molecular weight glycol based frother, which was used neat at a dosage of 40 g/t.

Di-sodium tetraborate decahydrate ($Na_2B_4O_7.10H_20$) was supplied by Sigma-Aldrich Co. and sodium sulphate (Na_2SO_4) was supplied by Associated Chemical Enterprises. These two salts

were dissolved with distilled water to concentrations of 0.05 M and 0.1 M, respectively, to achieve a pH of 9.4. The solution mixture was used as a buffer and an electrolyte for all electrochemical measurements.

4.6 Mineralogy

The copper sulphide ore was subjected to Powder X-Ray Diffraction (PXRD) for mineral phase analysis as shown in Table 4.3. Samples prepared for phase quantification were micronised in ethanol using a McCrone micronizer for homogeneous particle size distribution. PXRD spectra were obtained using a Bruker D8 Advance powder diffractometer with Vantec detector and fixed divergence and receiving slits with Co-Ka radiation. The phases were identified using Bruker Topas 4.1 software (Coelho, 2007) and the relative phase amounts (weight %) were estimated using the Rietveld method.

Table 4.3: PXRD characterisation of the high grade copper sulphide ore (Kalichini, 2015).

Mass (%)	**Minerals**
Major (>30%)	none
Moderate (10-30%)	calcite; muscovite; quartz; bytownite
Minor (2-10%)	chalcopyrite; chalcocite; kaolinite
Trace (<2%)	bornite; chlorite; malachite

4.7 Batch flotation tests

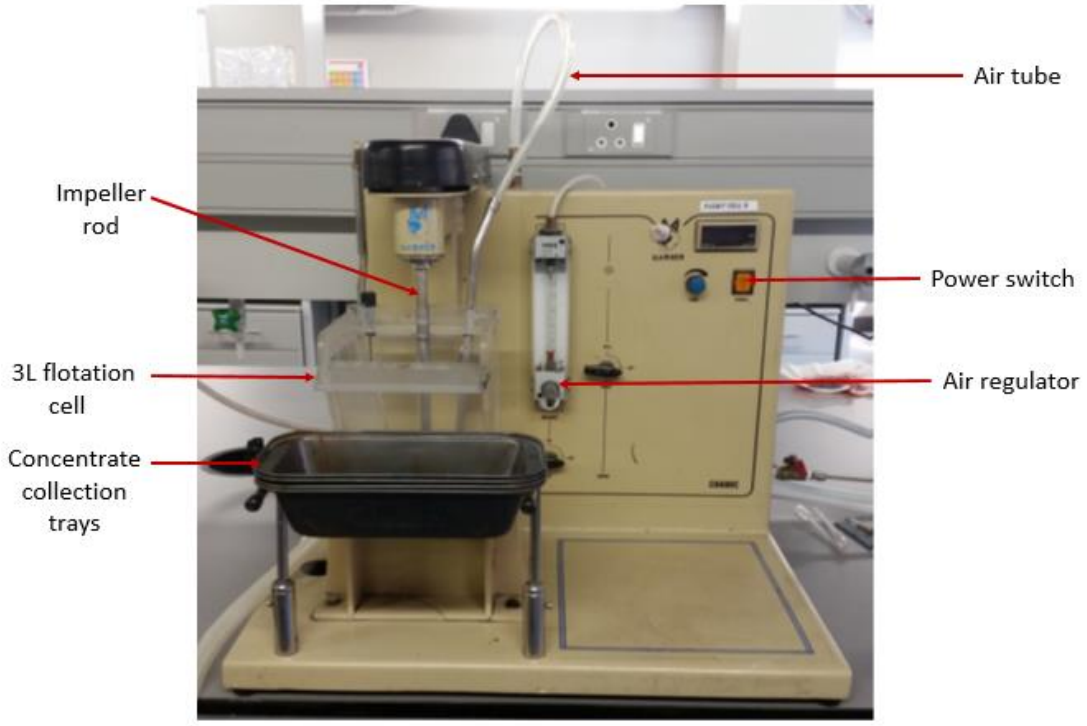

Figure 4.2: UCT 3L Barker Laboratory batch flotation cell.

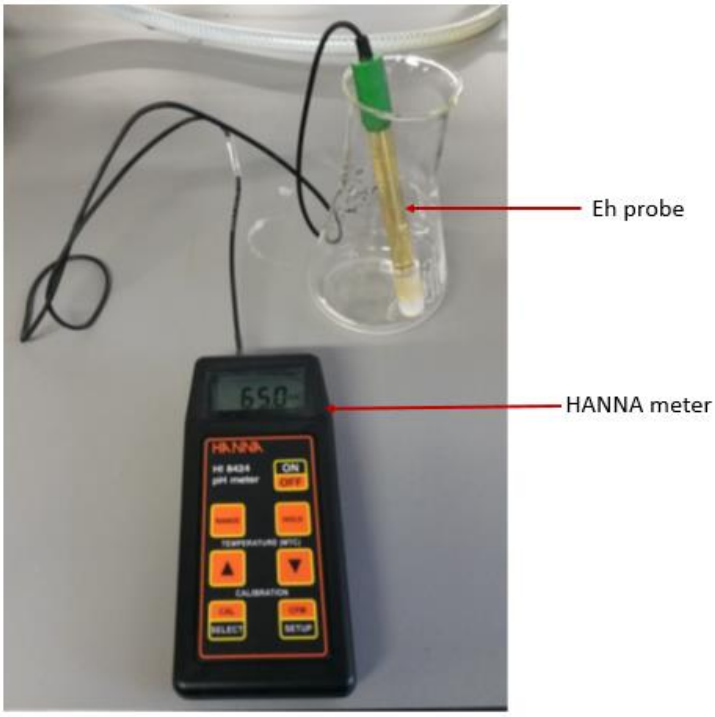

Figure 4.3: HANNA meter with Eh probe for Eh measurements.

All batch flotation tests were carried out in duplicates using the standard UCT batch flotation procedure, which was developed within the CMR. The tests were performed in a 3 L Barker flotation cell (Figure 4.2), with a top driven impeller and a Wilkerson ¼ inch 0-8 bar air regulator for air flow control. The cell was made of clear Perspex, to help visually maintain the required froth height in all the batch flotation experiments. The impeller speed was 1200 rpm and the air flow rate was 7 L/min. The Eh probe used for all batch tests was supplied by Hanna Instruments. The probe was a single junction, HI3230B electrode composed of a platinum sensor and a polyetherimide resin body.

For each test, the milled slurry was transferred to the flotation cell and topped up to the 3 L mark using synthetic plant water, in order to make up a solids concentration of 35%. The impeller was switched on instantly to keep the solids suspended. Prior to the addition of any reagents, a 40 ml feed sample was taken for head grade assays. The Eh of the natural ore was recorded by the Eh probe (Figure 4.3). For each test $1x10^{-4}$ mols, $1x10^{-3}$ mols and $1x10^{-2}$ mols of each potential modifier were added in the 3L flotation cell and the Eh recorded. 10 ml of a 1% solution of SIBX, equivalent of 100 g/t, was added and allowed to condition for 2 minutes, after which 40 µl pure DOW 200 frother, equivalent of 40 g/t, was added and allowed to condition for one minute. After reagent conditioning, air was introduced into the pulp phase via the air regulator. Froth was scrapped every 15 seconds and four concentrates (C1, C2, C3 and C4) were collected into weighed and labelled concentrate collection trays. Each concentrate stage had a corresponding wash bottle which was weighed before and after the flotation runs for water balance calculations. The concentrates were collected for 2, 4, 6 and 8 minutes respectively (Figure 4.4). A froth height of 1 cm was maintained by continuously replenishing synthetic plant water into the flotation cell. At the end of each run, air was turned off and two 40 ml samples of tailings were collected. The bulk remainder of tailings were collected into a bucket, filtered using an Eriez Magnetics MASCLAB filter press, dried and weighed. The filled concentrate trays were weighed; and the concentrates filtered using a vacuum filter and dried at 80 ^{0}C in ovens manufactured by Memmert. The dried feeds, concentrates and tailings were sent for Cu analysis by X-ray Fluorescence (XRF) using a Bruker S4 Explorer XRF Spectrometer. The weighed material was used to calculate the solids recoveries and assay results were used to calculate copper recoveries and grades.

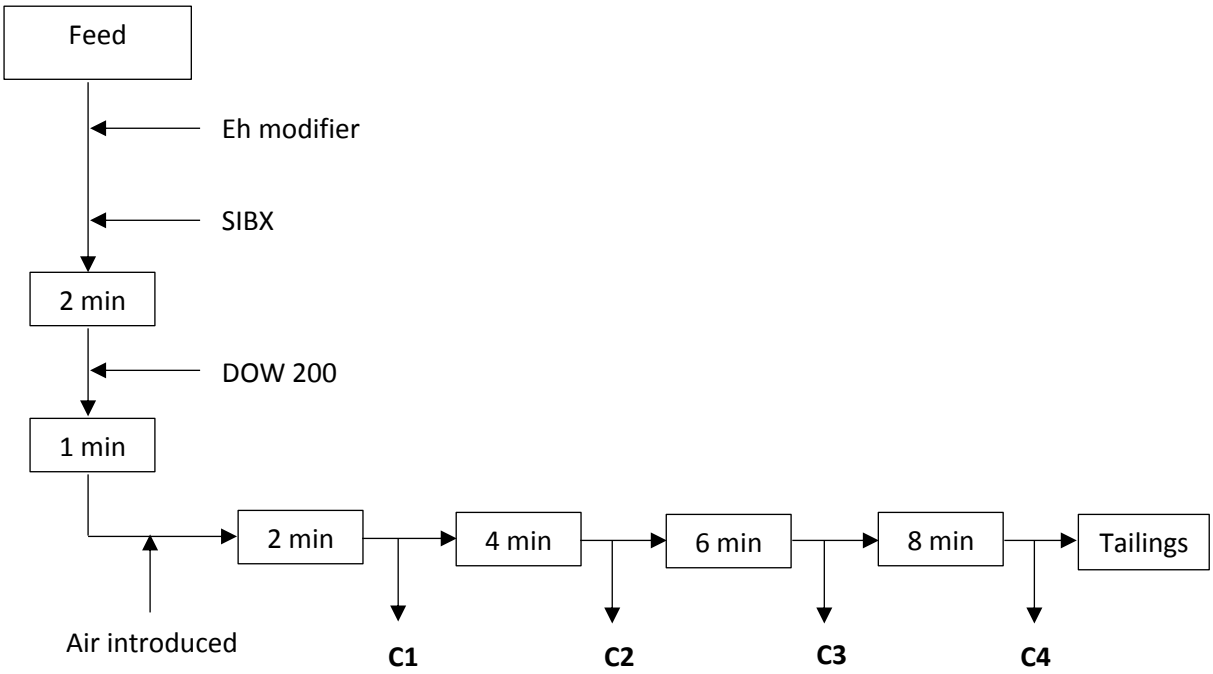

Figure 4.4: Summary of batch flotation procedure.

4.6 Froth stability tests

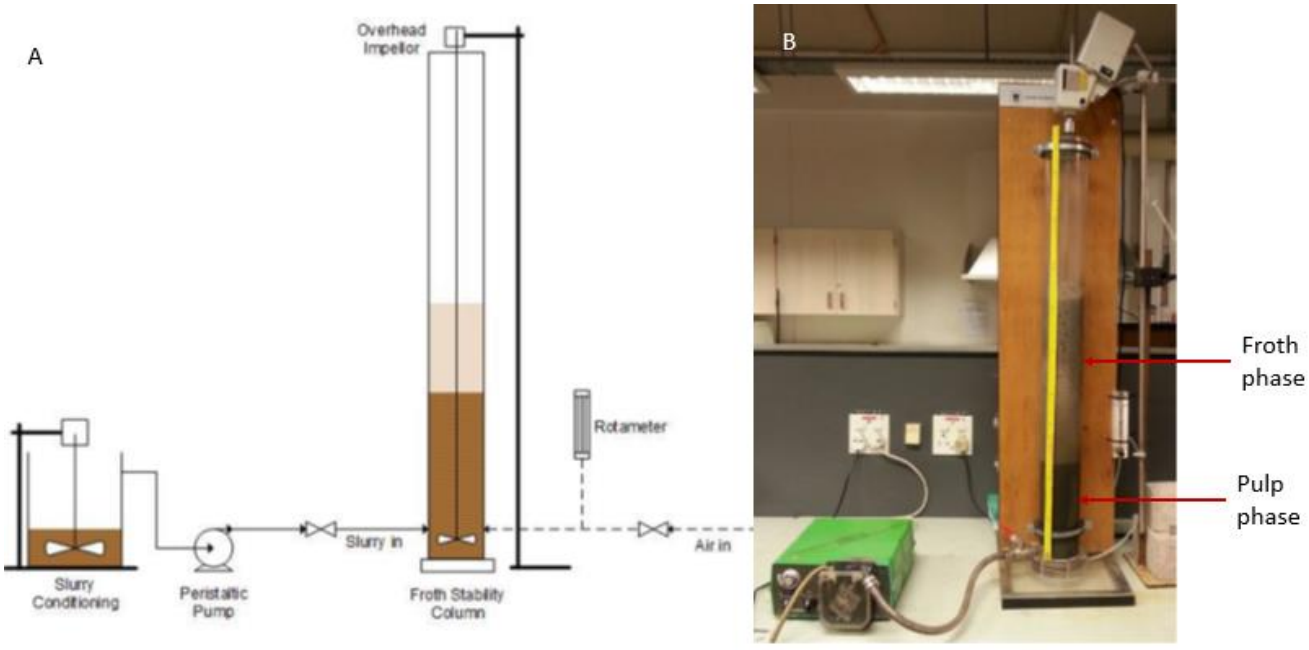

Figure 4.5: Froth stability column and ancillary equipment B and a schematic diagram of the experimental set-up A.

Froth stability column tests were carried out to determine the effect of potential modifiers on the froth phase. Both two phase (air and water) and three phase tests (air, water and solids) were done in the absence and presence of potential modifiers with SIBX. The froth stability column is made of Perspex to allow for froth height measurements at pre-determined time intervals. The column has a diameter of 10 cm and height of 1 m; and it is fitted with a 60 mm diameter sintered ceramic frit with pore size 2, at the bottom of the column, through which air is bubbled into the column. The air flow rate used for all experiments was kept constant at 7 L/min. An over-head impeller was used to aid in maintaining a homogeneous mixture of solids in the three phase system. All experiments were performed in duplicates. The experimental set-up is as shown in Figure 4.5.

The milled slurry was made up to a solids density of 35% in a feed bucket. Reagents were added to the feed bucket and allowed to condition prior to running each column test. The conditioned slurry/plant water were fed into the column using a peristaltic pump. The valve through which the slurry/solution was fed, was closed to avoid backflow. As soon as the feed was introduced into the column, the impeller was instantly switched on to avoid settling of solids for the three phase tests. To commence the generation of the froth within the column for the dynamic test, air was introduced into the column and froth height was recorded after every 5 seconds for 1 minute after which recordings were taken every 30 seconds until the equilibrium froth height (H_{max}) was achieved. Dynamic stability factor for each experiment was calculated using Equation 4.1.

$$\sum = \frac{V_f}{Q} = \frac{H_{max} x A}{Q} \quad \text{.....Eqn 4.1}$$

Where V_f is the volume of foam or froth at equilibrium, Q is the gas volumetric flow rate, H_{max} is the foam or froth height at equilibrium and A is the cross sectional area of the column.

4.7 Electrochemical measurements

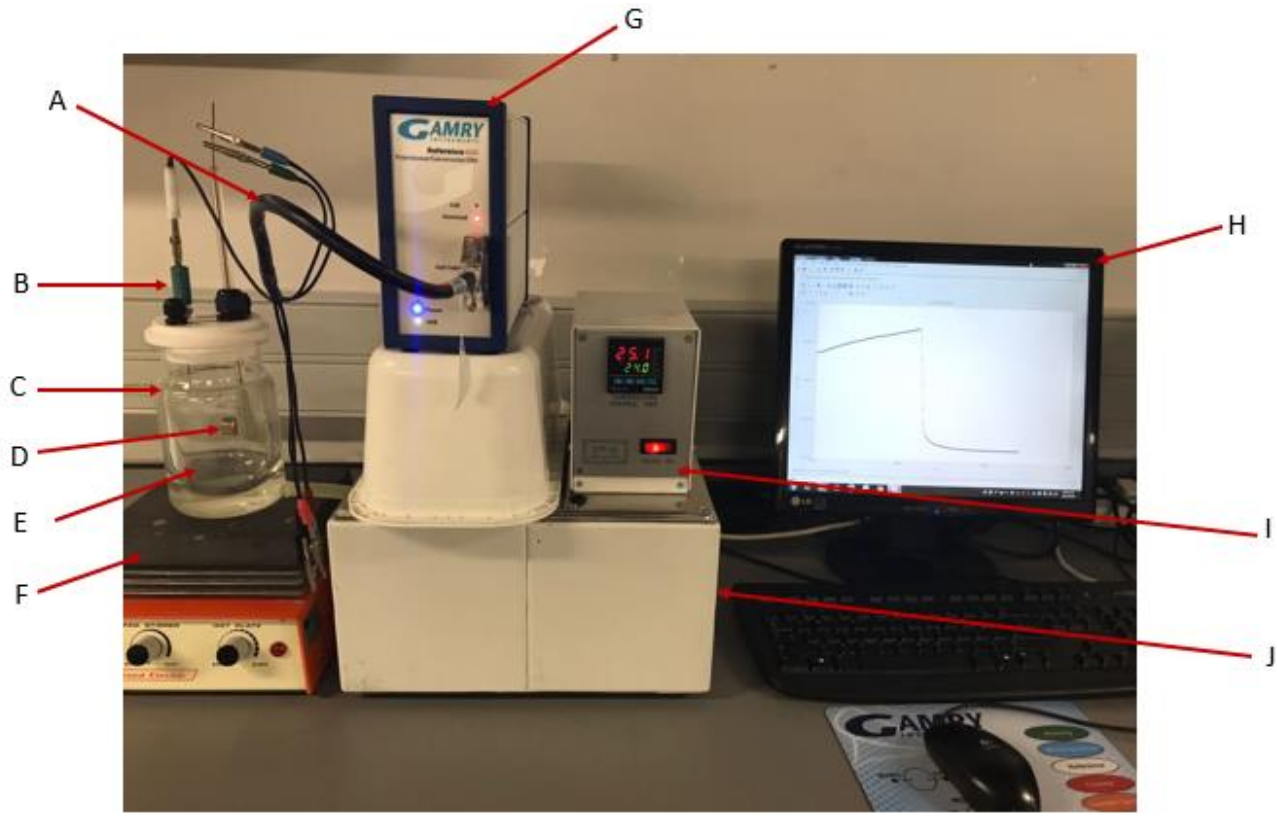

Figure 4.6: Equipment used for electrochemical measurements.

In this study, electrochemical measurements were conducted in a 500 ml double jacketed glass vessel (C), into which a Ag/AgCl reference electrode (B) and a working electrode (D) were suspended. The electrodes were immersed in a buffer solution/electrolyte (E), which was continuously stirred using a 15 mm magnetic stirrer bar during all experimental runs. The electrochemical cell was mounted on a Freed Electric magnetic stirrer (F). Temperature within the cell was maintained at 25±1 ^{0}C by pumping water through the outside of the glass vessel and the temperature of the water was regulated by a water bath (J) using a Shinha DCS Model 300 temperature controller (I). A Gamry Instruments Reference 600^{TM} Potentiostat/Galvanostat/Zero Resistance Ammeter (G) was used to measure required potentials. The Potentiostat and the computer (H), were coordinated through a USB cable. Connections between the Potentiostat and electrodes were made via a cell cable that has six connections (A). The blue crocodile clip was connected to the working electrode and measures the voltage. The green crocodile clip was connected to the working electrode and

carries the cell current. The red crocodile clip was connected to the counter/auxiliary electrode. The orange crocodile clip measures the counter electrode potential used in Zero Resistance Ammeter (ZRA) mode. The white crocodile clip was connected to the reference electrode and measures the voltage and the black crocodile clip for the floating ground which either connects to the Faraday cage or can be left suspended. Connections were made based on the electrochemical technique used for analysis.

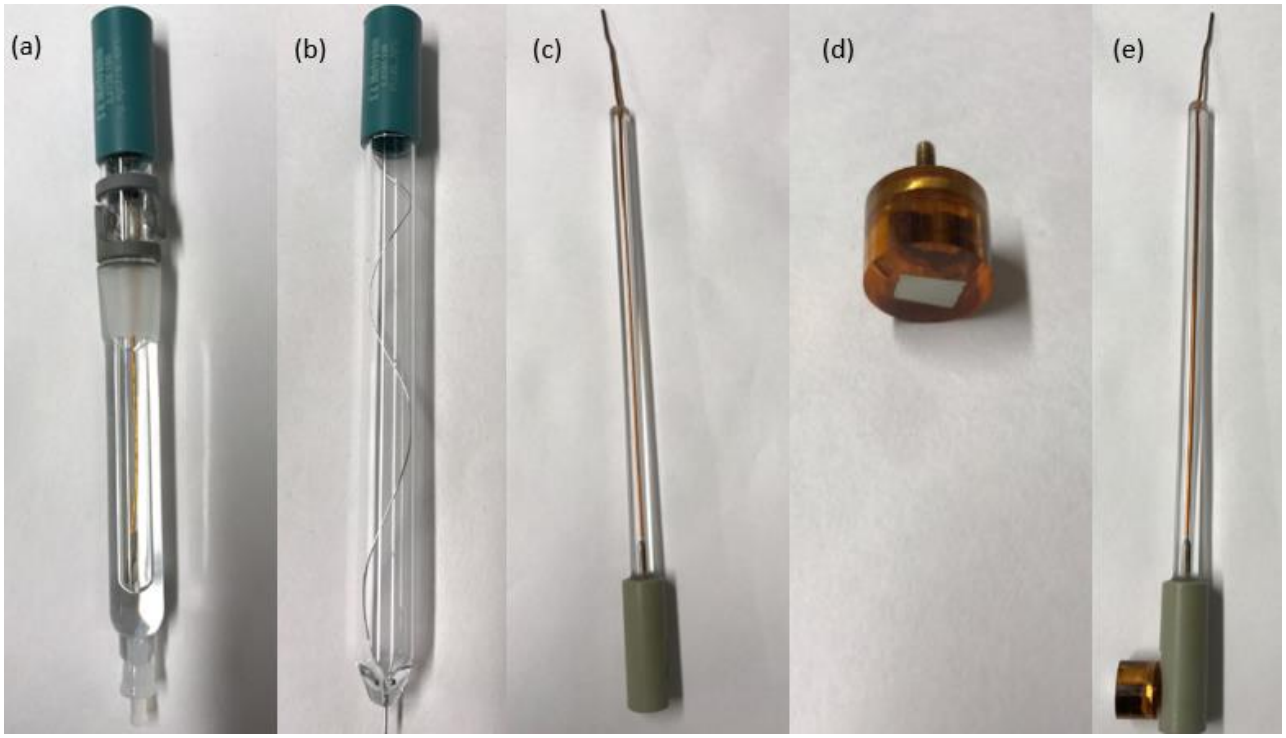

Figure 4.7: Electrodes used for electrochemical measurements.

A two and a three electrode system were used for open circuit measurements and equilibrium potential measurements, respectively. The counter electrode was a platinum wire electrode (b), the working electrode/mineral electrode (d) was moulded in epoxy resin and mounted on a copper wire encased in a plastic material (c – unmounted, e - mounted) and the reference electrode (a) was a double junction Ag/AgCl electrode with a potential of -0.207 V against the standard hydrogen electrode. The Ag/AgCl reference electrode was filled with a 3 M KCl solution. All prefabricated electrodes were supplied by Metrohm. The mineral electrode was manufactured at Murdoch University (Tadie, 2015) from a pure mineral sample and had 97% purity. The mineral was embedded in a non-conductive resin to obtain an electrode of about

15 mm in diameter and 10 mm in height. Before commencing with the electrochemical measurements, the reference electrode was measured against a standard Ag/AgCl electrode, as a means of calibration.

The user interface used with the Potentiostat was Gamry Framework which enabled instrument calibration, open circuit and current measurements. Results obtained were analysed by the Gamry Instruments Echem^{TM} Analyst Software. All the measured potentials were exported to Microsoft Excel and converted to the SHE scale.

4.7.1 Mineral working electrode preparation

The chalcopyrite electrode used was cleaned prior to each run in order to remove any oxidation products generated during storage or during previous runs. The mineral was initially wet ground on a 600 Grit Silica Carbide paper and rinsed with de-ionised water after which it was wet polished using alumina powders of 1 µm, 0.3 µm and 0.05 µm, respectively. The mineral was finally rinsed with de-ionised water and dried by lightly dabbing the surface with a paper towel. The alumina powders were supplied by IMP Scientific and Precision (Pty) Ltd.

4.7.2 Rest potential measurements

Rest potential measurements determined the rest/open circuit potentials of chalcopyrite in the electrolyte solution. The measurements were carried out using a two electrode system, Ag/AgCl reference electrode and the mounted working electrode. The electrodes were immersed into 450 ml electrolyte solution and connections were made from the cell cable to the electrodes. The rest potential measurements were conducted in the presence of SIBX and in the absence and presence of potential modifiers. Module PHE^{TM} 200 was run under open circuit and potential modifiers were dosed into the cell at 300 seconds after which the collector was dosed at 600 seconds (Chimonyo, 2016). The total run for each experiment was 1200 seconds.

4.7.3 Equilibrium potential measurements

The equilibrium potential measurements measured the oxidation potential of SIBX. The measurements were carried out using a three electrode system, a Ag/AgCl reference electrode, a counter electrode and a platinum working electrode. The electrodes were immersed into 450 ml electrolyte solution and connections were made from the cell cable to the electrodes. The measurements were conducted in the presence of SIBX. The potential was held anodic for 5 minutes, to allow for the oxidation reaction of xanthate to dixanthogen on the platinum electrode surface. The electrode was then open circuited for 1200 seconds and the final rest potential measured. The equilibrium potential of the collector was measured at three different concentrations of $1X10^{-3}$ M, $6.24X10^{-4}$ M and $1X10^{-4}$ M.

5 Results

5.1 Introduction

The objectives of this work are to evaluate the effect of potential modifiers on flotation recoveries and froth stability of a copper sulphide ore, to measure the oxidation potentials of a thiol collector at three different concentrations and further determine the rest potentials of a pure chalcopyrite mineral in the absence and presence of both the potential modifiers and the thiol collector. The detailed procedures for all tests investigated have been fully described in Chapter 4. This chapter will therefore report on the results obtained from the tests carried out in relation to the above-mentioned objectives.

The chapter has been split into six sections. Section 5.2 will show reproducibility of the tests conducted. Section 5.3 will show preliminary results for pH stability with time in the presence of each potential modifier. Section 5.4 will present results that show the effect of potential modifiers on water recoveries, solids recoveries, copper recoveries and copper grades. Section 5.5 will indicate how potential modifiers affect the stability of foam and froth in two phase and three phase systems, respectively. Section 5.6 will report on the oxidation/equilibrium potentials of SIBX at $1x10^{-3}$ M, $6.24X10^{-4}$ M and $1x10^{-4}$ M; and subsequently analyse the rest potentials of chalcopyrite in the absence and presence of both $6.24x10^{-4}$ M SIBX and each potential modifier. It is important to experimentally determine the rest potentials of minerals and equilibrium potentials for thiol collectors in order to gain insight on the possible mechanisms and species forming on mineral surfaces at specific conditions. Section 5.6 was carried out in order to complement results obtained from sections 5.4 and 5.5.

The baseline case/control run for all experiments investigated had SIBX as a collector, with no potential modifier addition.

5.2 Reproducibility

It was important to determine how reproducible the results obtained were. Repeatability is the degree of agreement of the same tests/measurements taken by a single instrument/individual under the same conditions whereas reproducibility measures whether an entire study or experiment can be reproduced in its entirety under the same conditions. Both of which are ways to measure precision. To ensure reproducibility on the experimental repeats, the same conditions were applied, both physical and chemical.

5.2.1 Statistical Analysis Tools

All experiments were carried out in duplicates to minimise experimental error. The experimental results were then averaged in order to obtain the arithmetic mean ($\bar{x}$), which is a measure of central tendency given by the Equation 5.1:

$$\bar{x} = \frac{1}{N}\sum_{X=i}^{N} x_i \quad \text{.....Eqn 5.1}$$

In equation 5.1, x_i represents values from a data set and N is the sample size.

From the arithmetic mean, standard error was calculated. This is defined as a measure of the statistical accuracy of an estimate, which is equal to the standard deviation of the theoretical distribution of a large population of such estimates. Error bars were indicated on all graphs to show error of corresponding points, using standard error calculations.

5.2.2 Flotation recoveries, froth stability and electrochemical measurements

A high level of reproducibility was obtained in all the tests conducted, which included batch flotation tests, froth stability tests and rest potential measurements.

Figure 5.1 shows cumulative solids recovery as a function of time in the presence of $1x10^{-4}$ mols $K_2Cr_2O_7$. The UCT standard batch flotation procedure used, depicts that in relation to mass, the standard error for solids recovery for each concentrate in similar tests should not exceed 5%. For all the test conditions carried out, the standard errors were within the 5% limit as shown in Figure 5.1.

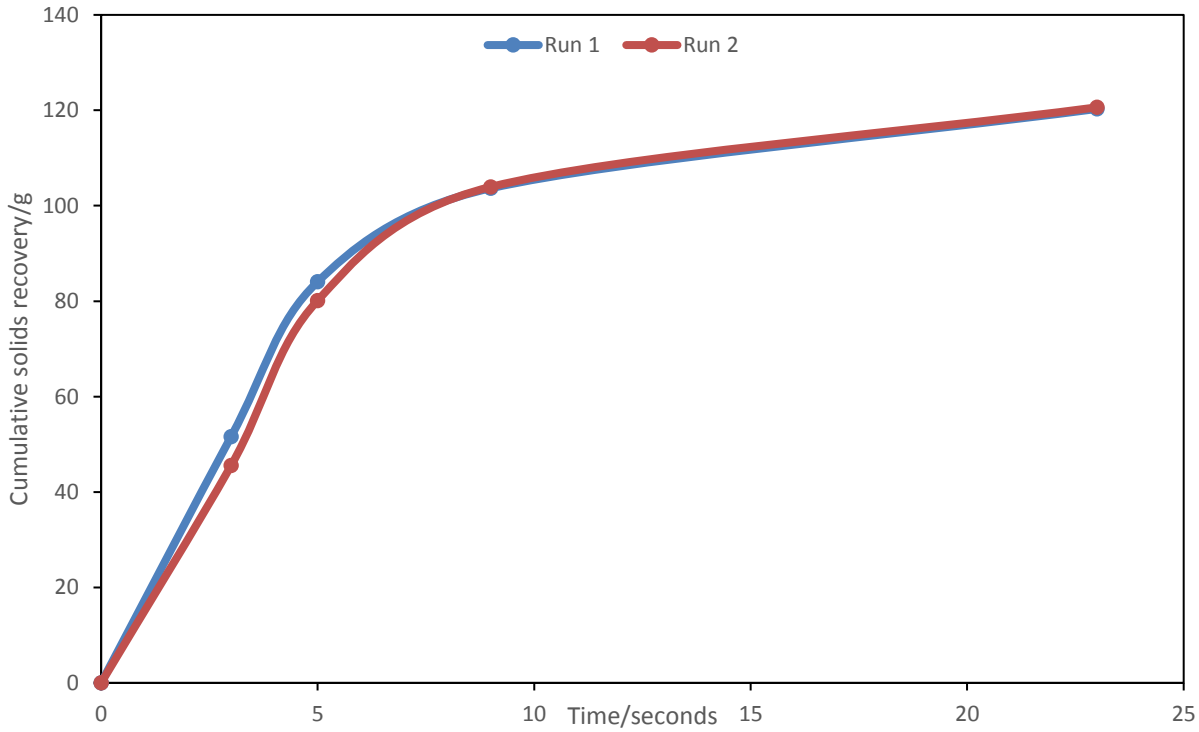

Figure 5.1: Reproducibility of cumulative solids as a function of time in $1x10^{-4}$ mols $K_2Cr_2O_7$, 100 g/t SIBX and 40 g/t DOW 200.

Figure 5.2 shows reproducibility of froth stability tests for conditions under investigation. The tests were carried out with a high degree of reproducibility, as a range of ±0.17 seconds difference in dynamic stability factors was obtained for all repeats.

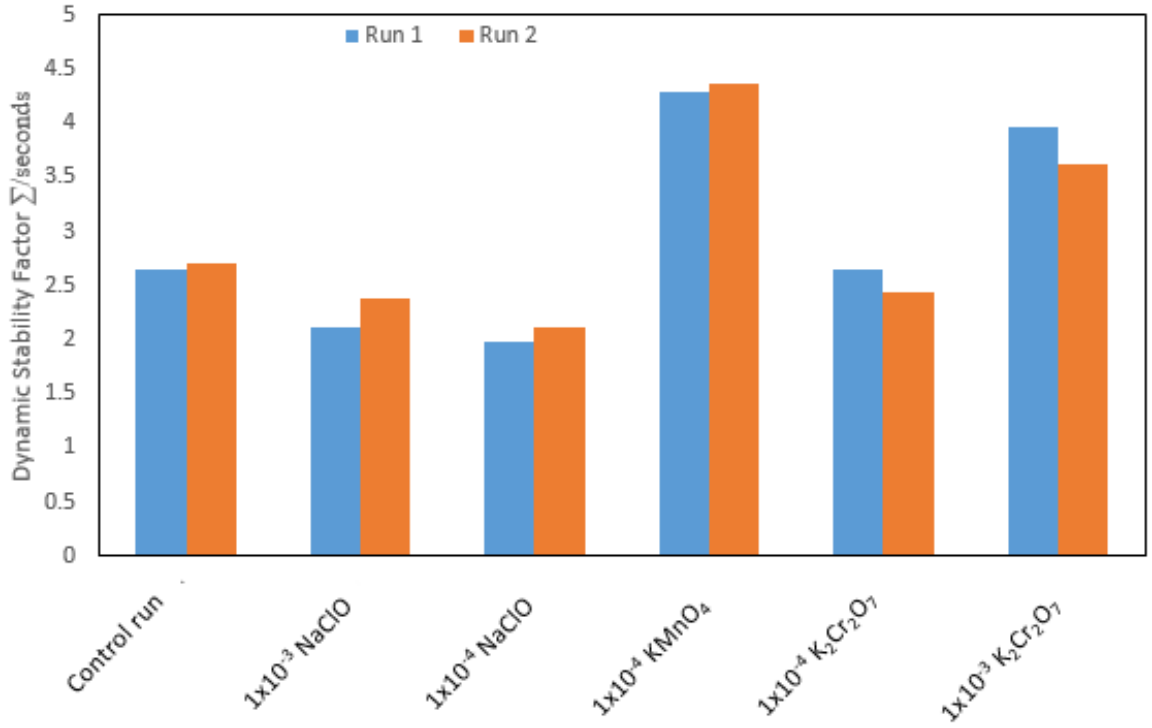

Figure 5.2: Reproducibility for the dynamic froth stability factor for conditions investigated.

Figure 5.3 indicates reproducibility of rest potential measurements carried out in $1x10^{-3}$ mols NaClO. The Gamry instrument operator's manual highlights that electrochemical measurements are considered to be reproducible if the potentials measured between repeats are not more than 10 mV apart. The current study obtained potential differences that were less than 5 mV for all repeats.

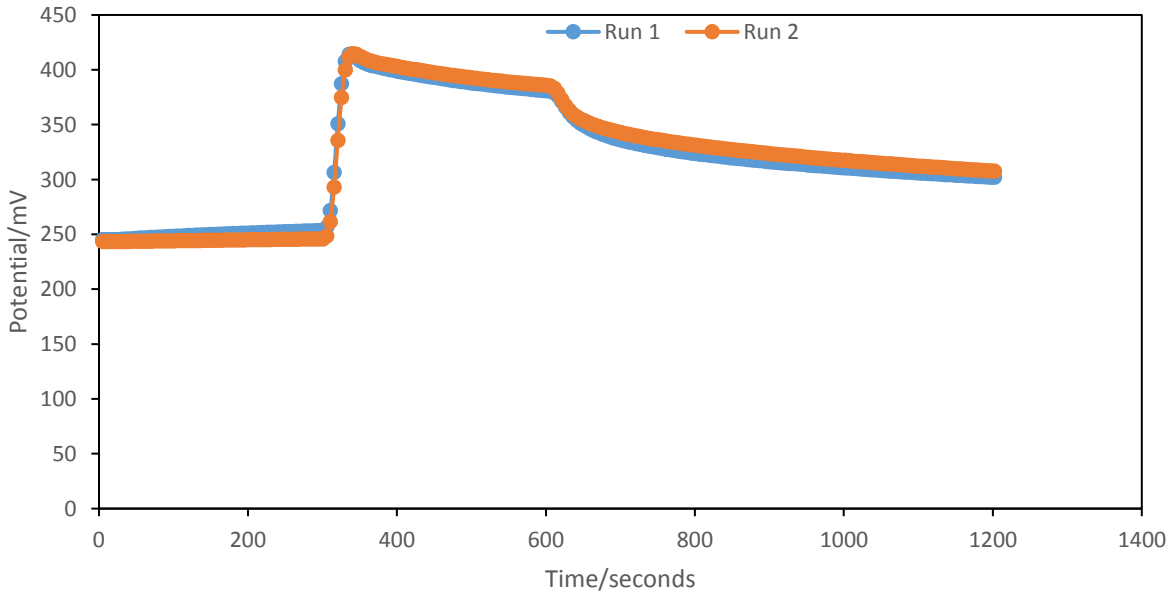

Figure 5.3: Reproducibility of rest potentials for chalcopyrite in $1x10^{-3}$ mols NaClO & $6.24x10^{-4}$ M SIBX.

5.3 Changes in pH with time

Preliminary experiments were carried out to investigate pH changes of ore slurry in plant water with time, in the presence of various potential modifiers at various Eh values. Figure 5.4 evidently shows that there are no significant changes in pH with time at different Eh values in the presence of NaClO, $KMnO_4$ and $K_2Cr_2O_7$. The pH ranges were recorded to be 8.18-8.46, 8.4-8.46 and 8.19-8.4, respectively. Therefore, it was deduced that pH is constant for this system under all conditions investigated. Hence, all test work was carried out at the ore's natural pH of 8.16-8.70.

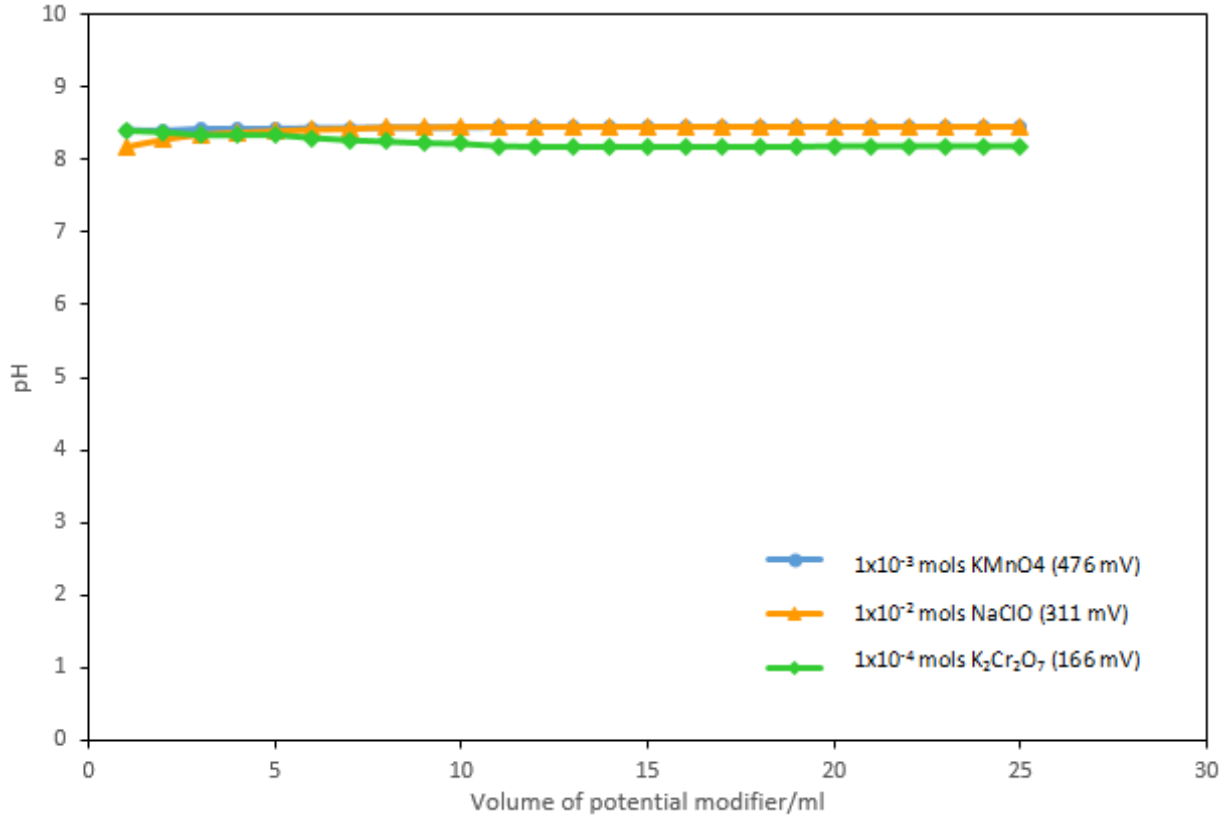

Figure 5.4: Changes in pH with time at various Eh values in $1x10^{-3}$ mols NaClO; $KMnO_4$ and $K_2Cr_2O_7$.

5.4 The effect of potential modifiers on flotation recoveries

The effect of potential modifiers, NaClO, $KMnO_4$ and $K_2Cr_2O_7$ each at $1x10^{-4}$; $1x10^{-3}$ and $1x10^{-2}$ mols, on solids recoveries, water recoveries, copper recoveries and copper grades was investigated and compared with the control run.

With regards to all the line graphs reported in this chapter, the first point on each line graph represents C1, which is the first concentrate recovered from 3 minutes to 5 minutes, the second point represents C2 which is the cumulative concentrate recovered from C1 up to 9 minutes, the third point represents C3 which is the cumulative concentrate recovered from C1, C2 up to 15 minutes and the fourth point represents C4 which is the cumulative concentrate recovered from C1, C2, C3 up to 23 minutes.

5.4.1 Solids recoveries as a function of flotation time

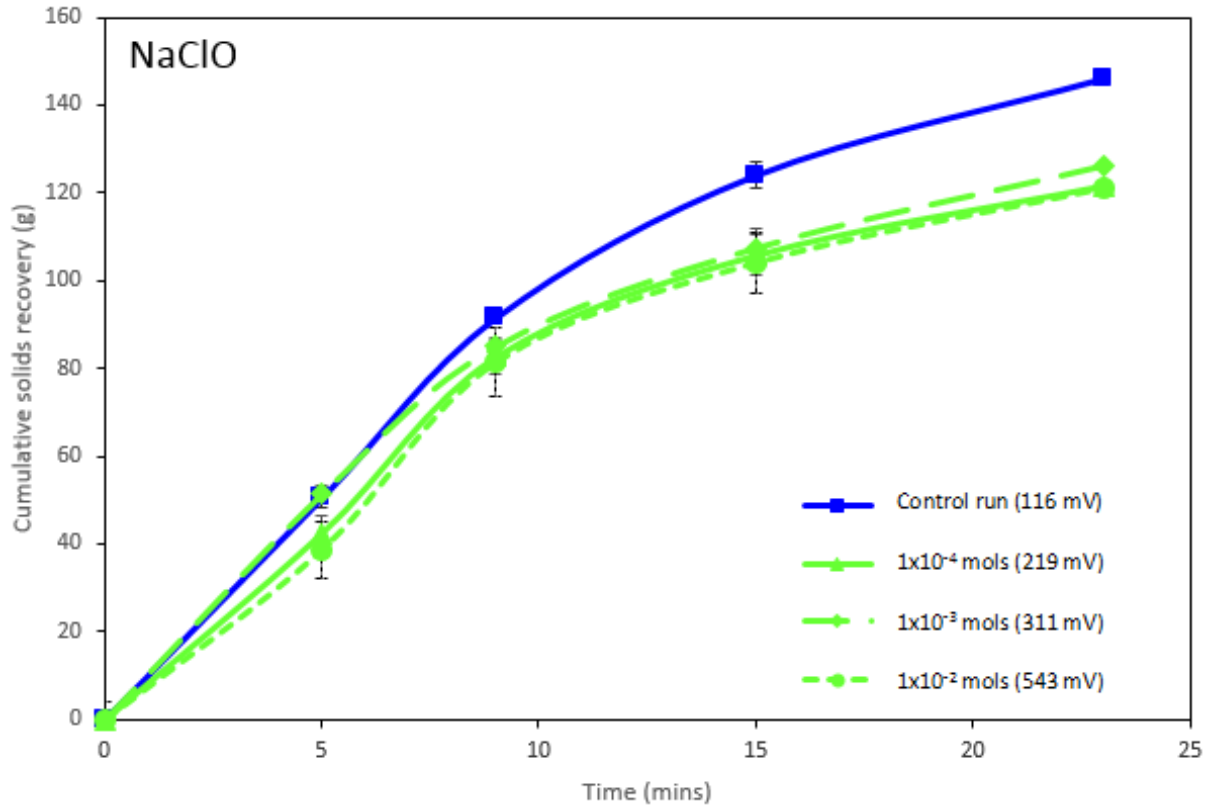

Figure 5.5: Cumulative solids recovery as a function of flotation time in 100 g/t SIBX & 40 g/t DOW 200 at $1x10^{-4}$, $1x10^{-3}$ and $1x10^{-2}$ mols of NaClO. Error bars represent standard error between duplicate tests.

Figure 5.5 shows cumulative solids recovery as a function of time. The highest solids recovery was obtained with the control run. Upon addition of NaClO at different concentrations, similar final recoveries were obtained with a slightly higher recovery at a concentration of $1x10^{-3}$ mols (Eh of 311 mV). Interestingly similar solids recoveries were obtained at the highest and lowest concentration of NaClO.

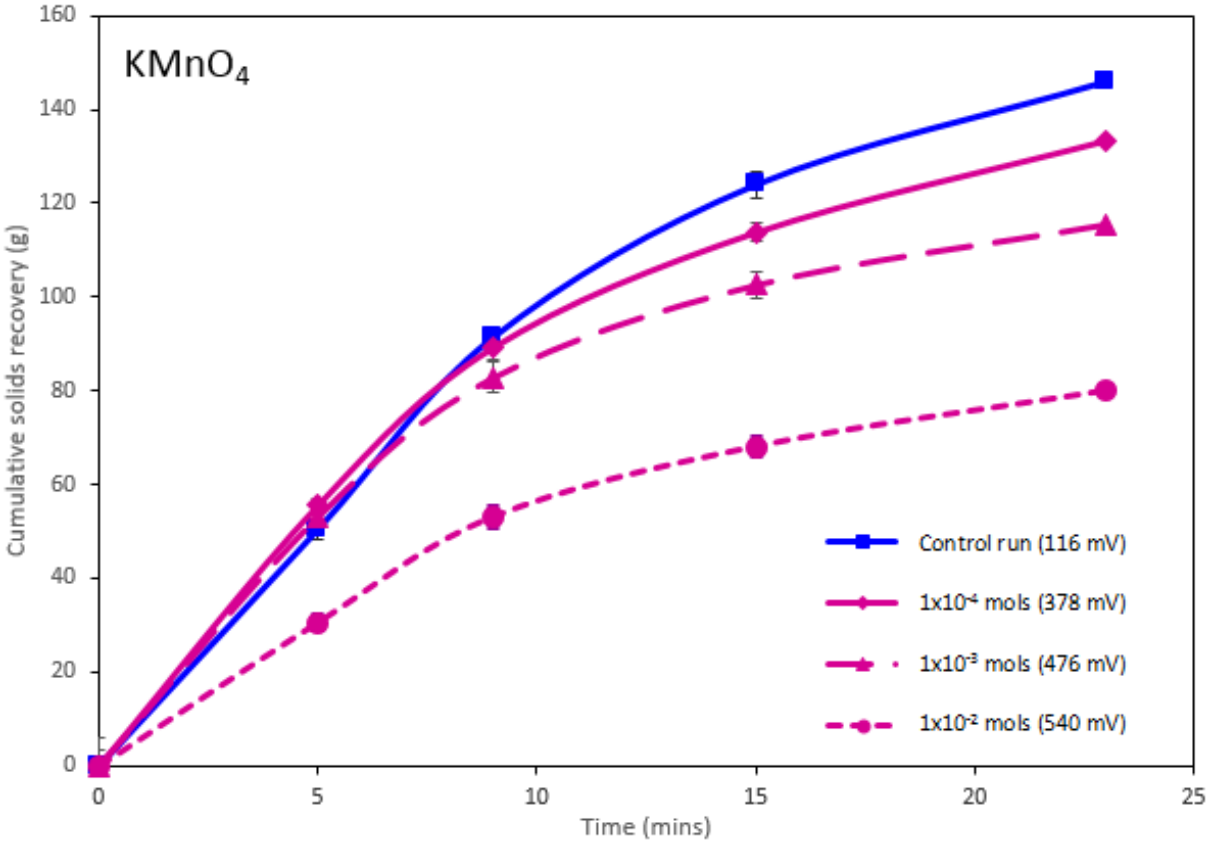

Figure 5.6: Cumulative solids recovery as a function of flotation time in 100 g/t SIBX & 40 g/t DOW 200 at $1x10^{-4}$, $1x10^{-3}$ and $1x10^{-2}$ mols of $KMnO_4$. Error bars represent standard error between duplicate tests.

As indicated in Figure 5.6, an increase in concentration of $KMnO_4$, thus an increase in Eh, reduced the amount of solids recovery with time. The highest solids recovery was 146.06 g and the lowest solids recovery was 79.9 g for the test with no modifier and $1x10^{-2}$ mols $KMnO_4$, respectively. It is apparent from Figure 5.6 that addition of $KMnO_4$ reduces the cumulative solids recovery with time.

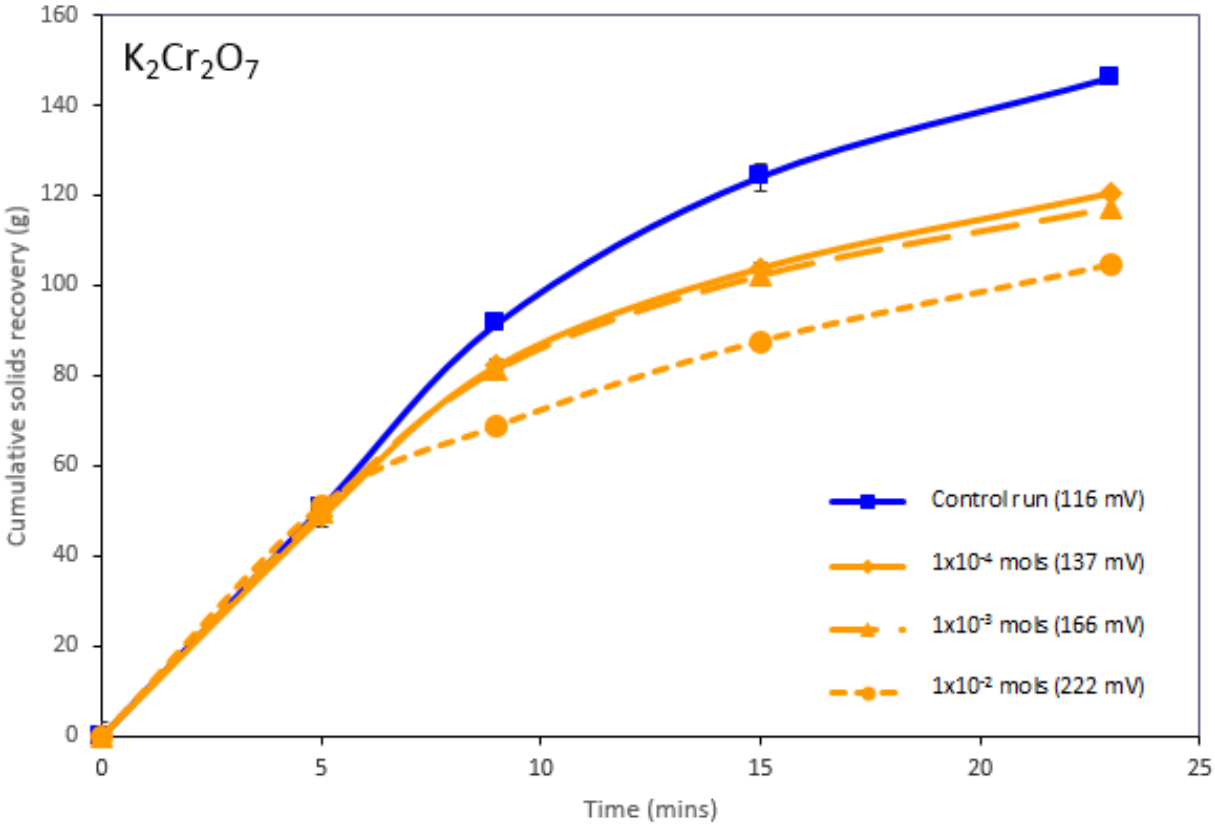

Figure 5.7: Cumulative solids recovery as a function of flotation time in 100 g/t SIBX & 40 g/t DOW 200 at $1x10^{-4}$, $1x10^{-3}$ and $1x10^{-2}$ mols of $K_2Cr_2O_7$. Error bars represent standard error between duplicate tests.

According to Figure 5.7, it is evident that when $K_2Cr_2O_7$ is used as a potential modifier, an increase in concentration and thus an increase in Eh reduces final solids recoveries. These results are consistent with Figure 5.6, where $KMnO_4$ was used. With reference to Figure 5.7, the same solids recoveries were acquired in the first concentrates of all the conditions. The highest final solids recovery was obtained in the absence of any modifier (Eh of 116 mV), whereas the lowest final solids recovery obtained was at a concentration of $1x10^{-2}$ mols $K_2Cr_2O_7$ (Eh of 222 mV). Interestingly there was no significant difference in solids recoveries at concentrations of $1x10^{-4}$ mols $K_2Cr_2O_7$ (Eh of 137 mV) and at $1x10^{-3}$ mols $K_2Cr_2O_7$ (Eh of 166 mV).

5.4.2 Water recoveries as a function of flotation time

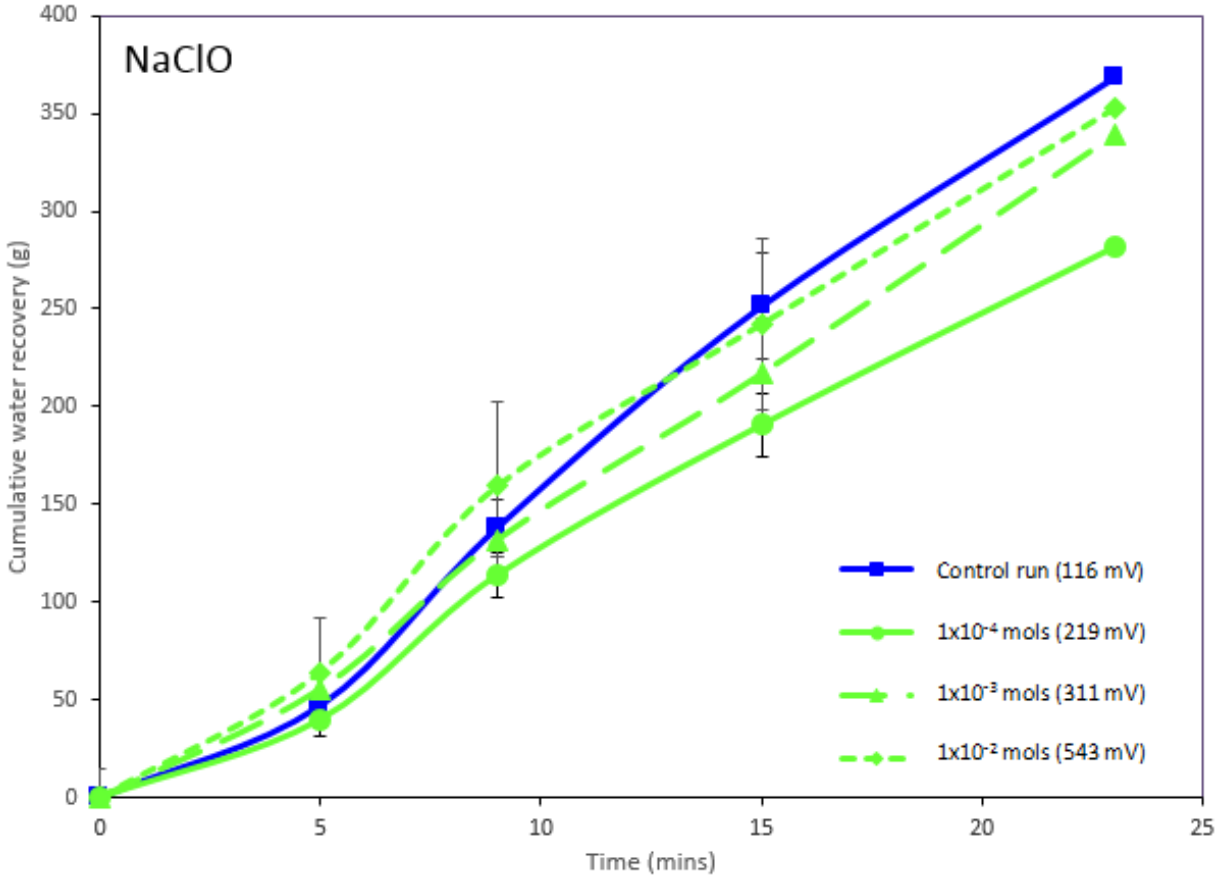

Figure 5.8: Cumulative water recovery as a function of flotation time in 100 g/t SIBX & 40 g/t DOW 200 at $1x10^{-4}$, $1x10^{-3}$ and $1x10^{-2}$ mols of NaClO. Error bars represent standard error between duplicate tests.

Figure 5.8 illustrates the cumulative water recovery as a function of flotation time in the presence of NaClO. The control run gave slightly higher final water recovery compared to all other conditions for NaClO. The lowest final water recovery was acquired at the lowest concentration (Eh of 219 mV) in the presence of NaClO, with concentrations of $1x10^{-3}$ mols NaClO (Eh of 311 mV), $1x10^{-2}$ mols NaClO (Eh of 543 mV) and the condition without modifier giving almost similar water recoveries of around 350 g. However, in the presence of NaClO, an increase in concentration and thus increase in Eh increased the water recoveries.

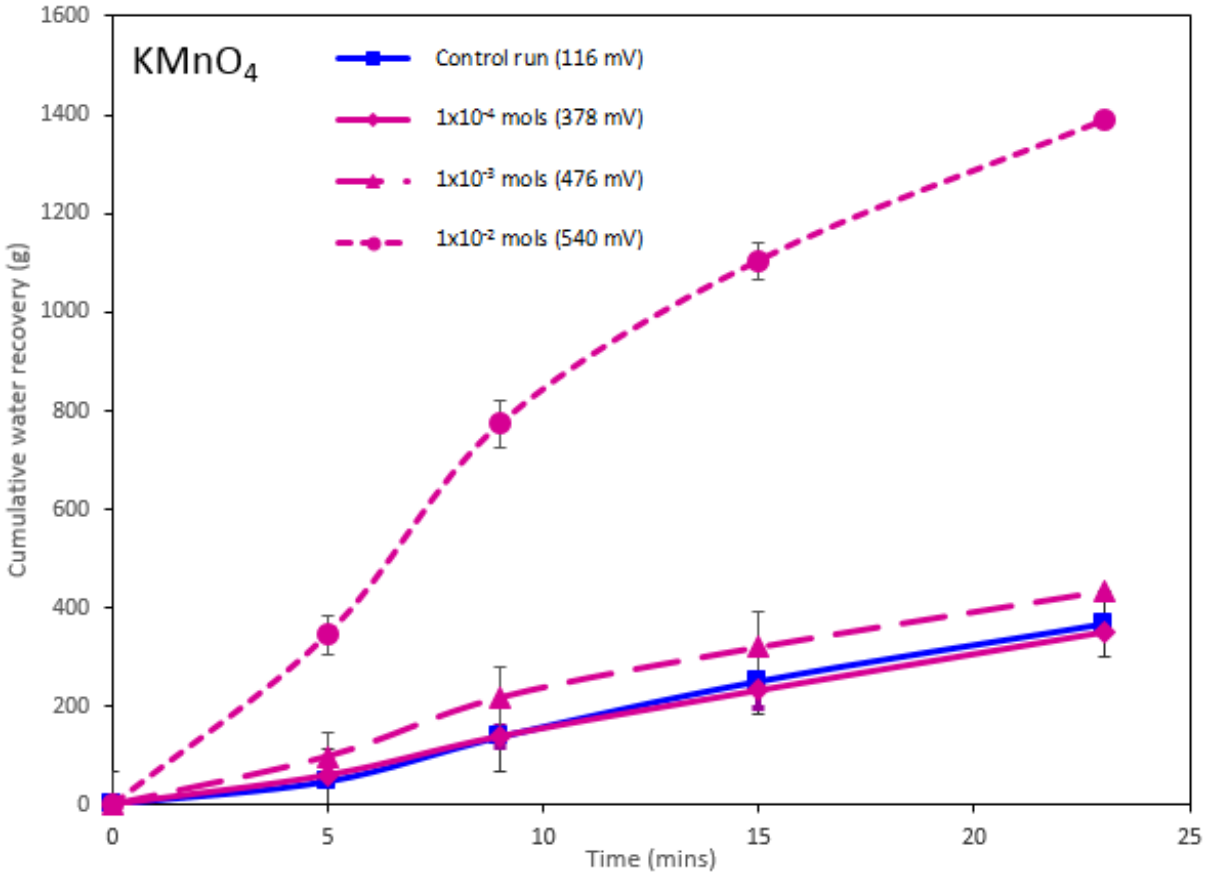

Figure 5.9: Cumulative water recovery as a function of flotation time in 100 g/t SIBX & 40 g/t DOW 200 at $1x10^{-4}$, $1x10^{-3}$ and $1x10^{-2}$ mols of $KMnO_4$. Error bars represent standard error between duplicate tests.

Figure 5.9 shows cumulative water recovery as a function of time in the presence of $KMnO_4$. It is evident that the addition of $1x10^{-2}$ mols $KMnO_4$ with an Eh value of 540 mV, resulted in remarkably high water recoveries compared to other conditions. The control run including other conditions of $KMnO_4$ resulted in almost similar water recoveries of about 350 g. Overall, an increase in concentration increased water recoveries and a decrease in concentration decreased water recoveries.

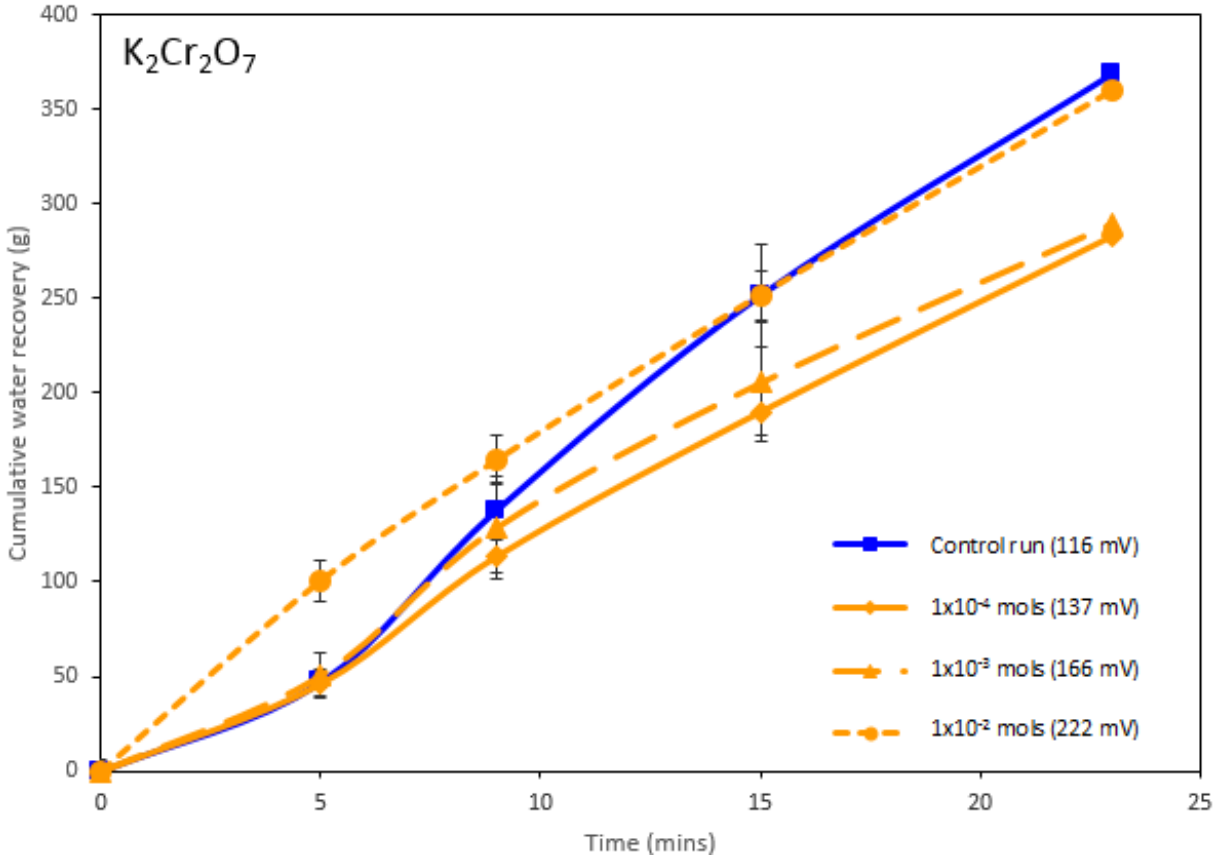

Figure 5.10: Cumulative water recovery as a function of flotation time in 100 g/t SIBX & 40 g/t DOW 200 at $1x10^{-4}$, $1x10^{-3}$ and $1x10^{-2}$ mols of $K_2Cr_2O_7$. Error bars represent standard error between duplicate tests.

Figure 5.10 shows that the highest final water recovery, of about 350 g was obtained at an Eh of 116 mV with no modifier and at the highest concentration of $K_2Cr_2O_7$ (Eh of 137 mV). Contrarily, the lowest concentrations of $K_2Cr_2O_7$ with Eh values of 137-166 mV gave lower water recoveries.

5.4.3 Solids recoveries as a function of water recoveries

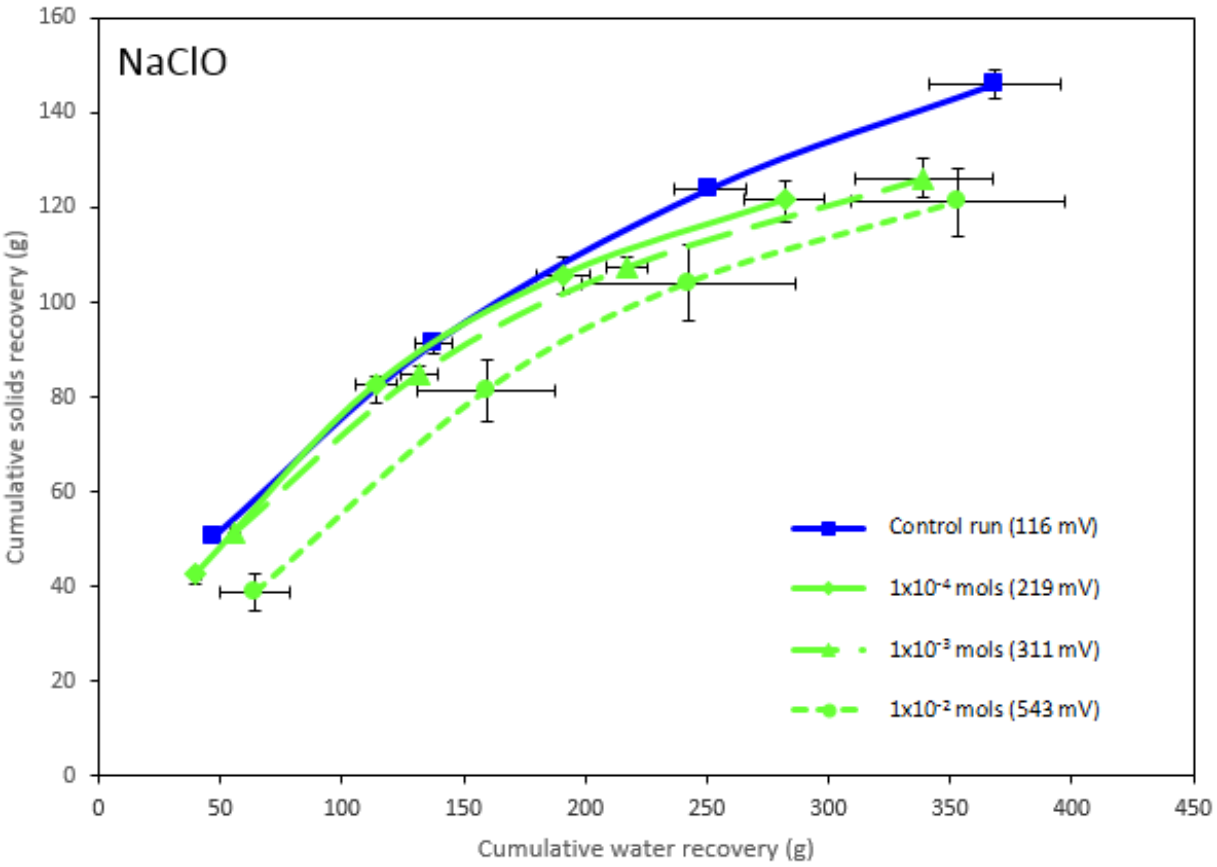

Figure 5.11: Cumulative solids recovery as a function of cumulative water recovery in 100 g/t SIBX & 40 g/t DOW 200 at $1x10^{-4}$, $1x10^{-3}$ and $1x10^{-2}$ mols of NaClO. Error bars represent standard error between duplicate tests.

Figure 5.11 indicates cumulative solids recovery as a function of water recovery in the presence of NaClO. The highest solids recovery and highest water recovery were observed at the condition with no modifier. Interestingly the use of NaClO at different concentrations gave rise to similar final solids recoveries. However more water was recovered at higher concentrations of NaClO compared to the lowest concentration of $1x10^{-4}$ mols NaClO.

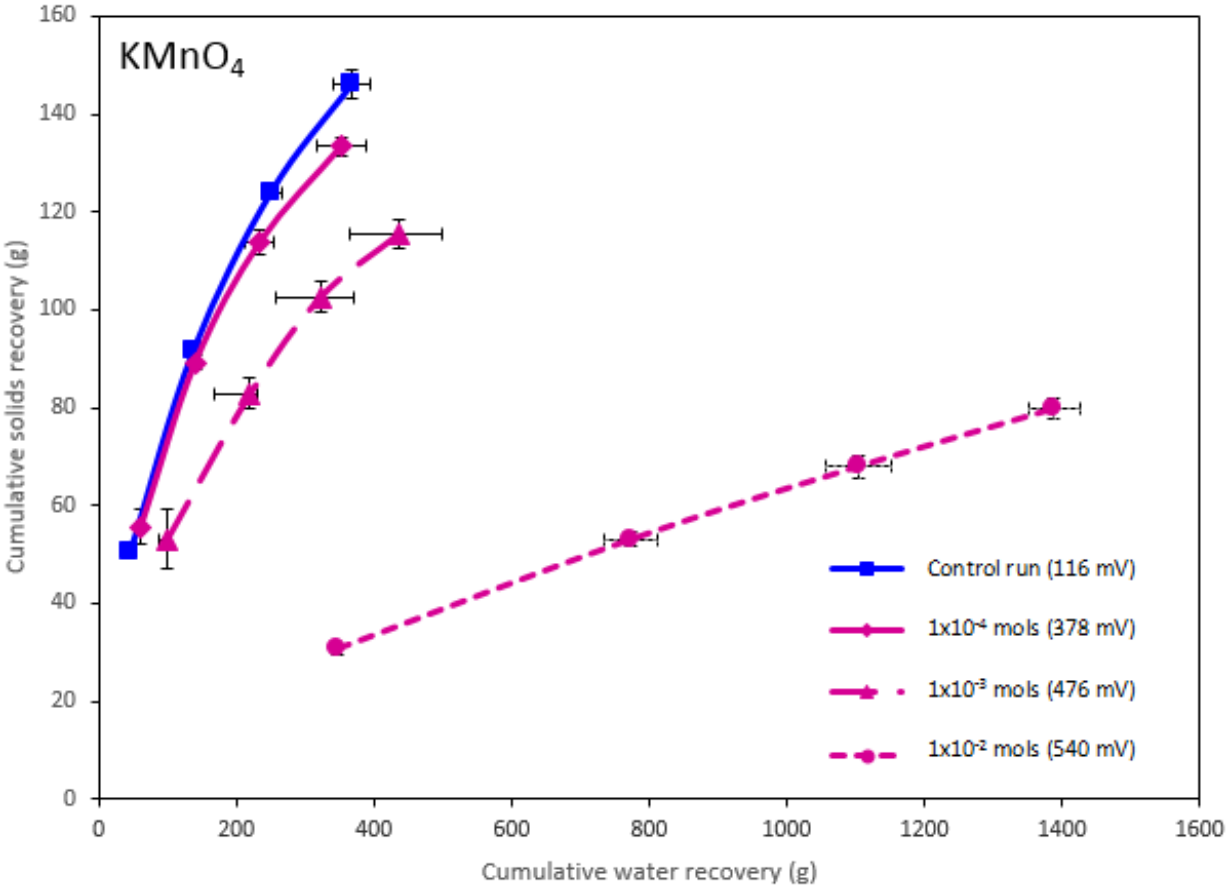

Figure 5.12: Cumulative solids recovery as a function of cumulative water recovery in 100 g/t SIBX & 40 g/t DOW 200 at $1x10^{-4}$, $1x10^{-3}$ and $1x10^{-2}$ mols of $KMnO_4$. Error bars represent standard error between duplicate tests.

It is apparent from Figure 5.12 that the highest concentration of $KMnO_4$ (Eh of 540 mV) resulted in the least amount of solids recovery per unit water. It is shown that the highest concentration gave rise to the lowest solids recovery with a very high water recovery compared to other conditions investigated. An increase in concentration and thus an increase in Eh decreased solids recoveries and conversely increased water recoveries.

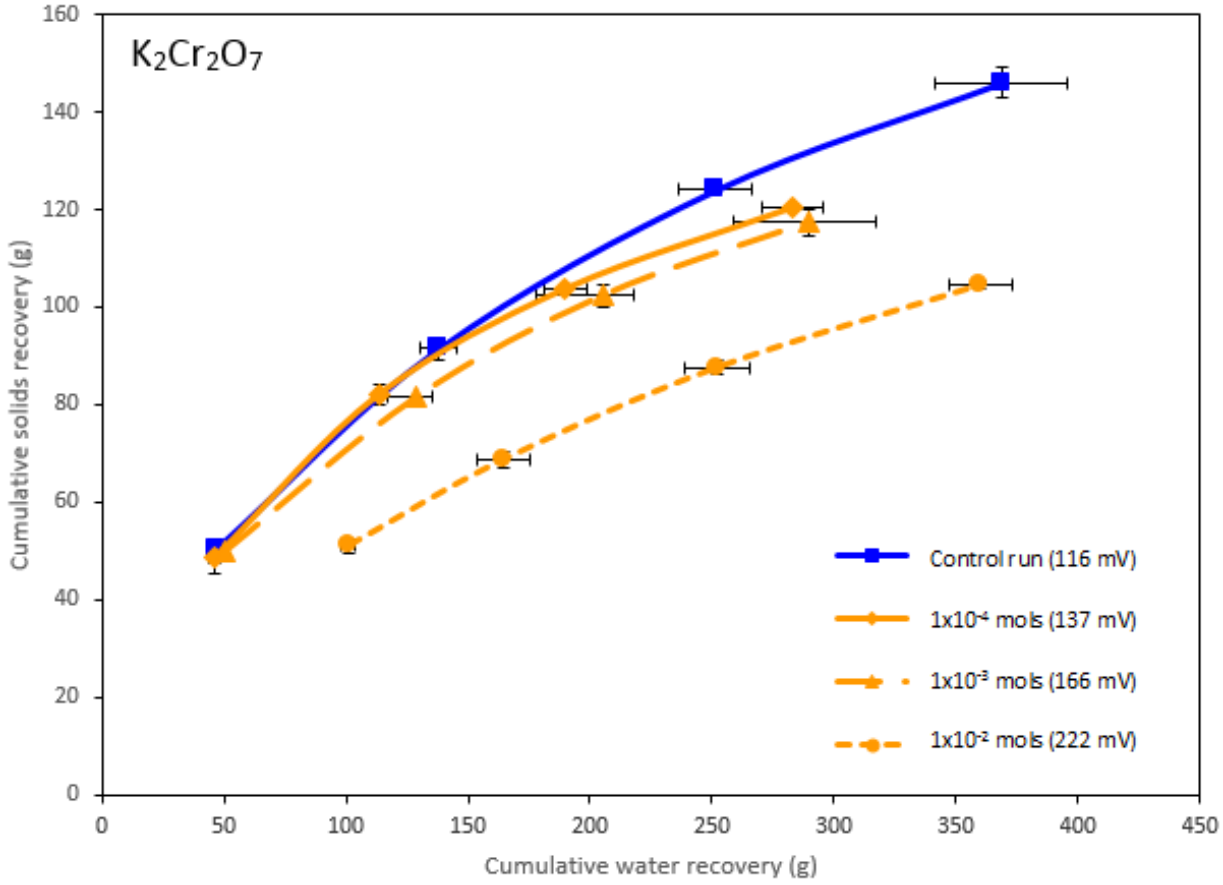

Figure 5.13: Cumulative solids recovery as a function of cumulative water recovery in 100 g/t SIBX & 40 g/t DOW 200 at $1x10^{-4}$, $1x10^{-3}$ and $1x10^{-2}$ mols of $K_2Cr_2O_7$. Error bars represent standard error between duplicate tests.

As shown in Figure 5.13, the amount of solids recovery per unit water recovery decreased with an increase in concentration of $K_2Cr_2O_7$. However, the condition without a modifier and the highest concentration of $K_2Cr_2O_7$ at 222 mV, had similar high final water recoveries whereas the lowest concentrations of $K_2Cr_2O_7$ at $1x10^{-4}$ mols and $1x10^{-3}$ mols both had lower water recoveries compared to the aforementioned. Moreover, lower concentrations of $K_2Cr_2O_7$ also gave rise to similar solids recoveries.

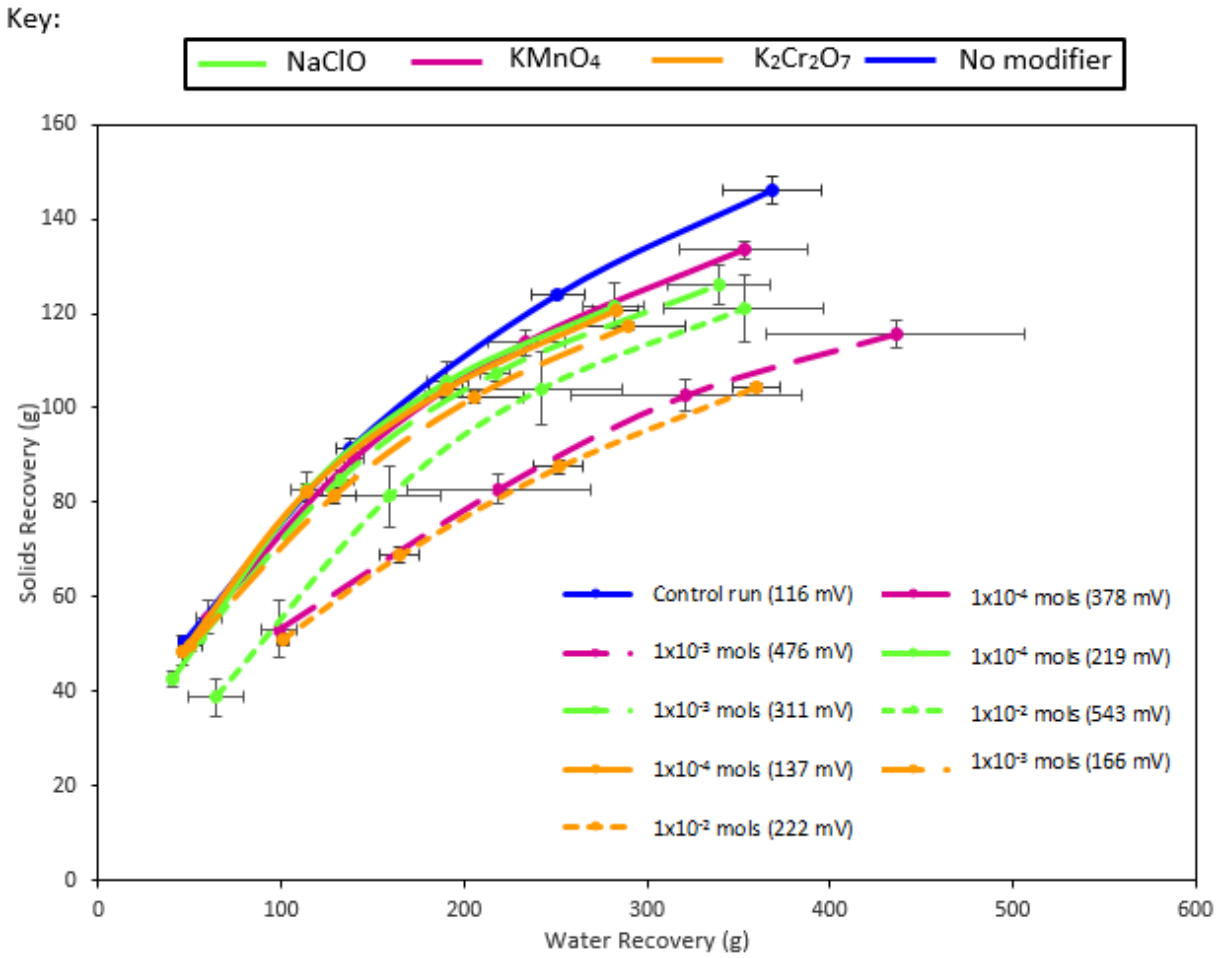

Figure 5.14: Cumulative solids recovery as a function of cumulative water recovery in 100 g/t SIBX & 40 g/t DOW 200 at given conditions. Error bars represent standard error between duplicate tests.

Figures 5.14 shows cumulative solids recovery as a function of cumulative water recovery for all conditions under investigation. Higher solids recoveries per unit water recovery were obtained without any potential modifier. Lower solids recoveries per unit water recovery were obtained for tests with a highest concentration for each potential modifier. A slightly higher water recovery was observed at a concentration of $1x10^{-3}$ mols $KMnO_4$ (Eh of 476 mV). Lower water recoveries were obtained in the presence of NaClO and $K_2Cr_2O_7$ at their lower concentrations, thus lower Eh values. For each potential modifier a trend can be observed where an increase in concentration and thus an increase in Eh results in a decrease in solids recovery per unit water recovery and vice versa.

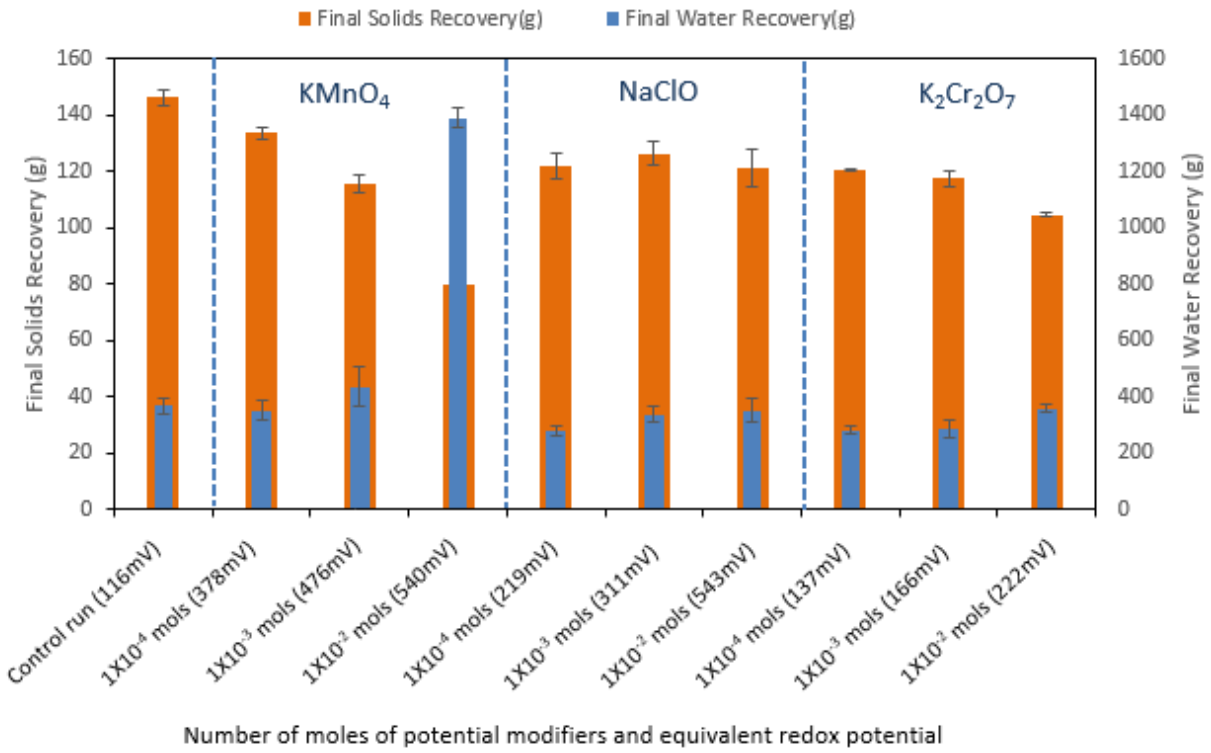

Figure 5.15: Final solids recovery as a function of final water recovery in 100 g/t SIBX & 40 g/t DOW 200 at given conditions. Error bars represent standard error between duplicate tests.

Figure 5.15 shows final solids and water recoveries for all conditions. The highest solids recovery was 146.06 g, which was for the control run, in which the Eh was 116 mV. The other conditions did not show very significant changes both in the solids or water recoveries. However, solids recoveries decreased slightly with an increase in concentration for each modifier and conversely water recoveries increased slightly with an increase in concentration. $KMnO_4$ at a high concentration of $1x10^{-2}$ mols is an outlier, a significant drop in solids recovery to 79.9 g was obtained. Moreover the same condition gave a pronounced increase in water recoveries from 368.41 g to 1388.35 g.

5.4.4 Copper recoveries as a function of time

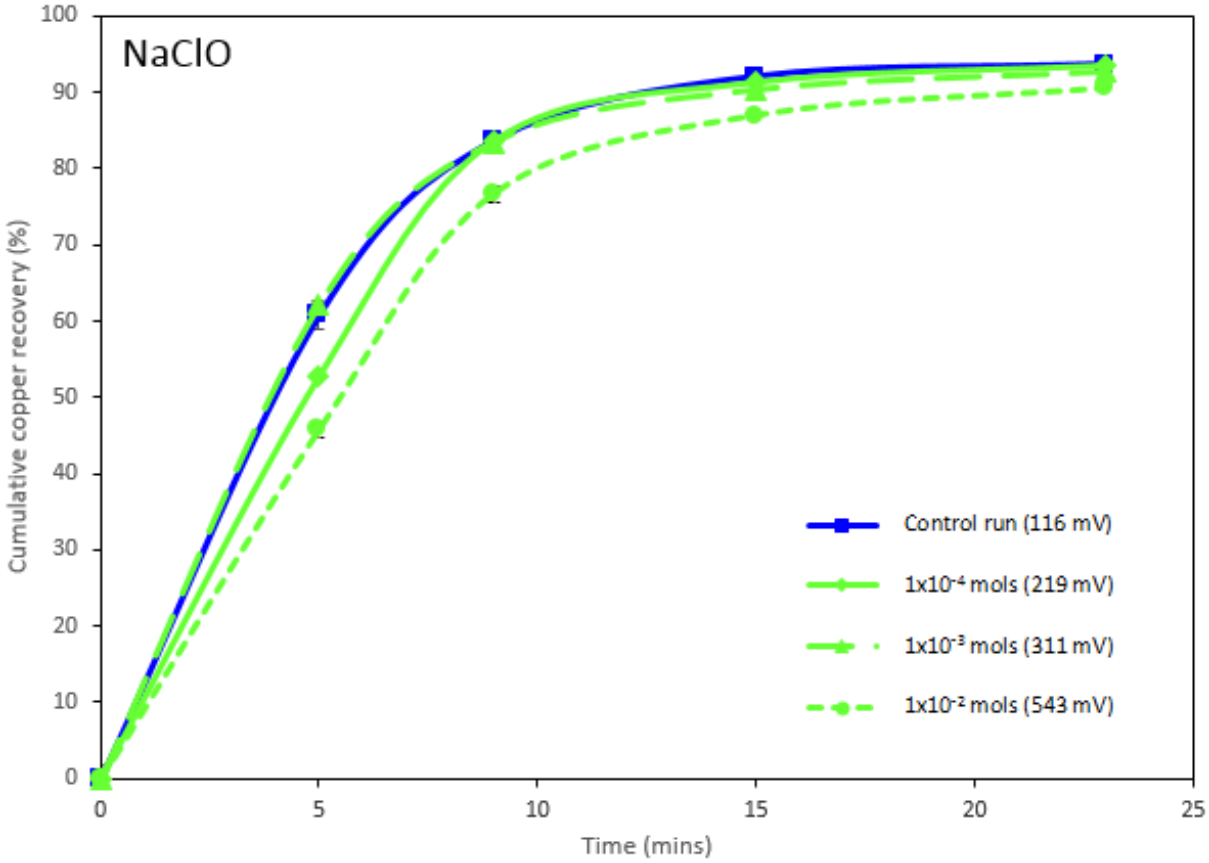

Figure 5.16: Cumulative copper recovery as a function of flotation time in 100 g/t SIBX & 40 g/t DOW 200 at $1x10^{-4}$, $1x10^{-3}$ and $1x10^{-2}$ mols of NaClO. Error bars represent standard error between duplicate tests.

As shown in Figure 5.16, very high copper recoveries >90% were obtained with and without NaClO. The graph shows that the same copper recovery can be achieved over the Eh range of 116-543 mV both in the absence and in the presence of NaClO. However, a very slight decrease in copper recovery with an increase in concentration and thus an increase in Eh was observed. It is clear from the graph that the rates of final copper recoveries for all conditions under investigation are the same.

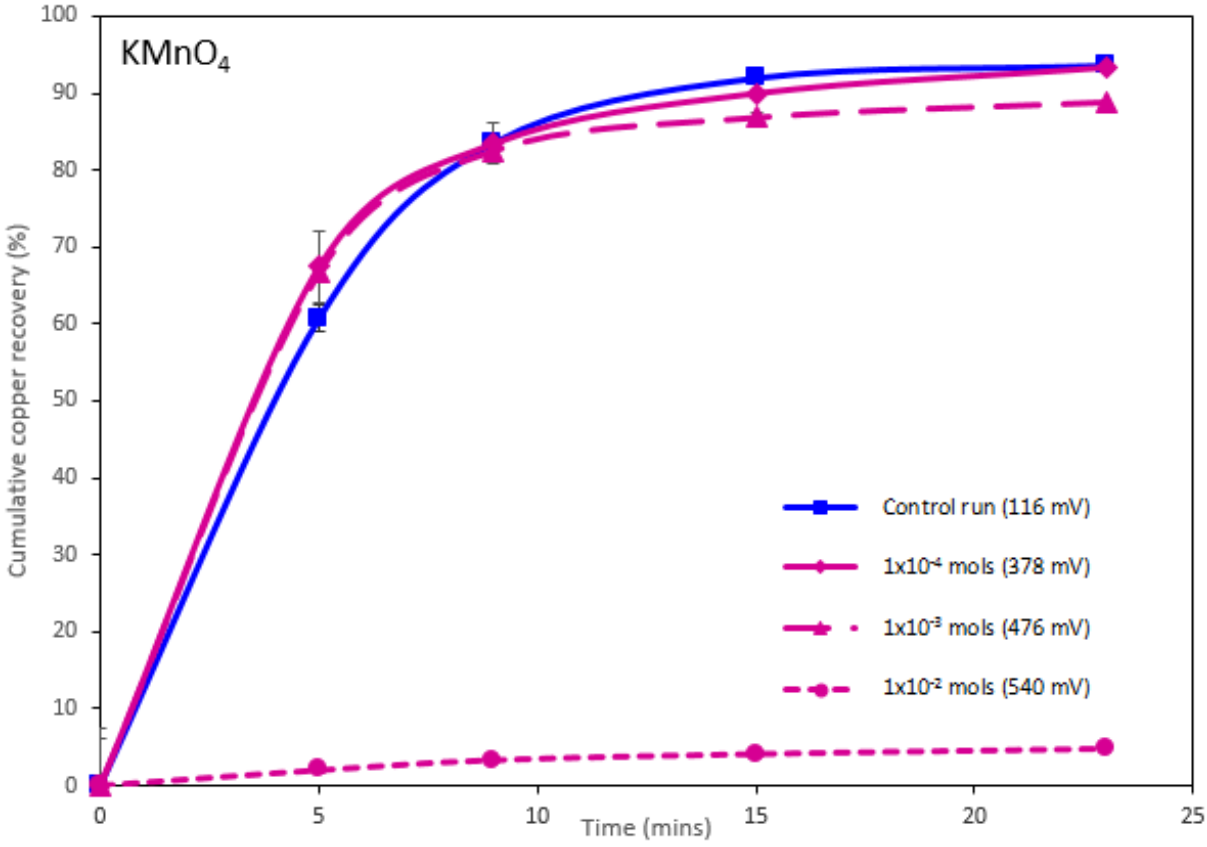

Figure 5.17: Cumulative copper recovery as a function of flotation time in 100 g/t SIBX & 40 g/t DOW 200 at $1x10^{-4}$, $1x10^{-3}$ and $1x10^{-2}$ mols of $KMnO_4$. Error bars represent standard error between duplicate tests.

Figure 5.17 shows cumulative copper recovery as a function of time in the presence of $KMnO_4$. Adverse effects of $KMnO_4$ on copper recoveries are observed at a concentration level of $1x10^{-2}$ mols (Eh of 500 mV), below which higher recoveries above 88% were acquired. This indicates that the rate of copper recovery is extremely reduced at a concentration of $1x10^{-2}$ mols $KMnO_4$, with the highest rate of copper recovery obtained without $KMnO_4$ and at the lowest concentration of $KMnO_4$.

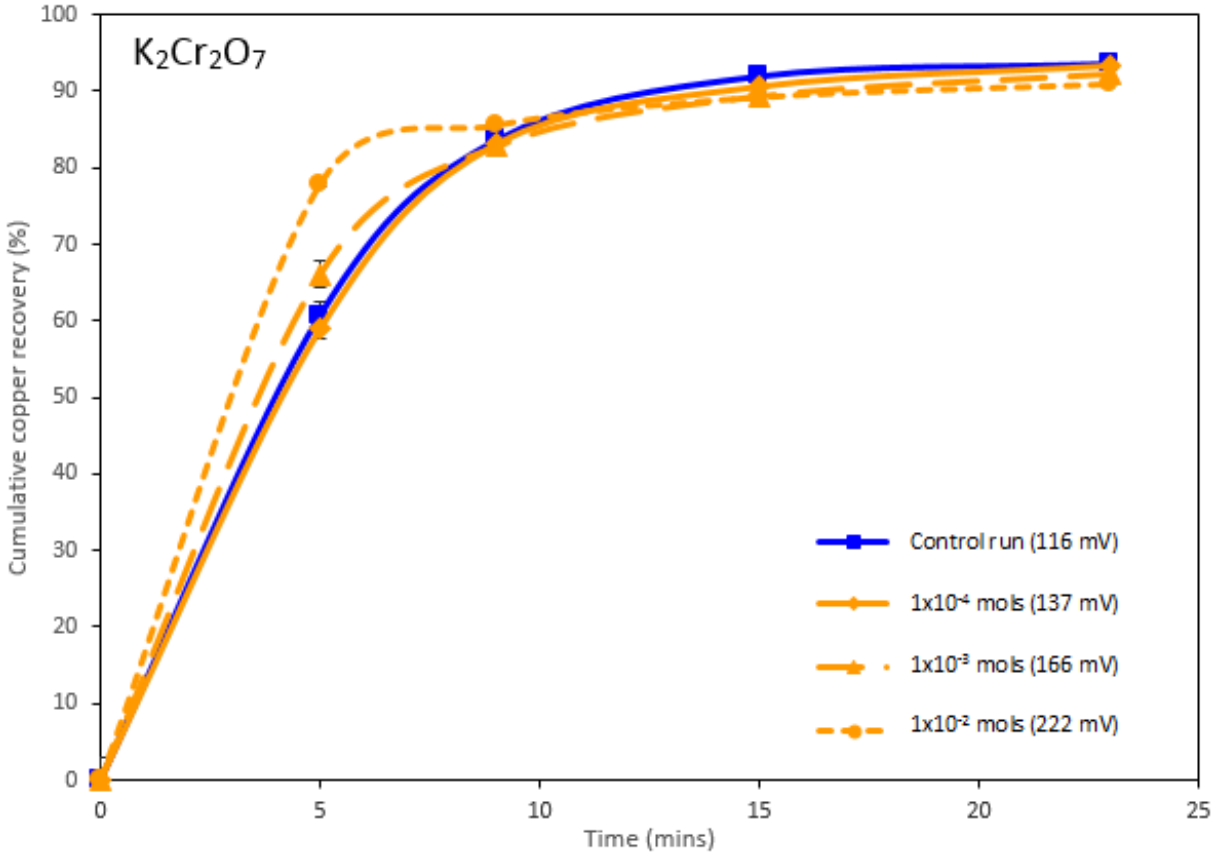

Figure 5.18: Cumulative copper recovery as a function of flotation time in 100 g/t SIBX & 40 g/t DOW 200 at $1x10^{-4}$, $1x10^{-3}$ and $1x10^{-2}$ mols of $K_2Cr_2O_7$. Error bars represent standard error between duplicate tests.

It is evident that in Figure 5.18 the final copper recoveries with and without $K_2Cr_2O_7$ are comparable. However, a slight reduction in copper recoveries is observed with an increase in concentration. It is illustrated in Figure 5.18 that the rates of maximum copper recovery for all conditions with and without $K_2Cr_2O_7$ are similar.

5.4.5 Copper recoveries as a function of water recovery

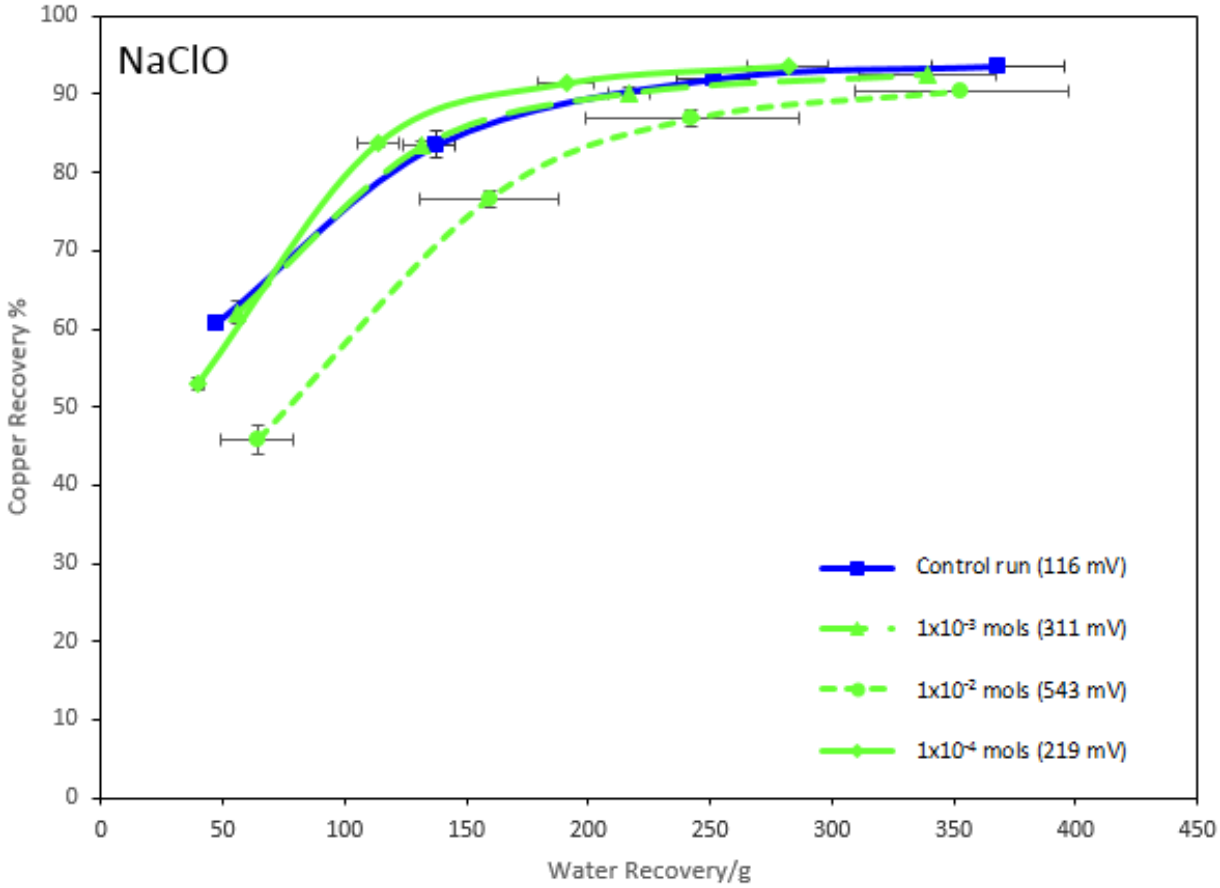

Figure 5.19: Cumulative copper recovery as a function of water recovery in 100 g/t SIBX & 40 g/t DOW 200 at $1x10^{-4}$, $1x10^{-3}$ and $1x10^{-2}$ mols of NaClO. Error bars represent standard error between duplicate tests.

Figure 5.19 shows the cumulative percentage of copper recovery per unit water recovery for NaClO at various concentrations. The data shown illustrates that an increase in NaClO concentration decreases copper recovery per unit water recovery. It is evident that the condition with no modifier at an Eh of 116 mV and the condition with $1x10^{-3}$ mols NaClO (311 mV) showed a similar trend. However NaClO at a concentration of $1x10^{-4}$ mols (219 mV) and $1x10^{-3}$ mols (311 mV) together with the condition without modifier all had the same final copper recoveries. Nevertheless, higher water recoveries were obtained with no modifier whereas the least water recovery was obtained at the least NaClO concentration, $1x10^{-4}$ mols (219 mV).

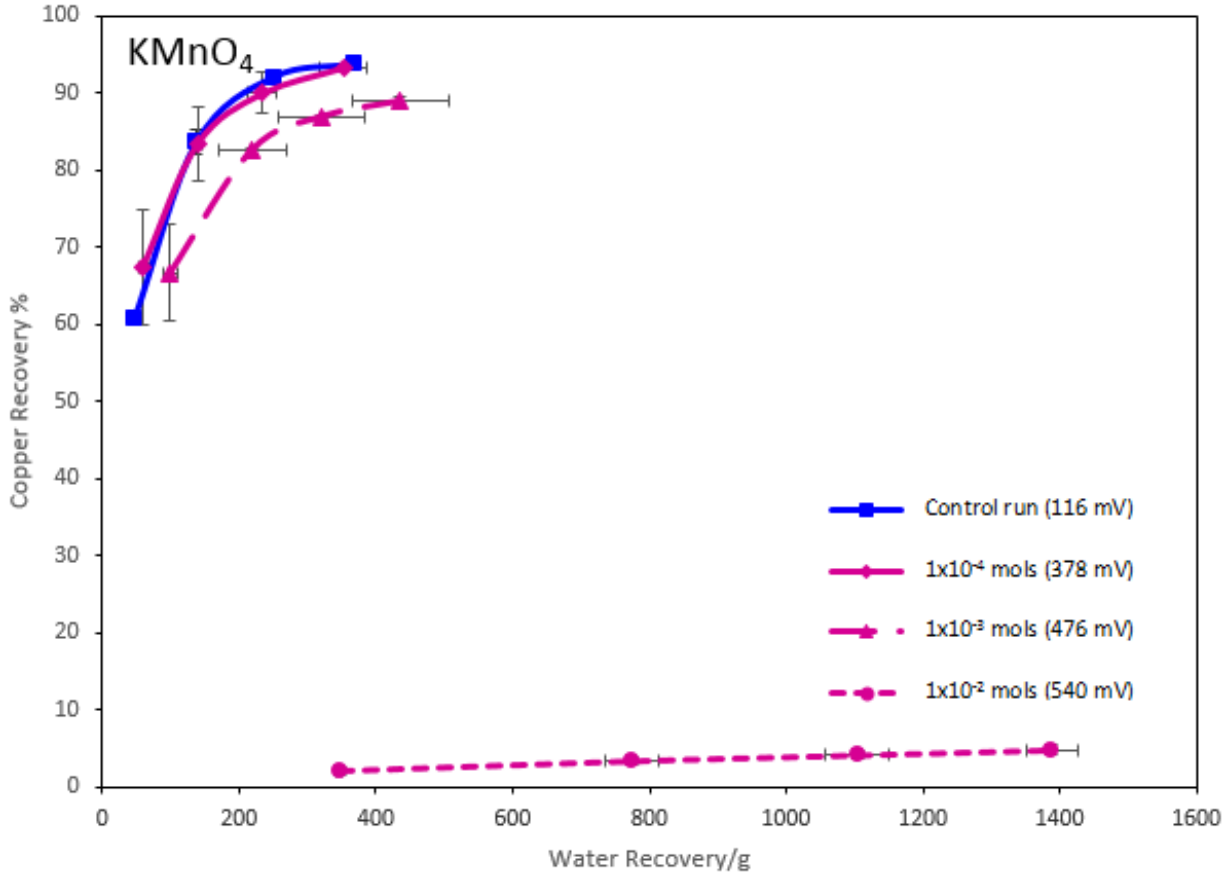

Figure 5.20: Cumulative copper recovery as a function of water recovery in 100 g/t SIBX & 40 g/t DOW 200 at $1x10^{-4}$, $1x10^{-3}$ and $1x10^{-2}$ mols of $KMnO_4$. Error bars represent standard error between duplicate tests.

The cumulative copper recovery as a function of water recovery for $KMnO_4$ at various concentrations is shown in Figure 5.20. It is evident that $1x10^{-2}$ mols of $KMnO_4$ (540 mV) drastically reduces final copper recoveries to 4.8%, yet a very high amount of water was recovered. Furthermore, the straight line obtained at this condition is an indication of entrainment. Overall, an increase in concentration of $KMnO_4$ reduces copper recoveries per unit water recovery. The trend for the condition with no modifier was similar to that of $1x10^{-4}$ mols $KMnO_4$ (378 mV).

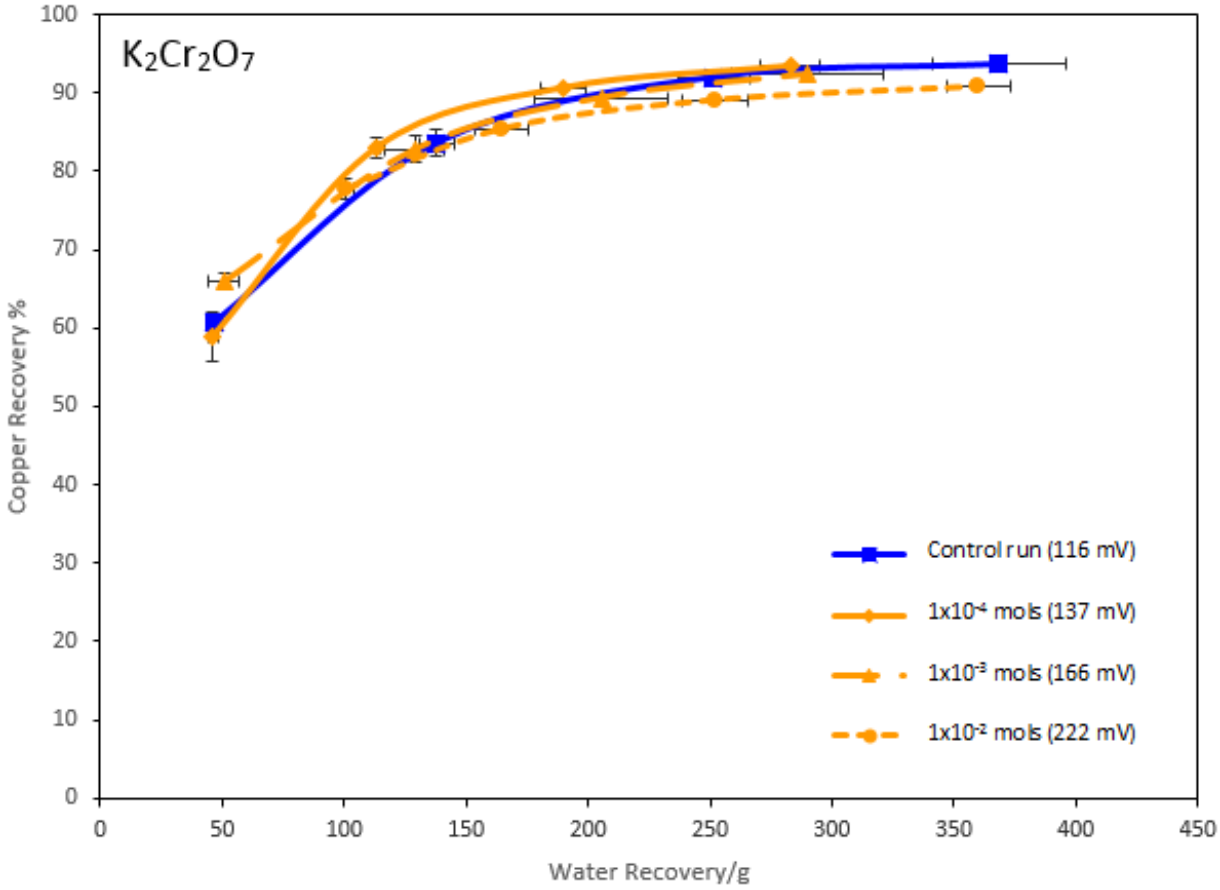

Figure 5.21: Cumulative copper recovery as a function of water recovery in 100 g/t SIBX & 40 g/t DOW 200 at $1x10^{-4}$, $1x10^{-3}$ and $1x10^{-2}$ mols of $K_2Cr_2O_7$. Error bars represent standard error between duplicate tests.

Figure 5.21 illustrates cumulative copper recovery as a function of water recovery with $K_2Cr_2O_7$ at various concentrations. The graph shows similar final copper recoveries for all conditions, however a slight decrease in copper recoveries with an increase in $K_2Cr_2O_7$ concentration was acquired. Higher water was recovered without $K_2Cr_2O_7$ and at the highest concentration of $1x10^{-2}$ mols $K_2Cr_2O_7$ at an Eh of 222 mV.

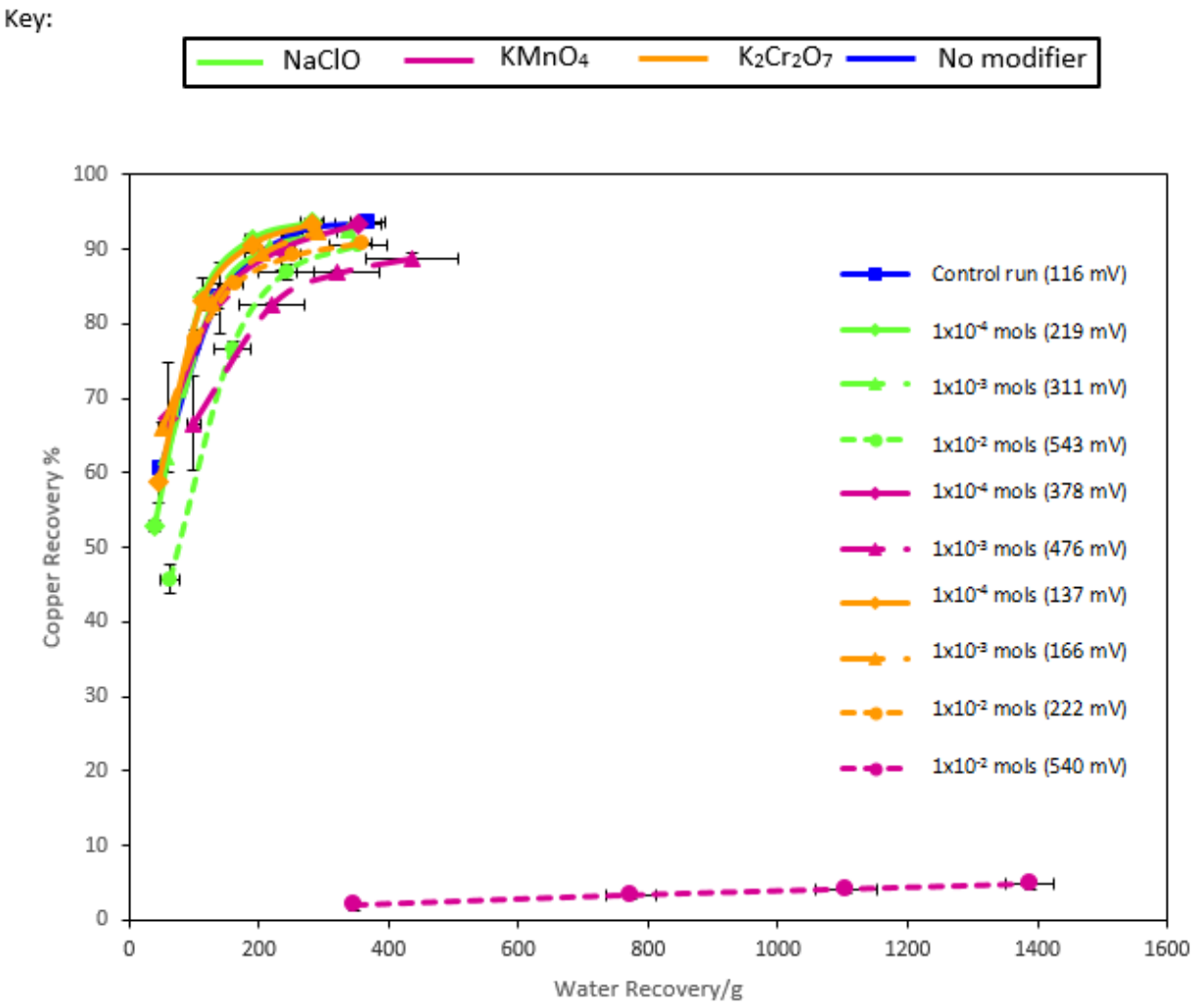

Figure 5.22: Copper recovery as a function of water recovery in 100 g/t SIBX & 40 g/t DOW 200 for all test conditions. Error bars represent standard error between duplicate tests.

Figure 5.22 shows copper recoveries versus water recovery for all test conditions. Maximum copper recoveries and minimum water recoveries were attained at lower concentrations/Eh for all potential modifiers. Alternatively, minimum copper recoveries and maximum water recoveries were obtained at higher concentrations and thus higher Eh values. A prominent change can be seen at $1x10^{-2}$ mols $KMnO_4$, where copper recovery was significantly decreased and a very high water recovery was obtained.

5.4.6 Copper grades as a function of copper recoveries

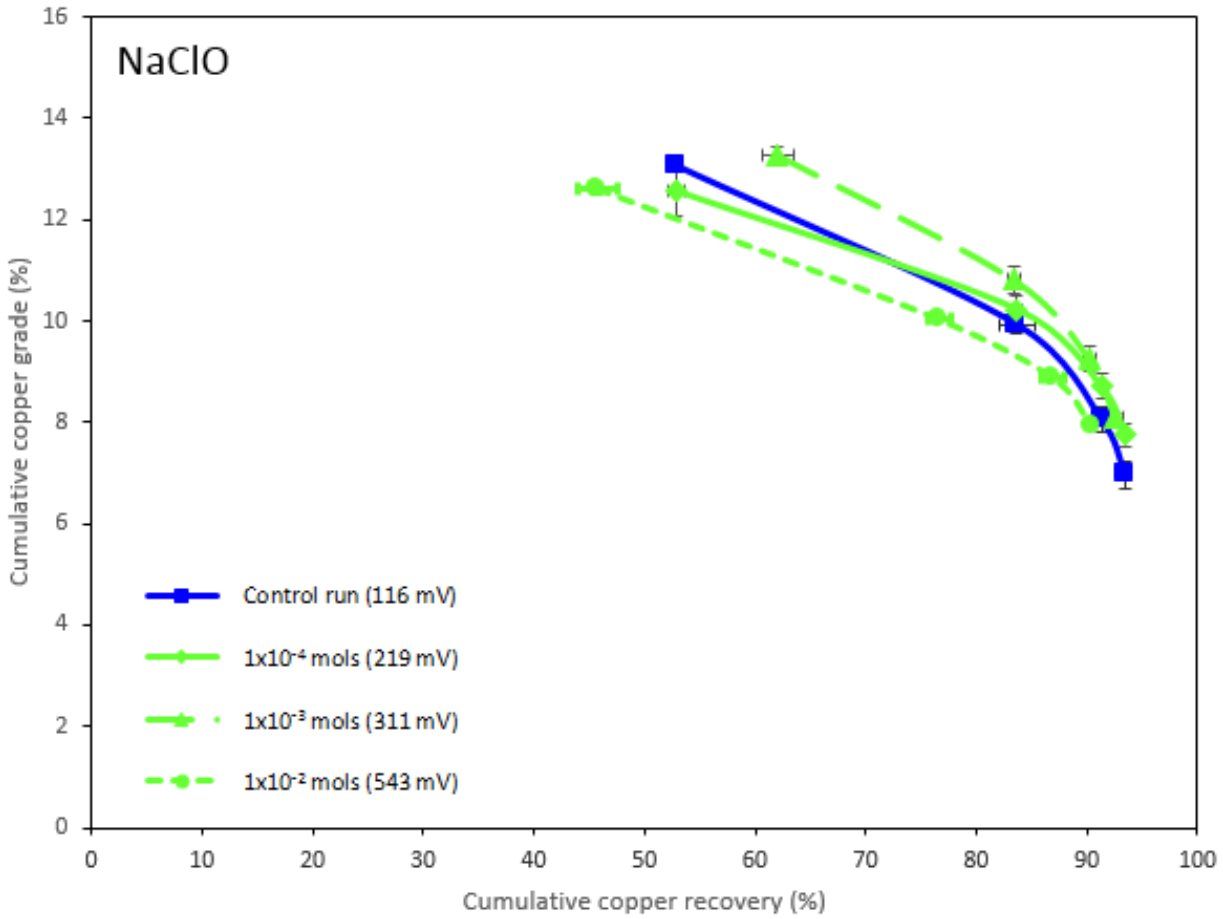

Figure 5.23: Cumulative copper grade as a function of cumulative copper recovery in 100 g/t SIBX & 40 g/t DOW 200 at $1x10^{-4}$, $1x10^{-3}$ and $1x10^{-2}$ mols of NaClO. Error bars represent standard error between duplicate tests.

As shown in Figure 5.23, the use of NaClO at any concentration improved copper grades. Final copper recoveries obtained for the conditions investigated in Figure 5.23 did not show significant differences. However, the use of NaClO under the conditions investigated resulted in improved final copper grades compared to the condition without NaClO.

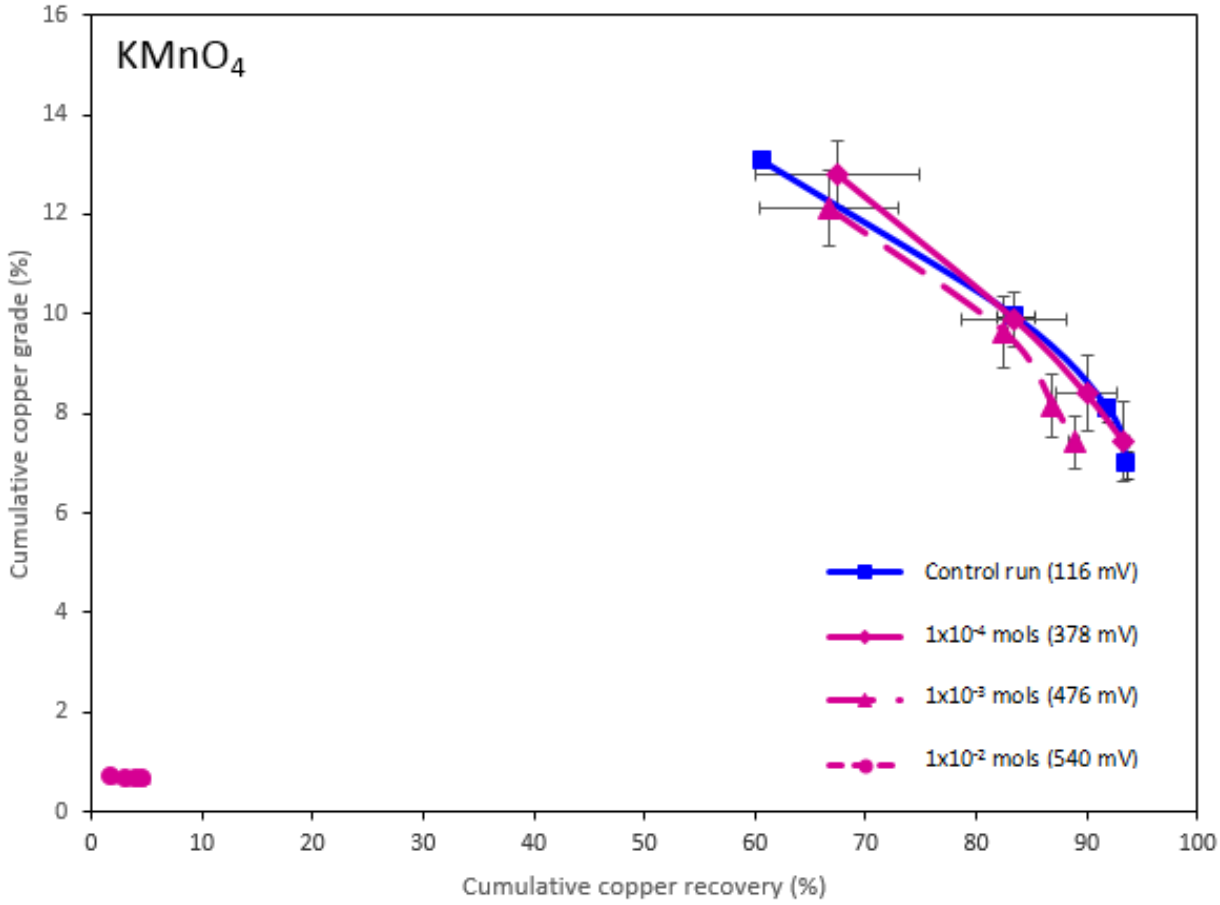

Figure 5.24: Cumulative copper grade as a function of cumulative copper recovery in 100 g/t SIBX & 40 g/t DOW 200 at $1x10^{-4}$, $1x10^{-3}$ and $1x10^{-2}$ mols of $KMnO_4$. Error bars represent standard error between duplicate tests.

Figure 5.24 illustrates cumulative copper grade as a function of cumulative copper recovery in the presence of $KMnO_4$. It is shown that the use of $KMnO_4$ at an Eh of 540 mV had an adverse effect on both copper recovery and copper grade. The graph shows that a decrease in concentration of $KMnO_4$ increased the final copper recoveries. It is clear that the condition with no modifier and the condition with the lowest concentration of $KMnO_4$ resulted in higher copper recoveries compared to conditions with higher concentrations of $KMnO_4$. With regards to final copper grades, the condition without $KMnO_4$ and conditions with lower concentrations of $KMnO_4$ did not significantly differ, with the exception of the highest concentration of $KMnO_4$, where the copper grade obtained was below 1%.

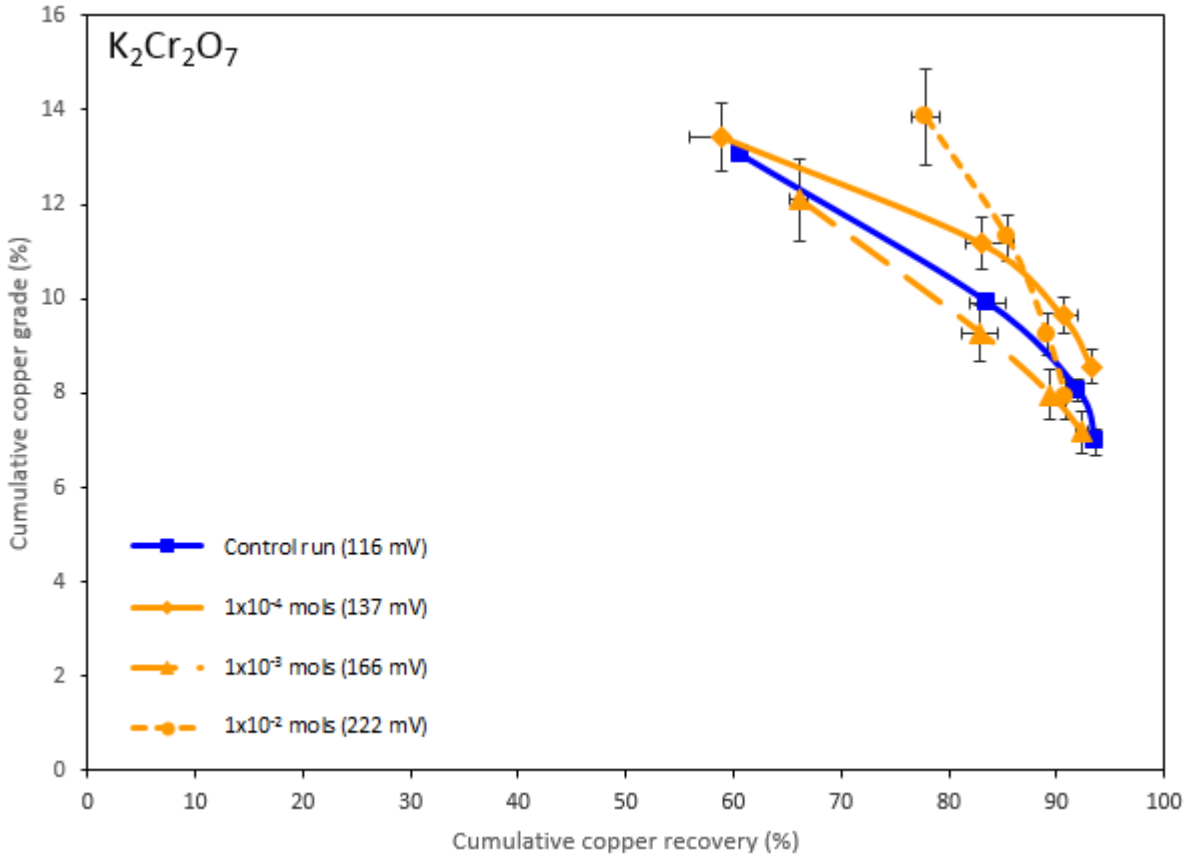

Figure 5.25: Cumulative copper grade as a function of cumulative copper recovery in 100 g/t SIBX & 40 g/t DOW 200 at $1x10^{-4}$, $1x10^{-3}$ and $1x10^{-2}$ mols of $K_2Cr_2O_7$. Error bars represent standard error between duplicate tests.

Figure 5.25 indicates cumulative copper grade as a function of cumulative copper recovery in the presence of $K_2Cr_2O_7$. Final copper recoveries for the conditions investigated were not significantly different, however an increase in concentration of $K_2Cr_2O_7$ (increase in Eh), slightly decreased final copper recoveries. With reference to copper grades, the highest and the lowest concentrations of $K_2Cr_2O_7$ improved final copper grades compared to the other conditions under investigation.

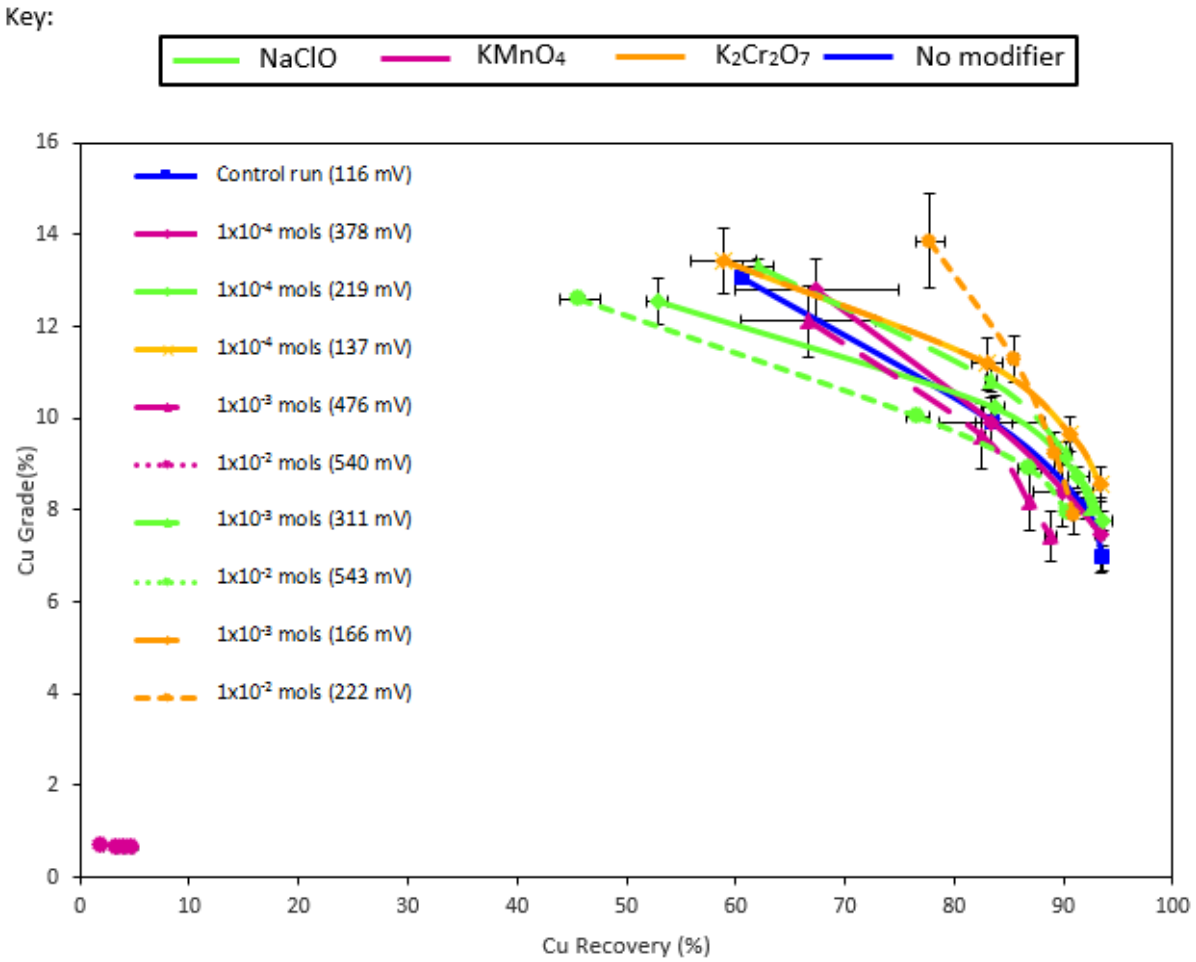

Figure 5.26: Cumulative copper grades as a function of cumulative copper recoveries in 100 g/t SIBX & 40 g/t DOW 200 at given conditions. Error bars represent standard error between duplicate tests.

The results for cumulative copper grades as a function of cumulative copper recoveries for all conditions are shown in Figure 5.26. The graph indicates that higher copper recoveries were obtained at lower concentrations and thus lower Eh values for all potential modifiers investigated. The highest concentration of $KMnO_4$ had a drastic effect on both copper recovery and copper grade compared with other potential modifiers. However, all other conditions of potential modifiers improved copper grades compared to the control test.

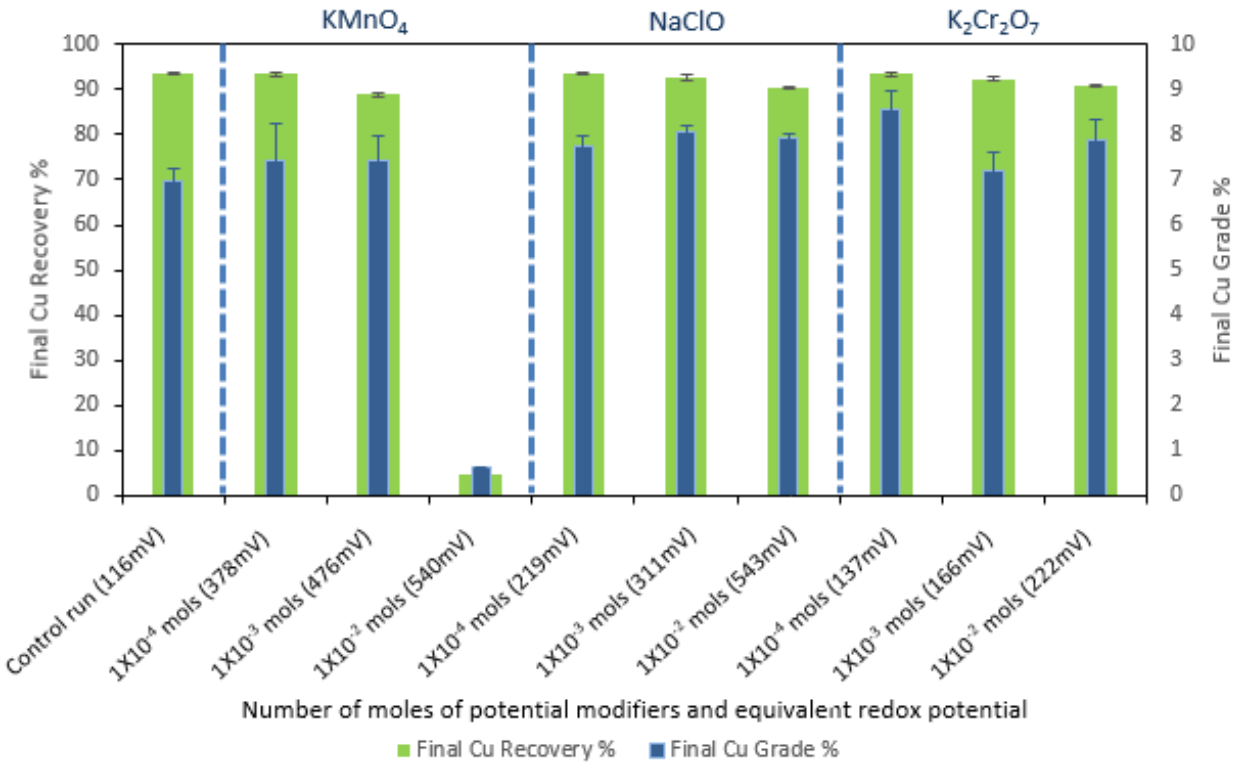

Figure 5.27: Final copper recoveries as a function of final copper grades in 100 g/t SIBX & 40 g/t DOW 200 at given conditions. Error bars represent standard error between duplicate tests.

Figure 5.27 shows final copper recoveries and copper grades for all conditions evaluated. High copper recoveries of ≥90% were obtained for most conditions, with the control run having the highest copper recovery of 93.64%. Compared to the control run, all other conditions did not show significant differences in copper recoveries and copper grades. However, $KMnO_4$ had a detrimental effect on copper at higher concentrations of $1x10^{-2}$ mols (Eh of 540 mV). A very low copper recovery of 4.8% and a low copper grade of 0.62% were obtained. It is interesting to note that at $1x10^{-2}$ mols, NaClO and $KMnO_4$ resulted in the same redox potential range but gave significantly different copper recoveries and copper grades. It is evident that albeit potential modifiers may give the same redox potential, their effect on mineral recoveries could differ, which indicates that this could be an effect contributed by the concentration and type of potential modifier. Though the graph shows no significant changes in copper recoveries and grades for most conditions, an increase in concentration and thus redox potential, upon addition of each potential modifier resulted in a slight decrease in copper recoveries and conversely in a slight increase in copper grades, which is consistent with the solids and water recoveries.

5.4.7 Flotation kinetics

Batch flotation tests were further analysed and interpreted using flotation kinetics with the aid of a kinetic model called the Klimpel model. The Klimpel model is considered as one of the most successful models in flotation by Mineral Technologies International, Inc. (2010). The Klimpel model was proposed by Klimpel (1980) and has been applied to most flotation tests. It is the simplest formulation of the distributed rate constant model and it is used for the simulation of single flotation cells. This model was based on earlier experimental flotation kinetic studies, where it was observed that not all particles are recovered during a flotation process no matter how much residence time is given. It assumes that each particle type has ultimate recovery that is less than 100% and that the particles that float can be recovered at a rate that is governed by a simple first order kinetic law. The Klimpel model describes recovery, R, as shown in equation 5.3 below:

$$R = R_{max}\left[1 - \frac{1-e^{-kt}}{kt}\right] \quad \text{.....Eqn 5.3}$$

In equation 5.3, R represents the recovery; R_{max} represents the final recovery, t represents flotation time and k represents the flotation rate constant.

The Klimpel model was used to fit the flotation data obtained, in order to determine the flotation kinetics by predicting the flotation rate constant. In this section, graphs of copper recovery as a function of time were used to describe the flotation kinetics of the investigated conditions. Therefore the term rate shall be used to refer to the percentage of copper recovery per minute.

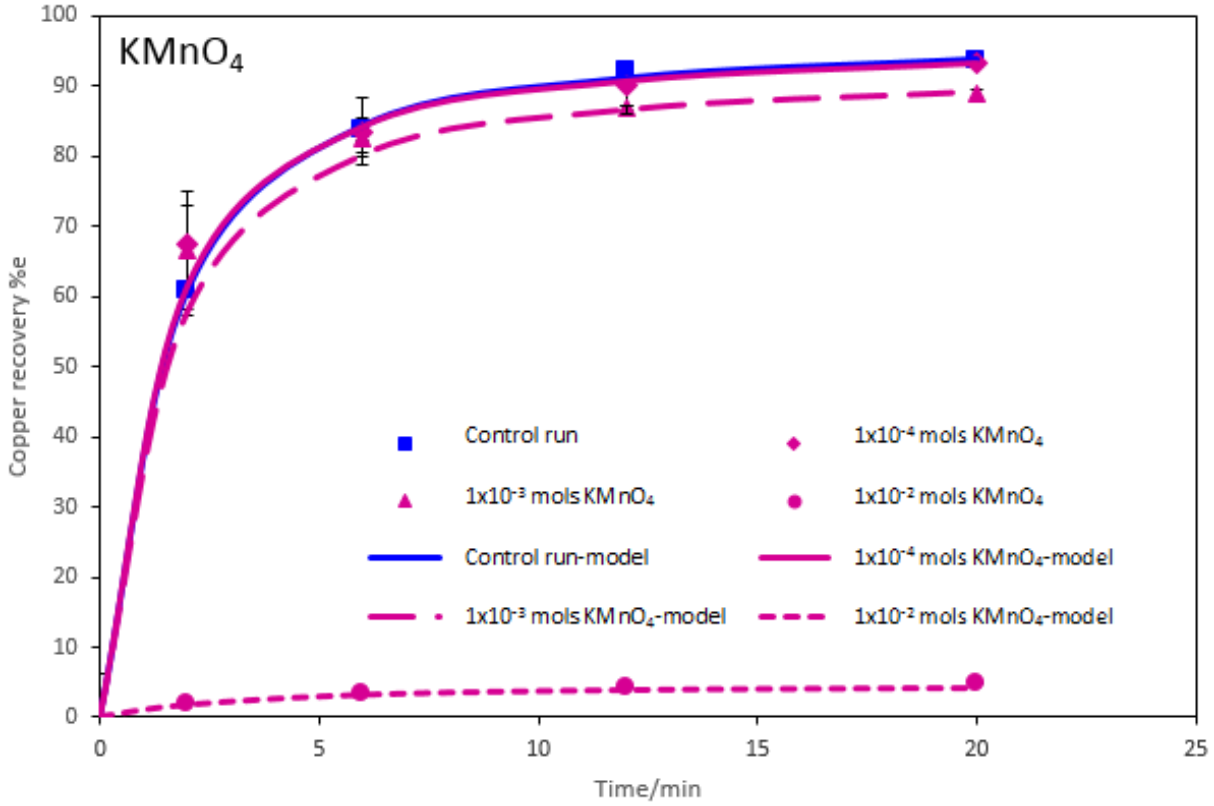

Figure 5.28: Copper recovery as a function of time for $KMnO_4$ .The experimental runs are represented by the data points and the respective fitted models are represented by solid lines. Error bars represent standard error between duplicate tests.

The theoretical maximum recovery (R_{max}) and the rate constants obtained from fitting data for $KMnO_4$ conditions to the Klimpel model are shown in Table 5.1.

Table 5.1: Maximum copper recoveries and flotation rate constants obtained with $KMnO_4$.

Condition	**Rmax (%)**	**k (min^{-1})**
Control run (116 mV)	98	1.2
$1x10^{-4}$ mols $KMnO_4$ (378 mV)	97	1.25
$1x10^{-3}$ mols $KMnO_4$ (476 mV)	93	1.2
$1x10^{-2}$ mols $KMnO_4$ (540 mV)	4.8	0.5

Figure 5.28 shows the flotation kinetics for copper under $KMnO_4$ addition. It is evident that the addition of $KMnO_4$ at different concentrations changed the cumulative copper recovery since different R_{max} values were obtained for the conditions investigated. The control run and

$1x10^{-4}$ mols $KMnO_4$ has almost similar R_{max} values with a slight decrease in copper recovery observed at $1x10^{-3}$ mols $KMnO_4$. A significantly low copper recovery was obtained at $1x10^{-2}$ mols $KMnO_4$ were decreased reaction kinetics were obtained as evidenced by the low rate constant value. Furthermore the Klimpel model constants show increased reaction kinetics for other conditions under investigation as shown in Table 5.1. Overall, in the presence of $KMnO_4$, within an Eh range of 116 mV- 476mV, high copper recoveries were observed with almost similar but increased reaction kinetics. Above 500 mV, significantly low copper recoveries were obtained in conjunction with very low reaction kinetics.

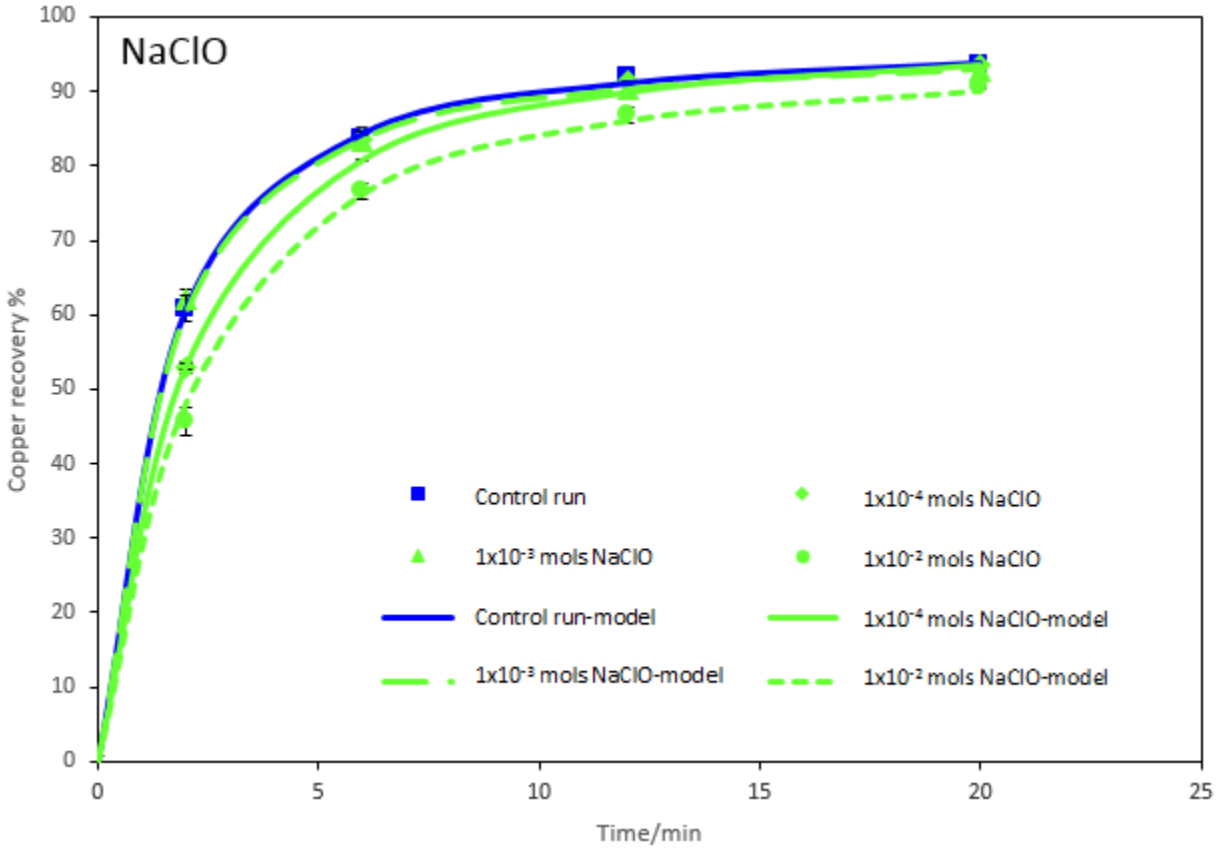

Figure 5.29: Copper recovery as a function of time for NaClO. The experimental runs are represented by the data points and fitted models are represented by solid lines. Error bars represent standard error between duplicate tests.

The theoretical maximum recovery (R_{max}) and the rate constants obtained from fitting data for NaClO conditions to the Klimpel model are shown in Table 5.2.

Table 5.2: Maximum copper recoveries and flotation rate constants obtained with NaClO.

Condition	Rmax (%)	k (min^{-1})
Control run (116 mV)	98	1.2
$1x10^{-4}$ mols NaClO (219 mV)	99	0.9
$1x10^{-3}$ mols NaClO (311 mV)	97	1.2
$1x10^{-2}$ mols NaClO (543 mV)	96	0.8

Figure 5.29 illustrates the flotation kinetics for copper in NaClO. It is evident that the addition of NaClO at different concentrations did not significantly change the cumulative copper recovery since the R_{max} values obtained were not significantly different. However, a slight decrease in copper recoveries at $1x10^{-3}$ mols and $1x10^{-2}$ mols NaClO was observed. The Klimpel model constants in Table 5.2 show that increased reaction kinetics were obtained in the absence of NaClO (Eh of 116 mV) and at $1x10^{-3}$ mols NaClO (Eh of 311mV) with the lowest reaction kinetics obtained in the presence of $1x10^{-2}$ mols NaClO (Eh of 543 mV).

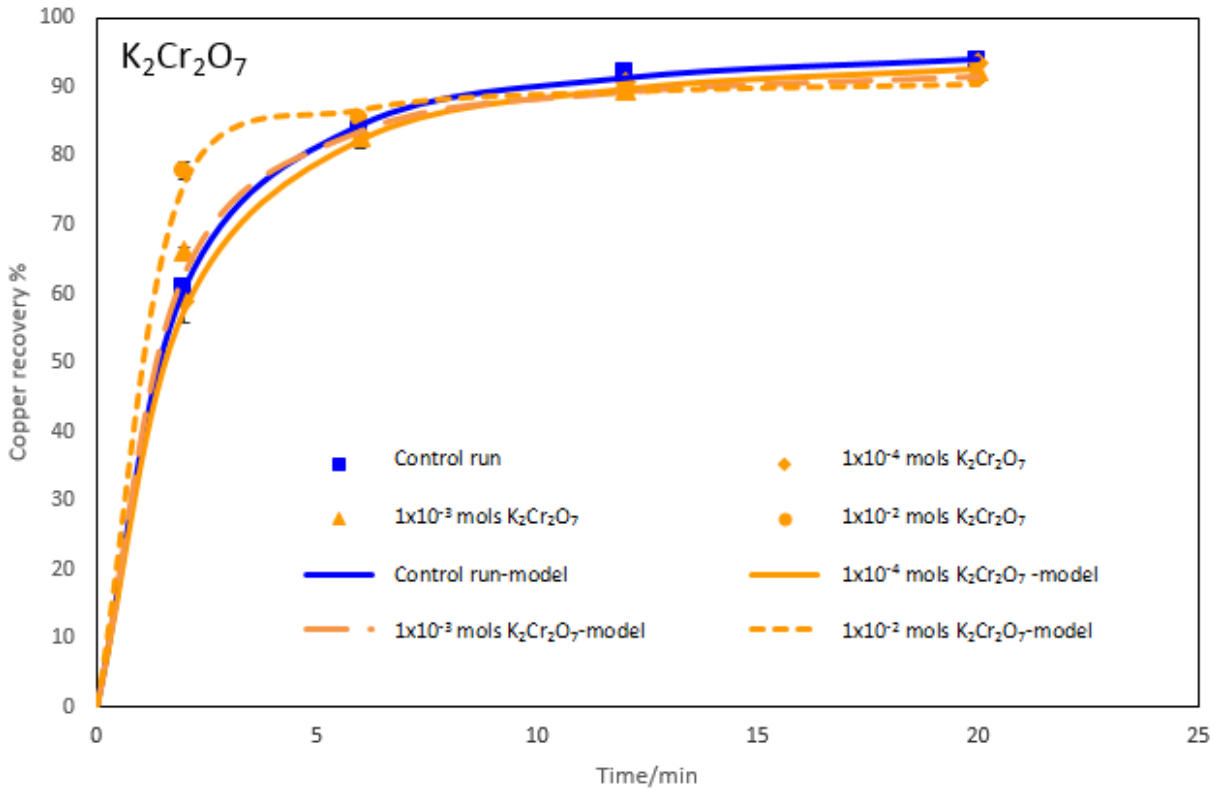

Figure 5.30: Copper recovery as a function of time for $K_2Cr_2O_7$. The experimental runs are represented by the data points and fitted models are represented by solid lines. Error bars represent standard error between duplicate tests.

The theoretical maximum recovery (R_{max}) and the rate constants obtained from fitting data for $K_2Cr_2O_7$ conditions to the Klimpel model are shown in Table 5.3.

Table 5.3: Maximum copper recoveries and flotation rate constants obtained with $K_2Cr_2O_7$.

Condition	**Rmax (%)**	**k (min^{-1})**
Control run (116 mV)	98	1.2
$1x10^{-4}$ mols $K_2Cr_2O_7$ (137 mV)	97	1.1
$1x10^{-3}$ mols $K_2Cr_2O_7$ (166 mV)	95	1.4
$1x10^{-2}$ mols $K_2Cr_2O_7$ (222 mV)	92	2.9

Figure 5.30 shows copper recoveries as a function of time in the presence of $K_2Cr_2O_7$. The highest R_{max} values were obtained in the absence of $K_2Cr_2O_7$ and at the lowest concentration of $K_2Cr_2O_7$ ($1x10^{-4}$ mols). In addition, the aforementioned conditions have the lowest reaction

kinetics as shown. Alternatively, at the highest concentration of $K_2Cr_2O_7$, at $1x10^{-2}$ mols, the lowest R_{max} value was obtained which corresponds to a higher reaction kinetics as evidenced by the high rate constant value obtained.

5.4.8 Gangue recovery

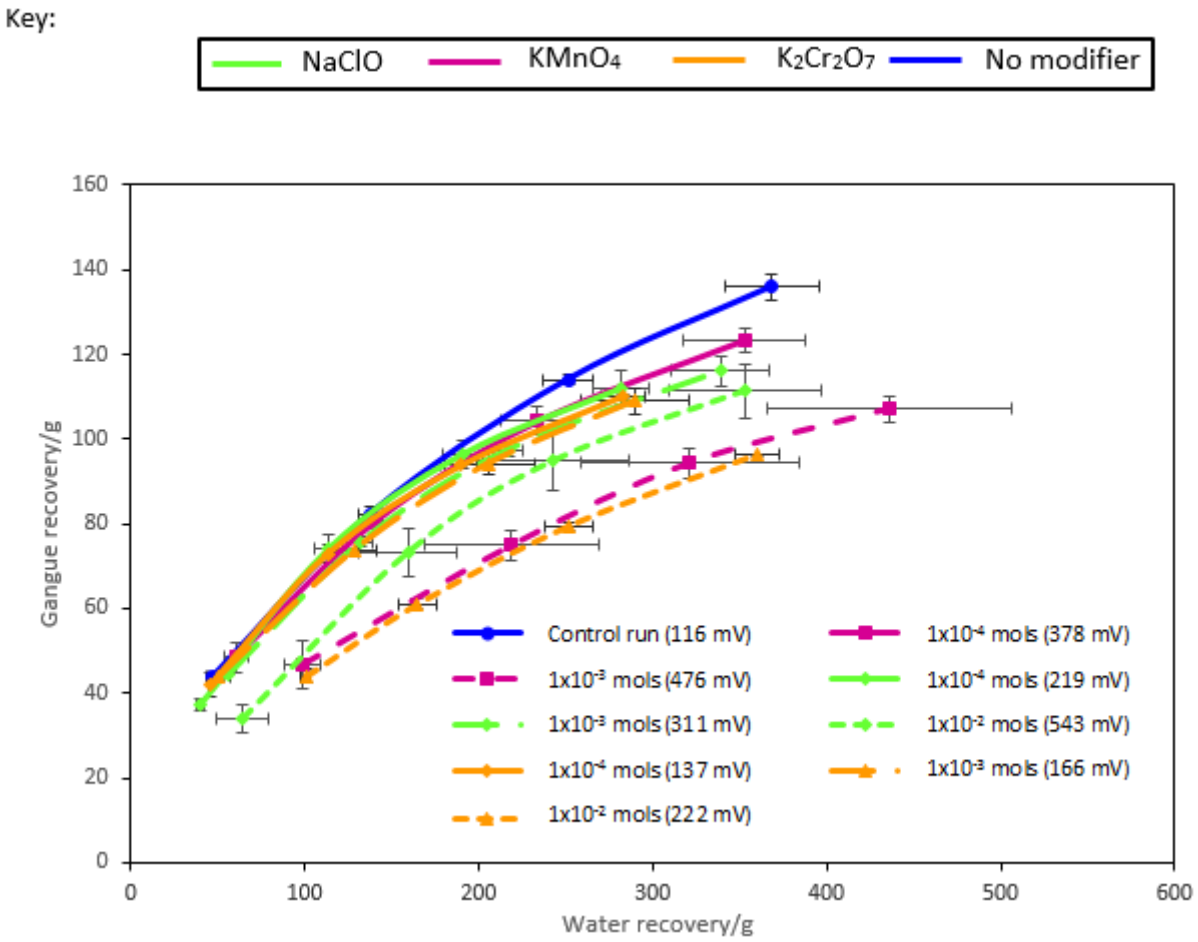

Figure 5.31: Gangue recovery as a function of water recovery at given conditions in 100 g/t SIBX & 40 g/t DOW 200. Error bars represent standard error between duplicate tests.

Figure 5.31 shows cumulative gangue recovery as a function of cumulative water recovery for all conditions under investigation. It is evident from this graph that the highest amount of gangue recovery was obtained with the control run. On the contrary, the lowest gangue recovery was attained at $1x10^{-2}$ mols $K_2Cr_2O_7$. It is clear that more gangue per unit water was recovered at lower concentrations of potential modifiers which gave an Eh range of 137-219 mV and consequently decreased with an increase in concentration/Eh. It can be inferred that the use of potential modifiers reduces gangue recovery. Similar trends are observed with the cumulative solids and water recoveries graph, Figure 5.14. Please note that the graph for the

highest concentration of $KMnO_4$ was excluded to allow for a better presentation of data for other conditions as the former was an outlier.

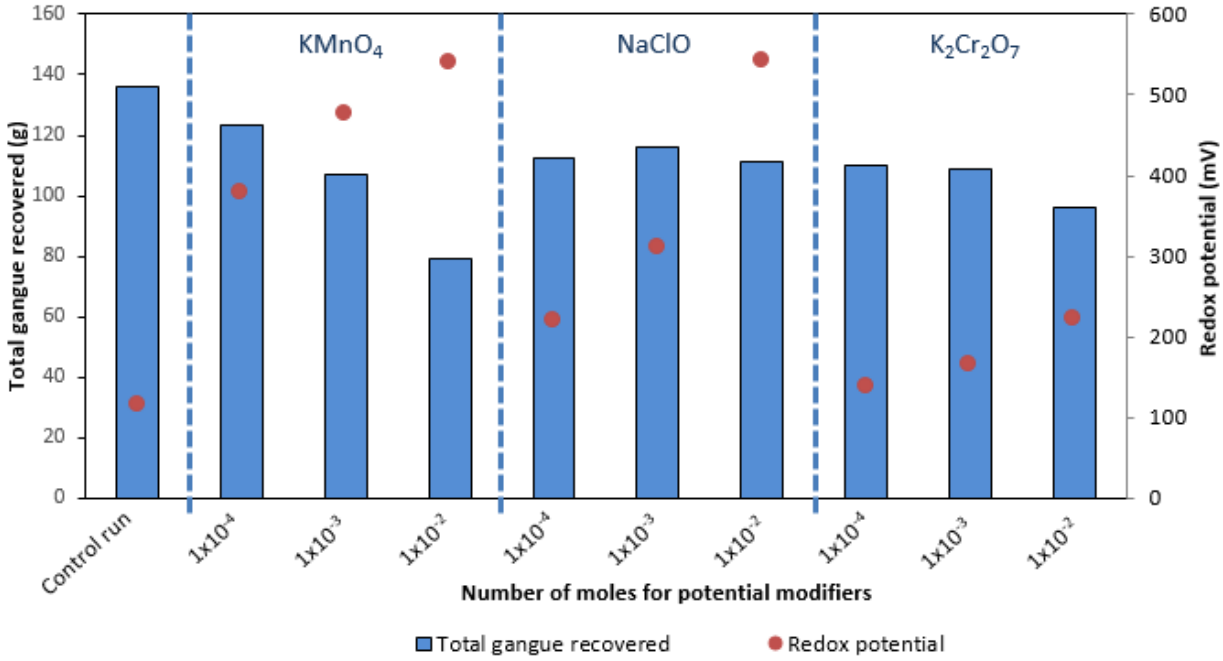

Figure 5.32: Total gangue recovery for conditions under investigation in 100 g/t SIBX & 40 g/t DOW 200. Error bars represent standard error between duplicate tests.

According to Figure 5.32, the highest gangue recovered was obtained with the control run. The lowest amount of gangue recovered was 79.4 g at $1x10^{-2}$ mols $KMnO_4$. A pronounced decrease in gangue recovery with increase in concentration/Eh can be seen for $KMnO_4$. However, pertaining to NaClO, an increase in concentration and thus increase in Eh did not significantly change gangue recovery. Overall, it can be seen that the addition of potential modifiers aids in reducing gangue recovery. Figure 5.32 is consistent with the final solids and water recoveries shown in Figure 5.15.

5.5 The effect of potential modifiers on froth stability

In this section, the effect of potential modifiers on froth stability is analysed. Results for the two phase and three phase systems are reported. A comparison of the dynamic stability factor for all conditions under investigation is given.

As highlighted in Chapter 4, the dynamic test was used to determine H_{max}, which is the maximum froth height achieved at specific conditions (Barbian et al., 2005). The H_{max} measured in the test was in turn used to calculate the dynamic stability factor, $\sum$, as shown in Equation 5.4:

$$\sum = \frac{V_f}{Q} = \frac{H_{max} x A}{Q} \quad \text{.....Eqn 5.4}$$

Where V_f is the volume of foam or froth at equilibrium, Q is the gas volumetric flow rate, H_{max} is the foam or froth height at equilibrium and A is the cross sectional area of the column.

All the potential modifiers used in this investigation at a concentration of $1x10^{-2}$ mols, were excluded from the form and froth stability tests due to the fact that $1x10^{-2}$ mols $KMnO_4$ caused extreme froth instability as shown in Figure 5.33 and hence became an outlier to other conditions.

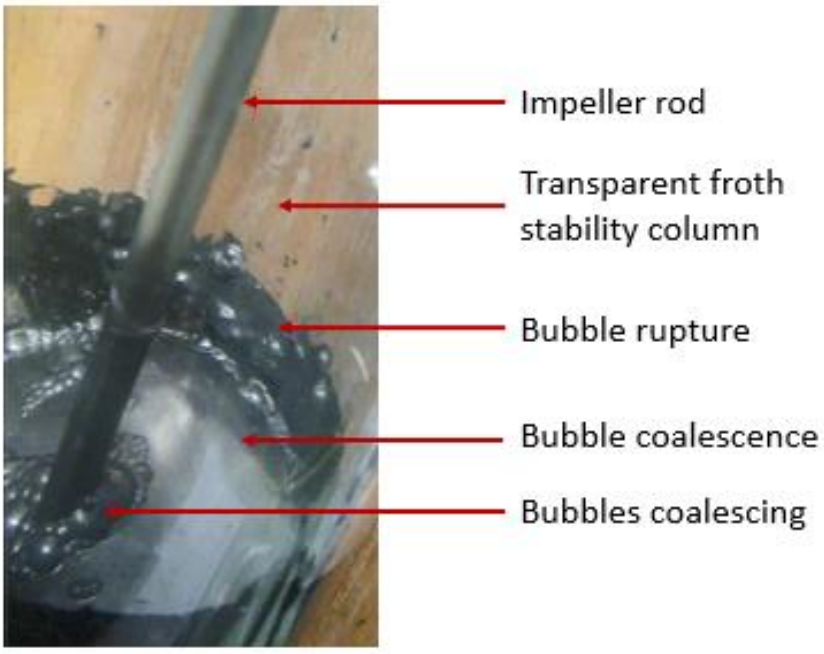

Figure 5.33: Froth instability with $1x10^{-2}$ mols $KMnO_4$.

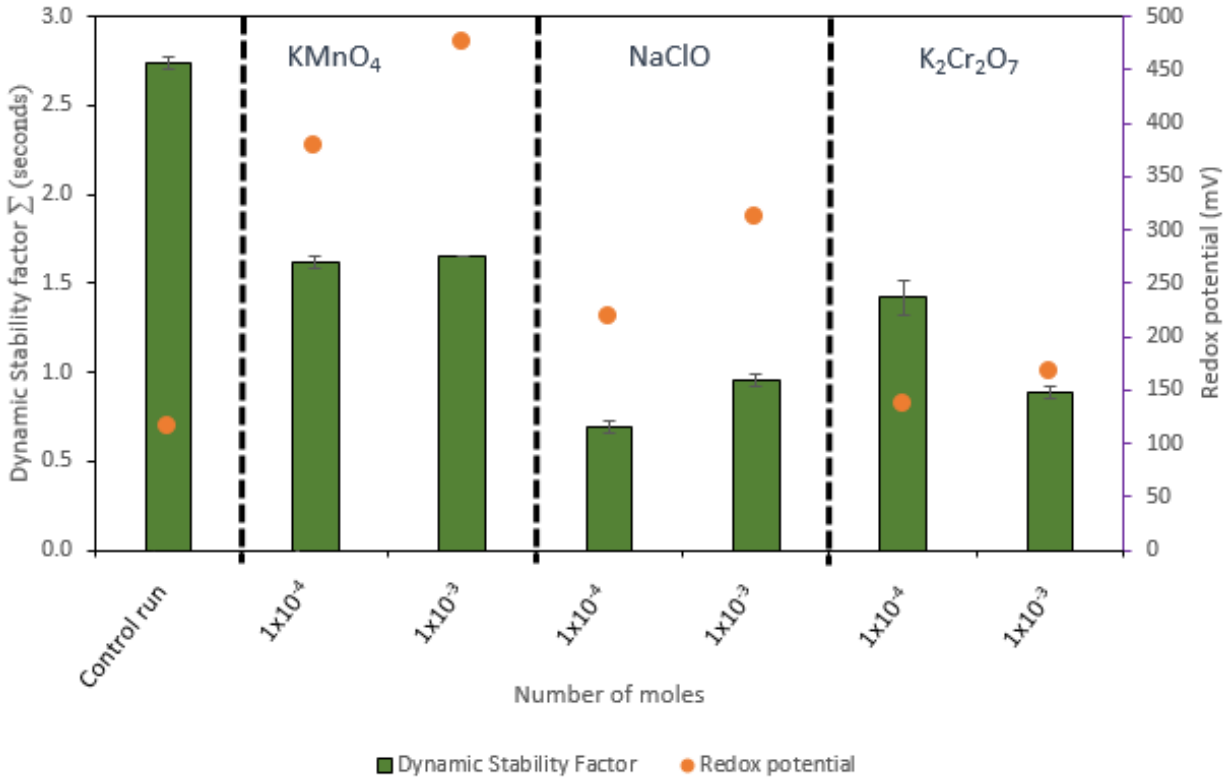

Figure 5.34: Dynamic stability factor for two phase tests for all conditions under investigation in 100 g/t SIBX & 40 g/t DOW 200. Error bars represent standard error between duplicate tests.

Figure 5.34 indicates that the addition of potential modifiers resulted in a decrease in foam stability compared to the control run, in the two phase system. Changing the concentration of $KMnO_4$ and thus Eh did not have an effect on the foam phase. With regards to NaClO, a direct relationship between the concentration/Eh and foam stability was observed. An increase in concentration/Eh increased foam stability. Conversely, addition of $K_2Cr_2O_7$ resulted in a decrease in foam stability with increase in concentration/Eh.

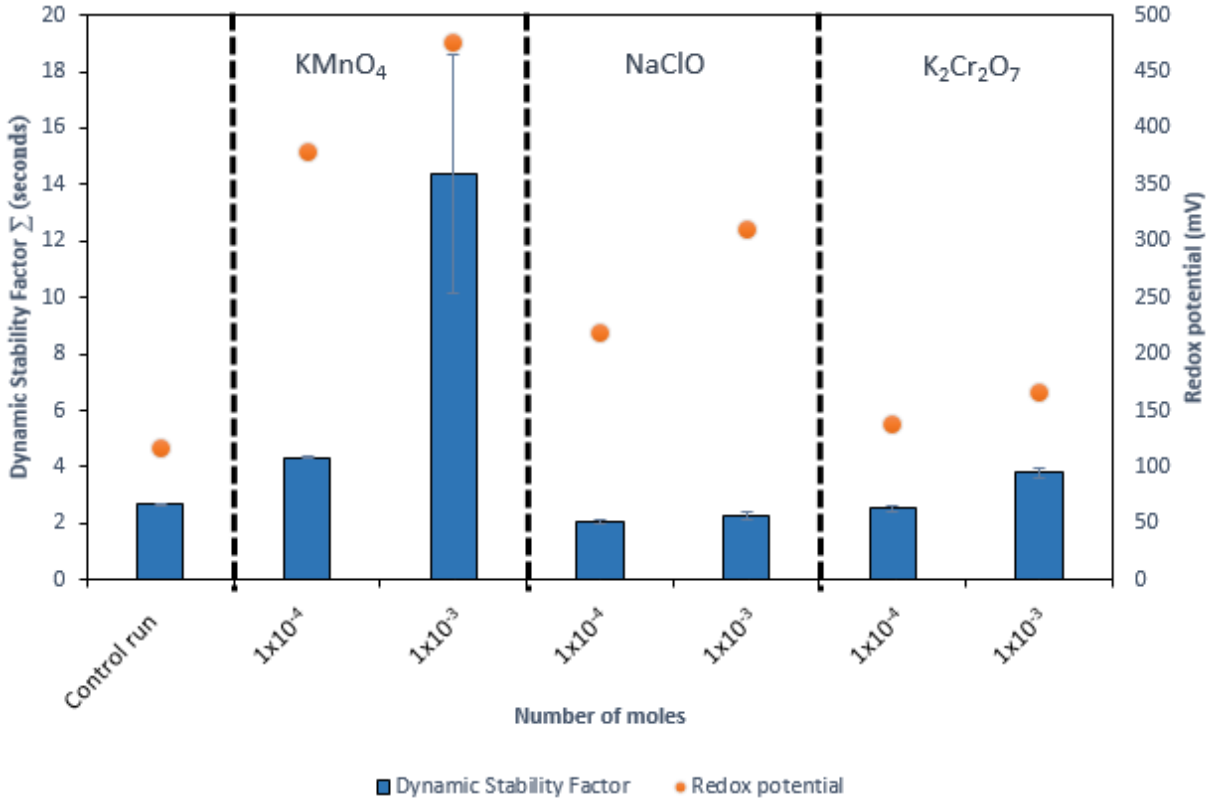

Figure 5.35: Dynamic stability factor for three phase tests for all conditions under investigation in 100 g/t SIBX & 40 g/t DOW 200. Error bars represent standard error between duplicate tests.

From Figure 5.35 it can be deduced that compared to the two phase tests, higher dynamic stability factors were obtained for the three phase system, in the presence of mineral particles. Higher dynamic stability factors were attained with $KMnO_4$, however this observation cannot be linked to high stability as depicted by the graph because $KMnO_4$ caused increased bubble coalescence and bubble breakage as shown in Figure 5.33, thus $KMnO_4$ caused highly unstable froth. An increase in concentration of NaClO from $1x10^{-4}$ mols to $1x10^{-3}$ mols (Eh of 219 to 311 mV), respectively did not change the stability of the froth. Interestingly an increase in concentration, thus increase in Eh from 137-166 mV for $K_2Cr_2O_7$, increased the froth stability. Furthermore $K_2Cr_2O_7$ at a concentration of $1x10^{-3}$ mols (Eh of 166 mV) showed a slightly higher dynamic stability factor compared to the control run (Eh of 116 mV). It can be deduced from Figure 5.35 that an increase in concentration/Eh resulted in a slight increase in the dynamic stability factor for most conditions investigated.

Since it was observed that $KMnO_4$ at higher concentrations causes froth instability, it was interesting to investigate the effect of $KMnO_4$ on the foam and froth phase in both collector

and collectorless conditions. Experiments were carried out in the absence and presence of SIBX both in the two phase and three phase systems.

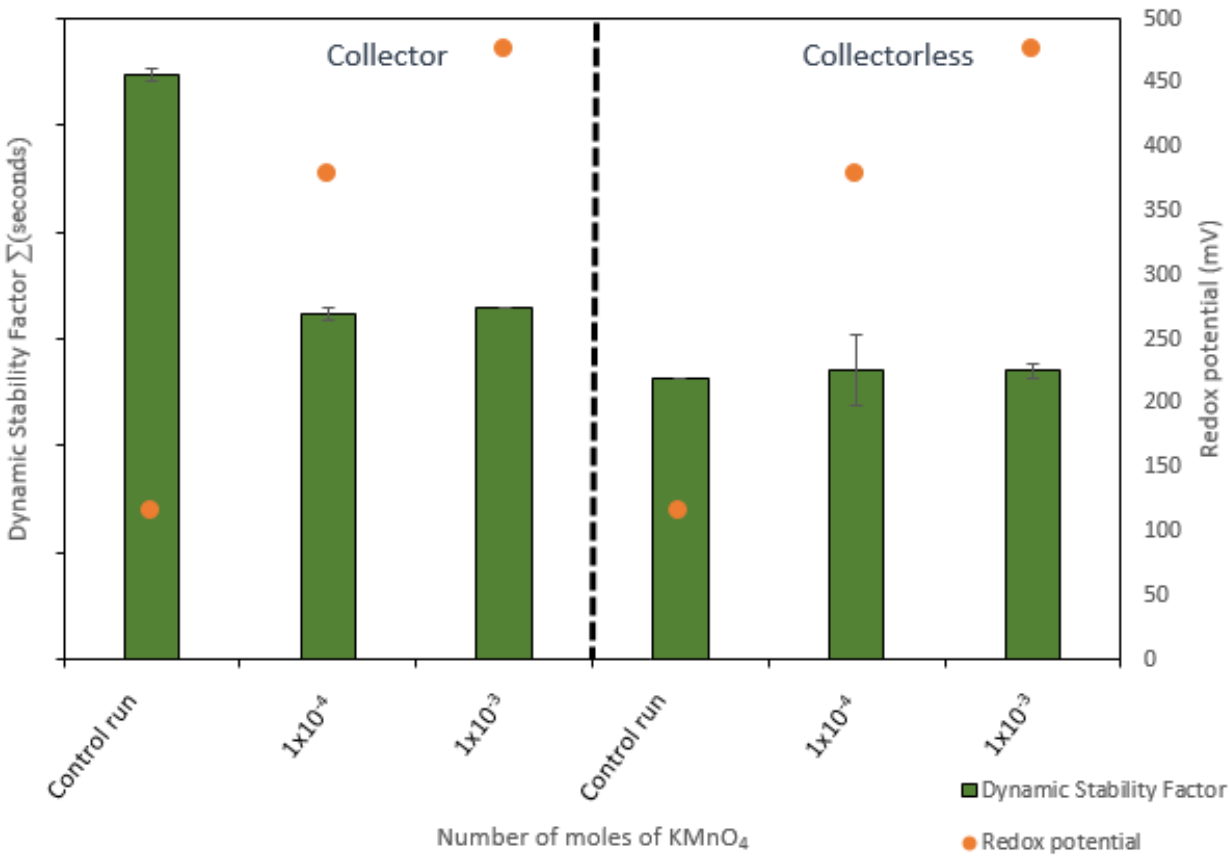

Figure 5.36: Dynamic stability factors for two phase tests for collector and collectorless baseline tests at $1x10^{-4}$ mols & $1x10^{-3}$ mols $KMnO_4$ in 100 g/t SIBX & 40 g/t DOW 200. Error bars represent standard error between duplicate tests.

Figure 5.36 indicates that $KMnO_4$ alone does not have a direct effect on the stability of the foam. This can be deduced from the non-collector runs that show no change in the dynamic stability factors with and without $KMnO_4$. In the collector tests, it was seen that the presence of collector and $KMnO_4$ reduced the stability of the foam compared with the test conducted in the presence of collector only. The control run in the presence of SIBX resulted in a higher stability compared with the baseline collectorless test. It was shown that the addition of $KMnO_4$ reduced foam stability, though the presence of SIBX and $KMnO_4$ gave higher foam stabilities compared to tests carried out in the presence of $KMnO_4$ only. However, an increase in concentration/Eh upon addition of $KMnO_4$ did not have an effect on the foam stability both in the presence and absence of a collector.

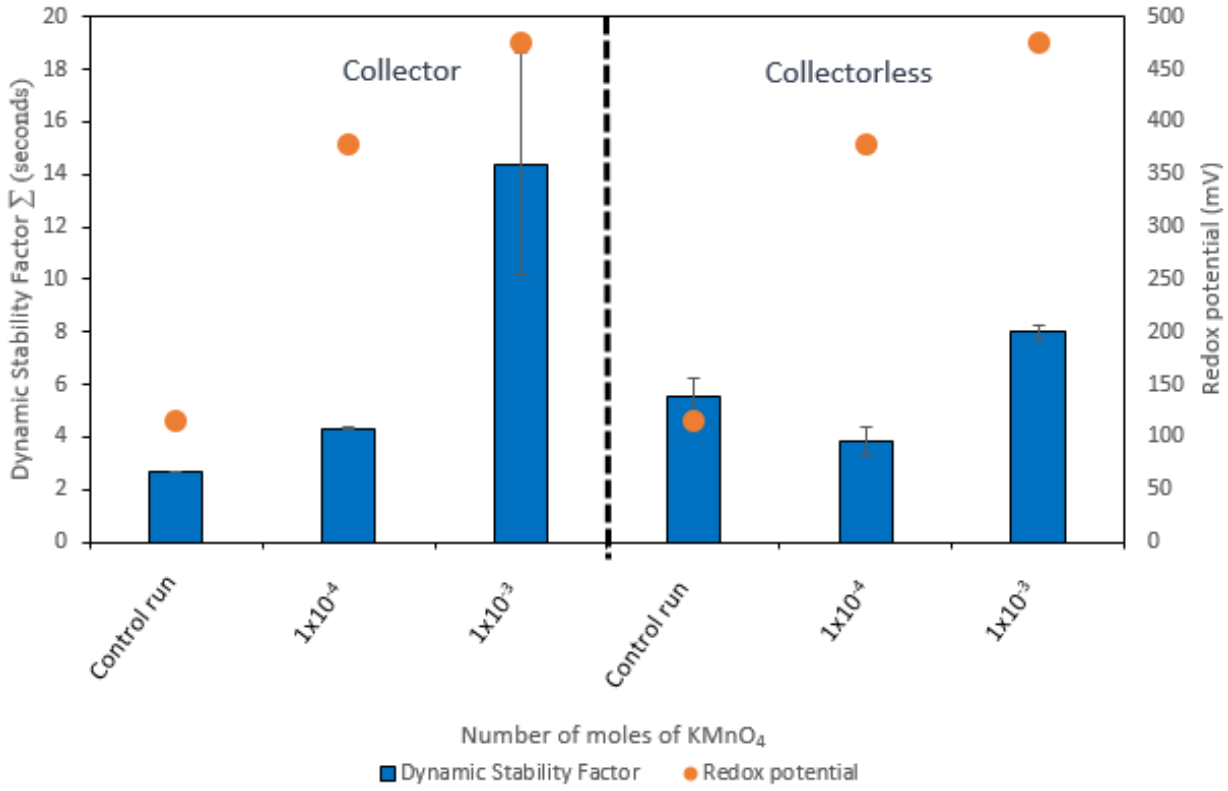

Figure 5.37: Dynamic stability factors for three phase tests for collector and collectorless baseline tests at $1x10^{-4}$ mols & $1x10^{-3}$ mols $KMnO_4$ in 100 g/t SIBX & 40 g/t DOW 200. Error bars represent standard error between duplicate tests.

Figure 5.37 shows the dynamic stability factors for the three phase system with $KMnO_4$ in collector and collectorless systems. With reference to the control runs, higher froth stability was obtained in the collectorless system compared to the collector system, despite the fact that the Eh values were similar. Contrarily, the addition of $KMnO_4$ in the absence of a collector gave lower froth stability compared to the collector system. Overall, it is evident that froth stability increased with an increase in concentration/Eh both in the presence and in the absence of a SIBX except for condition $1x10^{-4}$ mols $KMnO_4$ where a slight decrease was observed.

5.6 The effect of potential modifiers on rest potentials of pure chalcopyrite

This section considers the mixed or rest potential measurements obtained for pure chalcopyrite in the absence and presence of both potential modifiers and SIBX. These tests were carried out in order to complement the batch flotation and froth stability results reported earlier in the chapter. Potential modifiers were added at 300 seconds and the SIBX

collector was added at 600 seconds as executed by Chimonyo (2016). The total run for each experiment was 1200 seconds.

5.6.1 Equilibrium potentials of the xanthate/dixanthogen couple

Most electrochemical studies have reported the equilibrium potentials of the xanthate/dixanthogen couple for potassium/sodium ethyl xanthate (Majima, 1968). Very limited literature has reports on the equilibrium potentials for SIBX (Buswell, 1998). Therefore this study will explore the effect of changing concentrations on the equilibrium potentials of SIBX.

It has been proposed in literature that the interaction of thiols with mineral surfaces is electrochemical in nature (Allison et al., 1972), with an anodic oxidation reaction involving the collector to form the corresponding dimer (Equation 5.4) and a cathodic reduction reaction involving the reduction of oxygen and/or oxidising reagents (Equation 5.5).

$$2X^- \leftrightarrow X_2 + 2e^- \quad \text{Eqn 5.4}$$

$$\frac{1}{2}O_{2(ads)} + H_2O + 2e^- \leftrightarrow 2OH^- \quad \text{Eqn 5.5}$$

In equation 5.4, X^- represents the xanthate ion and X_2 represents dixanthogen. Depending on the type of sulphide mineral used for an investigation, the anodic oxidation mechanism can follow different paths (Buswell et al., 2002).

The Nernst equation is considered as an important equation in electrochemistry. It is an equation that relates the reduction potential of an electrochemical reaction to the standard electrode potential, temperature and activities of chemical species undergoing reduction and oxidation reactions.

For unit activity X_2, the Nernst equation predicts that:

$$E = E^0 - {}^{RT}/_{2F}\,.\,In(X^-)^2 \quad \text{Eqn 5.6}$$

Where R represents the universal gas constant, T represents the temperature in Kelvin, F represents the Faraday constant, E represents the cell potential and E^0 represents the standard cell potential.

The Nernst equation (Equation 5.6) predicts a 59 mV increase in equilibrium potential for every order of magnitude decrease in xanthate concentration (Buswell, 1998) . As shown in Table 5.4, Buswell (1998) observed a 58 mV change, and was similar to what was obtained in this study. The results indicated in the table are in agreement with the prediction from the Nernst equation. E^0 for each concentration of SIBX was calculated using the Nernst's equation and tabulated as shown in Table 5.4. It has been postulated that rest potentials of minerals that are observed above the equilibrium potential of a thiol collector indicate the formation of the dithiolate species whereas rest potentials that are measured below the equilibrium potential indicate the formation of a metal thiolate species on the mineral surface.

Table 5.4: Equilibrium potentials for xanthate/dixanthogen couple (SIBX).

Conc. of SIBX (M)	E/(mV vs SHE)		E^0/(mV vs SHE)	
	Buswell (1998)	**Experimentally Measured**	**Buswell (1998)**	**Calculated**
$1x10^{-3}$	49	68	-127	-109
$6.24X10^{-4}$	-	80	-128	-110
$1x10^{-4}$	108	126	-128	-110

5.6.2 Rest potential measurements

The potential measured at the mineral/liquid interface is important in that it gives an indication of the mineral surface conditions and how a reagent may react with such a surface. Figures 5.38 to 5.47 show rest potential profiles generated for all conditions under investigation. The rest potentials were measured at a pH of 9.4 at a concentration of $6.24x10^{-4}$ M SIBX and at various concentrations of potential modifiers.

5.6.2.1 SIBX

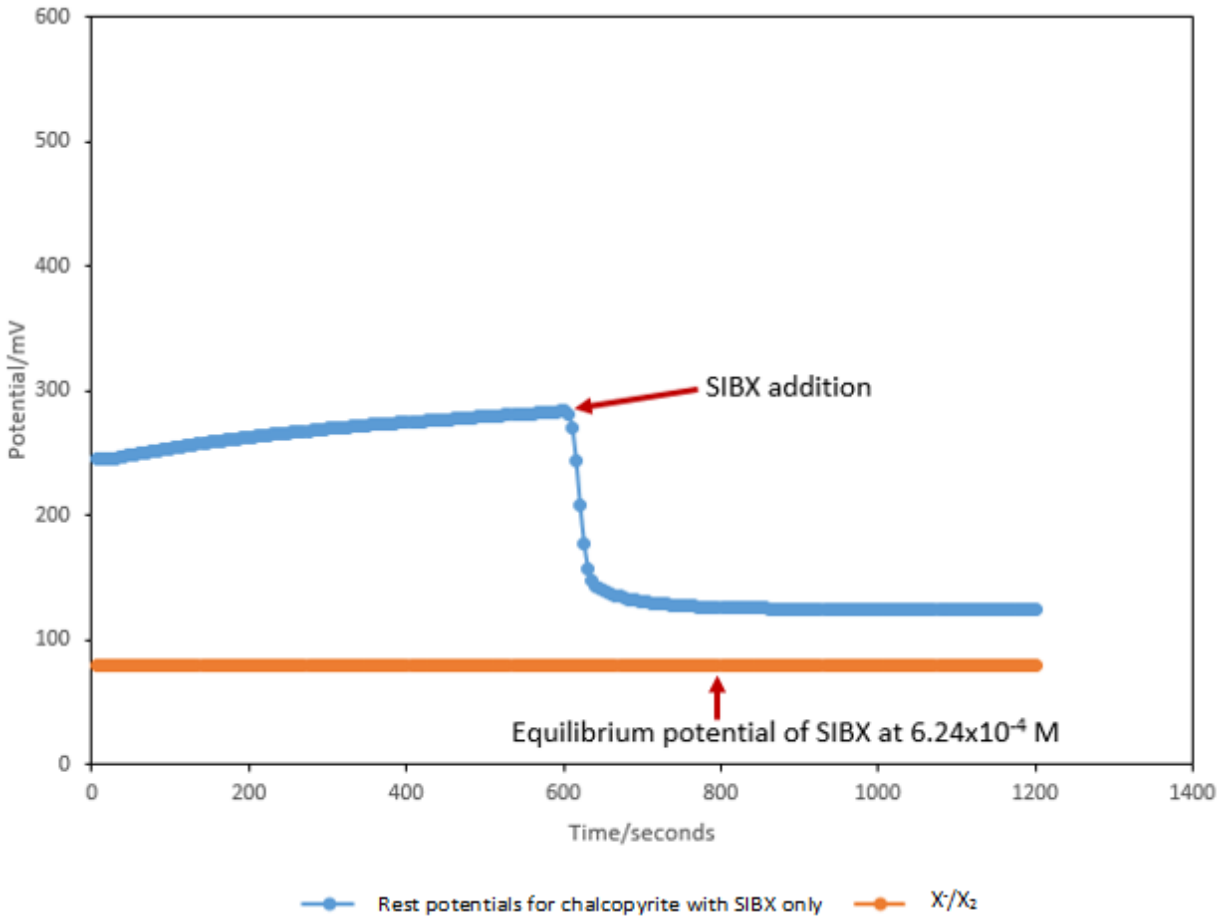

Figure 5.38: Equilibrium potential of SIBX at 6.24x10^{-4} M and the rest potentials for chalcopyrite in the absence and presence of SIBX only.

Figure 5.38 illustrates the changes in rest potentials upon addition of SIBX. Prior to collector addition, the rest potentials measured for chalcopyrite were fairly constant at an average potential of around 250 mV. Upon addition of the collector, a pronounced decrease in rest potentials was observed, to 130 mV. The final rest potential observed was 124 mV. It can be seen from Figure 5.38, that the rest potentials measured were above the equilibrium potential for formation of the xanthate dimer, which was experimentally determined to be 80 mV.

5.6.2.2 NaClO

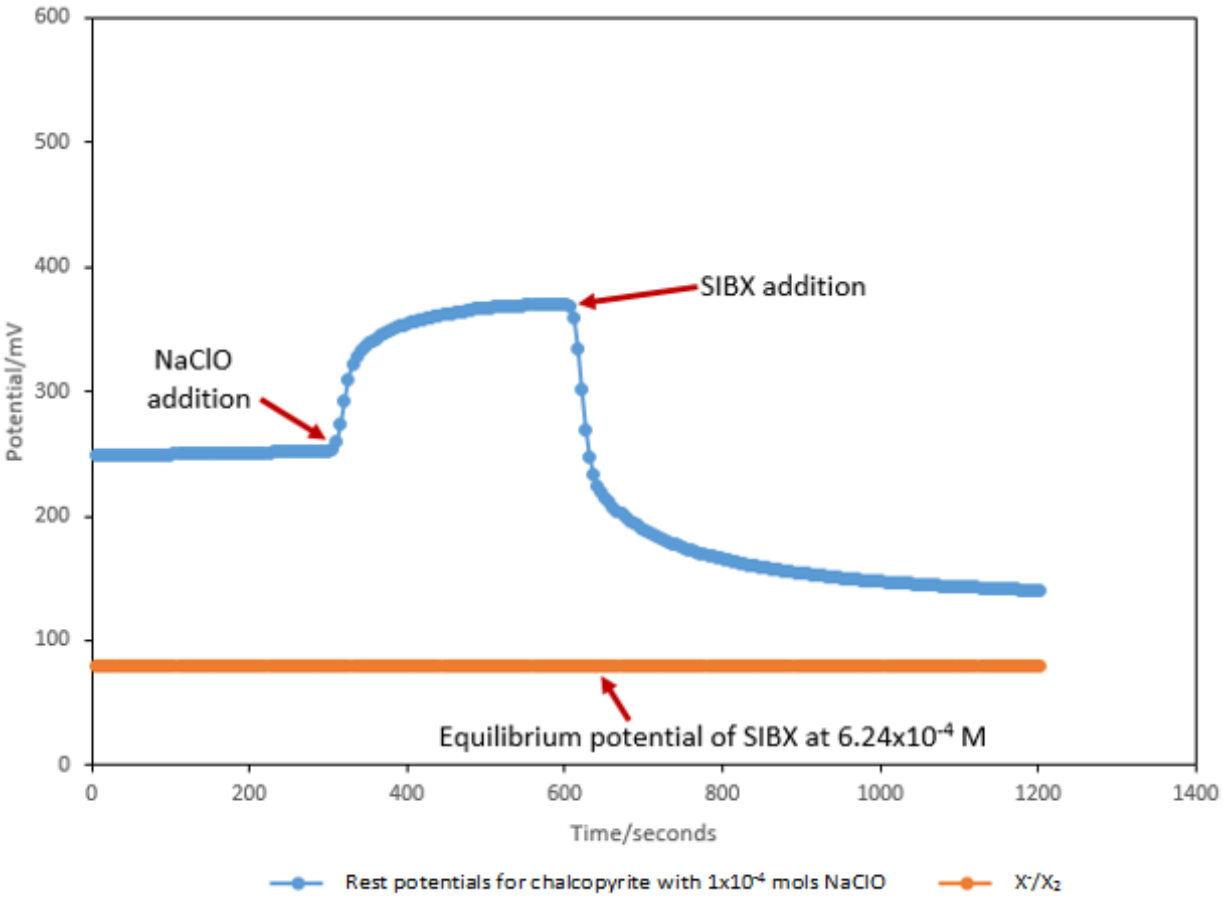

Figure 5.39: Equilibrium potential of SIBX at 6.24×10^{-4} M and the rest potentials for chalcopyrite in the absence and presence of 1×10^{-4} mols NaClO and SIBX.

Figure 5.39 illustrates the changes in rest potentials upon addition of 1×10^{-4} mols NaClO and SIBX. The rest potentials before addition of 1×10^{-4} mols NaClO were determined to be at 250 mV. Upon addition of 1×10^{-4} mols NaClO, an increase in potential to about 370 mV was observed. Thereafter, SIBX was added and a reduction in rest potential to a potential of 150 mV was observed. Under the investigated conditions, the final rest potential measured was above the equilibrium potential of SIBX.

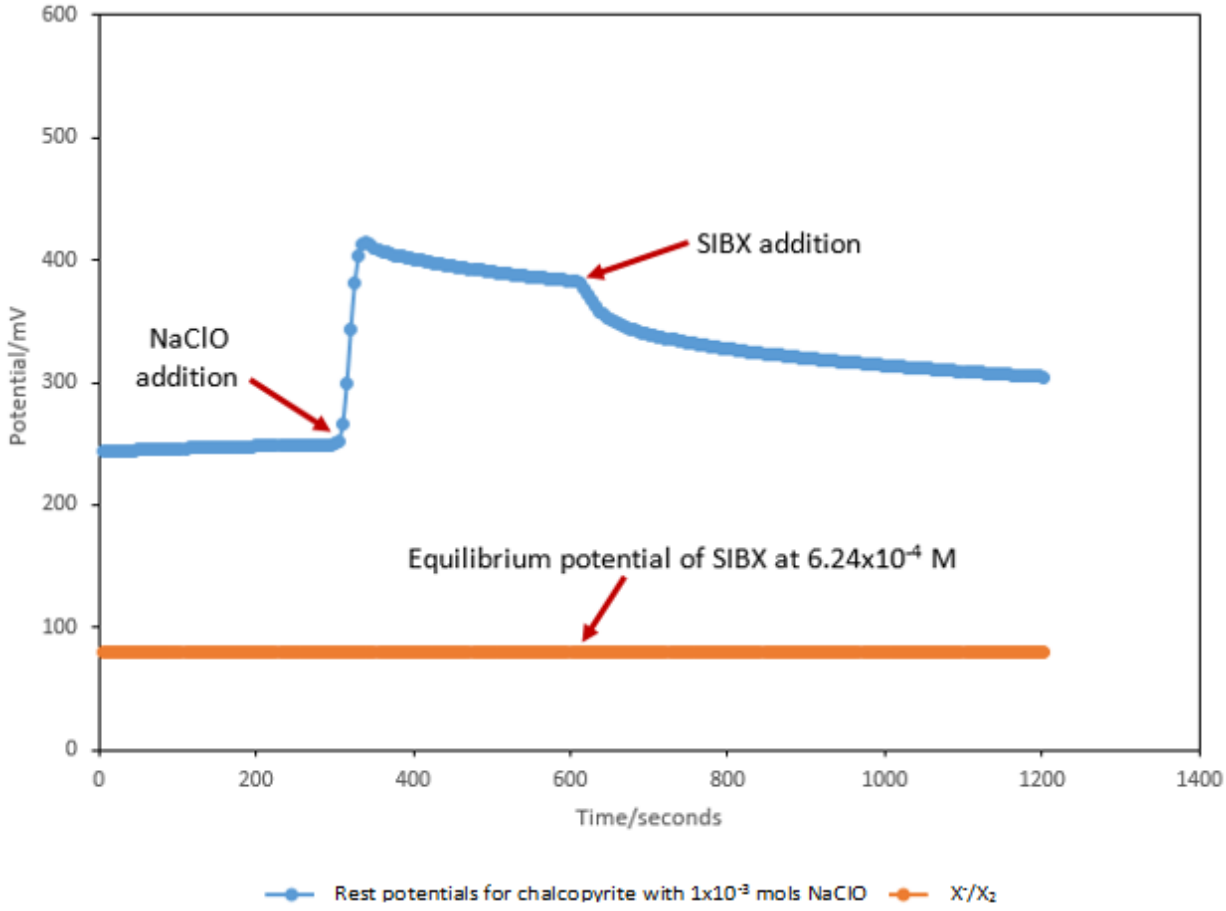

Figure 5.40: Equilibrium potential of SIBX at 6.24x10^{-4} M and the rest potentials for chalcopyrite in the absence and presence of 1x10^{-3} mols NaClO and SIBX.

Figure 5.40 illustrates the changes in rest potentials upon addition of 1x10^{-3} mols NaClO and SIBX. Prior to addition of the 1x10^{-3} mols NaClO, the potential was determined to be about 250 mV. After addition of the potential modifier, a pronounced increase in potential to about 415 mV was observed. A subsequent addition of SIBX had a less pronounced effect as the rest potential was only reduced to 300 mV. Again under the investigated conditions, the final rest potential was above the equilibrium potential of SIBX.

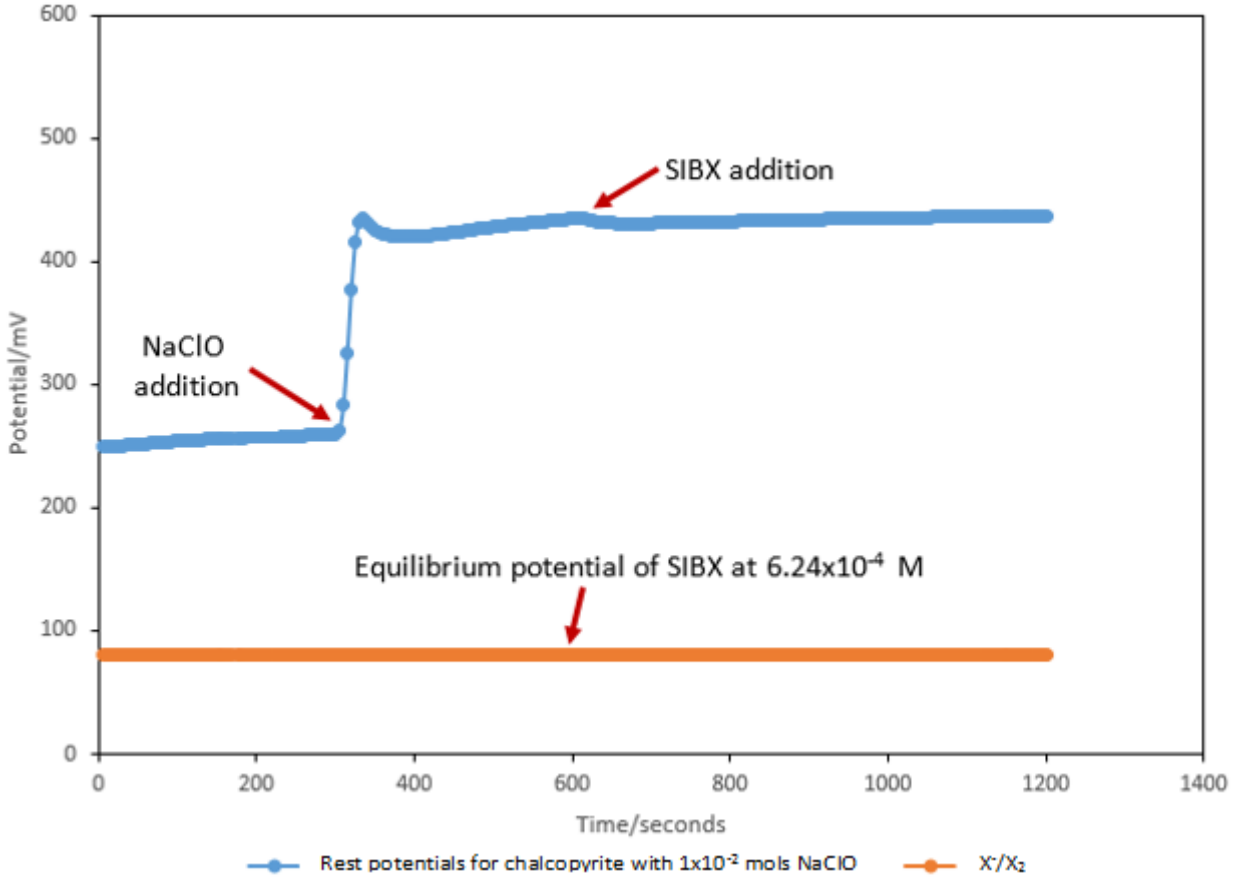

Figure 5.41: Equilibrium potential of SIBX at 6.24x10^{-4} M and the rest potentials for chalcopyrite in the absence and presence of 1x10^{-2} mols NaClO and SIBX.

Figure 5.41 illustrates the changes in rest potentials upon addition of 1x10^{-2} mols NaClO and SIBX. Before the addition of 1x10^{-2} mols NaClO, the rest potential was about 250 mV. Upon addition of the 1x10^{-2} mols NaClO, a prominent increase in the rest potentials to 432 mV was noted. Thereafter, SIBX was added and the reduction in rest potentials was not significant. A final rest potential of about 430 mV was observed. Evidently, the rest potentials measured throughout the experiment were above the equilibrium potential of SIBX. In summary, increase in concentration of NaClO resulted in a significant increase in potential after-which a less significant reduction in potential upon addition of SIBX was observed and vice-versa.

5.6.2.3 $KMnO_4$

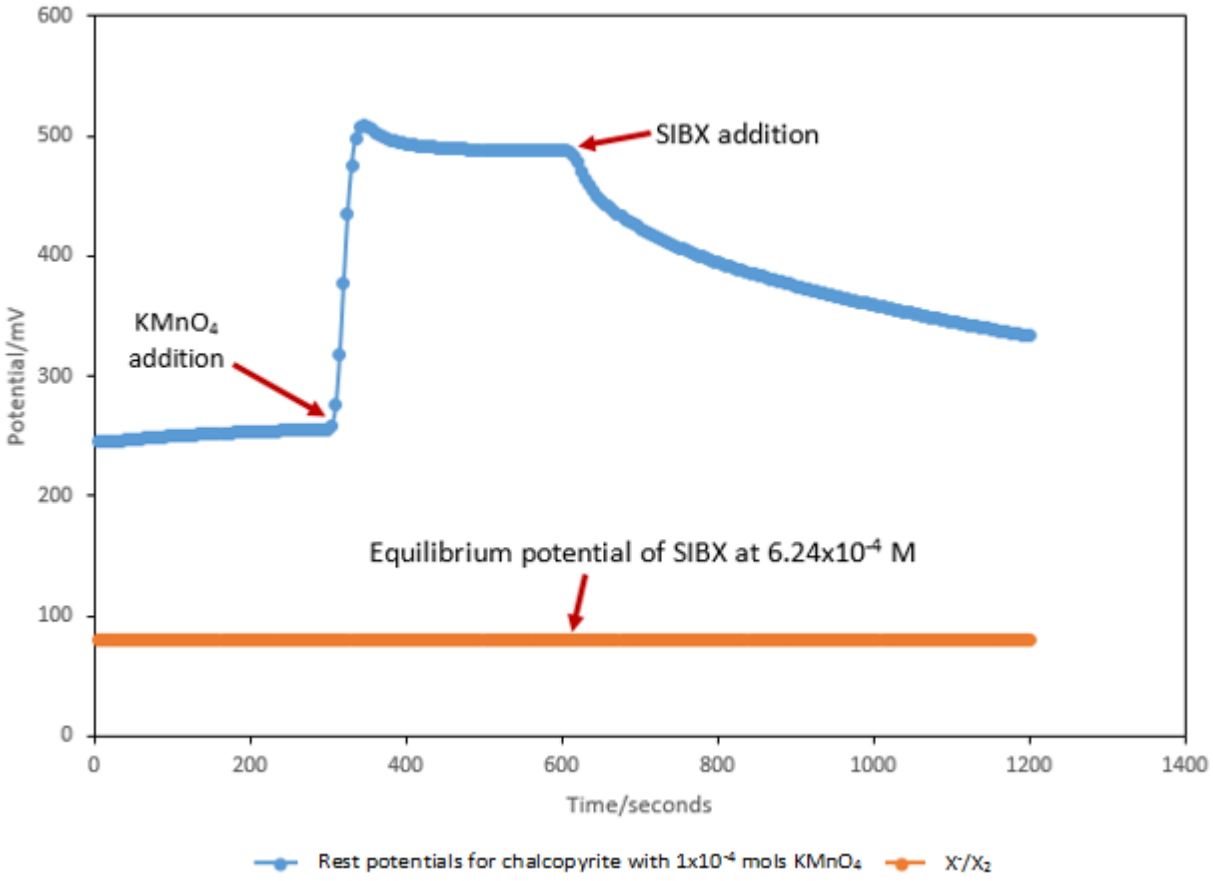

Figure 5.42: Equilibrium potential of SIBX at $6.24x10^{-4}$ M and the rest potentials for chalcopyrite in the absence and presence of $1x10^{-4}$ mols $KMnO_4$ and SIBX.

Figure 5.42 illustrates the changes in rest potentials upon addition of $1x10^{-4}$ mols $KMnO_4$ and SIBX. From an initial rest potential value of about 250 mV, a very pronounced increase in potential was observed after addition of $1x10^{-4}$ mols $KMnO_4$. A rest potential of about 500 mV was obtained, after-which a subsequent addition of SIBX gave a rest potential value of about 320 mV. As shown in the graph, the rest potentials measured under the investigated conditions, were clearly above the equilibrium potential of SIBX.

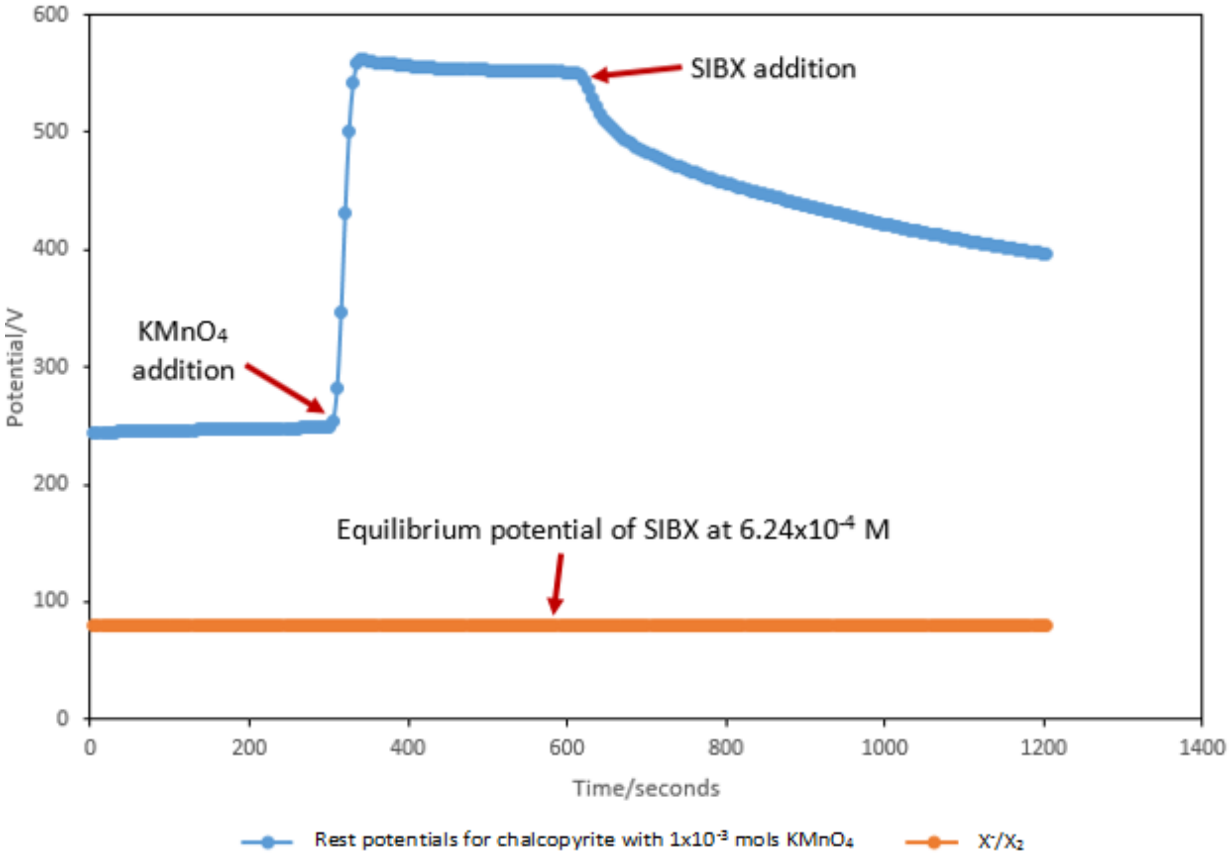

Figure 5.43: Equilibrium potential of SIBX at $6.24x10^{-4}$ M and the rest potentials for chalcopyrite in the absence and presence of $1x10^{-3}$ mols $KMnO_4$ and SIBX.

Figure 5.43 illustrates the changes in rest potentials upon addition of $1x10^{-3}$ mols $KMnO_4$ and SIBX. The graph indicates that addition of $1x10^{-3}$ mols $KMnO_4$ gave a higher rest potential of around 550 mV, compared to $1x10^{-4}$ mols $KMnO_4$. Upon addition of SIBX, the reduction in rest potentials was less pronounced and a final potential of about 400 mV was obtained. All rest potentials measured under the condition investigated in Figure 5.43 were above the equilibrium potential of SIBX.

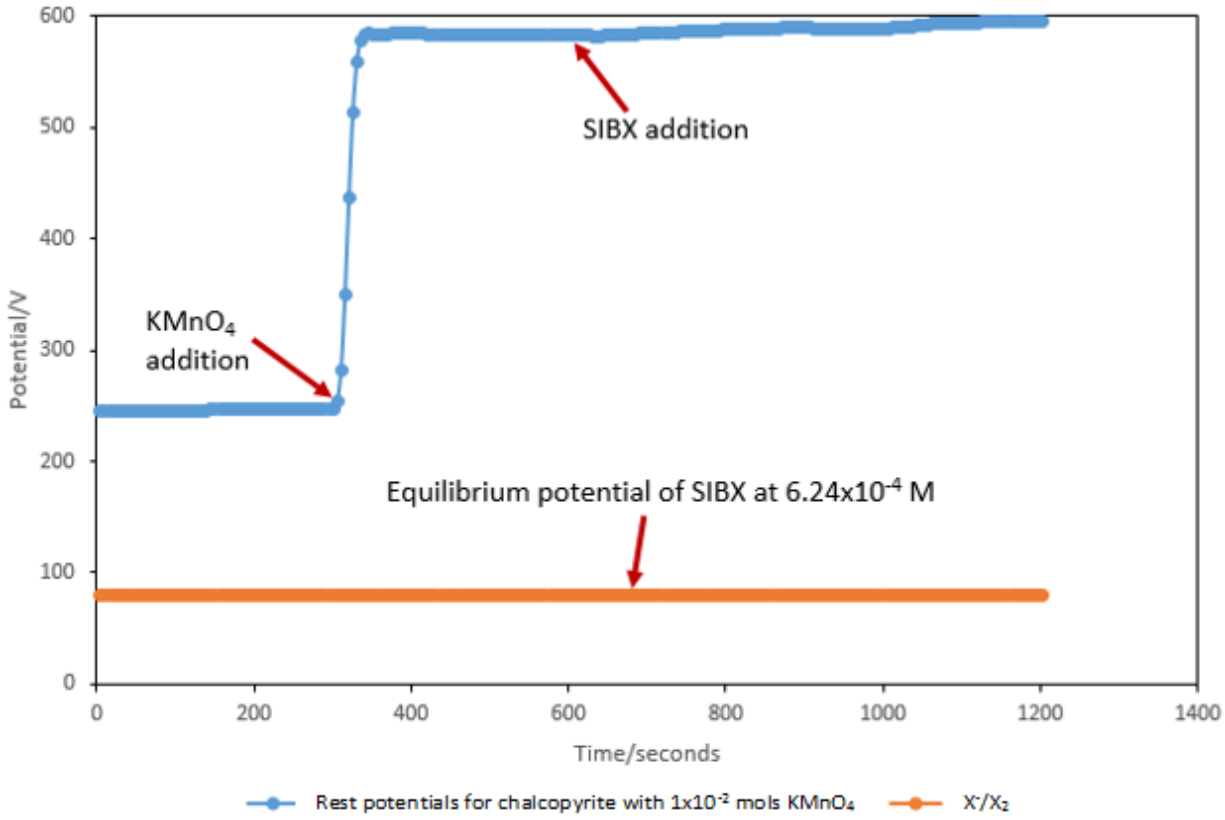

Figure 5.44: Equilibrium potential of SIBX at $6.24x10^{-4}$ M and the rest potentials for chalcopyrite in the absence and presence of $1x10^{-2}$ mols $KMnO_4$ and SIBX.

Figure 5.44 illustrates the changes in rest potentials upon addition of $1x10^{-2}$ mols $KMnO_4$ and SIBX. The graph shows that before addition of the potential modifier, the rest potential value measured was about 250 mV. Addition of $1x10^{-2}$ mols $KMnO_4$ resulted in the highest rest potential value attained of all the conditions investigated. The rest potential recorded after addition of the modifier was about 600 mV. It was interesting to note that under these conditions, the effect of the collector was not noticeable, as no change in rest potentials upon addition of SIBX was observed. Similar to other conditions, the rest potential measured with $1x10^{-2}$ mols $KMnO_4$ was above the equilibrium potential of SIBX. The non-response of the rest potential to the addition of SIBX after $1x10^{-2}$ mols $KMnO_4$ addition is consistent with the flotation results.

5.6.2.4 $K_2Cr_2O_7$

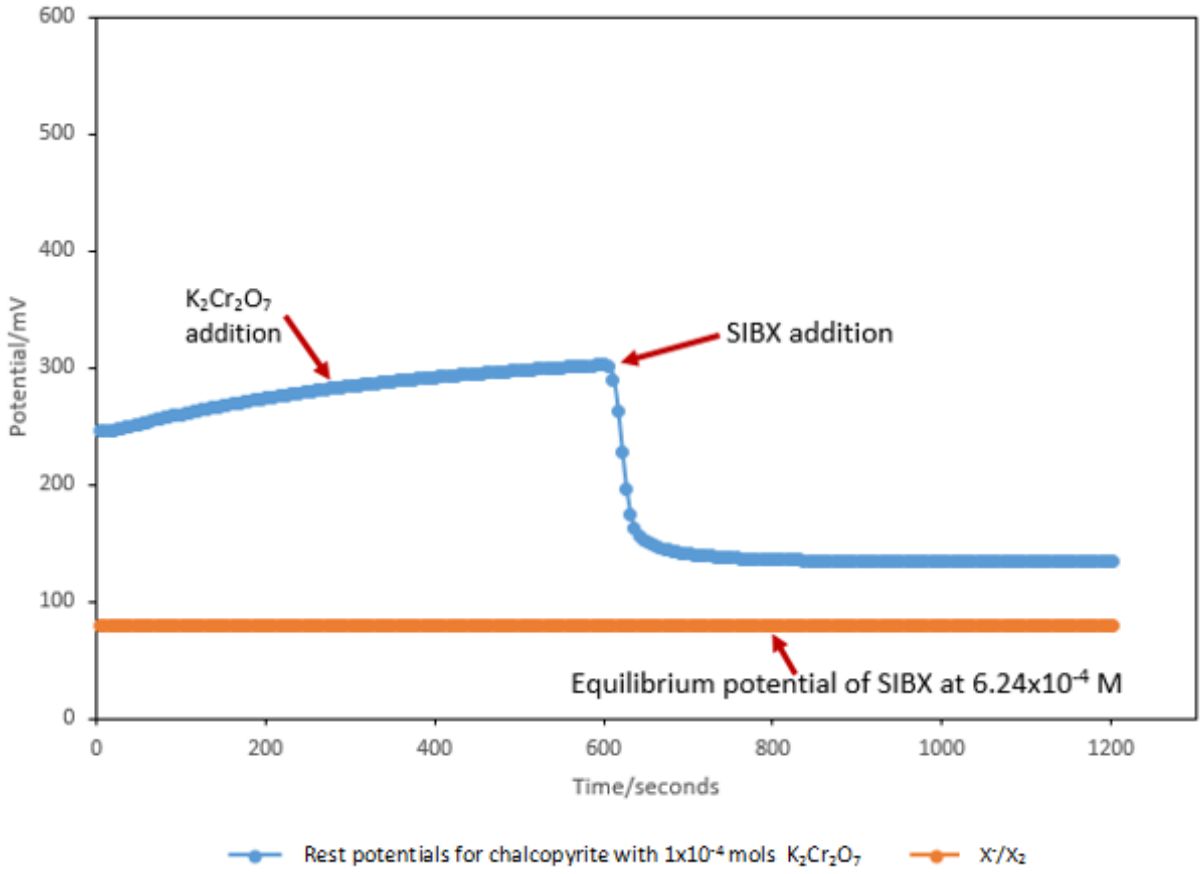

Figure 5.45: Equilibrium potential of SIBX at $6.24x10^{-4}$ M and the rest potentials for chalcopyrite in the absence and presence of $1x10^{-4}$ mols $K_2Cr_2O_7$ and SIBX.

Figure 5.45 illustrates the changes in rest potentials upon addition of $1x10^{-4}$ mols $K_2Cr_2O_7$ and SIBX. It is of interest to note that addition of $1x10^{-4}$ mols $K_2Cr_2O_7$ did not change the initial rest potentials measured prior to its addition. A subsequent drop in rest potentials was observed after addition of the collector to a potential of about 134 mV. It can be seen that the shape of the graph is similar to the control test though the final rest potential for SIBX only was 124 mV, which is 10 mV lower than the final rest potential obtained in Figure 5.45. The final rest potentials obtained for the two conditions corresponded to their respective copper recoveries of 93.64% and 93.36% for the control test and $1x10^{-4}$ mols $K_2Cr_2O_7$, respectively. All rest potentials measured under the condition investigated in Figure 5.45 were above the equilibrium potential of SIBX.

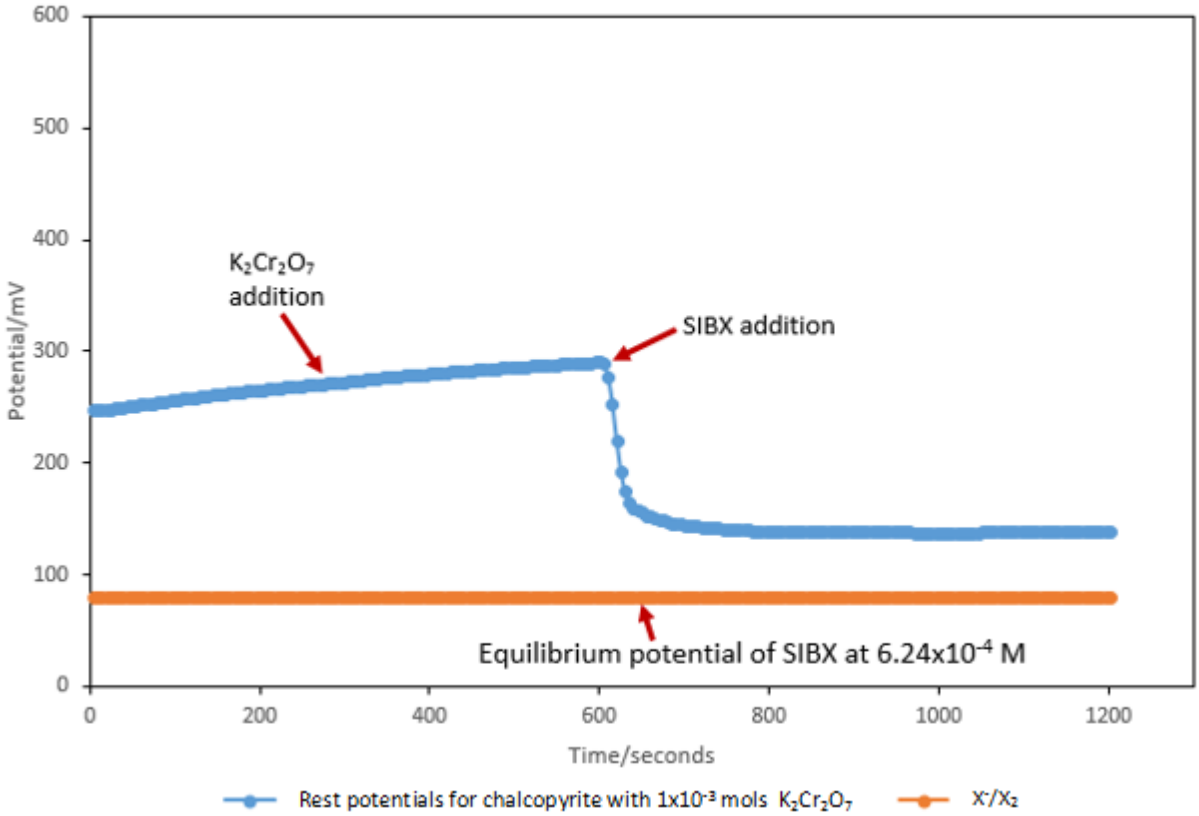

Figure 5.46: Equilibrium potential of SIBX at $6.24x10^{-4}$ M and the rest potentials for chalcopyrite in the absence and presence of $1x10^{-3}$ mols $K_2Cr_2O_7$ and SIBX.

Figure 5.46 illustrates the changes in rest potentials upon addition of $1x10^{-3}$ mols $K_2Cr_2O_7$ and SIBX. Similar to Figure 5.45, Figure 5.46 also showed no significant changes in rest potentials upon addition of $K_2Cr_2O_7$. The potentials measured after addition of the potential modifier were similar to the potentials measured prior to the addition of the potential modifier. The graph obtained in Figure 5.46 is similar to that obtained in Figure 5.45 and Figure 5.38. The three graphs show that the final rest potentials obtained were 138 mV, 134 mV and 124 mV, respectively and their corresponding copper recoveries were 92.36%, 93.36% and 93.64%. It can be seen that there is an inverse relationship between final rest potential values and copper recoveries obtained in the batch flotation tests. Therefore the lower the final rest potential acquired, the higher the copper recovery. The equilibrium potential of SIBX was determined to be below the rest potential measurements for the conditions under investigation.

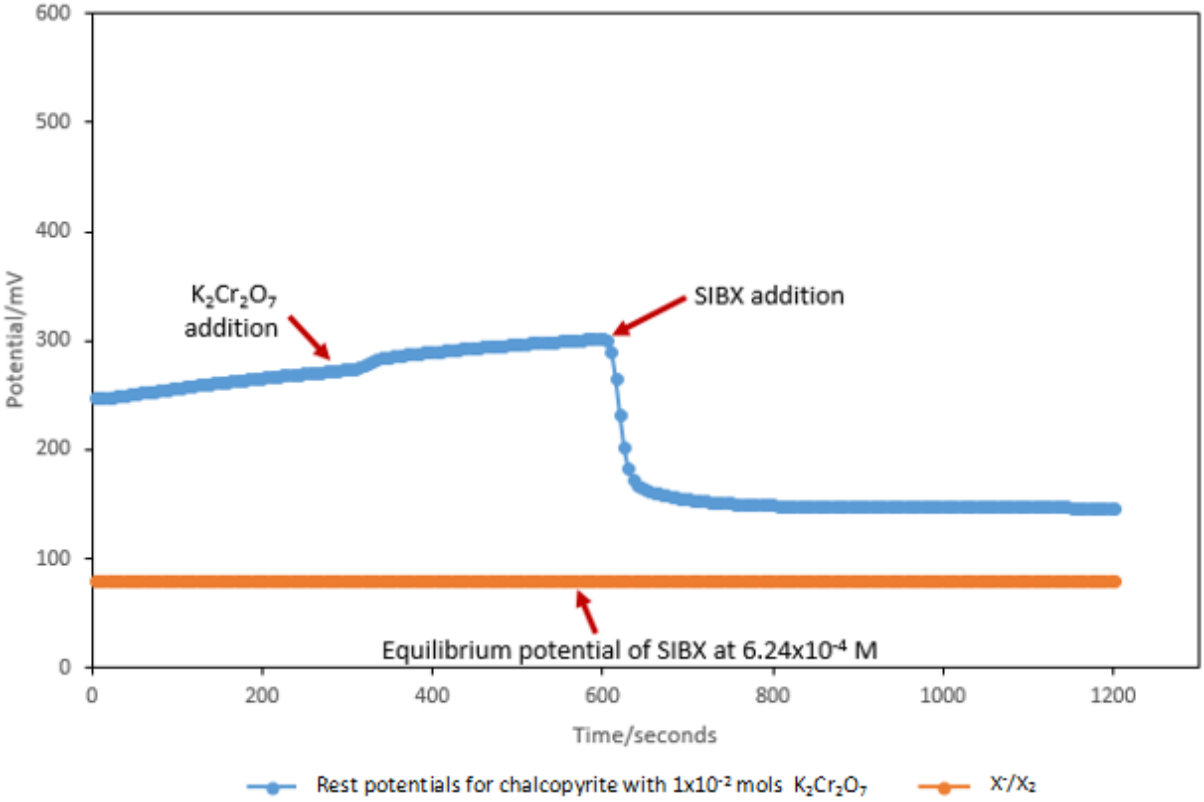

Figure 5.47: Equilibrium potential of SIBX at $6.24x10^{-4}$ M and the rest potentials for chalcopyrite in the absence and presence of $1x10^{-2}$ mols $K_2Cr_2O_7$ and SIBX.

Figure 5.47 illustrates the changes in rest potentials upon addition of $1x10^{-2}$ mols $K_2Cr_2O_7$ and SIBX. The figure shows that contrary to what was observed in Figures 5.46 and 5.47, a slight increase in potential was observed upon addition of $1x10^{-2}$ mols $K_2Cr_2O_7$. Rest potentials increased from 270 mV to about 300 mV, after-which a decrease to about 150 mV was seen, upon addition of SIBX. Similar to other conditions, the final rest potential measured with $1x10^{-2}$ mols $K_2Cr_2O_7$ was above the equilibrium potential of SIBX.

6 Discussion

6.1 Introduction

This chapter provides a critical analysis of the results presented in Chapter 5. The critical analysis has been reinforced by literature findings. Froth stability and batch flotation tests are analysed to elucidate the flotation performance of a copper sulphide ore. Furthermore the results obtained from electrochemical measurements are examined to thermodynamically complement the results obtained from the flotation performance tests. Ultimately, the flotation recoveries are linked to the electrochemical measurements.

6.2 Effect of potential modifiers on flotation performance of a copper sulphide ore

6.2.1 Flotation recoveries as a function of froth stability

It has been reported in previous studies that the floatability of sulphide minerals is feasible by the control of potential using chemical reagents (Goktepe, 2010, Razmjouee et al., 2012, Plackowski et al., 2014, Chimonyo et al., 2017). Though various potential modifiers have been used to enhance the floatability of sulphide minerals, to date no detailed comparison of the potential modifiers, at different concentrations or Eh levels, on floatability has been conducted.

The present study linked chemical conditions applied by the addition of potential modifiers in the pulp phase to the behaviour of the froth phase. Froth stability tests were performed to show the effect of potential modifiers on the froth phase both in the absence and presence of solids as shown in Figures 5.34 and 5.35, respectively. Comparing the two phase (foam stability) to the three phase (froth stability) systems, it is evident that higher stability was obtained in the presence of solids than in the absence of solids. It has been reported in literature that the presence of solid particles in a flotation system may enhance froth stability (Subrahmanyam and Forssberg, 1988, Horozov, 2008, Hunter et al., 2008, Farrokhpay, 2011, Nyabeze, 2015). Subrahmanyam & Forssberg (1988) linked froth stabilisation to an increase in surface viscosity of films whereas Horozov (2008) and Hunter et al. (2008) identified the

main determining factors as being the particle shape, size, concentration and hydrophobicity. Horozov (2008) identified the mechanism of particle stabilisation of foams to be as a result of the interplay between the ability of the solid particles to form dense coherent particle shells around the bubbles, the stabilisation of liquid films separating bubbles and the formation of a three-dimensional network in the bulk aqueous phase. In the present study, the increase in froth stability from the two-phase system to the three phase system might have been due to the increase in particle hydrophobicity which resulted from the addition of potential modifiers. Sheni (2016) attributed the increase in hydrophobicity after an increase in concentration of potential modifiers and thus Eh to be associated with the presence of more oxidised minerals, resulting in greater froth stability. However, Ata et al. (2003) reported a stabilising effect on the froth phase due to the presence of hydrophilic particles, which was attributed to the increasing effective viscosity or possibly mechanical blockage due to particle obstructions to the flow in the liquid films. It was further highlighted that hydrophobicity of particles in the bubble film has a significant effect on bubble size growth. It was determined that particles with strong hydrophobicity result in increased bubble coalescence compared to moderately hydrophobic particles and decreased coalescence in the presence of weakly hydrophobic particles (Ata et al., 2003). The former observation supports the results obtained in the present study for $1x10^{-2}$ mols $KMnO_4$ as shown in Figure 5.33. Due to the high froth instability induced by this condition, it was of importance to investigate the flotation performance of the copper sulphide ore under different $KMnO_4$ conditions.

Figure 5.36 shows that $KMnO_4$ had no significant effect on the foam phase, in the absence of solid particles, both in the presence and in the absence of a collector. However, Figure 5.37 indicates that the froth stabilising effect was brought about by the interaction of the solids with both $KMnO_4$ and SIBX. With reference to the control run, it was observed that the presence of SIBX destabilised the froth and this observation was attributed to the destabilising properties of the more hydrophobic xanthate-coated sulphide minerals in the froth phase (Wiese et al., 2011, Nyabeze, 2015).

It has been shown in the present study that flotation recoveries are a function of froth stability. Their correlation has been graphically presented in Figure 6.1-6.3. Froth structure

and froth stability are parameters that regulate mineral recovery and grade in mineral processing (Farrokhpay, 2011).

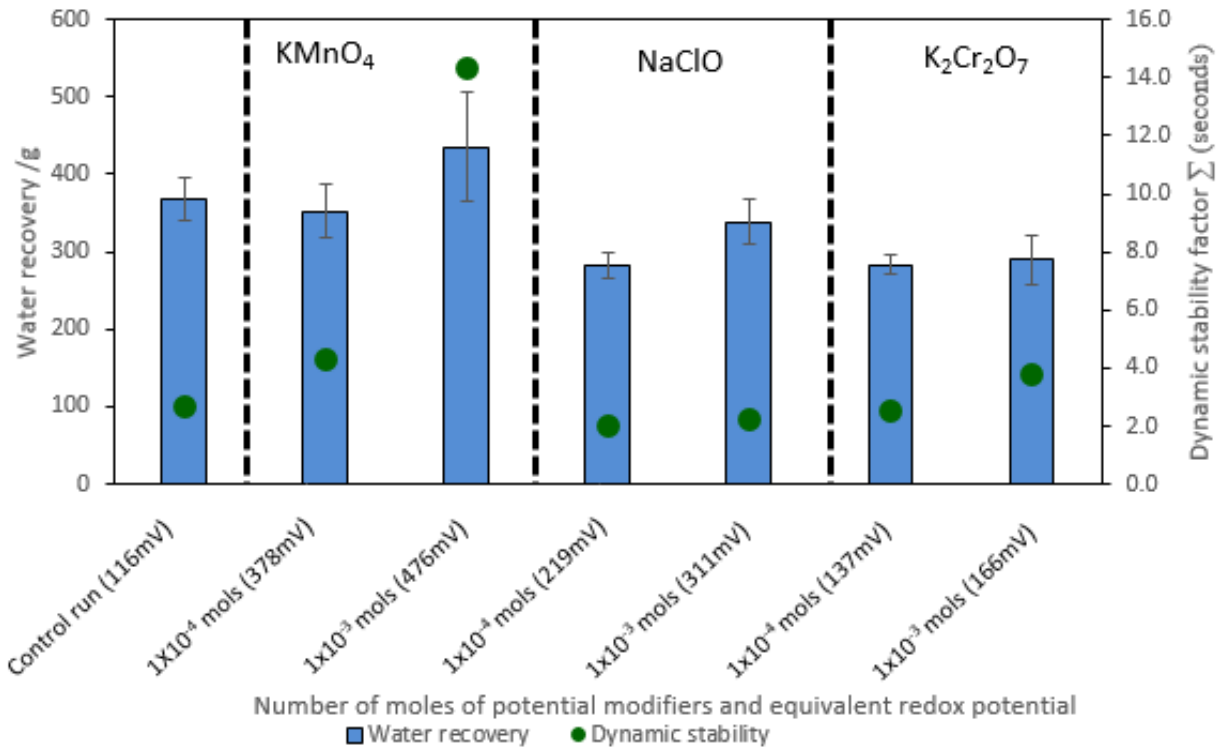

Figure 6.1: Dynamic froth stability as a function of water recovery for all conditions under investigation in 100 g/t SIBX & 40 g/t DOW 200. Error bars represent standard error between duplicate tests.

Figure 6.1 shows the link between froth stability and water recovery. Water recovery obtained in concentrates is an important aspect that signifies the extent of froth stability (Ekmekci et al., 2006). High water recoveries have been shown to be an indicator of greater froth stability enhanced by the presence of hydrophobic mineral particles (Johansson and Pugh, 1992, Horozov, 2008, Wiese, 2009). It has been reported that an increase in concentration of potential modifiers and subsequently an increase in the Eh results in an increase in water recovery (Chimonyo, 2016, Sheni, 2016). These findings agree with the results obtained in the present study, as shown in Figures 5.15 and 6.1. It has been postulated that pulp conditions such as concentration of chemical reagents used, concentration of suspended particles in the system, bubble surface area flux and bubble loading to a large degree determine the amount of water recovery in the froth phase from the pulp phase (Zheng et al., 2005). The results obtained in the present study agree with literature findings. It was determined that high water recoveries obtained at $1x10^{-2}$ $KMnO_4$ in Figure 5.15, may

be associated with an increase in the surface area of air bubbles, which may have increased the liquid film around the air bubbles thus increasing water recovery. However, the rate of bubble coalescence for this condition was visibly higher than the rate of bubble breakage as indicated by the high dynamic stability factor obtained.

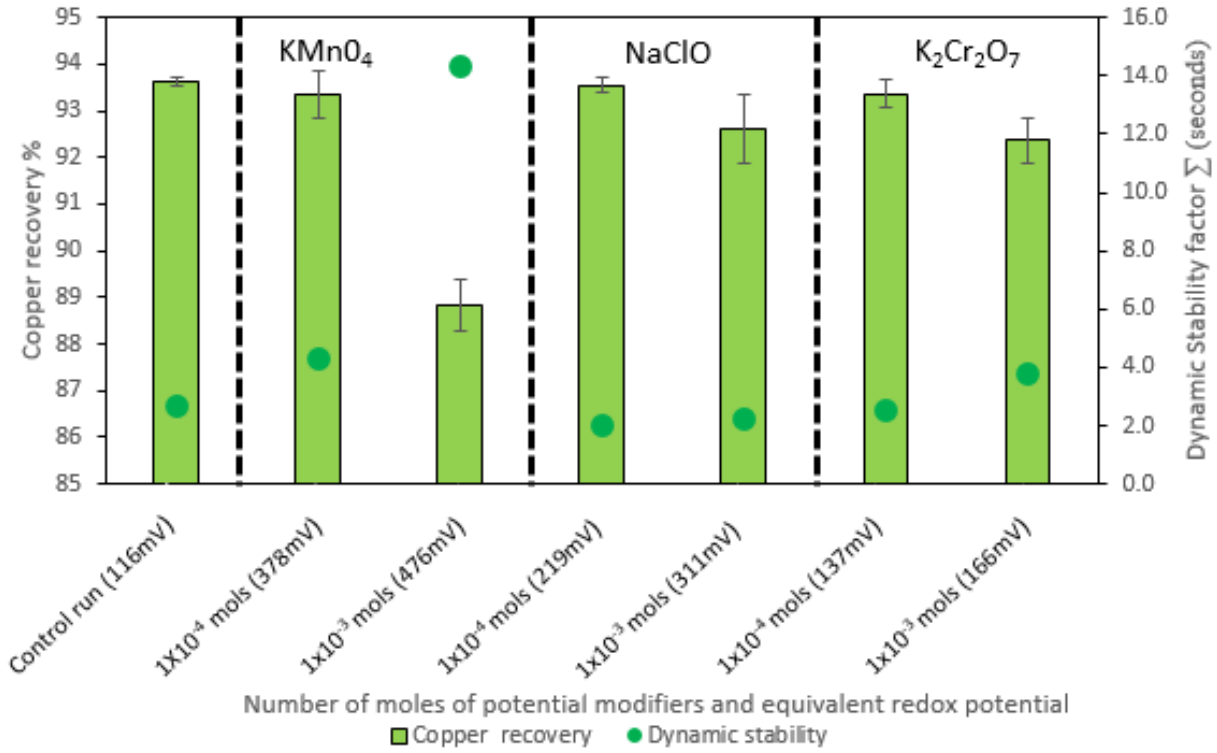

Figure 6.2: Copper recovery as a function of dynamic froth stability for all conditions under investigation in 100 g/t SIBX & 40 g/t DOW 200. Error bars represent standard error between duplicate tests.

Figure 6.2 illustrates copper recoveries as a function of froth stability. Literature highlights that froth stability plays a crucial role in flotation recoveries (Barbian et al., 2003). It is apparent from Figure 6.2 that an increase in concentration and thus Eh for each potential modifier, increased froth stability and in turn reduced copper recoveries. A moderately stable froth is essential for optimum recovery of valuable minerals, as a more stable froth is allied to the recovery of more gangue material (Farrokhpay, 2011). Furthermore, it has been reported in literature that a highly stable froth may result in the loss of the valuable mineral from the froth phase to the pulp phase and eventually to the tailings stream (Tsatouhas et al., 2006), as indicated by the result obtained with 1x10^{-3} mols $KMnO_4$.

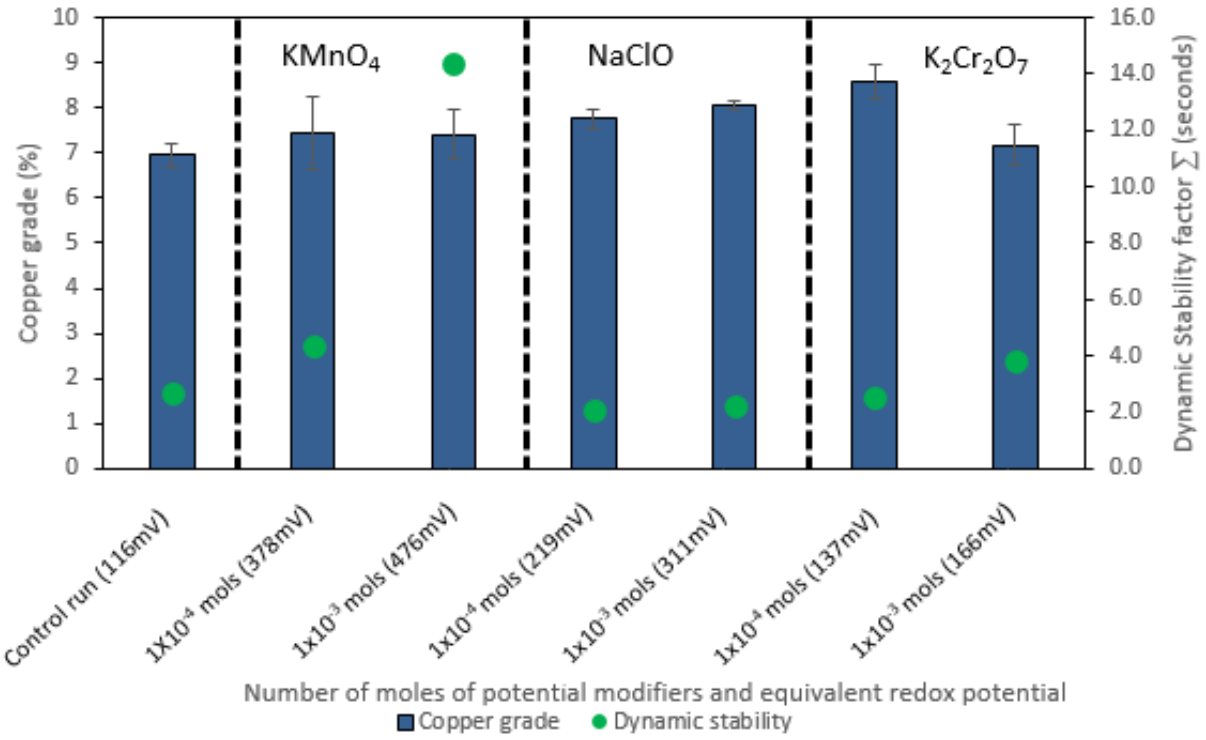

Figure 6.3: Copper grade as a function of dynamic froth stability for all conditions under investigation in 100 g/t SIBX & 40 g/t DOW 200. Error bars represent standard error between duplicate tests.

Figure 6.3 shows the relationship between froth stability and copper grades. Froth stability is known to play a significant role in determining mineral grade (Dippenaar, 1982). It is clear from Figure 6.3 that the use of potential modifiers in a flotation process aids in suppressing gangue material recovery (Chimonyo, 2016), as can be seen by the relatively higher grades obtained for all conditions except the baseline case. The decrease in copper grade observed with an increase in froth stability at $1x10^{-3}$ mols $K_2Cr_2O_7$, could be attributed to an increase in gangue material recovery due to entrainment (Manono, 2012), whereas with other potential modifiers, as their concentrations increased, a slight increase in copper grade was observed implying that there was a reduction in gangue material recovery. The higher solids recovery (Figure 5.15) observed for the control run may also be attributed to gangue material that may have reported to the concentrate through true flotation, entrainment and entrapment (Wiese, 2009), thus a lower copper grade obtained.

Since gangue material recovery is a direct indicator of copper grade, the present study shows no direct correlation between Eh and gangue mineral floatability and thus copper grade, as shown in Figures 5.32 and 6.3. This suggests that the most dominant factor affecting

floatability could be the type of potential modifier used. This argument can be rationalized by the fact that similar concentrations resulting in similar Eh values for $KMnO_4$ and NaClO were obtained with substantially different flotation recoveries. It was observed that an increase in concentration of potential modifiers and Eh decreased gangue material recovery with the exception of NaClO, where no substantial difference was observed. Contrarily, Sheni (2016) reported an increase in gangue material recovery with an increase in Eh, which was attributed to entrainment. However, in the present study, gangue material recovery due to entrainment was observed at $1x10^{-2}$ mols $KMnO_4$, as revealed by the straight line obtained in Figure 5.28. This observation is in agreement with literature studies that report that entrainment has a linear relationship with water recovery (Yang and Aldrich, 2005). Furthermore, factors such as solids suspension in the pulp phase and drainage in the froth phase have been reported to be related to entrainment (Wang et al., 2016).

6.2.2 Copper recoveries as a function of potential modifier concentration/Eh

Most conditions investigated in the present study produced very high copper recoveries above 90%. This may be attributed to the formation of dixanthogen, which is well known to be the most hydrophobic species that is responsible for chalcopyrite flotation (Guo and Yen, 2002, Kocabag and Guler, 2007). However, all potential modifiers had a similar trend, where a slight decrease in copper recoveries was obtained with an increase in concentration or Eh. This may be attributed to the formation of a thin oxidation product film on the mineral surface (Guo and Yen, 2002). The possible presence of the oxidation film can result in an increase in hydrophilicity due to a reduction in the affinity between the mineral surface and elemental sulphur and a reduction in the amount of dixanthogen adsorbed on the mineral surface. In the present study, as concentration of modifiers and thus Eh was increased, the thickness of the possible oxidation product film may have increased which would result in less adsorption of the dixanthogen on the mineral surfaces and thus lower copper recoveries. Each potential modifier will be critically analysed and possible respective entities forming on the mineral surfaces were proposed with the aid of respective Pourbaix diagrams.

6.2.2.1 NaClO

NaClO has been used in previous studies to enhance valuable mineral recoveries (Senior et al., 2009, Smith et al., 2012, Plackowski et al., 2014, Chimonyo et al., 2017). Plackowski et al. (2014) reported enargite recoveries of 82% at an Eh of +500 mV using xanthate as a collector with reduced recoveries of 52% at Eh +100 mV and a further reduction in recoveries to 11% at an Eh of -400 mV. Chimonyo et al. (2017) investigated the effect of 0.0067 moles of NaClO and reported no significant effect on copper recoveries within an Eh range of 500-600 mV at a pH of 9. However, the authors reported an improvement in recoveries at a pH of 11 within an Eh range of 200-300 mV. In the present study, there was no substantial change in copper recoveries at different concentrations of NaClO within an Eh range of 219-543 mV. The results obtained could be explained by the fact that different types of sulphide ores were investigated in these studies, suggesting that different sulphide minerals exhibit different rates of redox reactions from an electrochemical perspective (Woods, 1971, Corin et al., 2013). From a mixed potential viewpoint, the reduction reaction of either oxygen or NaClO, as shown in equations 6.1 and 6.2, is an essential step that should occur on the mineral surface to enhance floatability. It should be noted that these reactions are clearly pH dependent.

$$ClO^- + H_2\ O + 2e^- \rightarrow Cl^- + 2OH^- \qquad E^0(V) = 0.89V \quad \text{..... Eqn 6.1}$$

$$O_2 + 2H_2O + 4e^- \leftrightarrow\ 4OH^- \quad \text{..... Eqn 6.2}$$

The control of potential by use of chemical reagents may have two implications on flotation recoveries, improvement of valuable mineral recoveries as a result of the formation of hydrophobic entities on the mineral surface or reduction of valuable mineral recoveries due to the formation of the hydrophilic entities. Though it is presumed that an increase in potential modifier concentration and thus Eh resulted in more hydrophobic mineral particles, as mentioned earlier, it may also be possible that a minute amount of Cl^- hydrophilic entities might have formed on the mineral surfaces, as suggested by the Pourbaix diagram in Figure 2.18. The increase in concentration of NaClO and thus Eh might have increased the oxidation film formed thereby confirming the slight decrease in copper recoveries obtained.

6.2.2.2 $KMnO_4$

It has been postulated that $KMnO_4$ has a depressing effect on sulphide minerals such as sphalerite, pyrrhotite and chalcopyrite (Bulatovic, 2007). However, the author did not highlight the concentration levels of $KMnO_4$ that yield depressing effects. Tajadod (1997) investigated the effect of $KMnO_4$ on chalcopyrite in the presence of a xanthate collector and determined that copper recoveries ranged between 78-81% for a concentration of 0.1-10 mg/l $KMnO_4$. The author reported the threshold level to be 10 mg/l and further reported lower recoveries of 39% at 100 mg/l $KMnO_4$. These findings are consistent with the present study where copper recoveries were above 88% for concentrations of $1x10^{-4}$ mols $KMnO_4$ (Eh of 378 mV) and $1x10^{-3}$ mols $KMnO_4$ (Eh of 476 mV). The threshold level was determined to be above a concentration of $1x10^{-3}$ mols $KMnO_4$ (Eh of 476 mV), after-which a very low copper recovery of 4.8% was obtained at a higher concentration of $1x10^{-2}$ mols $KMnO_4$ (Eh of 540 mV). However, Tajadod (1997) did not report on how the copper grades and froth stability were affected by the use of $KMnO_4$ which have been highlighted in the present study. Good floatability of chalcocite was obtained in reducing conditions with a maximum recovery of 73% at an Eh of -222 mV whereas increasing the Eh to 602 mV reduced recoveries to 18% (Razmjouee et al., 2012). The lower copper recoveries obtained with higher concentrations of $KMnO_4$ have been ascribed to the strong depressing effect of hydrated forms of manganese oxides (Rinelli et al., 1980). These oxidation products coat the mineral surface with a hydrophilic layer thereby reducing/inhibiting the flotation of chalcopyrite (Guo and Yen, 2002). From an electrochemical perspective, it has been reported that depression of chalcopyrite may be associated with the creation of a more cathodic mixed potential than the xanthate/dixanthogen potential, which would not favour the formation of dixanthogen on the mineral surface (Janetski et al., 1977). This statement may apply depending on the type of mineral surface used and the chemical environment to which it is exposed. The findings of Rinelli et al. (1980) are consistent with the results obtained in the present study, where reduced forms of manganese oxides are presumed to have formed on the mineral surface, as indicated in the Pourbaix diagram in Figure 2.19.

It has been proposed that the potential at which a mineral is depressed highly depends on the affinity of ions for that particular mineral surface, therefore depressive effects vary

depending on the nature of ion involved (Kocabag and Guler, 2008, Razmjouee et al., 2012). Kocabag and Guler (2008) further prescribed the forces on the mineral surfaces to determine floatability, implying that floatability is a function of the relative number of hydrophilic and hydrophobic sites present on the mineral surface.

6.2.2.3 $K_2Cr_2O_7$

With regards to $K_2Cr_2O_7$, most studies in literature that have investigated the use of $K_2Cr_2O_7$ as a potential modifier have mainly reported on its depressing effect on galena (Palsson, 1991, Kocabag and Guler, 2008). The effect of $K_2Cr_2O_7$ on chalcopyrite recoveries has not been clearly discussed in previous studies (Kocabag and Guler, 2007). Kocabag (2007) investigated on floatability of high purity chalcopyrite, in which recoveries of 65% were reported at an Eh of 400 mV and a pH range similar to that of the present study. However, the present study obtained higher copper recoveries above 90% for all concentrations of $K_2Cr_2O_7$ which resulted in an Eh range of 137-222 mV. Copper recoveries obtained in the present study at concentrations under investigation were therefore not significantly different. The Pourbaix diagram in Figure 2.20, suggests that the hydrophilic species Cr_2O_3 was formed in very minute quantities with an increase in concentration of $K_2Cr_2O_7$ and thus Eh. This also confirms the lower recoveries obtained by Kocabag (2007) at an Eh of 400 mV. Kocabag and Guler (2008) suggested that copper and iron chromates are soluble in water and that the mineral surface is composed mainly of the oxidation products of the mineral rather than metal chromate or dichromate and suggested that the reaction in equation 3 could be one of the cathodic reactions that occur on a mineral surface:

$$Cr_2O_7^{-2} + H_2O + 2e^- \leftrightarrow 2HCrO_4^{-2} \leftrightarrow 2CrO_4^{-2} + 2H^+ + 2e^- \quad \text{Eqn 6.3}$$

Overall, it has been observed in this study that there is no correlation between Eh and copper recovery as shown by Corin et al. (2013), for it may be that the flotation recoveries could be dominated by the mineral type, the potential modifier type and probably the concentration of a particular potential modifier. Standard operating conditions were used in Figures 2.18, 2.19 and 2.20, the findings of this work could further be substantiated by future research work under the same experimental conditions.

6.3 Equilibrium potentials of SIBX

Anodic polarization of a platinum working electrode is a technique often used in determining equilibrium potentials of xanthate collectors. The polarization step results in the oxidation of xanthate to its dimer form, dixanthogen on the platinum electrode surface (Buswell, 1998, Tadie, 2015). The final rest potential measured after open circuiting the platinum electrode, is referred to as the dimerization potential of the respective xanthate collector.

Most studies have focussed on the equilibrium potential of sodium/potassium ethyl xanthate (Majima, 1968, Allison et al., 1972, Tadie, 2015) with very little having been reported for SIBX. In the present study the equilibrium potential of SIBX at 6.24×10^{-4} M was measured as 80 mV. It was observed that the equilibrium potential for SIBX is fully dependent on its concentration as shown in Table 5.4. These findings are supported by the work of Buswell (1998). The present study further determined the increase in equilibrium potential for every order of magnitude decrease in concentration of SIBX to be 58 mV. These findings are in good agreement with what is predicted by the Nernst equation. Using the Nernst equation, E^0 values were calculated and showed similar trends to what has been reported previously by Buswell (1998).

6.4 Effect of potential modifiers on rest potential measurements

An attempt is made in this section to identify the thermodynamic reactions taking place on the mineral surface and to identify the characteristic species formed. Special reference will be made to the mixed potential/rest potential theory, as described in Chapter 2 and in this context the term rest potential is used. In addition to the aforementioned, it is presumed that rest potential measurements also make it possible to determine rates of reactions occurring on a mineral surface (Hu et al., 2009).

The existence of a rest potential involves the anodic oxidation of a thiol collector that transfers a charge to the mineral surface and the simultaneous cathodic reduction of oxygen (or oxidising agents) returns the charge to solution (Kocabag and Guler, 2008, Hu et al., 2009). It has been established that surface composition of sulphide minerals such as formation of

dithiolate or a metal-thiolate is highly dependent upon whether the final rest potential of a particular mineral lies below or above the thio ion/dithiolate couple, which is commonly referred to as the equilibrium/oxidation potential (Allison et al., 1972, Tolley et al., 1996). Over potentials that are established during the electrochemical reactions drive the cathodic and anodic reactions away from the equilibrium potential, and proceed at a definite speed (Kocabag and Guler, 2008). Therefore, the over potential is a crucial parameter in determining the progress of a particular reaction.

The equilibrium potential of SIBX measured prior to the rest potential, was used as a baseline to determine which species were formed on the mineral surface. It was determined in the present study that all rest potentials measured under all conditions were in excess of the equilibrium potential of the xanthate/dixanthogen couple, thereby indicating that the dixanthogen species was formed on the mineral surface (Allison et al., 1972). This fully confirms the copper recoveries obtained in the present study. The formation of the dixanthogen species is presumed to proceed through a chemisorption step in which the multilayers of dixanthogen formed bind to the chemisorbed xanthate monolayer by interaction of the hydrocarbon moieties of the molecule (Vermaak et al., 2004).

A standard rest potential measurement profile in the presence of an oxidising potential modifier has been proposed in this study in modification of the standard rest potential measurement profile derived by Tadie (2015). With regards to this system, it is indicated in Figure 2.24 that prior to the addition of the oxidising potential modifiers, the open-circuit potential was a result of the oxidation of the mineral surface and the reduction of oxygen. After addition of an oxidising potential modifier, the open-circuit potential measured is presumed to be as a result of three factors, namely the oxidation of the mineral surface, the reduction of oxygen and the reduction of the oxidising potential modifier. Upon addition of SIBX, the potential measured was as a result of the oxidation of the mineral surface, the reduction of oxygen, the reduction of the oxidising potential modifier and the oxidation of SIBX. However, the preceding interpretations apply to all rest potential graphs (Figures 5.38-5.47), with the degree of increase and decrease in potential after addition of oxidising

potential modifiers and SIBX, respectively, being determined by the type and concentration of potential modifier used.

Relevant to the rest potential curves as shown in Figures 5.39-5.47 for NaClO, $KMnO_4$ and $K_2Cr_2O_7$, it is evident that the higher the concentration of potential modifier, the higher the magnitude of increase in potential and the lower the magnitude of decrease upon addition of SIBX. This suggests that collector adsorption is affected by its extent of oxidation on the mineral surface, depending on the conditions in the solution phase and subsequently affects floatability as oxidation products found on mineral surfaces also determine the degree of floatability. Compared to other potential modifiers, it has been proposed that the reduction of $KMnO_4$ is rapid due to its high oxidising nature (Bulatovic, 2007). This agrees with the large increase in rest potential obtained after addition of $KMnO_4$ in the present study. Previous studies have indicated that $KMnO_4$ has depressive effects on sphalerite, pyrrhotite, pyrite, galena and chalcopyrite (Tajadod, 1997, Bulatovic, 2007, Hu et al., 2009). This observation is confirmed by Figure 5.44, which shows that no collector oxidation occurred on the mineral surface after addition of the collector due to the formation of an oxidation product film on the mineral surface that either prevented or reduced the amount of dixanthogen that adsorbed on the mineral surface. With regards to $K_2Cr_2O_7$, the non-responsive trends observed may suggest that concentrations used in this investigation for $K_2Cr_2O_7$ were not effective enough to increase the rest potential of the mineral. It can be inferred that no reduction of $K_2Cr_2O_7$ occurred on the mineral surface at lower concentrations as shown in Figures 5.45 and 5.46.

6.5 Relationship between final rest potentials and copper recoveries

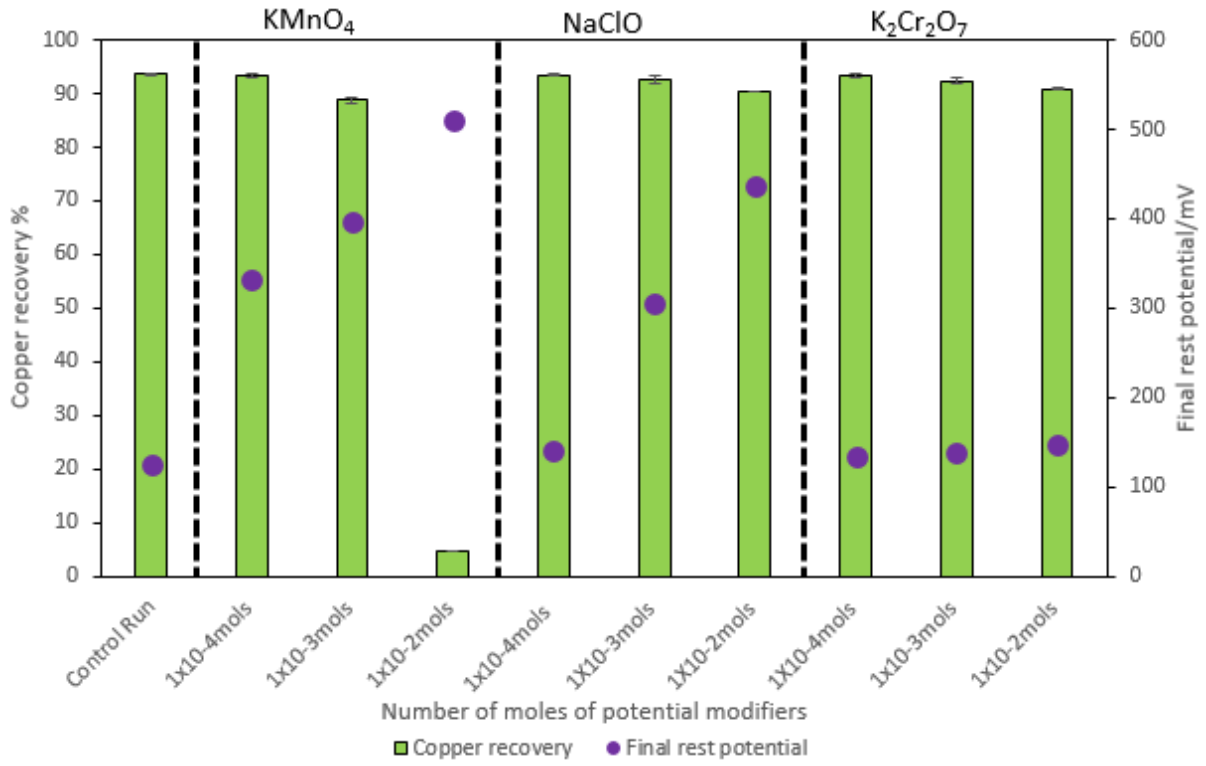

Figure 6.4: Copper recovery as a function of final rest potential of chalcopyrite for all conditions under investigation in 100 g/t SIBX & 40 g/t DOW 200. Error bars represent standard error between duplicate tests.

An attempt was made to relate copper recoveries with final rest potential measurements, as shown in Figure 6.4. It is clear that an inverse relationship exists between copper recoveries and rest potentials values. There is no evidence in literature reporting on the relationship of the aforementioned parameters. It is evident that the highest copper recovery was obtained at a lower rest potential and conversely the lowest copper recovery was attained at the highest rest potential. The final rest potentials obtained are indicative of the extent of oxidation of the respective xanthate collector. The lower rest potentials indicate that a higher level of collector oxidation occurred on the mineral surface, thereby allowing for more collector adsorption on the mineral surface resulting in higher copper recoveries. Inversely, higher rest potentials show that little or no degree of collector oxidation occurred, as indicated by the lower copper recoveries of 4.8% obtained at $1x10^{-2}$ mols $KMnO_4$. These findings are in contradiction with what was reported by Janetski et al. (1977), where the authors ascribe the depression of chalcopyrite to a mixed potential more cathodic than the

xanthate/dixanthogen potential in which no dixanthogen formation occurs. Notwithstanding the observations made by Janetski et al. (1977), the observations from the present study could be an additional explanation. It is important to highlight that the aforestated explanations could also be dependent on the type of system used for an investigation.

7 Conclusions and Recommendations

The key findings from the present study are presented as answers to the key questions developed in Chapter 3. The contribution of the current work provides a comprehensive insight into the effect of potential modifiers on the flotation of a copper sulphide ore, using an electrochemical approach. The key questions are outlined below and the conclusions drawn from the present study are given. Thereafter, a list of recommendations is given for future work.

7.1 Conclusions

To what extent do potential modifiers affect froth stability, copper recoveries and copper grades?

On the basis of previous studies, it was hypothesized at the commencement of this study that concentrations of potential modifiers that result in an Eh range of 100-400 mV would promote high valuable mineral recoveries due to the formation of hydrophobic mineral particles which would result in a moderately stable froth. Very high concentrations of potential modifiers that induce Eh values ≥500 mV, may result in reduced copper recoveries due to the presence of very hydrophobic mineral particles, which would increase bubble coalescence and bubble breakage or result in highly stable froth. This study has certainly shown that an increase in concentration of potential modifiers increases froth stability or bubble coalescence depending on the potential modifier used. Furthermore, concentrations of potential modifiers resulting in Eh values of 137-476 mV resulted in high copper recoveries >88%, with $1x10^{-2}$ mols of $KMnO_4$ at an Eh of 540 mV giving a very low copper recovery of 4.8%. However, though high copper recoveries were obtained between concentrations that gave rise to an Eh range of 137-476 mV, a slight decrease in copper recoveries of approximately <4%, was observed with even larger increases in concentrations of potential modifiers.

The key findings of this study were that the use of potential modifiers improved copper grades as a result of the reduction in gangue material recovery. Due to significantly different flotation recoveries obtained for $KMnO_4$ and NaClO at the same concentration and at the same Eh

values, it was surmised that there is no correlation between concentration of potential modifiers or Eh and flotation recoveries. Although Eh and concentration of potential modifiers have an effect of flotation performance, it has been determined that the nature of a potential modifier has a dominant effect. Comparing the findings of this work to literature findings on the results obtained for NaClO, it was determined that indeed different sulphide minerals exhibit different rates of redox reactions.

What is the equilibrium potential of SIBX (thiol collector) at $6.24x10^{-4}$ M?

The equilibrium potential of SIBX at $6.24x10^{-4}$ M in this study was measured to be 80 mV.

Does varying concentration affect the equilibrium potential of SIBX?

This study has shown that varying the concentration of the thiol collector SIBX, changes its equilibrium potential. It was determined that the increase in equilibrium potential for every order of magnitude decrease in concentration of SIBX is 58 mV.

What is the effect of using potential modifiers on the rest potentials of chalcopyrite and the subsequent species forming on the mineral surface?

The rest potential measurements demonstrated the interaction of potential modifiers and SIBX with a chalcopyrite surface and the possible characteristic species formed. The evaluation of the use of potential modifiers on rest potentials has shown that an increase in concentration of potential modifiers resulted in a higher magnitude of increase in potential and subsequently a lower magnitude of decrease upon addition of SIBX and vice-versa. The magnitude of increase of potential after addition of the potential modifiers is indicative of the extent of reduction of the particular potential modifier whereas the magnitude in the decrease of potential after addition of SIBX is indicative of the extent of oxidation of SIBX.

It was hypothesized that the dixanthogen species will be the most dominant species forming on the mineral surfaces. It has been shown in this study that indeed the dixanthogen species readily formed on the mineral surface in all conditions under investigation. This was demonstrated by the rest potential measurements obtained, which were all in excess of the

equilibrium potential of the SIBX xanthate/dixanthogen couple. The study shows that no metal thiolate species was formed given the investigated conditions. The final rest potential for the control run was the lowest of all conditions investigated and thus closer to the equilibrium potential, thereby indicating a lower rate of dixanthogen formation on the mineral surface. It was evident that an increase in rest potentials for all conditions investigated resulted from an increase in concentrations of the potential modifiers, thereby shifting the final rest potential away from the equilibrium potential. It can be inferred that an increase in concentration of the potential modifiers investigated increased the rate of dixanthogen formation on the mineral surface. However, $K_2Cr_2O_7$ had rest potentials for all concentrations investigated closer to the equilibrium potential, implying that compared to other potential modifiers, $KMnO_4$ and NaClO, $K_2Cr_2O_7$ produced the lowest rate of dixanthogen formation despite the increase in concentration.

Is there a relationship between rest potentials and flotation recoveries?

This work has demonstrated that an inverse relationship exists between copper recoveries and rest potential measurements. It was apparent that the highest copper recovery was obtained at a lower final rest potential measurement and conversely the lowest copper recovery was obtained at the highest final rest potential measurement. It was of high interest to note that SIBX did not interact with the mineral surface at $1x10^{-2}$ $KMnO_4$, which therefore resulted in a drastic decrease in copper recovery.

7.2 Recommendations

Based on the contributions and key findings of this study, the following recommendations have been proposed:

1. Since a high grade copper sulphide ore was investigated in this study, it will be interesting to investigate the effect of the same potential modifiers on other sulphide ores, either with lower grades or with different valuable minerals.
2. More potential modifiers could be investigated on this particular system.
3. Conditioning time for potential modifiers could be assessed to determine how it can affect copper recoveries.
4. It was difficult to directly relate the dynamic stability factors obtained for the $KMnO_4$ tests with froth stability, as quantified by the Bikerman's test. Therefore, it is recommended that other methods may be used in future to quantify froth stability for potential modifiers like $KMnO_4$.
5. Complementing electrochemical investigations with techniques such as UV-VIS (Ultraviolet and visible absorption) Spectroscopy, FTIR (Fourier Transform Infrared Spectroscopy), X-ray Photoelectron Spectroscopy (XPS) and Raman spectroscopy, provides valuable information on the nature of surface species.
6. The use of in-situ spectro-electrochemical methods such as transmission spectroscopy or Internal Reflection Spectroscopy (IRS). These optically coupled electrochemical methods allow for direct access to kinetic data of electrode reactions, quantitative and qualitative information on the state of the interface at electrochemical conditions.

References

ALLISON, S. A., GOOLD, L., NICOL, M. & GRANVILLE, A. 1972. A determination of the products of reaction between various sulfide minerals and aqueous xanthate solution, and a correlation of the products with electrode rest potentials. *Metallurgical and materials transactions A Physical metallurgy and materials science, Volume* 3, pp 2613-2618.

ATA, S., AHMED, N. & JAMESON, G. J. 2003. A study of bubble coalescence in flotation froths. *International Journal Of Mineral Processing,* 72, pp 255-266.

BARBIAN, N., HADLER, K., VENTURA-MEDINA, E. & CILLIERS, J. J. 2005. The froth stability column: linking froth stability and flotation performance. *Minerals Engineering,* 18, pp 317-324.

BARBIAN, N., VENTURA-MEDINA, E. & CILLIERS, J. J. 2003. Dynamic froth stability in froth flotation. *Minerals Engineering,* 16, pp 1111-1116.

BIKERMAN, J. J. 1973. *Foams,* New York, Springer-Verlag.

BOZKURT, V., XU, Z. & FINCH, J. A. 1998. Pentlandite/pyrrhotite interaction and xanthate adsorption. *International Journal of Mineral Processing,* 52, pp 203-214.

BROUGHTON, D. W., HITZMANN, M. A. & STEPHENS, A. J. 2002. Exploration history and Geology of the Kansanshi Cu(-Au) deposit, Zambia. *R. Goldfarb & R. Nielsen (Eds). Society of Economic Geologists, Special Publication 9-Integrated Methods for Discovery: Global Exploration in the 20th century.* 1st ed : Boulder, Colorado: Society of Economic Geologists.

BUCKLEY, A. N., HOPE, G. A. & WOODS, R. 2003. Metals from sulfide minerals: The role of adsorption of organic reagents in processing technologies , in Solid-Liquid Interfaces Macroscopic Phenomena-Microscopic Understanding. *Topics in Applied Physics SpringerVerlag pp.* Berlin: *Springer-Verlag*.

BUCKLEY, A. N. & WOODS, R. 1990. X-Ray Photoelectron Spectroscopic and Electrochemical Studies of the Interaction of Xanthate with Galena in Relation to the Mechansim Proposed by Page and Hazell. *International Journal of Mineral Processing,* 28**,** pp 310-311.

BUCKLEY, A. N. & WOODS, R. 1994. Xanthate chemisorption on lead sulfide. *Colloids and Surfaces,* 89, pp 71-76.

BUCKLEY, A. N. & WOODS, R. 1997. Chemisorption-the thermodynamically favoured process in the interaction of thiol collectors with sulphide minerals. *International Journal of Mineral Processing,* 51, pp 15-26.

BULATOVIC, S. M. 2007. *Handbook of Flotation Reagents*, Elsevier Science Technology Books.

BUSWELL, A. M. 1998. *An electrochemical investigation into the floatability of pyrrhotite.* Master's thesis, University of Witwatersrand.

BUSWELL, A. M., BRADSHAW, D. J., HARRIS, P. J. & EKMEKCI, Z. 2002. The use of electrochemical measurements in the flotation of a platinum group minerals (PGM) bearig ore. *Minerals Engineering,* 15**,** pp 395-404.

BUSWELL, A. M. & NICOL, M. J. 2002. Some aspects of the elctrochemistry of the flotation of pyrrhotite. *Journal of Applied Electrochemistry,* 32, pp 1321-1329.

CHADWICK, J. 2011. Great Mines- Zambia.

CHIMONYO, W. 2016. *An investigation into the relationship between electrochemical properties and flotation of sulphide mineras.* Master's thesis, University of Cape Town.

CHIMONYO, W., CORIN, K. C., WIESE, J. G. & O'CONNOR, C. T. 2017. Redox potential control during flotation of a sulphide mineral ore. *Minerals Engineering,* 110, pp 57-64.

COELHO, A. 2007. Coelho Software. Brisbane, Australia: TOPAS, Academic.

COOK, M. A. & NIXON, J. C. 1949. Theory of water-repellent films on solids formed by adsorption from aqueous solutions of heteropolar compounds. *Salt Lake City University of Utah Utah.* Salt Lake City: University of Utah, Utah.

CORIN, K. C., MISHRA, J. & O'CONNOR, C. T. 2013. Investigating the role of pulp chemistry on the floatability of a Cu-Ni sulphide ore. *International Journal of Mineral Processing,* 120, pp 8-14.

DIPPENAAR, A. 1982. The destabilization of froth by solids. I. The mechanism of film rupture. *International Journal of Mineral Processing,* 9, pp 1-14.

EKMEKCI, Z., BRADSHAW, D. J., HARRIS, P. J. & BUSWELL, A. M. 2006. Interactive effects of the type of milling media and CuSO4 addition on the flotation perfomance of sulphide minerals from Merensky ore Part II: Froth stability. *International Journal of Mineral Processing,* 78, pp 164-174.

EKMEKCI, Z., MEGAN, B., TEKES, E. B. & BRADSHAW, D. 2010. The relationship between the electrochemical, mineralogical and flotation characteristics of pyrrhotite samples from different Ni ores. *Journal of Electroanalytical Chemistry,* 647, pp 133-143.

FARROKHPAY, S. 2011. The significance of froth stability in mineral flotation. *Advances in Colloid and Interface Science,* 166, pp 1-7.

FARROKHPAY, S. & ZANIN, M. 2011. *Effect of water quality on froth stability in flotation*. *Engineering a Better World.* New South Wales, Austalia.

FINCH, J. A., NESSET, J. E. & ACUNA, C. 2008. Role of frother on bubble production and behaviour in flotation. *Minerals Engineering,* 21, pp 949-957.

FINKELSTEIN, N. P. 1997. Addendum to: The activation of sulphide minerals for flotation: A review. *International Journal of Mineral Processing,* 55, pp 283-286.

GOKTEPE, F. 2010. Effect of hydrogen peroxide and sodium hydrogen sulphide addition to change the electrochemical potential in flotation of chalcopyrite and pyrite minerals. *Mineral Processing and Extractive Metallurgy Review,* 32, pp 24-29.

GONZENBACH, U. T., STUDART, A. R., TERVOORT, E. & GAUCKLER, L. J. 2007. Tailoring the microstructure of particle-stabilised wet foams. *Langmuir,* 32, pp 1025-1032.

GUO, H. & YEN, W. 2002. Pulp potential and flotability of chalcopyrite. *Minerals Engineering,* 16, pp 247-256.

HOROZOV, T. S. 2008. Foams and foam films stabilised by solid particles. *Current opinion in Colloid and Interface Science,* 13, pp 134-140.

HU, Y., SUN, W. & WANG, D. 2009. *Electrochemistry of Flotation of Sulphide Minerals,* Beijing, *Tsinghua University Press & Springer Dordrecht Heidelberg*.

HUNTER, T. N., PUGH, R. J., FRANKS, G. V. & JAMESON, G. J. 2008. The role of particles in stabilising foams and emulsions. *Advances in Colloid and Interface Science,* 137, pp 57-81.

JANETSKI, A., WOODBURN, S. & WOODS, R. 1977. An electrochemical investigation of pyrite flotation and depression. *International Journal of Mineral Processing,* 4, pp 227-239.

JOHANSSON, G. & PUGH, R. J. 1992. The influence of particle size and hydrophobicity on the stability of mineralized froths. *International Journal of Mineral Processing,* 34, pp 1-21.

KALICHINI, M. S. 2015. *A study of the flotation characteristics of a complex copper ore.* Master's thesis, University of Cape Town.

KAMPUNZU, A. B., CAILTEUX, J. L. H., KAMONA, A. F., INTIOMALE, M. M. & MELCHER, F. 2009. Sediment hosted Zn-Pd-Cu deposits in the Central African Copperbelt. *Ore Geology Reviews,* 35**,** pp 263-297

KAWATRA, S. & EISELE, T. 2014. *Froth Flotation-Fundamental Principles* [Online]. Available: http://www.chem.mtu.edu/chemeng/faculty/kawatra/FlotationFundamentals.pdf [Accessed].

KHAN, A. & KELEBEK 2004. Electrochemical aspects of pyrrhotite and pentlandite in relation to their flotation with xanthate.Part 1: Cyclic voltammetry and rest potential measurements. *Journal of Applied Electrochemistry,* 34, pp 849-856.

KLIMPEL, R. R. 1995. The influence of Frother Structure on Industrial Coal Flotation. High Efficiency Coal Preparation (Kawatra, ed). Littleton: *Society for Mining, Metallurgy and Exploration*.

KOCABAG, D. & GULER, T. 2007. Two liquid flotation of sulphides: An electrochemical approach. *Minerals Engineering,* 20, pp 1246-1254.

KOCABAG, D. & GULER, T. 2008. A comparative evaluation of the response of platinum and mineral electrodes in sulfide mineral pulps. *International Journal of Mineral Processing,* 87, pp 51-59.

KOH, P. T. L. & SMITH, L. K. 2011. The effect of stirring speed and induction time on flotation. *Minerals Engineering,* 24, pp 442-448.

LANGA, N. T. N., ADELEKE, A. A., MENDONIDIS, P. & THUBAKGALE, C. K. 2014. Evaluation of sodium isobutyl xanthate as a collector in the froth flotation of a carbonatitic copper ore. *International Journal of Industrial Chemistry,* 5, pp 107-110.

LASKOWSKI, J. 1993. Frothers and flotation froth. *Mineral Processing and Extractive Metallurgy Review,* 12, pp 61-89.

MAJIMA, H. T., M 1968. Electrochemical studies of the xanthate-dixanthogen system on pyrite. *Trans.AIME,* 241**,** pp 431-436.

MANONO, M. S. 2012. *An investigation into the effect of ionic strength of plant water on vauable mineral and gangue recovery of a platinum bearing ore from the Merensky Reef.* Master's thesis, University of Cape Town.

MORAR, S. H. A comparison of froth stability measurements and their use in the prediction of concentrate grade 23rd International Mineral Processing Conference, 2006 Istanbul Turkey.

NYABEZE, W. 2015. *The effect of Copper Sulphate on froth stability.* Master's thesis, University of Cape Town.

PAGE, P. W. & HAZELL, L. B. 1989. X-ray photoelectron spectroscopy (XPS) studies of potassium amyl xanthate (KAX) adsorption on precipitated PdS related to galena flotation. *International Journal of Mneral Processing,* 25, pp 87-100.

PALSSON, B. I. 1991. Computer-assisted calculation of chemical equilibria with relevance to the chromate depression of galena. *International Journal of Mineral Processing,* 33, pp 207-221.

PENG, Y., WANG, B. & GERSON, A. 2012. The effect of electrochemical potential on the activation of pyrite by copper and lead ions during grinding. *International Journal of Mineral Processing* 102-103, pp 1141-149

PLACKOWSKI, C., BRUCKARD, W. J. & NGUYEN, A. V. 2014. Surface characterisation, collector adsorption and flotation response of enargite in a redox potential controlled environment. *Minerals Engineering,* 65, pp 61-73.

RALSTON, J. 1991. Eh and its consequences in sulphide mineral flotation. *Minerals Engineering,* 4, pp 859-878.

RAMACHANDRA RAO, S. 2004. *Surface Chemistry of Froth Flotation*, *Kluwer Academic/Plenum Publishers*.

RAZMJOUEE, S., ABDOLLAHY, M. & KOLEINI, S. M. J. 2012. Collectorless flotation of chalcocite by controlling redox potential. *Journal of Mining & Environment,* 3, pp 99-102.

RINELLI, G., MARABINI, A. M. & ALESSE, V. Depressing effect of permanganate on pyrite and galena flotation. Complex sulphide ores, 1980 Rome, Italy. IMM, pp 199-206.

ROSS, V. & VAN DEVENTER, J. 1985. The interactive effects of the sulphite ion, pH, and dissolved oxygen on the flotation of chalcopyrite ad galena from Black Mountain ore. *Journal of the South African Institute of Mining and Metallurgy,* 1, pp 13-21.

SASAKI, K., TAKATSUGI, K., ISHIKURA, K. & HIRAJIMA, T. 2010. Spectroscopic study on oxidative dissolution of chalcopyrite, enargite and tennantite at different pH values. *Hydrometallurgy,* 100**,** pp 144-151.

SENIOR, G. D., SMITH, L. K. S. E. & BRUCKARD, W. J. 2009. The flotation of gersdorffite in sulphide nickel systems-A single mineral study. *International Journal of Mineral Processing,* 93, pp 165-171.

SHENI, N. R. 2016. *Considering the effect of pulp chemistry during flotation on froth stability.* Master's thesis, University of Cape Town.

SMITH, L., DAVEY, K. & BRUCKARD, W. The use of pulp potential control to separate copper and arsenic. IMPC, 2012 New Delhi, India.

SUBRAHMANYAM, T. & FORSSBERG, E. 1988. Particle entrainment and drainage in flotation- A review. *International Journal of Mineral Processing,* 23, pp 33-53

TADIE, M. 2015. *An Electrochemical Investigation of Platinum Group Minerals.* PhD thesis, University of Cape Town.

TAJADOD, J. 1997. *Flotation chemistry of enargite and chalcopyrite using potassium amyl xanthate and depressants.* PhD thesis, Queen's University.

TOLLEY, W., KOTLYAR, D. & VAN WAGONER, R. 1996. Fundamental electrochemical studies of sulphide mineral flotation. *Minerals Engineering,* 9, pp 603-637.

TSATOUHAS, G., GRANO, S. R. & VERA, M. 2006. Case studies on the performance and characterisation of the froth phase in industrial flotation circuits. *Minerals Engineering,* 19, pp 774-783.

VENTURA-MEDINA, E., BARBIAN, N. & CILLIERS, J. J. Froth stability and flotation performance. 22nd International Mineral Processing Conference, 2003 Cape Town.

VERMAAK, M. K. G., PISTORIOUS, P. C. & VENTER, J. A. 2005. Electrochemical and Raman spectroscopic studies of the interaction of ethyl xanthate with Pd-Bi-Te. *Minerals Engineering,* 18, pp 575-584.

VERMAAK, M. K. G., VENTER, J. A. & PISTORIOUS, P. C. 2004. Electrochemical studies of the interaction of ethyl xanthate with Pd-Bi-Te. *The Journal of the South African Institure of Mining and Metallurgy.* Pretoria.

WANG, L., PENG, Y. & RUNGE, K. 2016. Entrainment in froth flotation: The degree of entrainment and its contributing factors. *Powder Technology,* 288, pp 202-211.

WIESE, J. G. 2009. *Investigating depressant behaviour in the flotation of selected Merensky ores.* Master's thesis, University of Cape Town.

WIESE, J. G., HARRIS, P. J. & BRADSHAW, D. J. 2005. The influence of the reagent suite on the flotation of ores from the Merensky reef. *Minerals Engineering,* 18, pp 189-198.

WIESE, J. G., HARRIS, P. J. & BRADSHAW, D. J. 2011. The effect of the reagent suite on the froth stability in laboratory scale batch flotation tests. *Minerals Engineering,* 9, pp 995-1003.

WILLS, B. A. & NAPIER-MUNN, T. 2006. *Mineral Processing Technology*, *Elsevier Science & Technology Books*.

WOODS, R. 1971. The oxidation of ethyl xanthate on platinum, gold, copper and galena electrodes: Relation to the mechanism of mineral flotation. *Journal of Physical Chemistry,* 75, pp 354-362.

WOODS, R. 2010. Electrochemical Aspects of Sulfide Mineral Flotation in: C.J GREET, ed, *Flotation Plant Optimisation: A Metallurgical Guide tO Identifying and Solving Problems in Flotation Plants*.

WOODS, R. & GARDNER, J. R. 1974. An electrochemical investigation of contact angle and of flotation in the presence of alkylxanthates. I Platinum and Gold surfaces. *Australian Journal of Chemistry,* 27, pp 2139-2148.

WOODS, R., YOUNG, C. A. & YOON, R. H. 1990. Ehtyl xanthate chemisorption isotherms and Eh-pH diagrams for the copper/water/xanthate and chalcocite/water/xanthate systems. *International Journal of Mineral Processing,* 30, pp 17-33.

YANG, X. & ALDRICH, C. 2005. Effects of impeller speed and aeration rate on flotation perfomance of sulphide ore. *Transactions of Nonferrous Metals Society of China,* 16, pp 185-190.

ZANIN, M., WIGHTMAN, E., GRANO, S. R. & FRANZIDIS, J. P. 2009. Quantifying contributions to froth stability in porphyry copper plants. *International Journal of Mineral Processing,* 91, pp 19-27.

ZHENG, X., FRANZIDIS, J. P. & JOHNSON, N. W. 2005. An evaluation of different models of water recovery in flotation. *Minerals Engineering,* 19, pp 871-882.

ZHENG, X., FRANZIDIS, J. P. & JOHNSON, N. W. 2006. An evaluation of different models of water recovery in flotation. *Minerals Engineering,* 19, pp 871-882.

Appendix A

Batch Flotation tests

Test Conditions	Sample ID	Time mins	Mass g	Water rec g	Cum mass g	Cum water g	Copper grade %	Copper rec %	Gangue rec %
SIBX 100 g/t	C1	2	49.67	43.92	49.67	43.92	13.0100	60.74	4.42
DOW 200 40 g/t	C2	4	39.55	86.59	89.22	130.51	9.7682	81.92	3.82
No Eh modifier	C3	6	35.64	106.14	124.86	236.65	7.82	91.78	3.54
	C4	8	24.13	104.49	148.99	341.14	6.69	93.74	2.45
	Feed		986.25						
	Tails		837.26						
SIBX 100 g/t	C1	2	51.35	50.05	51.35	50.05	13.09	60.72	4.63
DOW 200 40 g/t	C2	4	42.37	95.15	93.72	145.20	10.07	85.27	4.12
No Eh modifier	C3	6	29.48	120.79	123.20	265.99	8.29	92.23	2.98
	C4	8	19.92	129.69	143.12	395.68	7.24	93.55	2.05
	Feed		973.34						
	Tails		830.22						
SIBX 100 g/t	C1	2	52.02	53.72	52.02	53.72	13.47	59.98	4.37
DOW 200 40 g/t	C2	4	35.90	81.14	87.92	134.86	10.45	78.67	3.27
$1x10^{-4}$ mols $KMnO_4$	C3	6	23.28	78.03	111.20	212.89	9.17	87.28	2.16
	C4	8	20.23	104.83	131.43	317.72	8.25	92.84	1.90
	Feed		1042.38						
	Tails		910.95						
SIBX 100 g/t	C1	2	59.12	67.15	59.12	67.15	12.15	74.85	5.41
DOW 200 40 g/t	C2	4	31.42	77.73	90.54	144.88	9.35	88.23	3.14
$1X10^{-4}$ mols $KMnO_4$	C3	6	25.87	109.97	116.41	254.85	7.64	92.67	2.65
	C4	8	18.96	133.03	135.37	387.88	6.65	93.84	1.96
	Feed		968.73						
	Tails		833.36						

Test Conditions	Sample ID	Time mins	Mass g	Water rec g	Cum mass g	Cum water g	Copper grade %	Copper rec %	Gangue rec %
SIBX 100 g/t	C1	2	59.12	67.15	59.12	67.15	12.15	74.85	5.41
DOW 200 40 g/t	C2	4	31.42	77.73	90.54	144.88	9.35	88.23	3.14
$1x10^{-4}$ mols $KMnO_4$	C3	6	25.87	109.97	116.41	254.85	7.64	92.67	2.65
	C4	8	18.96	133.03	135.37	387.88	6.65	93.84	1.96
	Feed		968.73						
	Tails		833.36						
SIBX 100 g/t	C1	2	59.26	108.98	59.26	108.98	11.35	72.87	5.49
DOW 200 40 g/t	C2	4	26.70	159.82	85.96	268.80	8.90	82.87	2.69
$1x10^{-3}$ mols $KMnO_4$	C3	6	19.95	115.81	105.91	384.61	7.54	86.51	2.05
	C4	8	12.56	121.62	118.47	506.23	6.88	88.27	1.29
	Feed		967.36						
	Tails		848.89						
SIBX 100 g/t	C1	2	47.03	88.70	47.03	88.70	12.90	60.47	4.42
DOW 200 40 g/t	C2	4	32.65	80.50	79.68	169.20	10.34	82.14	3.29
$1x10^{-3}$ mols $KMnO_4$	C3	6	19.67	89.11	99.35	258.31	8.80	87.15	2.07
	C4	8	13.36	107.29	112.71	365.60	7.96	89.38	1.42
	Feed		935.40						
	Tails		822.69						
SIBX 100 g/t	C1	2	31.56	342.79	31.56	342.79	0.72	2.15	3.28
DOW 200 40 g/t	C2	4	20.03	391.59	51.59	734.38	0.68	3.33	2.09
$1X10^{-2}$ mols $KMnO_4$	C3	6	14.16	323.31	65.75	1057.69	0.66	4.08	1.48
	C4	8	12.08	293.73	77.83	1351.42	0.65	4.79	1.26
	Feed		964.85						
	Tails		887.02						

Test Conditions	Sample ID	Time mins	Mass g	Water rec g	Cum mass g	Cum water g	Copper grade %	Copper rec %	Gangue rec %
SIBX 100 g/t	C1	2	29.54	350.05	29.54	350.05	0.63	1.84	3.09
DOW 200 40 g/t	C2	4	24.96	462.95	54.50	813.00	0.61	3.30	2.61
1x10^{-2} mols $KMnO_4$	C3	6	15.77	338.18	70.27	1151.18	0.60	4.15	1.65
	C4	8	11.70	274.09	81.97	1425.27	0.59	4.81	1.22
	Feed		959.82						
	Tails		877.85						
SIBX 100 g/t	C1	2	44.29	42.01	44.29	42.01	13.04	53.64	4.03
DOW 200 40 g/t	C2	4	42.13	80.11	86.42	122.12	10.48	84.13	4.06
1x10^{-4} mols NaClO	C3	6	23.33	79.77	109.75	201.89	8.96	91.33	2.36
	C4	8	16.61	96.37	126.36	298.26	7.98	93.71	1.71
	Feed		966.11						
	Tails		839.75						
SIBX 100 g/t	C1	2	40.74	38.00	40.74	38.00	12.06	52.05	3.79
DOW 200 40 g/t	C2	4	38.07	67.49	78.81	105.49	9.97	83.25	3.71
1x10^{-4} mols NaClO	C3	6	23.09	74.17	101.90	179.66	8.46	91.38	2.36
	C4	8	15.08	85.73	116.98	265.39	7.54	93.40	1.57
	Feed		954.99						
	Tails		838.01						
SIBX 100 g/t	C1	2	51.52	57.32	51.52	57.32	13.45	60.66	4.71
DOW 200 40 g/t	C2	4	35.20	82.03	86.72	139.35	11.06	83.97	3.44
1X10^{-3} mols NaClO	C3	6	22.66	85.85	109.38	225.20	9.48	90.80	2.31
	C4	8	21.06	142.16	130.44	367.36	8.17	93.33	2.19
	Feed		957.18						
	Tails		826.74						

Test Conditions	Sample ID	Time mins	Mass g	Water rec g	Cum mass g	Cum water g	Copper grade %	Copper rec %	Gangue rec %
SIBX 100 g/t	C1	2	51.23	53.89	51.23	53.89	13.13	63.47	4.67
DOW 200 40 g/t	C2	4	31.99	70.28	83.22	124.17	10.56	82.89	3.14
$1x10^{-3}$ mols NaClO	C3	6	22.36	84.41	105.58	208.58	9.00	89.67	2.27
	C4	8	16.46	102.27	122.04	310.85	7.98	91.88	1.70
	Feed		964.04						
	Tails		842						
SIBX 100 g/t	C1	2	42.64	49.49	42.64	49.49	12.68	47.61	3.90
DOW 200 40 g/t	C2	4	45.21	81.60	87.85	131.09	10.04	77.66	4.38
$1x10^{-2}$ mols NaClO	C3	6	24.12	67.63	111.97	198.72	8.92	87.93	2.40
	C4	8	16.11	110.47	128.08	309.19	8.01	90.37	1.66
	Feed		965.72						
	Tails		837.64						
SIBX 100 g/t	C1	2	34.85	78.93	34.85	78.93	12.53	43.91	3.26
DOW 200 40 g/t	C2	4	40.07	108.61	74.92	187.54	10.04	75.62	3.95
$1x10^{-2}$ mols NaClO	C3	6	21.33	98.57	96.25	286.11	8.87	85.85	2.17
	C4	8	17.88	110.70	114.13	396.81	7.89	90.52	1.86
	Feed		944.84						
	Tails		830.71						
SIBX 100 g/t	C1	2	51.59	48.43	51.59	48.43	12.71	61.94	4.72
DOW 200 40 g/t	C2	4	32.47	66.56	84.06	114.99	10.63	84.39	3.16
$1X10^{-4}$ mols $K_2Cr_2O_7$	C3	6	19.60	65.88	103.66	180.87	9.27	90.78	1.99
	C4	8	16.63	89.64	120.29	270.51	8.19	93.05	1.72
	Feed		963.35						
	Tails		843.06						

Test Conditions	Sample ID	Time mins	Mass g	Water rec g	Cum mass g	Cum water g	Copper grade %	Copper rec %	Gangue rec %
SIBX 100 g/t	C1	2	45.52	44.07	45.52	44.07	14.14	55.87	4.09
DOW 200 40 g/t	C2	4	34.60	68.04	80.12	112.11	11.74	81.65	3.31
$1x10^{-4}$ mols $K_2Cr_2O_7$	C3	6	23.83	86.91	103.95	199.02	10.02	90.44	2.39
	C4	8	16.68	96.28	120.63	295.30	8.95	93.67	1.71
	Feed		965.23						
	Tails		844.60						
SIBX 100 g/t	C1	2	50.62	56.85	50.62	56.85	11.24	65.29	4.71
DOW 200 40 g/t	C2	4	30.78	84.14	81.40	140.99	8.69	81.18	3.08
$1x10^{-3}$ mols $K_2Cr_2O_7$	C3	6	23.34	91.78	104.74	232.77	7.43	89.36	2.37
	C4	8	15.29	88.36	120.03	321.13	6.74	92.84	1.57
	Feed		961.25						
	Tails		841.22						
SIBX 100 g/t	C1	2	49.17	44.42	49.17	44.42	12.94	66.89	4.53
DOW 200 40 g/t	C2	4	32.31	72.25	81.48	116.67	9.87	84.52	3.24
$1x10^{-3}$ mols $K_2Cr_2O_7$	C3	6	18.51	61.40	99.99	178.07	8.51	89.46	1.91
	C4	8	14.79	80.31	114.78	258.38	7.61	91.87	1.54
	Feed		955.04						
	Tails		840.26						
SIBX 100 g/t	C1	2	49.72	97.97	49.72	97.97	14.88	76.49	4.49
DOW 200 40 g/t	C2	4	20.75	77.47	70.47	175.44	11.77	85.77	2.10
$1X10^{-2}$ mols $K_2Cr_2O_7$	C3	6	18.47	89.93	88.94	265.37	9.70	89.16	1.92
	C4	8	16.35	107.67	105.29	373.04	8.34	90.76	1.72
	Feed		952.51						
	Tails		847.22						

Test Conditions	Sample ID	Time mins	Mass g	Water rec g	Cum mass g	Cum water g	Copper grade %	Copper rec %	Gangue rec %
SIBX 100 g/t	C1	2	52.41	103.70	52.41	103.70	12.83	79.11	4.83
DOW 200 40 g/t	C2	4	14.63	50.11	67.04	153.81	10.80	85.16	1.49
$1x10^{-2}$ mols $K_2Cr_2O_7$	C3	6	19.12	84.60	86.16	238.41	8.79	89.14	1.99
	C4	8	17.59	108.49	103.75	346.90	7.46	91.00	1.84
	Feed		954.23						
	Tails		840.48						

Appendix B

Determination of dynamic froth stability

Froth Height (mm)				
Run 1	Run 2	Average Height	STDEV	STDERROR
0	0	0	0	0
23	18	20.5	3.535534	2.5
30	24	27	4.242641	3
32	28	30	2.828427	2
38	29	33.5	6.363961	4.5
42	30	36	8.485281	6
44	37	40.5	4.949747	3.5
48	41	44.5	4.949747	3.5
52	45	48.5	4.949747	3.5
54	48	51	4.242641	3
56	50	53	4.242641	3
58	53	55.5	3.535534	2.5
60	55	57.5	3.535534	2.5

- The dynamic stability factors were calculated using equation 2.2. The value of H_{max} was determined by averaging the maximum froth heights obtained from duplicate tests. Results for each condition were tabulated as in table above, which shows the condition for $1x10^{-3}$ mols $K_2Cr_2O_7$ from three phase tests.

Appendix C

Electrochemical measurements

Time/secs	$1x10^{-4}$ mols NaClO/ V-SHE		$1X10^{-3}$ mols NaClO/ V-SHE		$1x10^{-2}$ mols NaClO/ V-SHE	
	Run 1	Run 2	Run 1	Run 2	Run 1	Run 2
5.01	0.25238	0.24478	0.24494	0.24321	0.24449	0.25459
10.02	0.25238	0.24479	0.24495	0.24321	0.24449	0.2546
15.03	0.25239	0.2448	0.24497	0.24322	0.24452	0.25467
20.04	0.25242	0.24482	0.24505	0.24324	0.24459	0.25485
25.05	0.25246	0.24488	0.24518	0.24327	0.24471	0.25518
30.06	0.25252	0.24495	0.24537	0.24331	0.24488	0.25561
35.07	0.25258	0.24503	0.24557	0.24336	0.24507	0.25609
40.08	0.25265	0.24511	0.24579	0.24341	0.24527	0.25656
45.09	0.25271	0.24519	0.246	0.24347	0.24547	0.25701
50.1	0.25278	0.24527	0.2462	0.24352	0.24566	0.25743
55.11	0.25285	0.24535	0.2464	0.24357	0.24585	0.25783
60.12	0.25291	0.24543	0.2466	0.24362	0.24603	0.25821
65.13	0.25298	0.24551	0.24679	0.24367	0.24621	0.25858
70.14	0.25304	0.24559	0.24699	0.24372	0.24639	0.25893
75.15	0.25311	0.24566	0.24718	0.24376	0.24657	0.25927
80.16	0.25317	0.24574	0.24736	0.24381	0.24673	0.25959
85.17	0.25324	0.24582	0.24754	0.24386	0.2469	0.25989
90.18	0.2533	0.24589	0.24772	0.24391	0.24706	0.26018
95.19	0.25337	0.24596	0.24789	0.24396	0.24721	0.26046
100.2	0.25343	0.24604	0.24806	0.244	0.24737	0.26073
105.2	0.25349	0.24611	0.24823	0.24405	0.24752	0.26099
110.2	0.25355	0.24618	0.2484	0.2441	0.24767	0.26124
115.2	0.25362	0.24626	0.24856	0.24414	0.24782	0.26148
120.2	0.25368	0.24633	0.24872	0.24419	0.24797	0.26171
125.3	0.25374	0.24641	0.24888	0.24424	0.24811	0.26194
130.3	0.2538	0.24648	0.24904	0.24428	0.24825	0.26215
135.3	0.25386	0.24655	0.2492	0.24433	0.24838	0.26237
140.3	0.25392	0.24662	0.24935	0.24438	0.24852	0.26257
145.3	0.25398	0.24669	0.2495	0.24442	0.24865	0.26276
150.3	0.25404	0.24676	0.24965	0.24447	0.24879	0.26295
155.3	0.2541	0.24683	0.2498	0.24452	0.24892	0.26314
160.3	0.25415	0.2469	0.24994	0.24456	0.24905	0.26331
165.3	0.25421	0.24697	0.25009	0.24461	0.24917	0.26349
170.3	0.25427	0.24704	0.25023	0.24465	0.24929	0.26365
175.4	0.25433	0.24711	0.25037	0.2447	0.24942	0.26381

180.4	0.25438	0.24717	0.2505	0.24474	0.24954	0.26396
185.4	0.25444	0.24724	0.25064	0.24479	0.24966	0.26411
190.4	0.2545	0.24731	0.25078	0.24484	0.24977	0.26425
195.4	0.25455	0.24738	0.25091	0.24488	0.24989	0.26438
200.4	0.2546	0.24744	0.25104	0.24492	0.25	0.26452
205.4	0.25466	0.2475	0.25117	0.24496	0.25011	0.26465
210.4	0.25471	0.24757	0.2513	0.24501	0.25022	0.26479
215.4	0.25476	0.24763	0.25143	0.24505	0.25032	0.26492
220.4	0.25482	0.2477	0.25155	0.2451	0.25043	0.26505
225.4	0.25487	0.24776	0.25168	0.24514	0.25053	0.26517
230.5	0.25492	0.24783	0.2518	0.24518	0.25063	0.26528
235.5	0.25497	0.24789	0.25192	0.24522	0.25074	0.26539
240.5	0.25502	0.24795	0.25204	0.24526	0.25084	0.2655
245.5	0.25508	0.24801	0.25216	0.24531	0.25094	0.2656
250.5	0.25513	0.24807	0.25227	0.24535	0.25104	0.26571
255.5	0.25519	0.24813	0.25239	0.24539	0.25113	0.26581
260.5	0.25524	0.24819	0.2525	0.24543	0.25123	0.26591
265.5	0.25529	0.24825	0.25261	0.24547	0.25133	0.266
270.5	0.25535	0.24831	0.25272	0.24551	0.25142	0.2661
275.5	0.2554	0.24837	0.25283	0.24555	0.25151	0.26618
280.6	0.25545	0.24843	0.25294	0.24559	0.2516	0.26627
285.6	0.2555	0.24849	0.25305	0.24563	0.25169	0.26635
290.6	0.25556	0.24855	0.25316	0.24566	0.25178	0.26644
295.6	0.25561	0.24861	0.25326	0.2457	0.25186	0.26651
300.6	0.25566	0.24867	0.25336	0.24574	0.25195	0.26659
305.6	0.25668	0.25001	0.25636	0.24824	0.25612	0.27046
310.6	0.26202	0.25686	0.2717	0.26154	0.27695	0.2897
315.6	0.27475	0.27238	0.30621	0.29279	0.3217	0.3307
320.6	0.29257	0.29275	0.3506	0.3356	0.3754	0.3794
325.6	0.3095	0.3105	0.3873	0.3745	0.4152	0.4148
330.7	0.3217	0.3219	0.4075	0.3997	0.4334	0.4307
335.7	0.3293	0.3282	0.414	0.4114	0.4367	0.4333
340.7	0.334	0.3319	0.4135	0.4146	0.4338	0.4306
345.7	0.3374	0.3345	0.4108	0.4139	0.4299	0.4272
350.7	0.3403	0.3368	0.4082	0.4121	0.4268	0.4247
355.7	0.3428	0.3389	0.4063	0.4104	0.4247	0.423
360.7	0.3451	0.3407	0.4049	0.4089	0.4233	0.4219
365.7	0.3471	0.3425	0.4039	0.4078	0.4222	0.4212
370.7	0.3488	0.3442	0.4031	0.4068	0.4214	0.4206
375.8	0.3504	0.346	0.4023	0.406	0.4208	0.4203
380.8	0.3519	0.3478	0.4016	0.4053	0.4204	0.4201
385.8	0.3533	0.3494	0.4008	0.4046	0.42	0.42
390.8	0.3547	0.3506	0.4001	0.404	0.4199	0.42

395.8	0.3559	0.3515	0.3993	0.4034	0.4198	0.4202
400.8	0.3569	0.3522	0.3986	0.4028	0.4198	0.4204
405.8	0.358	0.3529	0.398	0.4022	0.4199	0.4207
410.8	0.359	0.3536	0.3974	0.4016	0.4201	0.421
415.8	0.36	0.3543	0.3968	0.401	0.4203	0.4213
420.8	0.361	0.3552	0.3962	0.4004	0.4206	0.4217
425.9	0.362	0.3561	0.3956	0.3999	0.4208	0.4221
430.9	0.3629	0.3569	0.395	0.3994	0.4212	0.4225
435.9	0.3637	0.3576	0.3945	0.3988	0.4215	0.423
440.9	0.3643	0.3582	0.3939	0.3983	0.4218	0.4235
445.9	0.3648	0.3588	0.3934	0.3977	0.4222	0.4239
450.9	0.3653	0.3595	0.3929	0.3971	0.4225	0.4244
455.9	0.3657	0.3601	0.3923	0.3966	0.4229	0.4249
460.9	0.3662	0.3607	0.3918	0.3961	0.4233	0.4254
465.9	0.3669	0.3611	0.3912	0.3957	0.4237	0.4258
470.9	0.3675	0.3616	0.3907	0.3952	0.4242	0.4263
476	0.3681	0.3622	0.3902	0.3948	0.4246	0.4268
481	0.3687	0.3628	0.3897	0.3943	0.425	0.4273
486	0.3692	0.3633	0.3893	0.3939	0.4253	0.4278
491	0.3696	0.3637	0.3888	0.3934	0.4257	0.4282
496	0.37	0.364	0.3884	0.3929	0.4261	0.4286
501	0.3703	0.3643	0.3879	0.3925	0.4266	0.4291
506	0.3706	0.3646	0.3875	0.3921	0.427	0.4295
511	0.3708	0.3649	0.3871	0.3917	0.4273	0.4299
516	0.3711	0.3652	0.3868	0.3913	0.4277	0.4303
521	0.3714	0.3654	0.3863	0.3909	0.4281	0.4307
526	0.3715	0.3657	0.3859	0.3905	0.4284	0.4311
531.1	0.3715	0.3659	0.3855	0.3902	0.4288	0.4315
536.1	0.3715	0.3661	0.3852	0.3898	0.4292	0.4318
541.1	0.3718	0.3663	0.3848	0.3894	0.4295	0.4322
546.1	0.3721	0.3665	0.3844	0.389	0.4299	0.4326
551.1	0.3725	0.3666	0.3841	0.3887	0.4302	0.4329
556.1	0.3729	0.3668	0.3837	0.3883	0.4305	0.4333
561.1	0.3731	0.3671	0.3834	0.388	0.4308	0.4336
566.1	0.373	0.3674	0.3831	0.3877	0.4311	0.4339
571.1	0.3729	0.3677	0.3827	0.3874	0.4314	0.4343
576.2	0.3727	0.368	0.3824	0.3871	0.4317	0.4346
581.2	0.3727	0.3681	0.382	0.3868	0.432	0.4349
586.2	0.3728	0.3682	0.3817	0.3865	0.4323	0.4352
591.2	0.3729	0.3684	0.3814	0.3862	0.4326	0.4355
596.2	0.3729	0.3686	0.3812	0.3859	0.4329	0.4357
601.2	0.3728	0.3687	0.3809	0.3856	0.4332	0.436
606.2	0.3706	0.3672	0.3804	0.385	0.4335	0.4363

611.2	0.3591	0.3583	0.3791	0.383	0.4336	0.4364
616.2	0.3328	0.3366	0.376	0.3787	0.4332	0.4362
621.2	0.29771	0.30491	0.3712	0.373	0.4325	0.4356
626.3	0.26644	0.27313	0.3658	0.3673	0.4316	0.4347
631.3	0.24537	0.24865	0.3609	0.3629	0.4308	0.4339
636.3	0.23326	0.23268	0.357	0.3596	0.4303	0.4332
641.3	0.22632	0.22283	0.3539	0.3572	0.4299	0.4328
646.3	0.22163	0.216334	0.3513	0.3552	0.4297	0.4326
651.3	0.21783	0.211465	0.3491	0.3535	0.4296	0.4324
656.3	0.214442	0.2074545	0.3471	0.3519	0.4295	0.4323
661.3	0.211314	0.20397	0.3454	0.3505	0.4295	0.4322
666.3	0.208365	0.200845	0.3438	0.3493	0.4295	0.4322
671.3	0.205571	0.198028	0.3424	0.3481	0.4295	0.4321
676.3	0.202932	0.19549	0.3411	0.347	0.4295	0.4321
681.4	0.200448	0.19317	0.3399	0.346	0.4295	0.4321
686.4	0.198153	0.19097	0.3388	0.3451	0.4296	0.4321
691.4	0.19609	0.18889	0.3377	0.3442	0.4296	0.4321
696.4	0.19424	0.1869	0.3368	0.3434	0.4296	0.4321
701.4	0.19254	0.18502	0.3358	0.3425	0.4297	0.4321
706.4	0.19091	0.18328	0.335	0.3418	0.4298	0.4322
711.4	0.18928	0.18167	0.3342	0.341	0.4299	0.4322
716.4	0.18767	0.18011	0.3334	0.3403	0.43	0.4323
721.4	0.18611	0.17859	0.3326	0.3396	0.4301	0.4324
726.5	0.18463	0.17711	0.3319	0.339	0.4302	0.4325
731.5	0.18324	0.1757	0.3312	0.3383	0.4303	0.4325
736.5	0.18194	0.17439	0.3305	0.3377	0.4304	0.4326
741.5	0.1807	0.17319	0.3299	0.3371	0.4304	0.4327
746.5	0.17947	0.17208	0.3293	0.3365	0.4305	0.4328
751.5	0.17827	0.17104	0.3287	0.336	0.4306	0.4329
756.5	0.17711	0.17001	0.3281	0.3355	0.4307	0.4329
761.5	0.17598	0.169	0.3275	0.335	0.4308	0.433
766.5	0.1749	0.16801	0.327	0.3344	0.4309	0.433
771.5	0.17386	0.16707	0.3264	0.3339	0.4309	0.4331
776.5	0.17287	0.16615	0.3259	0.3334	0.431	0.4332
781.6	0.17196	0.16528	0.3254	0.3329	0.4311	0.4332
786.6	0.17109	0.16444	0.3249	0.3324	0.4312	0.4333
791.6	0.17025	0.16363	0.3244	0.332	0.4313	0.4334
796.6	0.16944	0.16284	0.324	0.3315	0.4314	0.4334
801.6	0.16865	0.16208	0.3235	0.3311	0.4315	0.4335
806.6	0.16786	0.16135	0.3231	0.3307	0.4315	0.4336
811.6	0.16709	0.16066	0.3227	0.3302	0.4316	0.4337
816.6	0.16634	0.15998	0.3223	0.3298	0.4317	0.4337
821.6	0.16561	0.15932	0.3219	0.3293	0.4318	0.4338

826.7	0.16489	0.15869	0.3215	0.3289	0.4319	0.4338
831.7	0.16418	0.15807	0.3211	0.3285	0.432	0.4338
836.7	0.16351	0.15746	0.3207	0.3281	0.4321	0.4339
841.7	0.1629	0.15686	0.3203	0.3277	0.4322	0.4339
846.7	0.16231	0.15628	0.3199	0.3273	0.4323	0.434
851.7	0.16174	0.15571	0.3196	0.327	0.4324	0.4341
856.7	0.16119	0.15517	0.3192	0.3266	0.4324	0.4342
861.7	0.16066	0.15465	0.3188	0.3262	0.4325	0.4342
866.7	0.16014	0.15417	0.3185	0.3259	0.4326	0.4343
871.7	0.15962	0.15371	0.3181	0.3255	0.4326	0.4344
876.8	0.15911	0.15325	0.3178	0.3252	0.4327	0.4344
881.8	0.15862	0.15279	0.3174	0.3248	0.4328	0.4345
886.8	0.15814	0.15234	0.3171	0.3245	0.4329	0.4345
891.8	0.15768	0.15191	0.3168	0.3241	0.433	0.4346
896.8	0.15724	0.15149	0.3164	0.3238	0.4331	0.4346
901.8	0.15679	0.15109	0.3161	0.3234	0.4332	0.4347
906.8	0.15635	0.15072	0.3158	0.3231	0.4333	0.4348
911.8	0.15594	0.15034	0.3155	0.3228	0.4333	0.4349
916.8	0.15555	0.14997	0.3152	0.3224	0.4334	0.435
921.8	0.15517	0.14959	0.3149	0.3221	0.4335	0.435
926.8	0.15478	0.14923	0.3146	0.3218	0.4336	0.435
931.9	0.15438	0.14888	0.3144	0.3214	0.4337	0.4351
936.9	0.15399	0.14854	0.3141	0.3211	0.4337	0.4351
941.9	0.15362	0.14821	0.3138	0.3208	0.4338	0.4352
946.9	0.15327	0.14789	0.3135	0.3205	0.4339	0.4352
951.9	0.15294	0.14758	0.3132	0.3202	0.434	0.4353
956.9	0.15263	0.14729	0.3129	0.3199	0.4341	0.4353
961.9	0.15233	0.147	0.3126	0.3196	0.4341	0.4354
966.9	0.15201	0.14671	0.3124	0.3193	0.4342	0.4354
971.9	0.1517	0.14643	0.3121	0.319	0.4342	0.4354
977	0.15139	0.14615	0.3118	0.3187	0.4343	0.4355
982	0.15109	0.14587	0.3116	0.3184	0.4344	0.4356
987	0.15081	0.14561	0.3113	0.3181	0.4344	0.4356
992	0.15053	0.14536	0.311	0.3178	0.4345	0.4357
997	0.15025	0.14511	0.3108	0.3175	0.4346	0.4358
1002	0.14999	0.14488	0.3105	0.3173	0.4347	0.4358
1007	0.14974	0.14465	0.3103	0.317	0.4348	0.4359
1012	0.1495	0.14442	0.31	0.3167	0.4348	0.4359
1017	0.14925	0.14418	0.3098	0.3164	0.4349	0.4359
1022	0.14901	0.14394	0.3096	0.3162	0.4349	0.4359
1027	0.14875	0.1437	0.3093	0.3159	0.435	0.436
1032	0.14851	0.14348	0.3091	0.3156	0.4351	0.436
1037	0.14828	0.14327	0.3088	0.3154	0.4352	0.436

1042	0.14807	0.14308	0.3086	0.3151	0.4352	0.4361
1047	0.14785	0.14288	0.3083	0.3148	0.4353	0.4361
1052	0.14763	0.14267	0.3081	0.3146	0.4354	0.4362
1057	0.1474	0.14247	0.3079	0.3143	0.4354	0.4363
1062	0.14717	0.14227	0.3076	0.3141	0.4355	0.4363
1067	0.14696	0.14209	0.3074	0.3138	0.4355	0.4363
1072	0.14677	0.1419	0.3072	0.3136	0.4356	0.4363
1077	0.14659	0.14171	0.30699	0.3133	0.4357	0.4364
1082	0.14642	0.14153	0.30678	0.3131	0.4357	0.4364
1087	0.14625	0.14135	0.30657	0.3128	0.4358	0.4365
1092	0.14608	0.14119	0.30635	0.3126	0.4359	0.4366
1097	0.1459	0.14103	0.30613	0.3123	0.4359	0.4367
1102	0.1457	0.14087	0.3059	0.312	0.436	0.4368
1107	0.14551	0.14071	0.30568	0.3118	0.436	0.4368
1112	0.14534	0.14056	0.30546	0.3116	0.4361	0.4368
1117	0.14519	0.1404	0.30526	0.3113	0.4361	0.4368
1122	0.14504	0.14025	0.30505	0.3111	0.4362	0.4368
1127	0.14489	0.14008	0.30485	0.3109	0.4362	0.4367
1132	0.14475	0.13992	0.30464	0.3106	0.4363	0.4367
1137	0.1446	0.13977	0.30444	0.3104	0.4363	0.4368
1142	0.14446	0.13962	0.30424	0.3102	0.4364	0.4369
1147	0.1443	0.13949	0.30404	0.3099	0.4364	0.4369
1152	0.14415	0.13936	0.30383	0.3097	0.4364	0.437
1157	0.144	0.13923	0.30363	0.3095	0.4365	0.4371
1162	0.14386	0.13911	0.30343	0.3092	0.4365	0.4371
1167	0.14371	0.13898	0.30323	0.309	0.4366	0.4372
1172	0.14356	0.13885	0.30304	0.3088	0.4366	0.4372
1177	0.14341	0.13871	0.30285	0.3086	0.4367	0.4372
1182	0.14327	0.13857	0.30266	0.3084	0.4367	0.4372
1187	0.14316	0.13843	0.30248	0.3081	0.4367	0.4373
1192	0.14305	0.1383	0.3023	0.3079	0.4368	0.4373
1197	0.14294	0.13817	0.3021	0.3077	0.4368	0.4373
1202	0.14283	0.13806	0.3019	0.3075	0.4369	0.4373

Time/secs	$1x10^{-4}$ mols $KMnO_4$/ V-SHE		$1X10^{-3}$ mols $KMnO_4$/ V-SHE		$1x10^{-2}$ mols $KMnO_4$/ V-SHE	
	Run 1	Run 2	Run 1	Run 2	Run 1	Run 2
5.01	0.2452	0.24457	0.24483	0.2444	0.24605	0.25177
10.02	0.24522	0.24457	0.24483	0.2444	0.24606	0.25179
15.03	0.24531	0.24459	0.24485	0.2444	0.24608	0.25192
20.04	0.24556	0.24463	0.2449	0.24442	0.24613	0.25228
25.05	0.246	0.24471	0.245	0.24444	0.24624	0.25292
30.06	0.24659	0.24481	0.24512	0.24448	0.24637	0.25378
35.07	0.24723	0.24493	0.24525	0.24453	0.24651	0.25473
40.08	0.24787	0.24505	0.24539	0.24457	0.24663	0.25568
45.09	0.24847	0.24517	0.24553	0.24462	0.24673	0.2566
50.1	0.24905	0.24529	0.24567	0.24466	0.24684	0.25747
55.11	0.24959	0.24541	0.2458	0.24471	0.24698	0.2583
60.12	0.25011	0.24553	0.24593	0.24476	0.24713	0.2591
65.13	0.2506	0.24565	0.24606	0.2448	0.2473	0.25987
70.14	0.25106	0.24576	0.24618	0.24485	0.24745	0.26061
75.15	0.25151	0.24588	0.2463	0.24489	0.24761	0.26133
80.16	0.25193	0.24599	0.24642	0.24494	0.24775	0.26203
85.17	0.25233	0.2461	0.24654	0.24498	0.2479	0.2627
90.18	0.25271	0.24621	0.24666	0.24503	0.24806	0.26335
95.19	0.25309	0.24632	0.24678	0.24507	0.24823	0.26398
100.2	0.25345	0.24642	0.2469	0.24511	0.24844	0.26458
105.2	0.2538	0.24652	0.24701	0.24515	0.24871	0.26517
110.2	0.25413	0.24662	0.24712	0.2452	0.249	0.26574
115.2	0.25446	0.24672	0.24723	0.24524	0.24923	0.2663
120.2	0.25477	0.24681	0.24734	0.24528	0.24939	0.26684
125.3	0.25506	0.24691	0.24745	0.24532	0.24948	0.26737
130.3	0.25535	0.24701	0.24756	0.24536	0.24953	0.2679
135.3	0.25563	0.2471	0.24767	0.24539	0.24958	0.26846
140.3	0.2559	0.2472	0.24778	0.24542	0.24964	0.26905
145.3	0.25616	0.24729	0.24788	0.24546	0.24973	0.26961
150.3	0.25641	0.24738	0.24798	0.2455	0.24984	0.27014
155.3	0.25665	0.24747	0.24808	0.24553	0.24996	0.27063
160.3	0.2569	0.24756	0.24818	0.24557	0.25009	0.27108
165.3	0.25713	0.24765	0.24828	0.24561	0.25023	0.27151
170.3	0.25736	0.24774	0.24838	0.24564	0.25038	0.27192
175.4	0.25758	0.24783	0.24847	0.24568	0.25055	0.27231
180.4	0.2578	0.24791	0.24857	0.24572	0.25072	0.27268
185.4	0.25801	0.24799	0.24867	0.24576	0.2509	0.27305
190.4	0.2582	0.24807	0.24875	0.2458	0.25106	0.27339
195.4	0.2584	0.24815	0.24884	0.24583	0.2512	0.27371
200.4	0.25859	0.24823	0.24892	0.24587	0.25135	0.274
205.4	0.25877	0.24831	0.24901	0.24591	0.2515	0.27429

210.4	0.25896	0.24839	0.2491	0.24594	0.25165	0.27457
215.4	0.25914	0.24847	0.24918	0.24598	0.25179	0.27485
220.4	0.25932	0.24855	0.24927	0.24602	0.25193	0.27513
225.4	0.25949	0.24863	0.24935	0.24606	0.25207	0.27542
230.5	0.25967	0.24871	0.24944	0.24609	0.25223	0.2757
235.5	0.25983	0.24878	0.24952	0.24613	0.2524	0.27598
240.5	0.25999	0.24886	0.24961	0.24617	0.25258	0.27625
245.5	0.26015	0.24893	0.24969	0.2462	0.25274	0.27651
250.5	0.2603	0.24901	0.24977	0.24624	0.2529	0.27677
255.5	0.26045	0.24908	0.24984	0.24627	0.25303	0.27703
260.5	0.26059	0.24916	0.24992	0.24631	0.25317	0.27728
265.5	0.26073	0.24923	0.25	0.24634	0.2533	0.27752
270.5	0.26087	0.2493	0.25008	0.24637	0.25343	0.27777
275.5	0.261	0.24937	0.25015	0.24641	0.25357	0.27801
280.6	0.26113	0.24944	0.25023	0.24644	0.25371	0.27825
285.6	0.26125	0.24951	0.2503	0.24648	0.25383	0.27848
290.6	0.26138	0.24958	0.25038	0.24651	0.25393	0.27871
295.6	0.26151	0.24965	0.25046	0.24654	0.254	0.27894
300.6	0.26163	0.24971	0.25053	0.24658	0.25406	0.27916
305.6	0.26467	0.25304	0.25596	0.25207	0.2595	0.28424
310.6	0.281	0.27111	0.28425	0.28083	0.28799	0.3104
315.6	0.3205	0.3148	0.3481	0.3459	0.3529	0.3704
320.6	0.377	0.377	0.4308	0.4304	0.4378	0.4495
325.6	0.432	0.4369	0.4998	0.5017	0.5093	0.5171
330.7	0.4717	0.4794	0.5396	0.5437	0.5502	0.5567
335.7	0.4939	0.5027	0.5553	0.5614	0.5654	0.572
340.7	0.5032	0.5123	0.5583	0.5662	0.5668	0.5738
345.7	0.5048	0.5145	0.557	0.5665	0.5634	0.5708
350.7	0.5028	0.5137	0.5552	0.5659	0.5596	0.5671
355.7	0.4995	0.512	0.5538	0.5657	0.5563	0.564
360.7	0.4961	0.5104	0.5529	0.5656	0.5538	0.5615
365.7	0.4933	0.5089	0.5521	0.5657	0.5517	0.5594
370.7	0.4911	0.5076	0.5514	0.5657	0.5498	0.5576
375.8	0.4893	0.5064	0.5507	0.5657	0.5482	0.556
380.8	0.4879	0.5054	0.55	0.5656	0.5467	0.5546
385.8	0.4868	0.5046	0.5493	0.5654	0.5453	0.5533
390.8	0.4859	0.5038	0.5487	0.5652	0.5441	0.5522
395.8	0.4852	0.5032	0.5481	0.565	0.5429	0.5512
400.8	0.4845	0.5026	0.5476	0.5648	0.5419	0.5503
405.8	0.484	0.502	0.5472	0.5646	0.5409	0.5495
410.8	0.4835	0.5014	0.5467	0.5645	0.54	0.5487
415.8	0.4831	0.5009	0.5464	0.5643	0.5392	0.5479
420.8	0.4828	0.5004	0.546	0.5642	0.5384	0.5472

425.9	0.4825	0.5	0.5457	0.564	0.5377	0.5466
430.9	0.4822	0.4997	0.5454	0.5639	0.5369	0.546
435.9	0.4819	0.4994	0.5452	0.5637	0.5363	0.5454
440.9	0.4817	0.4991	0.5449	0.5636	0.5356	0.5448
445.9	0.4815	0.4988	0.5447	0.5635	0.535	0.5442
450.9	0.4814	0.4985	0.5446	0.5633	0.5344	0.5436
455.9	0.4812	0.4983	0.5444	0.5632	0.5338	0.5431
460.9	0.481	0.4981	0.5442	0.563	0.5332	0.5426
465.9	0.4809	0.4979	0.5441	0.5629	0.5327	0.5421
470.9	0.4808	0.4977	0.544	0.5627	0.5322	0.5416
476	0.4806	0.4975	0.5439	0.5626	0.5316	0.5411
481	0.4805	0.4972	0.5438	0.5625	0.5311	0.5406
486	0.4804	0.497	0.5437	0.5624	0.5306	0.5401
491	0.4804	0.4968	0.5436	0.5623	0.5302	0.5397
496	0.4803	0.4967	0.5435	0.5622	0.5297	0.5392
501	0.4803	0.4966	0.5434	0.5622	0.5293	0.5388
506	0.4803	0.4965	0.5433	0.562	0.5288	0.5384
511	0.4803	0.4964	0.5432	0.5619	0.5284	0.5379
516	0.4802	0.4963	0.5432	0.5618	0.528	0.5375
521	0.4802	0.4962	0.5431	0.5617	0.5276	0.5371
526	0.4802	0.4961	0.5431	0.5615	0.5271	0.5367
531.1	0.4802	0.4961	0.543	0.5614	0.5267	0.5363
536.1	0.4802	0.4961	0.5429	0.5613	0.5264	0.5359
541.1	0.4802	0.4961	0.5429	0.5612	0.526	0.5355
546.1	0.4802	0.4961	0.5428	0.5611	0.5256	0.5352
551.1	0.4802	0.4962	0.5428	0.561	0.5252	0.5348
556.1	0.4802	0.4962	0.5427	0.5609	0.5249	0.5344
561.1	0.4802	0.4962	0.5427	0.5607	0.5245	0.534
566.1	0.4802	0.4962	0.5426	0.5606	0.5242	0.5337
571.1	0.4803	0.4963	0.5425	0.5605	0.5238	0.5333
576.2	0.4803	0.4963	0.5425	0.5604	0.5235	0.533
581.2	0.4804	0.4963	0.5425	0.5603	0.5232	0.5326
586.2	0.4804	0.4963	0.5424	0.5602	0.5229	0.5322
591.2	0.4804	0.4964	0.5424	0.5601	0.5225	0.5319
596.2	0.4805	0.4964	0.5423	0.56	0.5222	0.5316
601.2	0.4805	0.4965	0.5423	0.5598	0.5219	0.5312
606.2	0.4804	0.4964	0.5421	0.5596	0.5216	0.5309
611.2	0.4793	0.495	0.5415	0.559	0.5212	0.5305
616.2	0.4763	0.4911	0.5393	0.5568	0.5206	0.53
621.2	0.4711	0.4847	0.5347	0.5525	0.52	0.5294
626.3	0.4649	0.4772	0.528	0.546	0.5195	0.5289
631.3	0.4588	0.4699	0.5203	0.5385	0.519	0.5284
636.3	0.4536	0.4638	0.5131	0.5313	0.5186	0.528

641.3	0.4493	0.4588	0.5069	0.525	0.5183	0.5277
646.3	0.4457	0.4546	0.5019	0.5199	0.518	0.5274
651.3	0.4426	0.4509	0.4977	0.5156	0.5177	0.5272
656.3	0.4398	0.4476	0.4943	0.512	0.5175	0.5269
661.3	0.4372	0.4445	0.4912	0.5089	0.5172	0.5267
666.3	0.4347	0.4417	0.4884	0.5061	0.5169	0.5264
671.3	0.4325	0.4389	0.4859	0.5035	0.5167	0.5262
676.3	0.4303	0.4363	0.4836	0.5011	0.5165	0.526
681.4	0.4282	0.4338	0.4814	0.4989	0.5162	0.5258
686.4	0.4263	0.4315	0.4793	0.4967	0.516	0.5256
691.4	0.4244	0.4292	0.4773	0.4948	0.5158	0.5254
696.4	0.4226	0.427	0.4754	0.4929	0.5156	0.5252
701.4	0.4209	0.4249	0.4737	0.4911	0.5154	0.525
706.4	0.4192	0.4228	0.472	0.4894	0.5153	0.5248
711.4	0.4176	0.4209	0.4703	0.4877	0.5151	0.5246
716.4	0.4161	0.419	0.4687	0.4862	0.5149	0.5244
721.4	0.4146	0.4172	0.4672	0.4846	0.5147	0.5242
726.5	0.4132	0.4154	0.4657	0.4832	0.5146	0.5241
731.5	0.4118	0.4136	0.4643	0.4817	0.5144	0.5239
736.5	0.4104	0.412	0.4629	0.4803	0.5143	0.5237
741.5	0.4091	0.4103	0.4616	0.479	0.5141	0.5236
746.5	0.4078	0.4087	0.4603	0.4777	0.514	0.5235
751.5	0.4066	0.4071	0.459	0.4764	0.5138	0.5233
756.5	0.4053	0.4056	0.4577	0.4752	0.5137	0.5232
761.5	0.4042	0.4041	0.4565	0.474	0.5135	0.523
766.5	0.403	0.4026	0.4553	0.4728	0.5134	0.5229
771.5	0.4019	0.4012	0.4541	0.4716	0.5132	0.5227
776.5	0.4008	0.3998	0.4529	0.4705	0.5131	0.5226
781.6	0.3997	0.3984	0.4517	0.4694	0.513	0.5225
786.6	0.3986	0.397	0.4506	0.4683	0.5128	0.5223
791.6	0.3976	0.3957	0.4495	0.4672	0.5127	0.5222
796.6	0.3966	0.3944	0.4484	0.4661	0.5126	0.522
801.6	0.3956	0.3931	0.4474	0.4651	0.5124	0.5219
806.6	0.3947	0.3918	0.4463	0.4641	0.5123	0.5218
811.6	0.3937	0.3906	0.4453	0.4631	0.5122	0.5216
816.6	0.3928	0.3894	0.4442	0.4621	0.5121	0.5215
821.6	0.3919	0.3881	0.4432	0.4611	0.5119	0.5214
826.7	0.391	0.387	0.4422	0.4601	0.5118	0.5212
831.7	0.3901	0.3858	0.4412	0.4591	0.5117	0.5211
836.7	0.3892	0.3846	0.4402	0.4582	0.5116	0.521
841.7	0.3884	0.3835	0.4393	0.4572	0.5115	0.5209
846.7	0.3875	0.3824	0.4383	0.4563	0.5113	0.5207
851.7	0.3867	0.3813	0.4374	0.4553	0.5112	0.5206

856.7	0.3859	0.3802	0.4364	0.4544	0.5111	0.5205
861.7	0.3851	0.3791	0.4355	0.4535	0.511	0.5203
866.7	0.3843	0.378	0.4346	0.4525	0.5109	0.5202
871.7	0.3835	0.3769	0.4336	0.4516	0.5108	0.5201
876.8	0.3828	0.3759	0.4327	0.4507	0.5107	0.52
881.8	0.382	0.3748	0.4319	0.4498	0.5106	0.5198
886.8	0.3813	0.3738	0.431	0.449	0.5105	0.5197
891.8	0.3805	0.3728	0.4301	0.4481	0.5104	0.5196
896.8	0.3798	0.3717	0.4292	0.4472	0.5103	0.5195
901.8	0.3791	0.3707	0.4284	0.4463	0.5102	0.5194
906.8	0.3784	0.3697	0.4275	0.4454	0.5101	0.5192
911.8	0.3777	0.3687	0.4267	0.4446	0.51	0.5191
916.8	0.377	0.3677	0.4258	0.4437	0.5099	0.519
921.8	0.3763	0.3668	0.425	0.4428	0.5098	0.5189
926.8	0.3756	0.3658	0.4242	0.442	0.5097	0.5187
931.9	0.3749	0.3648	0.4234	0.4411	0.5095	0.5186
936.9	0.3743	0.3639	0.4226	0.4403	0.5094	0.5185
941.9	0.3736	0.3629	0.4218	0.4394	0.5093	0.5184
946.9	0.373	0.3619	0.421	0.4386	0.5093	0.5183
951.9	0.3723	0.361	0.4202	0.4377	0.5092	0.5182
956.9	0.3717	0.36	0.4194	0.4369	0.5091	0.518
961.9	0.3711	0.3591	0.4187	0.4361	0.509	0.5179
966.9	0.3704	0.3582	0.4179	0.4353	0.5089	0.5178
971.9	0.3698	0.3573	0.4172	0.4344	0.5088	0.5177
977	0.3692	0.3564	0.4164	0.4336	0.5087	0.5176
982	0.3686	0.3555	0.4157	0.4328	0.5086	0.5174
987	0.368	0.3545	0.415	0.4319	0.5085	0.5173
992	0.3674	0.3536	0.4143	0.4311	0.5084	0.5172
997	0.3668	0.3527	0.4136	0.4303	0.5083	0.5171
1002	0.3662	0.3518	0.4129	0.4295	0.5082	0.517
1007	0.3656	0.3509	0.4122	0.4287	0.5082	0.5169
1012	0.365	0.35	0.4115	0.4279	0.5081	0.5168
1017	0.3645	0.3491	0.4108	0.4271	0.508	0.5167
1022	0.3639	0.3483	0.4102	0.4264	0.5079	0.5165
1027	0.3633	0.3474	0.4095	0.4256	0.5078	0.5164
1032	0.3628	0.3466	0.4088	0.4249	0.5077	0.5163
1037	0.3622	0.3457	0.4082	0.4241	0.5077	0.5162
1042	0.3617	0.3449	0.4076	0.4234	0.5076	0.5161
1047	0.3611	0.344	0.4069	0.4227	0.5075	0.516
1052	0.3606	0.3432	0.4063	0.4219	0.5074	0.5159
1057	0.36	0.3423	0.4057	0.4212	0.5073	0.5158
1062	0.3595	0.3415	0.4051	0.4205	0.5072	0.5157
1067	0.359	0.3407	0.4045	0.4197	0.5072	0.5156

1072	0.3585	0.3399	0.4039	0.419	0.5071	0.5155
1077	0.3579	0.3391	0.4033	0.4183	0.507	0.5154
1082	0.3574	0.3383	0.4027	0.4176	0.5069	0.5153
1087	0.3569	0.3375	0.4021	0.4169	0.5069	0.5152
1092	0.3564	0.3367	0.4015	0.4162	0.5068	0.5151
1097	0.3559	0.3359	0.401	0.4155	0.5067	0.515
1102	0.3554	0.3351	0.4004	0.4148	0.5066	0.5149
1107	0.3549	0.3343	0.3999	0.4141	0.5066	0.5148
1112	0.3545	0.3336	0.3993	0.4134	0.5065	0.5147
1117	0.354	0.3328	0.3988	0.4127	0.5064	0.5146
1122	0.3535	0.332	0.3983	0.412	0.5063	0.5145
1127	0.353	0.3313	0.3977	0.4114	0.5063	0.5144
1132	0.3526	0.3305	0.3972	0.4107	0.5062	0.5143
1137	0.3521	0.3298	0.3967	0.4101	0.5061	0.5142
1142	0.3516	0.329	0.3962	0.4094	0.5061	0.5141
1147	0.3512	0.3283	0.3957	0.4088	0.506	0.514
1152	0.3507	0.3275	0.3952	0.4082	0.5059	0.514
1157	0.3503	0.3268	0.3947	0.4075	0.5058	0.5139
1162	0.3498	0.326	0.3942	0.4069	0.5058	0.5138
1167	0.3494	0.3253	0.3937	0.4063	0.5057	0.5137
1172	0.3489	0.3246	0.3932	0.4057	0.5056	0.5136
1177	0.3485	0.3239	0.3927	0.4051	0.5056	0.5135
1182	0.348	0.3231	0.3922	0.4045	0.5055	0.5134
1187	0.3476	0.3224	0.3918	0.4039	0.5054	0.5133
1192	0.3472	0.3217	0.3913	0.4033	0.5053	0.5132
1197	0.3468	0.321	0.3908	0.4027	0.5052	0.5131
1202	0.3463	0.3203	0.3904	0.4022	0.5051	0.513

Time/secs	$1x10^{-4}$ mols $K_2Cr_2O_7$/ V-SHE		$1X10^{-3}$ mols $K_2Cr_2O_7$/ V-SHE		$1x10^{-2}$ mols $K_2Cr_2O_7$/ V-SHE		SIBX only/ V-SHE	
	Run 1	Run 2	Run 1	Run 2	Run 1	Run 2	Run 1	Run 1
5.01	0.24627	0.24556	0.24577	0.24854	0.24631	0.24736	0.24565	0.24372
10.02	0.24629	0.24558	0.24578	0.24855	0.24632	0.24737	0.24567	0.24373
15.03	0.2464	0.24571	0.24585	0.24861	0.24637	0.24745	0.24576	0.24378
20.04	0.24671	0.24609	0.24607	0.24879	0.24654	0.24769	0.24604	0.24394
25.05	0.24726	0.24678	0.24646	0.2491	0.24685	0.24812	0.24653	0.24423
30.06	0.24801	0.2477	0.24699	0.24951	0.24728	0.2487	0.24721	0.24462
35.07	0.24886	0.24874	0.24759	0.24999	0.24777	0.24938	0.24797	0.24505
40.08	0.24973	0.24983	0.2482	0.25048	0.24827	0.25008	0.24875	0.24549
45.09	0.25061	0.25091	0.2488	0.25097	0.24876	0.25078	0.24951	0.24593
50.1	0.25148	0.25196	0.24941	0.25145	0.24924	0.25147	0.25024	0.24637
55.11	0.25236	0.25298	0.25001	0.25192	0.24973	0.25215	0.25095	0.24681
60.12	0.25324	0.25398	0.2506	0.25239	0.25021	0.25282	0.25165	0.24723
65.13	0.2541	0.25497	0.25119	0.25286	0.2507	0.25347	0.25234	0.24764
70.14	0.25492	0.25594	0.25176	0.25335	0.25117	0.2541	0.25302	0.24802
75.15	0.25571	0.25687	0.25233	0.25385	0.25164	0.25473	0.25368	0.2484
80.16	0.25646	0.25778	0.25289	0.25436	0.25211	0.25534	0.25433	0.24879
85.17	0.25719	0.25866	0.25345	0.25486	0.25257	0.25596	0.25497	0.2492
90.18	0.2579	0.25953	0.254	0.25535	0.25303	0.25658	0.25561	0.24961
95.19	0.25859	0.26039	0.25456	0.25583	0.25348	0.25722	0.25626	0.25001
100.2	0.25929	0.26123	0.2551	0.25632	0.25393	0.25786	0.2569	0.25041
105.2	0.26001	0.26206	0.25563	0.25681	0.25437	0.25849	0.25753	0.2508
110.2	0.26075	0.26287	0.25617	0.2573	0.25481	0.25909	0.25815	0.25119
115.2	0.2615	0.26367	0.25671	0.25777	0.25525	0.25967	0.25877	0.25156
120.2	0.26223	0.26446	0.25725	0.25825	0.25568	0.26024	0.2594	0.25194
125.3	0.26295	0.26522	0.25777	0.25874	0.25611	0.2608	0.26002	0.2523
130.3	0.26364	0.26596	0.25826	0.25924	0.25653	0.26135	0.26063	0.25266
135.3	0.26431	0.26669	0.25873	0.25971	0.25695	0.26189	0.26122	0.25301
140.3	0.26497	0.2674	0.25919	0.26014	0.25736	0.26243	0.2618	0.25334
145.3	0.26562	0.26809	0.25968	0.26055	0.25776	0.26297	0.26237	0.25366
150.3	0.26631	0.26877	0.26017	0.26095	0.25816	0.2635	0.2629	0.25398
155.3	0.26702	0.26947	0.26067	0.26133	0.25855	0.26401	0.26342	0.25431
160.3	0.26771	0.27015	0.26119	0.2617	0.25894	0.26453	0.26393	0.25466
165.3	0.26835	0.27081	0.26175	0.26207	0.25933	0.26503	0.26444	0.25501
170.3	0.26898	0.27145	0.26232	0.26244	0.25972	0.26553	0.26494	0.25537
175.4	0.26961	0.27207	0.26286	0.26282	0.26011	0.26602	0.26541	0.25571
180.4	0.27025	0.27268	0.26334	0.2632	0.26049	0.26649	0.26587	0.25605
185.4	0.27088	0.27328	0.26379	0.26357	0.26087	0.26696	0.26631	0.25639
190.4	0.27147	0.27389	0.26421	0.26394	0.26124	0.26743	0.26675	0.25674
195.4	0.27202	0.27451	0.26463	0.2643	0.26162	0.26791	0.26719	0.25709
200.4	0.27256	0.27515	0.26503	0.26466	0.262	0.26838	0.26762	0.25742
205.4	0.27311	0.27581	0.26543	0.26503	0.26238	0.26884	0.26805	0.25774

210.4	0.27368	0.27646	0.26583	0.26538	0.26275	0.2693	0.26847	0.25805
215.4	0.27425	0.27708	0.26622	0.26572	0.26311	0.26974	0.26889	0.25834
220.4	0.27481	0.27766	0.26661	0.26606	0.26347	0.27018	0.2693	0.25863
225.4	0.27534	0.27823	0.26698	0.26641	0.26383	0.27061	0.2697	0.25893
230.5	0.27586	0.27877	0.26736	0.26676	0.26418	0.27101	0.27011	0.25924
235.5	0.27638	0.27931	0.26773	0.2671	0.26453	0.27142	0.27052	0.25955
240.5	0.27691	0.27984	0.26812	0.26743	0.26488	0.27185	0.27092	0.25985
245.5	0.27748	0.28036	0.26852	0.26776	0.26524	0.27227	0.2713	0.26016
250.5	0.27809	0.28087	0.26891	0.26809	0.26558	0.2727	0.27168	0.26046
255.5	0.27872	0.28137	0.2693	0.26841	0.26593	0.27312	0.27205	0.26076
260.5	0.27932	0.28186	0.26966	0.26874	0.26628	0.27353	0.27242	0.26106
265.5	0.27987	0.28236	0.27003	0.26908	0.26662	0.27393	0.27277	0.26135
270.5	0.28038	0.28284	0.27039	0.26942	0.26697	0.27432	0.27313	0.26162
275.5	0.28086	0.28332	0.27076	0.26977	0.26731	0.27471	0.27348	0.26189
280.6	0.28132	0.28378	0.27113	0.27012	0.26765	0.27509	0.27383	0.26217
285.6	0.28176	0.28424	0.27149	0.27045	0.26798	0.27547	0.27418	0.26245
290.6	0.28221	0.2847	0.27185	0.27076	0.26831	0.27585	0.27453	0.26272
295.6	0.28265	0.28516	0.27221	0.27106	0.26863	0.27623	0.27488	0.26299
300.6	0.28308	0.28561	0.27256	0.27135	0.26896	0.2766	0.27523	0.26325
305.6	0.28351	0.28606	0.2729	0.27164	0.26933	0.27705	0.27557	0.26351
310.6	0.28395	0.28652	0.27327	0.27198	0.26994	0.27793	0.27592	0.26376
315.6	0.2844	0.28698	0.27369	0.27242	0.27107	0.27958	0.27627	0.26399
320.6	0.28486	0.28744	0.27416	0.27292	0.27271	0.28187	0.27661	0.26421
325.6	0.2853	0.28789	0.27466	0.27344	0.2745	0.2842	0.27693	0.26445
330.7	0.28572	0.28831	0.27513	0.27391	0.27605	0.28607	0.27726	0.26469
335.7	0.28612	0.28872	0.27557	0.27432	0.2772	0.28739	0.27757	0.26495
340.7	0.28652	0.28912	0.27598	0.2747	0.27803	0.28832	0.27789	0.26521
345.7	0.28691	0.28951	0.27636	0.27506	0.27865	0.28905	0.27819	0.26546
350.7	0.2873	0.28989	0.27673	0.27539	0.27917	0.28968	0.27849	0.2657
355.7	0.28766	0.29025	0.27709	0.27572	0.27964	0.29028	0.27878	0.26594
360.7	0.28801	0.29058	0.27744	0.27605	0.28009	0.29085	0.27906	0.26617
365.7	0.28834	0.29089	0.27779	0.27638	0.28052	0.2914	0.27934	0.26636
370.7	0.28866	0.29121	0.27814	0.27671	0.28094	0.29193	0.27962	0.2665
375.8	0.28897	0.29153	0.2785	0.27704	0.28134	0.29244	0.27989	0.26662
380.8	0.2893	0.29186	0.27884	0.27737	0.28174	0.29293	0.28015	0.26677
385.8	0.28964	0.29219	0.27917	0.27768	0.28214	0.29342	0.28039	0.26697
390.8	0.28998	0.29251	0.27949	0.27799	0.28253	0.29388	0.28063	0.26723
395.8	0.29032	0.29282	0.27981	0.2783	0.28293	0.29434	0.28088	0.26751
400.8	0.29065	0.29312	0.28013	0.2786	0.28334	0.29478	0.28113	0.26778
405.8	0.29096	0.29343	0.28046	0.2789	0.28376	0.29522	0.28139	0.26803
410.8	0.29122	0.29377	0.28081	0.2792	0.28416	0.29564	0.28165	0.26826
415.8	0.29145	0.29412	0.28116	0.27948	0.28455	0.29605	0.2819	0.26848
420.8	0.29168	0.29449	0.28152	0.27975	0.28493	0.29646	0.28214	0.26871

425.9	0.29193	0.29484	0.28188	0.28003	0.28531	0.29685	0.28235	0.26893
430.9	0.29223	0.29517	0.28225	0.28032	0.28567	0.29724	0.28252	0.26915
435.9	0.29255	0.29547	0.28261	0.2806	0.28602	0.29762	0.2827	0.26937
440.9	0.29285	0.29576	0.28294	0.2809	0.28636	0.298	0.28292	0.2696
445.9	0.29314	0.29605	0.28326	0.28119	0.28669	0.29837	0.28316	0.26982
450.9	0.29341	0.29635	0.28356	0.28146	0.28701	0.29874	0.28342	0.27005
455.9	0.29369	0.29666	0.28385	0.28172	0.28733	0.29911	0.28368	0.27029
460.9	0.29397	0.29698	0.28413	0.28196	0.28764	0.29948	0.28393	0.27054
465.9	0.29425	0.29731	0.28442	0.28219	0.28795	0.29983	0.28417	0.27078
470.9	0.29455	0.29766	0.2847	0.28244	0.28826	0.30018	0.2844	0.27102
476	0.29485	0.29799	0.28497	0.2827	0.28857	0.30051	0.28462	0.27126
481	0.29516	0.29829	0.28524	0.28298	0.28887	0.30084	0.28485	0.27151
486	0.29547	0.29854	0.2855	0.28326	0.28917	0.30116	0.28507	0.27178
491	0.29577	0.29877	0.28576	0.28353	0.28945	0.30147	0.28529	0.27204
496	0.29605	0.29899	0.28601	0.28379	0.28974	0.30178	0.28551	0.27229
501	0.29631	0.29922	0.28626	0.28405	0.29002	0.30209	0.28571	0.27251
506	0.29657	0.29946	0.28651	0.28433	0.29031	0.30239	0.28592	0.27272
511	0.29683	0.29974	0.28675	0.28462	0.29059	0.3027	0.28613	0.27293
516	0.29709	0.30003	0.28699	0.2849	0.29088	0.303	0.28633	0.27314
521	0.29735	0.30033	0.28722	0.28517	0.29115	0.3033	0.28652	0.27335
526	0.29761	0.30061	0.28744	0.28541	0.29142	0.30359	0.28672	0.27357
531.1	0.29787	0.30087	0.28766	0.28563	0.29167	0.30389	0.28691	0.27378
536.1	0.29811	0.30111	0.28788	0.28586	0.29193	0.30419	0.28711	0.27399
541.1	0.29834	0.30136	0.2881	0.28609	0.29218	0.3045	0.2873	0.2742
546.1	0.29855	0.3016	0.28831	0.28632	0.29242	0.30482	0.28749	0.27441
551.1	0.29875	0.30186	0.28853	0.28655	0.29265	0.30513	0.28769	0.27463
556.1	0.29897	0.30213	0.28875	0.28676	0.29288	0.30543	0.28788	0.27486
561.1	0.29921	0.3024	0.28899	0.28697	0.29313	0.30572	0.28808	0.27508
566.1	0.29945	0.30266	0.28923	0.28718	0.2934	0.306	0.28829	0.27532
571.1	0.2997	0.3029	0.28947	0.28738	0.29366	0.30626	0.2885	0.27558
576.2	0.29994	0.30313	0.28972	0.28759	0.29392	0.30652	0.28871	0.27589
581.2	0.30018	0.30336	0.28996	0.28779	0.29416	0.30677	0.28891	0.27622
586.2	0.30041	0.30358	0.2902	0.28801	0.29439	0.307	0.28912	0.27653
591.2	0.30063	0.30382	0.29044	0.28823	0.29462	0.3073	0.28933	0.27679
596.2	0.30084	0.30405	0.29067	0.28846	0.29484	0.3075	0.28953	0.27698
601.2	0.30104	0.30429	0.2909	0.2887	0.29505	0.3078	0.28972	0.27714
606.2	0.29917	0.30232	0.28905	0.28686	0.29322	0.30595	0.2876	0.27516
611.2	0.28824	0.29088	0.27843	0.27614	0.28254	0.2952	0.2756	0.26401
616.2	0.26242	0.26425	0.25408	0.25135	0.25761	0.27017	0.248	0.23829
621.2	0.22701	0.22863	0.22204	0.21856	0.22421	0.2368	0.21161	0.204202
626.3	0.19444	0.19695	0.19406	0.18986	0.19461	0.2073501	0.17996	0.17437
631.3	0.17212	0.17618	0.1759	0.17146	0.17544	0.18827	0.15989	0.15534
636.3	0.15962	0.16511	0.1661	0.16199	0.16551	0.17831	0.14974	0.14565

641.3	0.15326	0.15969	0.16104	0.15756	0.1609	0.17362	0.14513	0.14125
646.3	0.14981	0.15675	0.15805	0.15518	0.15849	0.17122	0.14279	0.13902
651.3	0.1475	0.15468	0.15585	0.15339	0.15678	0.16961	0.14117	0.13744
656.3	0.14565	0.15297	0.15399	0.15176	0.15522	0.16824	0.13979	0.13605
661.3	0.14408	0.1515	0.15241	0.15027	0.15378	0.16695	0.13854	0.13478
666.3	0.14272	0.15022	0.15105	0.14893	0.1525	0.16575	0.13739	0.13366
671.3	0.14155	0.14909	0.14984	0.14776	0.15145	0.16468	0.13635	0.13268
676.3	0.14055	0.14809	0.14874	0.14672	0.15058	0.16378	0.13544	0.13183
681.4	0.13967	0.14719	0.14771	0.1458	0.14978	0.16301	0.13465	0.13108
686.4	0.13888	0.14638	0.14677	0.145	0.14899	0.16231	0.13397	0.13042
691.4	0.13817	0.14565	0.14593	0.1443	0.1482	0.16167	0.13336	0.12981
696.4	0.13753	0.14502	0.14518	0.14371	0.14745	0.16109	0.13282	0.12927
701.4	0.13696	0.14447	0.14454	0.14318	0.14679	0.16055	0.13234	0.12879
706.4	0.13647	0.144	0.14401	0.1427	0.14622	0.16005	0.1319	0.12834
711.4	0.13605	0.14358	0.14358	0.14226	0.14571	0.15963	0.1315	0.12792
716.4	0.13566	0.1432	0.14319	0.14185	0.14526	0.15929	0.13113	0.12753
721.4	0.1353	0.14287	0.14282	0.14149	0.14486	0.15899	0.1308	0.12716
726.5	0.13496	0.14255	0.14246	0.14116	0.14445	0.15871	0.1305	0.12683
731.5	0.13462	0.14224	0.1421	0.14085	0.14401	0.15844	0.13024	0.12653
736.5	0.1343	0.14193	0.14173	0.14057	0.14354	0.15819	0.12999	0.12626
741.5	0.13398	0.14162	0.14139	0.1403	0.14308	0.15797	0.12975	0.126
746.5	0.1337	0.14132	0.14108	0.14007	0.14267	0.15782	0.12952	0.12574
751.5	0.13344	0.14102	0.14079	0.13987	0.14232	0.15772	0.12929	0.12549
756.5	0.13321	0.14077	0.14049	0.13968	0.14204	0.15764	0.12908	0.12526
761.5	0.133	0.14057	0.14019	0.1395	0.1418	0.15754	0.12887	0.12506
766.5	0.13281	0.14042	0.1399	0.13931	0.14156	0.15743	0.1287	0.12489
771.5	0.13264	0.14031	0.13962	0.13911	0.1413	0.15732	0.1286	0.12472
776.5	0.1325	0.14021	0.13937	0.13892	0.14104	0.15722	0.12854	0.12457
781.6	0.13238	0.14012	0.13916	0.13873	0.14078	0.1571	0.12848	0.12441
786.6	0.13226	0.14003	0.13897	0.13856	0.14052	0.15697	0.12842	0.12426
791.6	0.13215	0.13993	0.1388	0.13842	0.14028	0.15685	0.12837	0.12412
796.6	0.13204	0.13983	0.13864	0.1383	0.14004	0.15675	0.12834	0.12399
801.6	0.13193	0.13973	0.13849	0.1382	0.13982	0.15667	0.12831	0.12386
806.6	0.13184	0.13963	0.13834	0.13812	0.13962	0.15661	0.12825	0.12374
811.6	0.13176	0.13954	0.1382	0.13806	0.13943	0.15659	0.12817	0.12363
816.6	0.13169	0.13947	0.13807	0.13801	0.13927	0.15659	0.12809	0.12353
821.6	0.1316	0.13943	0.13796	0.13796	0.13914	0.15657	0.12802	0.12344
826.7	0.1315	0.13938	0.13788	0.13792	0.13902	0.15652	0.12794	0.12335
831.7	0.13141	0.13932	0.13782	0.13786	0.1389	0.15646	0.12786	0.12326
836.7	0.13134	0.13925	0.13779	0.13781	0.13879	0.15638	0.12776	0.12318
841.7	0.1313	0.13916	0.13782	0.13777	0.1387	0.15632	0.12766	0.1231
846.7	0.13126	0.13906	0.13786	0.13774	0.13862	0.15627	0.12754	0.12303
851.7	0.13119	0.13897	0.13786	0.13771	0.13858	0.15625	0.12744	0.12297

856.7	0.1311	0.1389	0.1378	0.13767	0.13856	0.15624	0.12734	0.12293
861.7	0.131	0.13885	0.13772	0.13765	0.13854	0.15623	0.12726	0.12287
866.7	0.1309	0.13881	0.13763	0.13763	0.1385	0.1562	0.12719	0.1228
871.7	0.13079	0.13879	0.13755	0.1376	0.13844	0.15617	0.12713	0.1227
876.8	0.13071	0.13878	0.13748	0.13757	0.13837	0.15615	0.12706	0.12263
881.8	0.13064	0.13878	0.13745	0.13754	0.13832	0.15614	0.12699	0.12259
886.8	0.1306	0.13877	0.13744	0.1375	0.13828	0.15613	0.12692	0.12257
891.8	0.13058	0.13875	0.13745	0.13748	0.13824	0.15612	0.12688	0.12255
896.8	0.13056	0.13872	0.13745	0.13746	0.13822	0.15609	0.12686	0.1225
901.8	0.13055	0.13868	0.13745	0.13745	0.13817	0.15605	0.12684	0.12245
906.8	0.13054	0.13865	0.13747	0.13745	0.1381	0.15603	0.12683	0.12241
911.8	0.13055	0.13863	0.13752	0.13745	0.13801	0.15603	0.12682	0.12238
916.8	0.13057	0.13862	0.13757	0.13745	0.13792	0.15603	0.1268	0.12235
921.8	0.13059	0.13863	0.13758	0.13745	0.13783	0.15604	0.12678	0.12231
926.8	0.13058	0.13867	0.13756	0.13746	0.13777	0.15603	0.12677	0.12228
931.9	0.13053	0.13872	0.13751	0.13747	0.13773	0.15602	0.12675	0.12224
936.9	0.13045	0.13878	0.13745	0.13748	0.1377	0.15605	0.12672	0.12221
941.9	0.13035	0.13883	0.13739	0.13749	0.13769	0.15611	0.12668	0.12218
946.9	0.13025	0.13887	0.13734	0.1375	0.1377	0.15617	0.12663	0.12216
951.9	0.13016	0.1389	0.1373	0.1375	0.13772	0.1562	0.12657	0.12214
956.9	0.13007	0.13891	0.13726	0.1375	0.13774	0.15619	0.12651	0.12213
961.9	0.12999	0.13891	0.13723	0.13749	0.13777	0.15616	0.12646	0.12211
966.9	0.12992	0.1389	0.13719	0.13748	0.13779	0.15613	0.12642	0.12208
971.9	0.12986	0.1389	0.13715	0.13747	0.1378	0.15612	0.12637	0.12205
977	0.12979	0.1389	0.1371	0.13747	0.13778	0.15612	0.12634	0.12202
982	0.12973	0.13888	0.13704	0.13746	0.13775	0.15614	0.12631	0.12199
987	0.12967	0.13887	0.13699	0.13745	0.13772	0.15619	0.12628	0.12197
992	0.12962	0.13885	0.13693	0.13743	0.1377	0.15626	0.12626	0.12194
997	0.12956	0.13883	0.13687	0.13743	0.13768	0.15633	0.12624	0.12192
1002	0.12952	0.13881	0.13681	0.13743	0.13767	0.15637	0.1262	0.1219
1007	0.12948	0.13879	0.13677	0.13744	0.13765	0.15639	0.12617	0.12188
1012	0.12945	0.13879	0.13674	0.13745	0.13763	0.15639	0.12614	0.12186
1017	0.12942	0.13879	0.13673	0.13747	0.13759	0.15638	0.12612	0.12183
1022	0.12938	0.13879	0.13673	0.13749	0.13757	0.15638	0.12613	0.12181
1027	0.12931	0.13877	0.13674	0.13751	0.13757	0.15639	0.12613	0.1218
1032	0.12923	0.13874	0.13676	0.13751	0.13758	0.15639	0.12614	0.12179
1037	0.12914	0.13871	0.13679	0.13751	0.13759	0.1564	0.12614	0.12178
1042	0.12908	0.13867	0.13686	0.13751	0.13761	0.15641	0.12613	0.12178
1047	0.12905	0.13865	0.13697	0.13752	0.13762	0.15642	0.12613	0.12177
1052	0.12905	0.13863	0.13714	0.13753	0.13761	0.15642	0.12611	0.12175
1057	0.12907	0.13862	0.13733	0.13755	0.1376	0.15642	0.12609	0.12174
1062	0.12911	0.13862	0.13752	0.13755	0.1376	0.15641	0.12608	0.12173
1067	0.12914	0.13865	0.13768	0.13756	0.13759	0.15641	0.12608	0.12173

1072	0.12914	0.13868	0.13781	0.13759	0.13758	0.1564	0.12607	0.12174
1077	0.12914	0.13871	0.13792	0.13763	0.13757	0.15639	0.12607	0.12174
1082	0.12913	0.13873	0.13801	0.13766	0.13756	0.15638	0.12608	0.12173
1087	0.12912	0.13876	0.13807	0.13767	0.13754	0.15635	0.12613	0.1217
1092	0.12912	0.13876	0.13812	0.13768	0.13755	0.15632	0.12623	0.12167
1097	0.1291	0.13875	0.13814	0.13769	0.13759	0.15627	0.12635	0.12164
1102	0.12909	0.13871	0.13818	0.1377	0.13765	0.15623	0.12646	0.12163
1107	0.12908	0.13868	0.13824	0.13769	0.1377	0.15619	0.12654	0.12162
1112	0.12908	0.13865	0.13832	0.13767	0.13771	0.15618	0.12657	0.12161
1117	0.12909	0.13864	0.13839	0.13764	0.13766	0.1562	0.12657	0.12161
1122	0.1291	0.13866	0.13843	0.1376	0.1376	0.15623	0.12657	0.12161
1127	0.1291	0.13872	0.13844	0.13758	0.13753	0.15624	0.12656	0.12162
1132	0.12908	0.13881	0.13842	0.13757	0.13744	0.15623	0.12656	0.12163
1137	0.12905	0.13891	0.13838	0.13756	0.13736	0.15617	0.12657	0.12163
1142	0.12903	0.13897	0.13837	0.13757	0.13728	0.15605	0.12659	0.12161
1147	0.12901	0.139	0.13847	0.13758	0.13721	0.1559	0.12661	0.12159
1152	0.12901	0.13902	0.13873	0.13759	0.13714	0.15577	0.12663	0.12157
1157	0.12902	0.13902	0.13909	0.1376	0.13708	0.15569	0.12666	0.12156
1162	0.12902	0.13903	0.13942	0.13762	0.13704	0.15565	0.12672	0.12156
1167	0.12903	0.13902	0.13964	0.13765	0.13703	0.15563	0.12679	0.12157
1172	0.12902	0.13901	0.13976	0.13767	0.13704	0.15562	0.12686	0.12158
1177	0.12903	0.13898	0.13981	0.13768	0.13703	0.15562	0.12693	0.1216
1182	0.12905	0.13895	0.13984	0.1377	0.13702	0.15561	0.12698	0.12161
1187	0.12909	0.13893	0.13986	0.13772	0.13699	0.15561	0.12703	0.12161
1192	0.12913	0.13892	0.13989	0.13774	0.13696	0.1556	0.12707	0.12163
1197	0.12914	0.13892	0.13993	0.13777	0.13693	0.1556	0.1271	0.12166
1202	0.12914	0.13891	0.13997	0.13779	0.13691	0.15562	0.12712	0.12169